

222
64

**RADICAL ANION REARRANGEMENTS. ARYL CYCLOPROPYL KETYL
ANIONS**

by

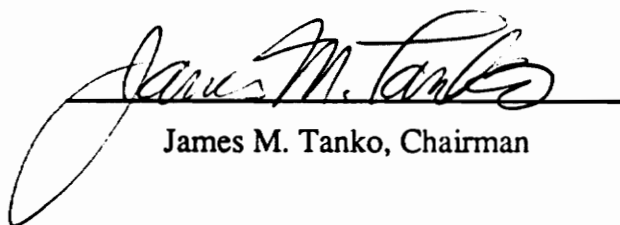
Ray E. Drumright

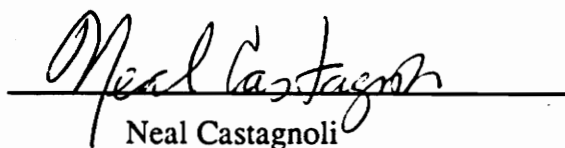
Dissertation submitted to the Faculty of the
Virginia Polytechnic Institute and State University
in partial fulfillment of the requirements for the degree of
DOCTOR OF PHILOSOPHY

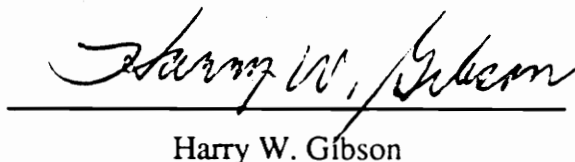
in

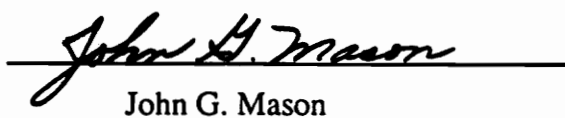
Chemistry

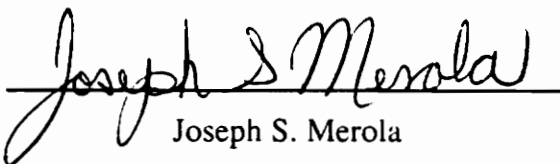
APPROVED:


James M. Tanko, Chairman


Neal Castagnoli


Harry W. Gibson


John G. Mason


Joseph S. Merola

January, 1991

Blacksburg, Virginia

LD

5655

V856

1991

D786

C.2

RADICAL ANION REARRANGEMENTS. ARYL CYCLOPROPYL KETYL ANIONS

by

Ray E. Drumright

James M. Tanko, Chairman
Chemistry

(ABSTRACT)

Aryl cyclopropyl ketones have often been employed as diagnostic probes for single electron transfer (SET) in organic chemical reactions. The implicit assumption in such studies is that the formation of rearranged product(s) can be ascribed to the intermediacy of a ketyl anion. Through a detailed examination of the decay of electrolytically generated aryl cyclopropyl ketyl anions, we have shown that the assumptions made in the use of these substrates as SET probes are not necessarily valid. Using derivative cyclic and linear sweep voltammetry it was discovered that the ketyl anions of alkyl- and unsubstituted aryl cyclopropyl ketones (class I), including phenyl cyclopropyl ketone (**28a**), 1-benzoyl-2-methylcyclopropane (**28b**), 1-benzoyl-2,2-dimethylcyclopropane (**28c**), *p*-tolyl cyclopropyl ketone (**28d**), and 1-benzoyl-1-methylcyclopropane (**28e**), undergo a slow and reversible cyclopropyl carbinyll type rearrangement followed by dimerization of the ring-opened and ring-closed radical anions. The equilibrium constant for the reversible ring opening lies highly in favor of the ring closed form. For (**28a**^{•-}) in anhydrous *N,N*-dimethylformamide containing 0.5 M *n*-Bu₄NBF₄ at 23 °C, the equilibrium constant was estimated at $K \approx 4.6 \times 10^{-8}$ with a maximum rate constant for ring opening and a minimum rate constant for ring closing at 2.0 s^{-1} and $4.3 \times 10^7 \text{ s}^{-1}$ respectively; the rate constant for dimerization was placed at $8.4 \times 10^7 \text{ M}^{-1}\text{s}^{-1}$. Semiempirical molecular orbital calculations (AM1) complement the above observations.

Similar results were obtained for all class I compounds. The ketyl anions of aryl cyclopropyl ketones with good radical stabilizing groups on the cyclopropane ring (class II), including trans-1-benzoyl-2-phenylcyclopropane (**66**), and 1-benzoyl-2-vinylcyclopropane (**76**) undergo rapid unimolecular ring opening. The rate constants for opening of (**66** \cdot^-) and (**76** \cdot^-) are greater than 10^3 s^{-1} but probably less than 10^7 s^{-1} and 10^5 s^{-1} respectively. Based upon our findings, class I ketones are extremely unreliable probes for SET; class II ketones may prove to be useful SET probes, but since absolute rate constants for their rearrangement are not yet known, they should be used only with extreme caution. The implications of these results are discussed in light of utilizing aryl cyclopropyl ketones as probes for SET.

ACKNOWLEDGMENTS

I would like to express my sincere gratitude to Dr. James M. Tanko for his patience, guidance, and friendship during my graduate career. I am very grateful to all of my committee members for their generous donation of time and critical reviews of my work and progress. I would also like to thank all faculty and students (past and present) in the Chemistry Department for making my stay at Virginia Tech very pleasant.

An extremely special thanks is sincerely extended to the donors of the Petroleum Research Fund of the American Chemical Society, Mobay Chemical Corporation (fellowship), Mr. George and Mrs. Gladys Cunningham (fellowship), Virginia Polytechnic Institute and State University (fellowship), and the department of chemistry at Virginia Tech for financial support.

Finally, and perhaps most importantly, I would like to thank my entire family for their unyielding support and understanding. An extremely warm and loving thanks to my dearest wife, Susan, and my faithful but recently deceased companion, Burt, who kept me sane through this whole ordeal.

TABLE OF CONTENTS

Chapter 1. Historical	01
Introduction	01
Literature Review	10
Free Radicals Related to Aryl Cyclopropyl Ketyl Anions	10
Use of Aryl Cyclopropyl Ketyl Anions to Detect Electron Transfer	14
Summary	26
Chapter 2. Alkyl- and Unsubstituted Aryl Cyclopropyl Ketones	27
Introduction	27
Kinetic Analysis of Ketyl Anion Decay	29
Electrolysis Products	47
Rate Constants for Ketyl Anion Decay	62
Stereoelectronic Effects in Ring Cleavage	68
Summary	77

Chapter 3. Development and Study of Potential Electron Transfer Probes	80
Introduction	80
<i>p</i> -Cyclopropyl Acetophenone (62)	81
<u>trans</u> -1-Benzoyl-2-phenylcyclopropane (66)	86
1-Benzoyl-2-vinylcyclopropane (76)	95
Summary	102
Chapter 4. Conclusions	105
Chapter 5. Experimental	108
Instrumentation	108
Materials and Purifications	110
Purification of Ethers	110
Activation of Alumina	110
Purification of N,N-Dimethylformamide	111
Purification of Argon	111
Synthesis of Starting Materials	112
<u>trans</u> -1-benzoyl-2-methylcyclopropane (28b)	112
1-benzoyl-1-methylcyclopropane (28e)	113
1-benzoyl-2-vinylcyclopropane (76)	113
2-vinylcyclopropane carboxylic acid	113

ethyl 2-vinylcyclopropane carboxylate	114
1-benzoyl-2,2-dimethylcyclopropane (28c)	114
1-(d5)benzoyl-2,2-dimethylcyclopropane (42)	114
p-tolyl cyclopropyl ketone (28d)	115
p-cyclopropyl acetophenone (62)	116
<u>trans</u> -1-benzoyl-2-phenylcyclopropane (66)	116
1-benzoyl-1-deuteriocyclopropane (45)	116
1-benzoyl-1-deuterio-2-phenylcyclopropane (75)	117
tetra-n-butylammonium tetrafluoroborate	117
Voltammetry	118
Solution Preparation	118
Voltammetric Cell	118
Working Electrode	119
Auxiliary Electrode	119
Reference Electrode	120
Positive Feedback IR Compensation	120
Voltammetric Runs	121
Electrolyses	123
Solution Preparation	123
Electrolysis Cell	123
Working Electrode	124
Auxiliary Electrode	124
Reference Electrode	124
Experimental Runs	125

Specific Electrolyses	127
Phenyl cyclopropyl ketone (28a)	127
Electrolysis quenched with H ₃ O ⁺	127
Electrolysis quenched with MeI	129
Electrolysis in presence of D ₂ O	130
1-benzoyl-1-deuteriocyclopropane (45)	132
<u>trans</u> -1-benzoyl-2-methylcyclopropane (28b)	134
1-benzoyl-2,2-dimethylcyclopropane (28c)	136
1-(d ₅)benzoyl-2,2-dimethylcyclopropane (42)	138
Coelectrolysis of 1-benzoyl-2,2-dimethylcyclopropane (28c) and 1-(d ₅)benzoyl-2,2-dimethylcyclopropane (42)	139
<p>-tolyl cyclopropyl ketone (28d)</p>	140
1-benzoyl-1-methylcyclopropane (28e)	142
<p>-cyclopropyl acetophenone (62)</p>	144
<u>trans</u> -1-benzoyl-2-phenylcyclopropane (66)	145
Electrolysis quenched with H ₃ O ⁺	145
Electrolysis quenched with MeI	146
Electrolysis monitored by CV	147
1-benzoyl-1-deuterio-2-phenylcyclopropane (75)	148
1-benzoyl-2-vinylcyclopropane (76)	149
Competition Kinetics	151
Independent Synthesis of Pivalophenone Ketyl Anion/ Radical Coupling Products	154
Coupling of Pivalophenone Ketyl Anion and the Δ ⁵ -hexenyl radical	155
Coupling of Pivalophenone Ketyl Anion and the cyclopentyl carbinyl radical	157
Synthesis of di(5-hexenyl)mercury (59)	159

Literature Cited	160
Appendix A. Use of Voltammetry for Mechanistic Studies	169
Introduction	169
Cyclic and Derivative Cyclic Voltammetry	170
Linear Sweep Voltammetry	177
Rate Constants	180
Summary	181
Appendix B. Collection and Handling of Electrochemical Data	182
Appendix C. Structural Determination by Ultraviolet Spectroscopy	184
Vita	186

LIST OF ILLUSTRATIONS

Figure 1.	Conventional reactions involving electron transfer	03
Figure 2.	Intramolecular rearrangement probes used to detect electron transfer	05
Figure 3.	Use of aryl cyclopropyl ketones as probes for electron transfer	07
Figure 4.	Comparison of free radical and ketyl anion rearrangements	08
Figure 5.	Effect of ion pairing on the rate of ring opening of cyclopropyl ketyl anions	09
Figure 6.	Product ratios derived from α -hydroxycyclopropyl benzyl free radical generated by reduction of the corresponding ketone and oxidation of the corresponding alcohol	12
Figure 7.	Possible mechanisms for tin hydride reduction of aromatic ketones	16
Figure 8.	Possible mechanisms for addition of trimethylsilyl-lithium to phenyl cyclopropyl ketone	17
Figure 9.	Reaction of 2-lithio-1,3-dithianes with phenyl cyclopropyl ketone	18
Figure 10.	Reaction of lithium dimethyl cuprate with phenyl cyclopropyl ketones	19
Figure 11.	Estimated half lives of phenyl cyclopropyl ketyl anions	19
Figure 12.	Nickel catalyzed additions of various organometallics to phenyl cyclopropyl ketones	21
Figure 13.	Proposed mechanism for nickel catalyzed addition of organometallics to phenyl cyclopropyl ketones	22
Figure 14.	Dissolving metal reduction of phenyl cyclopropyl ketones	24

Figure 15.	Electrochemical reduction of phenyl cyclopropyl ketones in aqueous ethanol	25
Figure 16.	General scheme for decay of electrode generated intermediates	28
Figure 17.	General structure of phenyl cyclopropyl ketones	28
Figure 18.	DCV reaction order plot for the decay of phenyl cyclopropyl ketyl anion (28a^{•-})	30
Figure 19.	DCV reaction order plot for the decay of <u>trans</u> -1-benzoyl-2-methylcyclopropyl ketyl anion (28b^{•-})	31
Figure 20.	DCV reaction order plot for the decay of 1-benzoyl-2,2-dimethylcyclopropyl ketyl anion (28c^{•-})	31
Figure 21.	DCV reaction order plot for the decay of <u>p</u> -tolyl cyclopropyl ketyl anion (28d^{•-})	32
Figure 22.	Linear sweep voltammetry reaction order plot for the decay of 1-benzoyl-2,2-dimethylcyclopropyl ketyl anion (28c^{•-})	34
Figure 23.	Linear sweep voltammetry reaction order plot for the decay of 1-benzoyl-2,2-dimethylcyclopropyl ketyl anion (28c^{•-})	34
Figure 24.	Plot for extraction of $\nu_{0.5}$ for phenyl cyclopropyl ketyl anion (28a^{•-})	37
Figure 25.	Plot for extraction of $\nu_{0.5}$ for <u>trans</u> -1-benzoyl-2-methylcyclopropyl ketyl anion (28b^{•-})	37
Figure 26.	Plot for extraction of $\nu_{0.5}$ for 1-benzoyl-2,2-dimethylcyclopropyl ketyl anion (28c^{•-})	38
Figure 27.	Plot for extraction of $\nu_{0.5}$ for <u>p</u> -tolyl cyclopropyl ketyl anion (28d^{•-})	38
Figure 28.	Plot for determination of activation energy for decay of phenyl cyclopropyl ketyl anion (28a^{•-})	41
Figure 29.	Plot for determination of activation energy for decay of <u>trans</u> -1-benzoyl-2-methylcyclopropyl ketyl anion (28b^{•-})	42

Figure 30.	Plot for determination of activation energy for decay of 1-benzoyl-2,2-dimethylcyclopropyl ketyl anion (28c ⁻)	42
Figure 31.	Proposed mechanism for the decay of phenyl cyclopropyl ketyl anions	45
Figure 32.	Electrolysis products for phenyl cyclopropyl ketones (28a), (28b), (28c), and (28e)	47
Figure 33.	Products of electrolysis of p-tolyl cyclopropyl ketone (28d)	49
Figure 34.	Coupling of ketyl anion and distonic radical anion to yield dianion	50
Figure 35.	Cyclic voltammogram of 1-benzoyl-2,2-dimethyl-cyclopropane (28c)	51
Figure 36.	Proposed mechanism for formation of dimeric product	52
Figure 37.	Results of electrolysis of 1-benzoyl-1-deuterio-cyclopropane (45)	53
Figure 38.	Results of electrolysis of phenyl cyclopropyl ketone in the presence of D ₂ O	54
Figure 39.	Compounds not observed in the electrolysis product mixture that would be expected if an intermolecular hydride transfer were operating	54
Figure 40.	Dimer products expected for coelectrolysis of labelled (42) and unlabelled (28c) 1-benzoyl-2,2-dimethyl-cyclopropanes if hydride transfer is intramolecular	55
Figure 41.	Dimer products expected for coelectrolysis of labelled (42) and unlabelled (28c) 1-benzoyl-2,2-dimethyl-cyclopropanes if hydride transfer is intermolecular	57
Figure 42.	DCV reaction order plot for the decay of 1-(d ₅)benzoyl-2,2-dimethylcyclopropyl ketyl anion (42 ⁻)	60
Figure 43.	Plot for extraction of $\nu_{0.5}$ for 1-(d ₅)benzoyl-2,2-dimethylcyclopropyl ketyl anion (42 ⁻)	60
Figure 44.	MMX calculated transition state for intramolecular hydride transfer	61

Figure 45.	Estimation of the rate constant for coupling of a free radical with a ketyl anion	63
Figure 46.	Products resulting from coupling of pivalophenone ketyl anion and Δ^5 -hexenyl radical	64
Figure 47.	Proposed mechanism for decay of alkyl- and unsubstituted phenyl cyclopropyl ketyl anions	69
Figure 48.	Plot of energy vs. reaction coordinate for the decay of phenyl cyclopropyl ketyl anions where dimerization is the rate limiting step	71
Figure 49.	Plot of energy vs. reaction coordinate for the decay of phenyl cyclopropyl ketyl anions where cyclopropane ring opening is the rate limiting step	72
Figure 50.	Walsh (Sudgen) model for cyclopropane	73
Figure 51.	Conformations of cyclopropane relative to an adjacent π system	74
Figure 52.	Effect of conformation on the rate of ring opening of cyclopropyl ketyl anions	75
Figure 53.	AM1 calculated least energy geometry for phenyl cyclopropyl ketyl anion (28a⁻)	75
Figure 54.	AM1 calculated least energy geometry for 1-benzoyl-1-methylcyclopropyl ketyl anion (28e⁻)	76
Figure 55.	Electron transfer reaction mechanism involving phenyl cyclopropyl ketone	78
Figure 56.	Resonance structures of <i>p</i> -cyclopropyl acetophenone ketyl anion (62⁻)	81
Figure 57.	DCV reaction order plot for the decay of <i>p</i> -cyclopropyl acetophenone (62)	83
Figure 58.	Fluoride catalyzed addition of silyl enol ethers to 4-cyclopropylnitrobenzene (65)	85
Figure 59.	Ring opening of 1-benzoyl-2-phenylcyclopropyl ketyl anion (67)	86
Figure 60.	Linear sweep voltammetry reaction order plot for the decay of 1-benzoyl-2-phenylcyclopropyl ketyl anion (67)	87

Figure 61.	Linear sweep voltammetry reaction order plot for the decay of 1-benzoyl-2-phenylcyclopropyl ketyl anion (67)	87
Figure 62.	Working curve for estimation of the upper limit of the unimolecular rate constant for ketyl anion decay	89
Figure 63.	Proposed mechanism for the decay of 1-benzoyl-2-phenylcyclopropyl ketyl anion (67)	90
Figure 64.	Results of methyl iodide quench after electrolysis of <u>trans</u> -1-benzoyl-2-phenylcyclopropane (66)	91
Figure 65.	Results of electrolysis of 1-benzoyl-1-deuterio-2-phenylcyclopropane (75)	92
Figure 66.	Cyclic voltammogram of <u>trans</u> -1-benzoyl-2-phenylcyclopropane (66)	93
Figure 67.	Cyclic voltammograms before and after electrolysis of <u>trans</u> -1-benzoyl-2-phenylcyclopropane (66)	94
Figure 68.	Electron transfer induced vinyl cyclopropane \rightarrow cyclopentene rearrangement	95
Figure 69.	Linear sweep voltammetry reaction order plot for 1-benzoyl-2-vinylcyclopropane (76)	97
Figure 70.	Linear sweep voltammetry reaction order plot for 1-benzoyl-2-vinylcyclopropane (76)	97
Figure 71.	Electrolysis products of 1-benzoyl-2-vinylcyclopropane (76)	98
Figure 72.	Proposed mechanism for the decay of 1-benzoyl-2-vinylcyclopropyl ketyl anion (77)	99
Figure 73.	Cyclic voltammogram of 1-benzoyl-2-vinylcyclopropane (76)	100
Figure 74.	Requirements for an effective electron transfer rearrangement probe	103
Figure 75.	Cleavage of a delocalized aryl cyclopropyl ketyl anion to its corresponding distonic radical anion	107
Figure 76.	Voltammetry cell and cap, two way purge valve, and bridge tube	122
Figure 77.	Electrolysis cell (H-cell) and cap	126

Figure 78.	Potential waveform for cyclic voltammetry	170
Figure 79.	Cyclic voltammogram	171
Figure 80.	Concentration profiles for both oxidized and reduced species during a CV experiment	172
Figure 81.	Cyclic voltammogram of system where the electrode generated species is involved in a homogeneous chemical reaction	174
Figure 82.	Derivative cyclic voltammogram of system where the electrode generated species is involved in a homogeneous chemical reaction	175
Figure 83.	Linear sweep voltammogram	177
Figure 84.	Possible isomeric structures for the cyclohexadiene containing product resulting from the coupling of a free radical with pivalophenone ketyl anion	184

LIST OF TABLES

Table 1.	Disputed rate constants for the decay of benzyl cyclopropyl free radicals	11
Table 2.	Reduction potentials of phenyl cyclopropyl ketones and the observed, integral orders for the rate laws for decay of their ketyl anions	30
Table 3.	Experimentally observed reaction orders for decay of phenyl cyclopropyl ketyl anions	32
Table 4.	Linear sweep voltammetry analysis of the decay of 1-benzoyl-2,2-dimethylcyclopropyl ketyl anion (28c ⁻)	35
Table 5.	Observed rate constants for decay of phenyl cyclopropyl ketyl anions	36
Table 6.	Relative stability of phenyl alkyl ketyl anions	39
Table 7.	Observed activation energies for the decay of phenyl cyclopropyl ketyl anions	40
Table 8.	AM1 calculated enthalpies for ring opening of cyclopropyl ketyl anions	44
Table 9.	Product yields for bulk electrolyses of phenyl cyclopropyl ketones (28a), (28b), (28c), and (28e)	48
Table 10.	Predicted and observed ratios of mass spectral peak intensities for coelectrolysis of labelled (42) and unlabelled (28c) 1-benzoyl-2,2-dimethylcyclopropanes	56
Table 11.	Equilibrium between radical anions and neutral substrates of isotopic isomers	58
Table 12.	Typical experimental results for coupling of Δ^5 -hexenyl radical with pivalophenone ketyl anion	65
Table 13.	Individual rate constants for the decay of phenyl cyclopropyl ketyl anion	66

Table 14.	AM1 calculated atomic orbital spin populations (ρ^{π}_i) in the p_z orbitals of phenyl alkyl and phenyl cyclopropyl ketyl anions	82
Table 15.	Results of competition experiments using 1-bromo-5-hexene as the radical source	153
Table 16.	Results of competition experiments using 5-hexenylmercuric chloride as the radical source	153

CHAPTER 1. HISTORICAL

INTRODUCTION

In general, organic chemists are trained to explain reaction mechanisms by invoking reactive intermediates that have all of their electrons paired. Therefore, intermediates such as carbanions and carbocations are often envisioned as reactive entities in organic chemical transformations. However, there exists a class of reactive intermediates, known as paramagnetic species, which do not have all of their electrons paired.

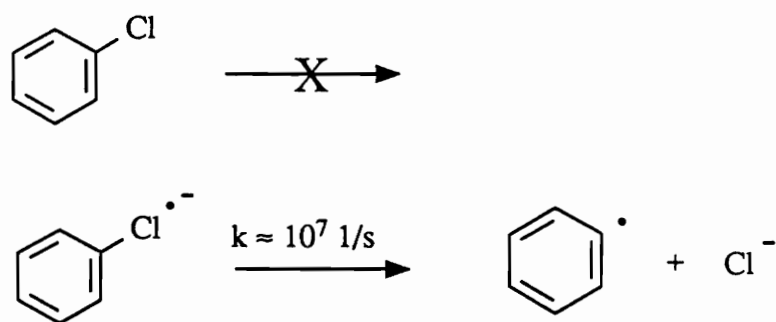
Paramagnetic species include the likes of free radicals and radical ions. Free radicals are not too esoteric because of their common use in such reactions as halogenations and polymerizations. Radical ions, on the other hand, are often overlooked. There are two basic types of radical ions:

- 1) a radical cation - formed by removal of an electron from a neutral, diamagnetic species (e.g. $M - e^- \rightarrow M^{\cdot+}$), and
- 2) a radical anion - formed by addition of an electron to a neutral, diamagnetic species (e.g. $M + e^- \rightarrow M^{\cdot-}$).

So, radical ions are formed by oxidation or reduction of neutral diamagnetic substrates. These simple changes in oxidation state of a molecule can drastically affect its reactivity.

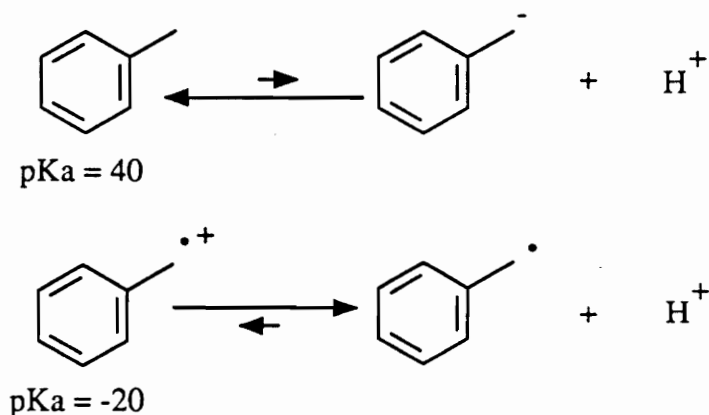
Radical ions are much more reactive than the corresponding neutral species. For example, chlorobenzene is a stable molecule which is not prone to homo- or heterolytic cleavage of the C-Cl bond. However, if chlorobenzene is reduced to its radical anion, it decomposes rapidly ($k \approx 10^7$ 1/s) to phenyl radical and chloride ion (Eqn. 1).¹

Eqn. 1



Similarly, toluene is an extremely weak acid with a pKa of around 40.² If toluene is oxidized to its radical cation, its pKa plummets to -20^{3,4} (Eqn. 2).

Eqn. 2



Recently, there has been a great deal of interest in single electron transfer (SET) reaction mechanisms as viable pathways in organic transformations. Radical ions are being implicated as intermediates in important biochemical transformations such as cytochrome oxidations⁵ and photosynthetic pathways⁶ as well as in conventional laboratory transformations.^{7,8} Reactions previously thought to proceed exclusively through conventional polar intermediates are now being shown to involve at least some component of electron transfer. Kochi has recently shown that SET is a viable mechanistic alternative to electrophilic aromatic substitution (Figure 1, I).^{9,10} Simple aliphatic nucleophilic substitutions¹¹ (S_N1 , S_N2) have also been shown to involve electron

transfer (Figure 1, II). For several systems, a free radical/radical ion chain process has been demonstrated and termed the $S_{RN}1$ reaction.¹² Also, nucleophilic addition of organometallics^{13-16a}, hydrides¹⁷, and carbanions^{16b-d} to carbonyl containing substrates are now believed to involve some component of electron transfer (Figure 1, III).

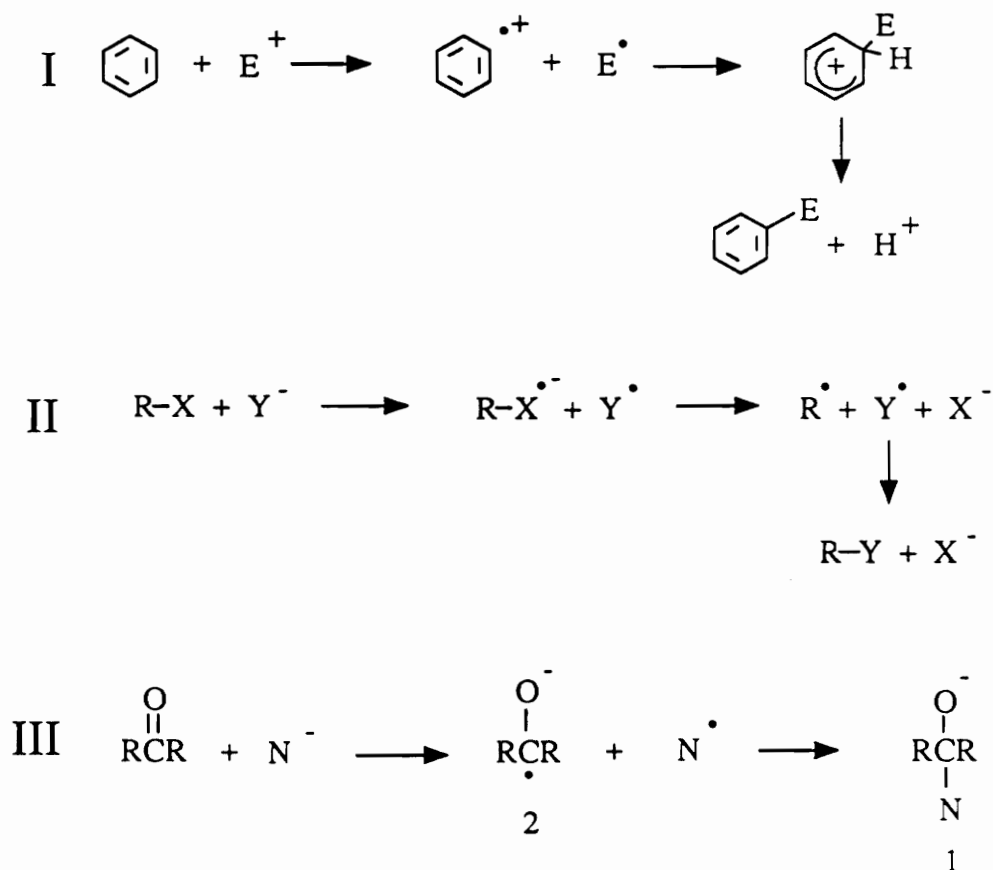


Figure 1. Conventional reactions involving electron transfer

As an example of an electron transfer mechanism, consider two mechanistic possibilities for addition of "nucleophiles" to carbonyl containing compounds (Figure 1, III). Conventional thought dictates that the nucleophile, N^- , adds to the electrophilic carbonyl compound in a concerted step yielding the final adduct (1). Suppose that instead of labelling N^- a nucleophile, it is considered a reducing agent; similarly, label the

carbonyl compound an oxidizing agent instead of an electrophile. One can then envision an electron transfer between N^- and the carbonyl compound to yield a ketyl anion (2) and a neutral radical, $N\cdot$. This pair of reactive intermediates can then collapse to the final adduct (1); the same product obtained from the conventional, concerted, polar path.

One would think that it would be a trivial matter to distinguish between conventional and electron transfer pathways, but this is often not the case. Because of the fleeting nature of radical ion intermediates they are extremely difficult to detect. Few cases exist where radical ions have been unambiguously observed during a chemical reaction by spectroscopic techniques. CIDNP¹⁸⁻²⁰ (chemically induced dynamic nuclear polarization) has been used as evidence for SET in reactions of alkyl iodides with alkyl lithium reagents. EPR (electron paramagnetic resonance) has provided evidence for SET in addition of hydrides to substituted benzophenones¹⁷ and reaction of anions with unsaturated organic molecules.²¹ Also, UV (ultraviolet) adsorption has allowed studies of electrophilic aromatic substitution^{9,10} and addition of hydrides to substituted benzophenones.¹⁷

In general, direct observation of radical ion intermediates is not feasible. It is more common to rely upon indirect methods to detect their presence. One method calls for the addition of a reagent into the reaction mixture which can "short circuit" the electron transfer such as a nitroaromatic compound (which acts as an electron sink). If rate inhibition is observed the reaction may involve some component of electron transfer. This method is most applicable in instances where a chain process is operating, but is often used outside of this context.

Another popular approach involves the use of intramolecular rearrangement probes to signal that an electron transfer mechanism is operating. For "appropriately substituted" molecules, it is assumed that radical ion formation will lead to a rapid rearrangement. Hence, if rearranged products are found in the final reaction mixture an electron transfer

process is implicated. The design philosophy of these probes is summarized in Figure 2.

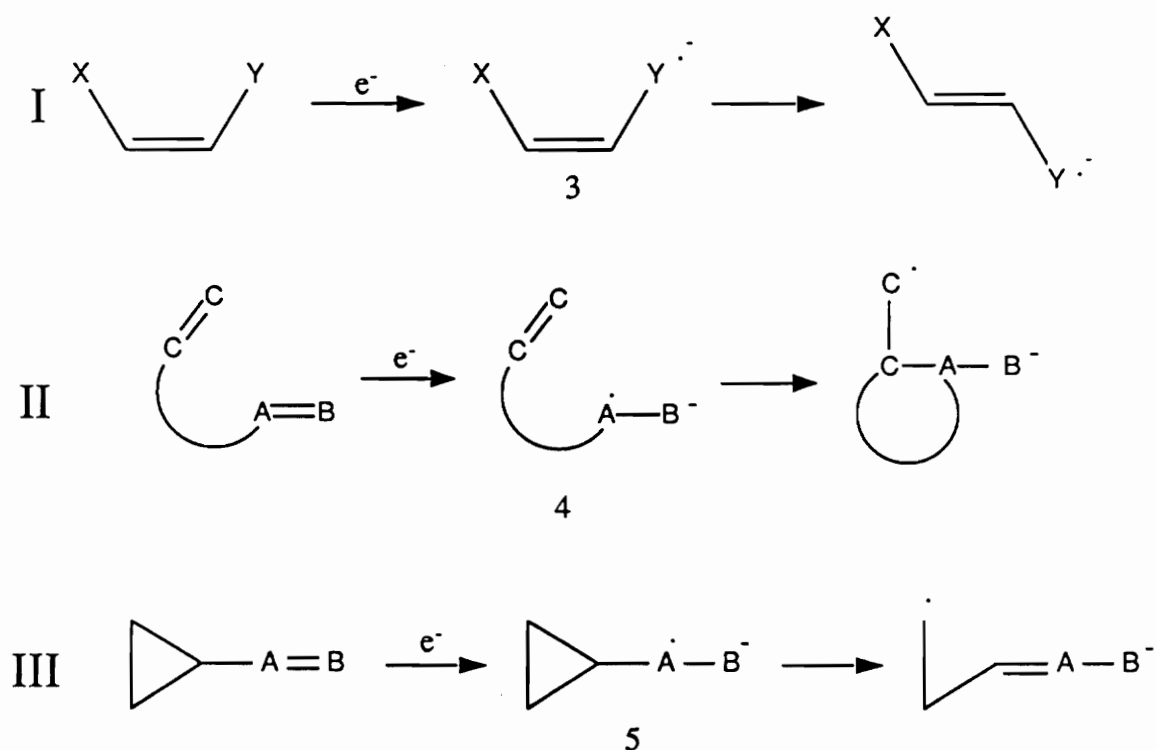


Figure 2. Intramolecular rearrangement probes used to detect electron transfer

The first example (Figure 2, I) is a geometric isomerization.²²⁻²⁵ Formation of the radical anion of the thermodynamically less stable isomer (3) reduces the bond order of the alkene allowing for facile isomerization. If isomerized starting material or products derived from isomerized material are found in the final reaction mixture, it may be inferred that the reaction proceeds through an electron transfer pathway. The second example (Figure 2, II) is a cyclization.²⁵⁻²⁹ For the purpose of this discussion let A=B be a functional group capable of accepting an electron (A=B = C=O, C-X, etc.). It is assumed that if the radical anion (4) is formed, it will rapidly cyclize. In most cases, these probes are designed to yield 5 or 6 membered rings. If ring closed product is found in the final reaction mixture, it may be inferred that the reaction proceeds through an electron transfer

pathway. The final example (Figure 2, III) is the formal opposite of the second example (Figure 2, II) and generally involves the rupture of 3 or 4 membered rings. Here it is assumed that if the radical anion (**5**) is formed it will rapidly ring open to relieve strain.^{24,30} Hence, if ring-opened product is found in the final reaction mixture an electron transfer mechanism is implicated.

The case that I would like to focus on is the cyclopropyl carbinylyl type rearrangement (Figure 2, III), and in particular, the cyclopropyl carbinylyl type rearrangement of aryl cyclopropyl ketyl anions (Figure 3). This particular rearrangement probe has seen an enormous amount of use in the last couple of decades. The general idea is that one takes a reagent ($X-Y$) suspected of undergoing electron transfer in its reaction with a carbonyl compound and treats it with a phenyl cyclopropyl ketone (i.e. **6**). If ring opened products (i.e. **7**) are found, an electron transfer process is implicated. Ring opened product is envisioned to be formed through an initial electron transfer to yield the aryl cyclopropyl ketyl anion (**8**) and the radical cation ($X-Y^{\cdot+}$). Radical anion (**8**) then rapidly ring opens to give distonic radical anion (**9**). Species (**9**) is called distonic because the anion portion and radical portion of this radical anion are no longer in conjugation. Distonic radical anion (**9**) and the radical cation ($X-Y^{\cdot+}$) then collapse in a bimolecular fashion to yield ring opened adduct (**7**). If only ring closed products (i.e. **10**) are found, the test is inconclusive. Ring closed products can arise from at least two mechanistic paths. The first possible path involves no electron transfer; the products arise from a traditional polar transformation. An alternate mechanistic explanation for observation of ring closed product is that indeed an electron transfer process is occurring but the bimolecular rate of collapse of (**8**) and ($X-Y^{\cdot+}$) is fast relative to the unimolecular rate of ring opening of (**8**) to (**9**).

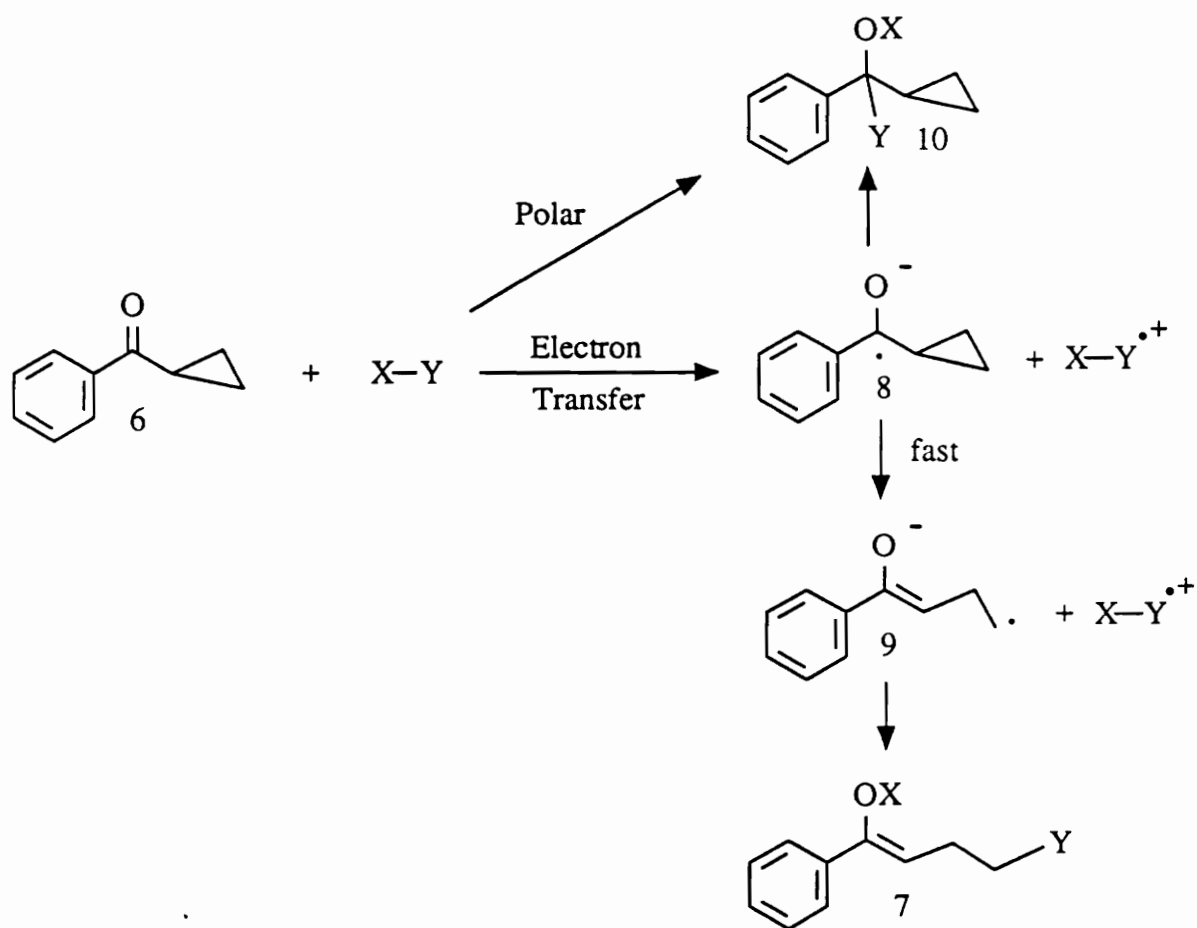


Figure 3. Use of aryl cyclopropyl ketones as probes for electron transfer

The justification for using rearrangement probes to detect electron transfer processes has its roots in free radical chemistry. Free radical rearrangements are well documented^{31,32} and in several cases their absolute rate constants are known.³³ It is implicitly assumed that structural features which lead to free radical rearrangements will also lead to rearrangement of radical ions. For example, the cyclopropyl carbinyl rearrangement is a cornerstone of free radical chemistry, proceeding with a rate constant of about 10^8 s^{-1} at room temperature (Figure 4, I).³³ This rearrangement is known as a "free radical clock" because absolute rate constants for competing bimolecular processes

can be determined from simple product analyses.

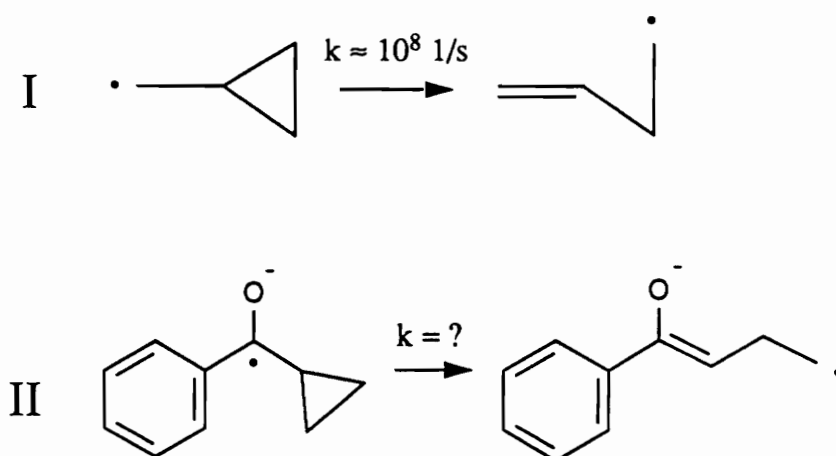


Figure 4. Comparison of free radical and ketyl anion rearrangements

The corresponding radical anion rearrangement (Figure 4, II) has not been studied in any detail. It is assumed that if the radical anion is formed, it will rapidly rearrange. No provisions are made for the extra delocalization which the radical anion enjoys over the free radical. This extra delocalization might be expected to slow the unimolecular rate of ring opening of the radical anion relative to the free radical. Also, solvent effects and ion pairing effects, which should drastically effect the radical anion but not the free radical, are ignored. Tighter ion pairing between the ketyl anion and the counter ion might be expected to speed the rate of ring opening of the ketyl anion relative to the free ketyl anion because ion pairing increases the spin density localized on the ketyl carbon atom (Figure 5).

EPR studies have shown that counter ion has a great effect upon the spin density localized on the ketyl carbon atom. For benzophenone ketyl anion labelled with carbon-13 at the ketyl carbon, the a_c^{13} coupling constants (hyperfine coupling of unpaired e^- and ^{13}C) are reported to be 15.8, 13.2, 12.1 and 9.6 Gauss when the counter ion is Mg^{2+} , Ca^{2+} , Ba^{2+} , and K^+ respectively.³⁴ Similarly, for fluorenone ketyl anion labelled with

C-13 on the ketyl carbon when the counter ion is varied from Li^+ , Na^+ , K^+ , to the "free" ion, the a_c^{13} coupling constants are reported to change from 6.20, 4.85, 4.20, to 2.87 Gauss respectively.³⁵ These trends show that spin density at the ketyl carbon atom is increased as the strength of the ion pair is increased. This increase in spin density at the ketyl carbon might be expected to be reflected in the rate of ring opening of the cyclopropyl ketyl anion. On the surface, the assumption that a ketyl anion will behave as a free radical seems unjustified.

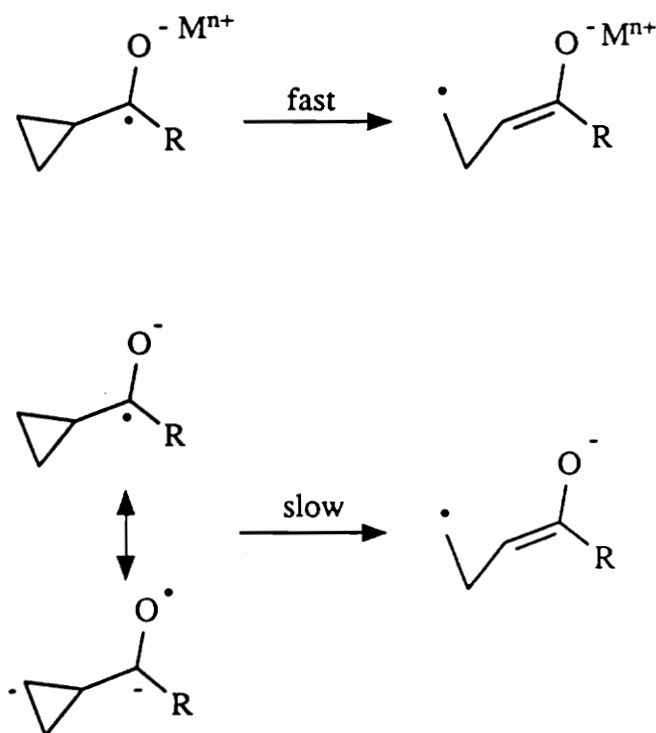


Figure 5. Postulated effect of ion pairing on the rate of ring opening of cyclopropyl ketyl anions

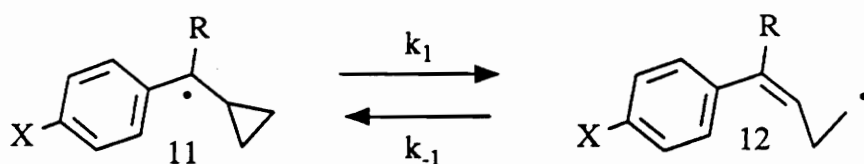
LITERATURE REVIEW

Free Radicals Related to Aryl Cyclopropyl Ketyl Anions

During the course of our studies, work on cyclopropyl benzyl radicals was reported³⁶ (Table 1). Pulse radiolysis of the benzoate esters of variously substituted cyclopropyl benzyl alcohols produced cyclopropyl benzyl radicals and allowed determination of the rate constant for the apparent ring opening (k_1) of the cyclopropane ring. The reverse rate constant (k_{-1}) was estimated to be at least an order of magnitude smaller than the forward rate constant. These claims were later questioned by Bowry et al.³⁷ who came to the conclusion that the cyclopropyl benzyl radical undergoes a reversible ring opening with the equilibrium favoring the ring closed form. They assigned the unimolecular rate constant for ring opening of cyclopropyl benzyl radical to be $k_1 = 1.3 \times 10^5$ 1/s and the unimolecular rate constant for ring closing to be $k_{-1} = 5.0 \times 10^6$ 1/s at 25 °C (Table 1, R = H, X = H). Therefore the equilibrium constant $K_1 = [12]/[11] = k_1/k_{-1} = 0.03$ at 25 °C.³⁸ Bowry³⁷ suggests that the earlier researchers³⁶ were not observing the decay of the cyclopropyl benzyl radicals but instead were observing fragmentation of radical anions of the benzoate esters generated by pulse radiolysis.

Table 1.

Disputed rate constants for the decay of benzyl cyclopropyl free radicals



X	R	k_1 (1/s)
H	H	2.7×10^5
Me	H	2.1×10^5
Cl	H	2.0×10^5
OMe	H	1.4×10^5
Ph	H	0.5×10^5
H	Me	3.6×10^5

Masnovi, J., Samsel, E., Bullock, R., *J. Chem. Soc., Chem. Commun.*, 1989, 1044.

Rate constants in dispute, see Bowry, V. Luszyk, J., Ingold, K., *J. Chem. Soc., Chem. Commun.*, 1990, 923.

Neckers et al^{39,40} have studied α -hydroxycyclopropyl benzyl free radicals (13), systems which are essentially protonated ketyl anions, in their investigation of the mechanism of photoinduced reduction of aromatic ketones (Figure 6). They conclude that the ring opening rearrangement of α -hydroxycyclopropyl benzyl free radicals is extremely rapid and nearly irreversible.

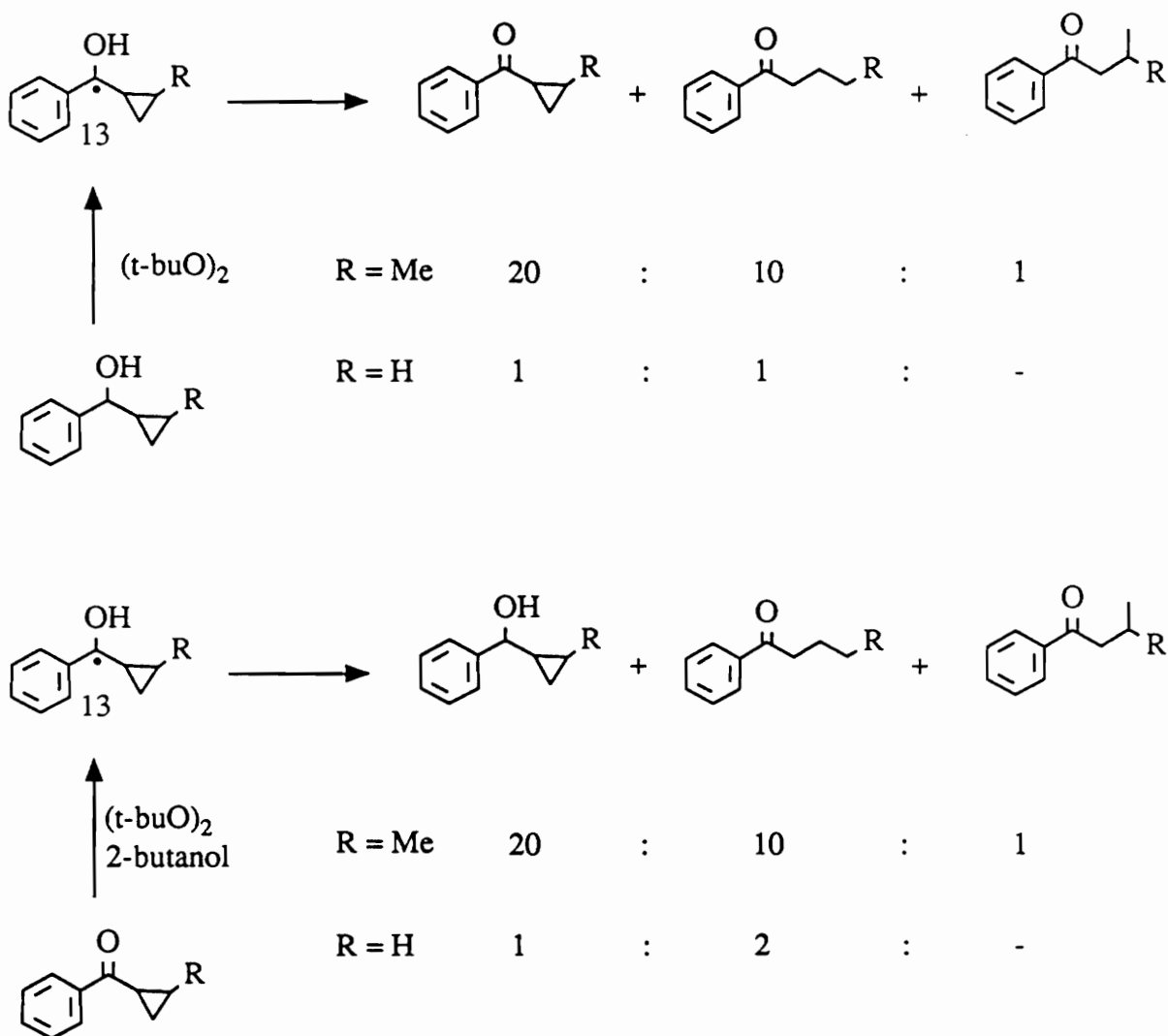
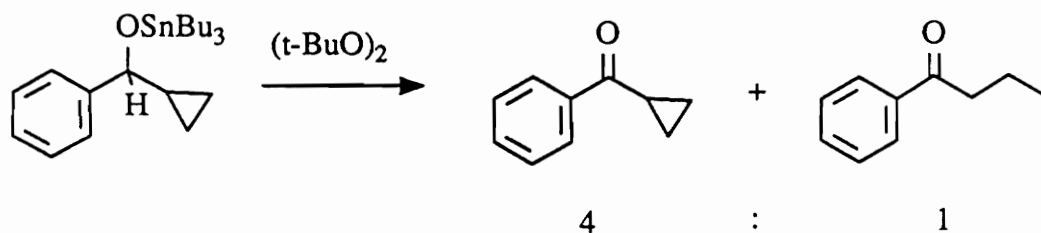


Figure 6. Product ratios derived from α -hydroxycyclopropyl benzyl free radicals generated by reduction of the corresponding ketone and oxidation of the corresponding alcohol

Another free radical closely related to aryl cyclopropyl ketyl anions has also been studied. The oxidation of cyclopropyltin alkoxides with di-*t*-butyl peroxide yields about four times more cyclopropyl ketone than non-cyclic ketone (Eqn. 3).⁴¹

Eqn. 3

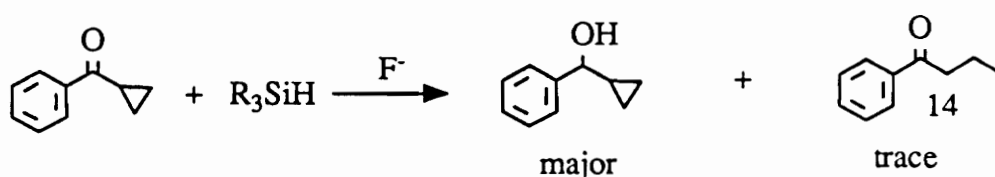


Use of Aryl Cyclopropyl Ketyl Anions to Detect Electron Transfer

Although little is known about the chemistry of aryl cyclopropyl ketyl anions, many researchers liberally employ these substrates as probes for electron transfer (Figure 3). It was surprising to find that despite the popularity of this approach, little concrete evidence for or against electron transfer has ever been gleaned from their use. Mechanistic studies on quite a diverse array of reagents have been performed utilizing phenyl cyclopropyl ketones as diagnostic probes. In the next few pages, a summary of the reagents tested for electron transfer by employing phenyl cyclopropyl ketones as rearrangement probes as well as the few sparse facts known about aryl cyclopropyl ketyl anions are presented.

The mechanism of fluoride ion catalyzed reduction of ketones with phenyldimethylsilane was investigated and determined to involve electron transfer (Eqn. 4).⁴² An SET pathway was implicated by observation of a dubious, unassigned EPR spectrum and the presence of an extremely small amount (< 1%) of butyrophenone (**14**) when phenyl cyclopropyl ketone was reacted with the reagent.

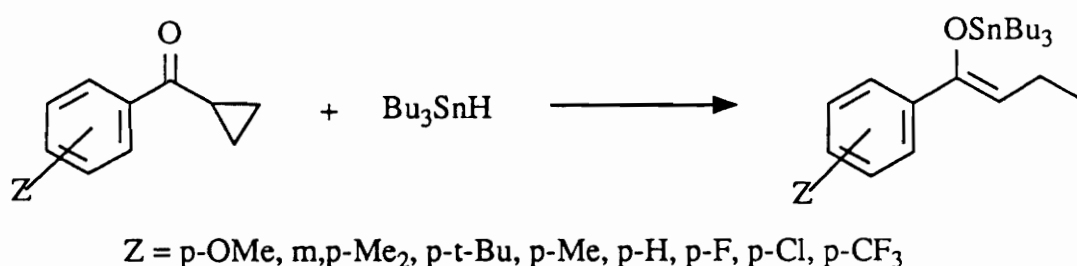
Eqn. 4



The reduction of phenyl cyclopropyl ketones by tin hydrides has received a great deal of attention. The reduction of a series of substituted phenyl cyclopropyl ketones with tri-*n*-butyl tin hydride led to ring opening in all cases (Eqn. 5).⁴³⁻⁴⁵ It was observed that electron withdrawing substituents on the phenyl ring increased the rate of reaction (log

$$k_z/k_h = 1.531\sigma - 0.034).$$

Eqn. 5



The effect of pressure on the addition of $n\text{-Bu}_3\text{SnH}$ to phenyl cyclopropyl ketone has also been studied.⁴⁶ It was found that increased pressure results in increased yields of product with the cyclopropane ring intact at the expense of the ring opened product. Tanner et al⁴⁷ have also studied addition of tin hydrides to phenyl cyclopropyl ketones. Through a convoluted set of experiments involving presence or absence of free radical initiators, presence or absence of electron transfer inhibitors, and product analyses, they conclude that several mechanisms are operating. They propose that a conventional heterolytic pathway (Figure 7, I), a conventional homolytic chain pathway (Figure 7, II), a conventional homolytic chain pathway initiated by an electron transfer step (Figure 7, III = initiation, II = propagation), and finally, an electron transfer-hydrogen abstraction pathway (Figure 7, IV) can all yield product depending upon the reaction conditions.

Reaction of phenyl cyclopropyl ketone with metal hydrides such as lithium aluminum hydride^{48a,48c}, sodium hydride^{48a,48b}, and sodium borohydride⁴⁹ yields only phenyl cyclopropyl carbinol; therefore, providing no evidence for an electron transfer mechanism.

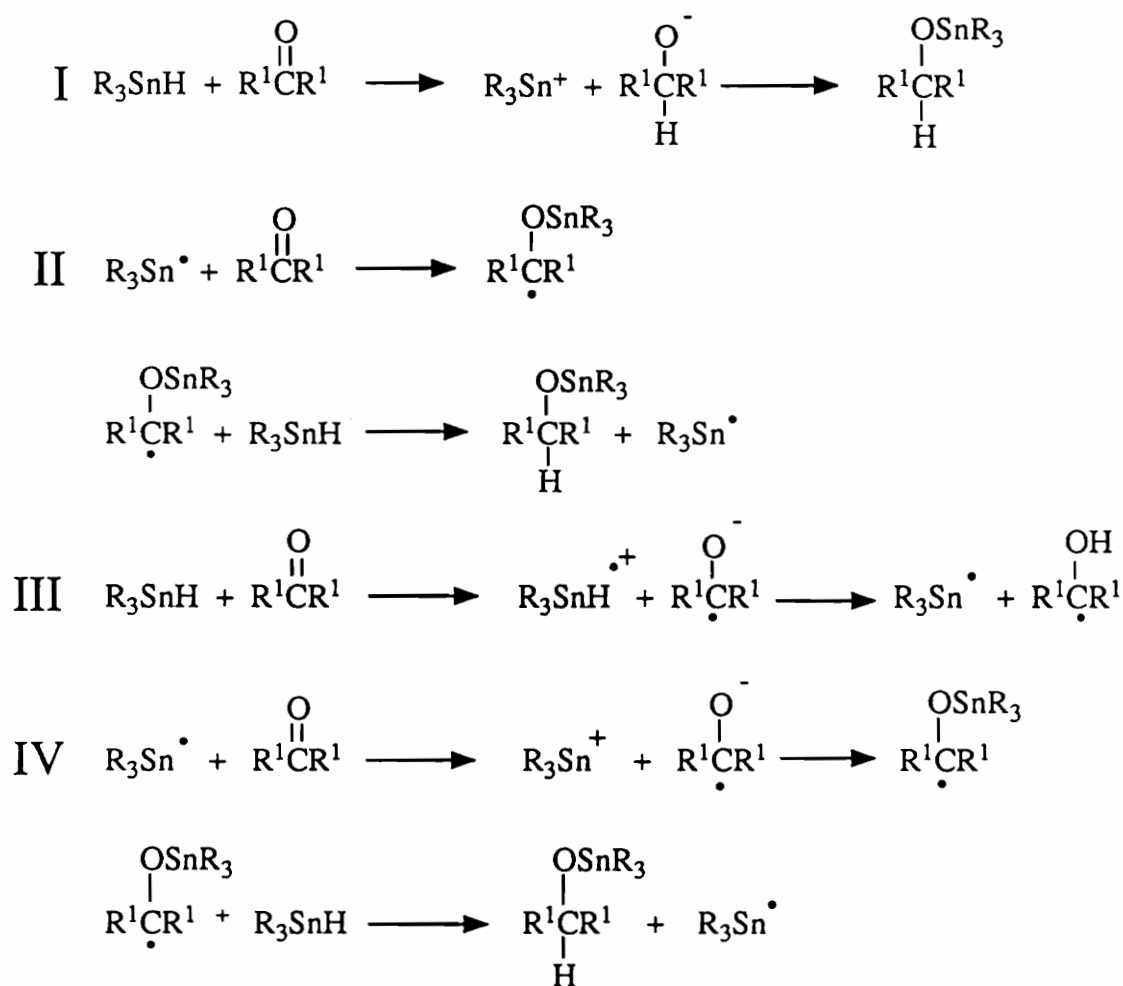


Figure 7. Possible mechanisms for tin hydride reduction of aromatic ketones

It has been reported that treatment of phenyl cyclopropyl ketone with trimethylsilyl lithium leads to products with the cyclopropane ring opened (Figure 8).⁵⁰ The author presents two possible mechanisms for product formation, but does not attempt to distinguish between the two. A Michael-type reaction (Figure 8, path A) is proposed where the trimethylsilyl anion directly attacks the cyclopropane ring. The other mechanistic alternative presented is an electron transfer pathway (Figure 8, path B) where the intermediate ketyl anion rearranges and then couples to yield ring opened products.

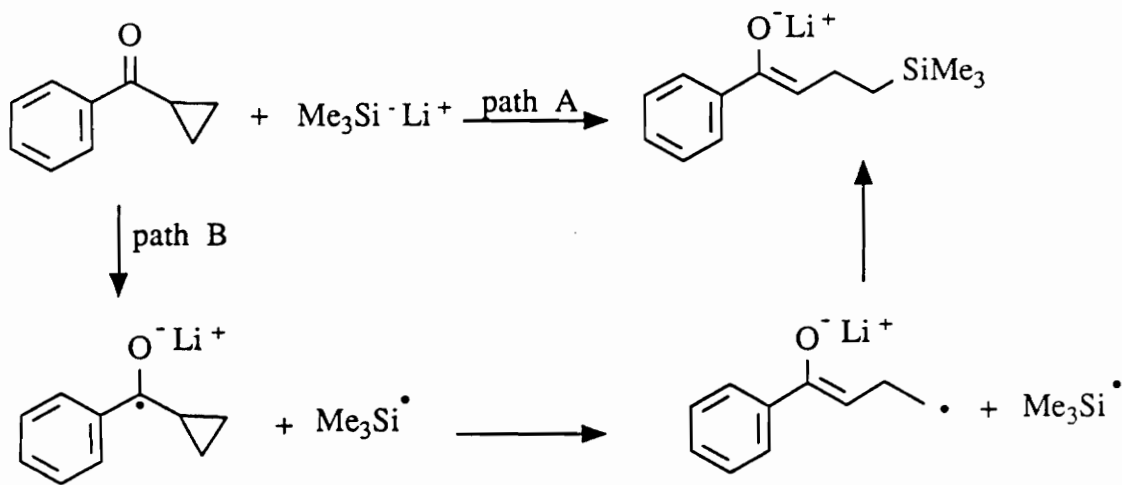
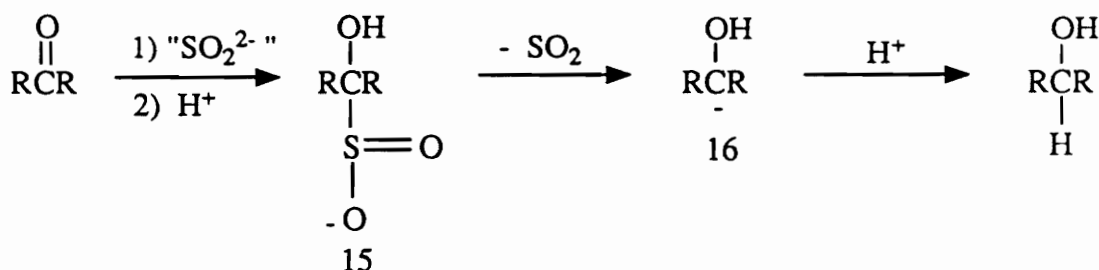


Figure 8. Possible mechanisms for addition of trimethylsilyllithium to phenyl cyclopropyl ketone

The mechanism of sodium dithionate ($\text{Na}_2\text{S}_2\text{O}_4$) reduction of carbonyl containing compounds⁵¹ has been determined not to involve electron transfer based on the lack of ring opened products when phenyl cyclopropyl ketone is reduced in aqueous *N,N*-dimethylformamide (DMF).⁵² Instead, the authors believe that reduction involves nucleophilic addition of SO_2 dianion or its equivalent to the carbonyl group to form an intermediate α -hydroxy sulfinate ion (**15**) which then loses SO_2 to give the carbanionic species (**16**) which is rapidly protonated to yield product (Eqn. 6).

Eqn. 6



The mechanism of reaction of 2-lithio-1,3-dithianes (**17**) with ketones has also

been studied.²⁵ Treatment of phenyl cyclopropyl ketone with this reagent leads only to products with the cyclopropane ring intact (Figure 9). Based on some anomalous results with other rearrangement probes, the authors conclude that a small component of electron transfer may sometimes be involved.

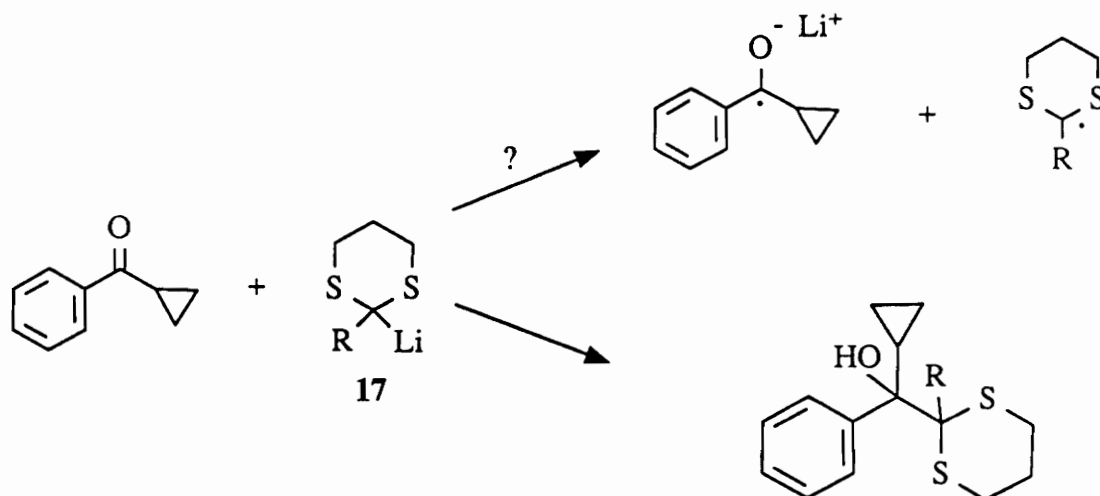
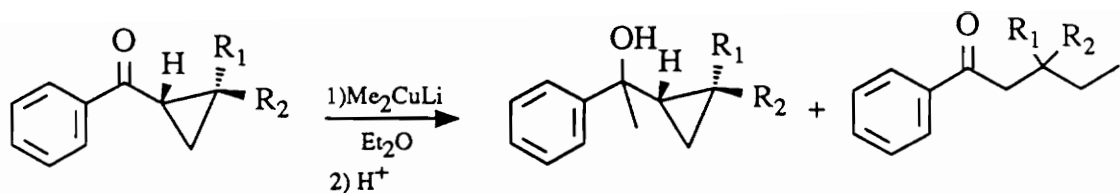


Figure 9. Reaction of 2-lithio-1,3-dithianes with phenyl cyclopropyl ketone

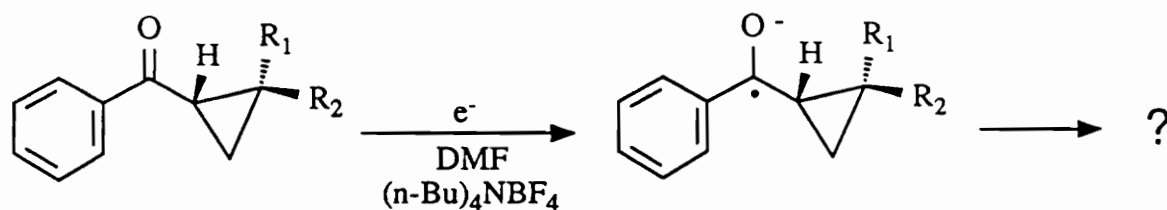
Phenyl cyclopropyl ketone and its derivatives have seen a large amount of utility as electron transfer probes in organocuprate chemistry. In a study of the reaction of lithium dimethyl cuprate with ketones, House et al⁵³ briefly examined phenyl cyclopropyl ketyl anions as qualitative probes for electron transfer. They found that addition of lithium dimethyl cuprate to phenyl cyclopropyl ketones (Figure 10) indeed led to small amounts of ring opened products. The regiochemistry of the ring opened products indicated that they were not formed by an electron transfer process but instead by a Michael-type addition of "CH₃⁻" to the least hindered carbon of the cyclopropane ring.



$R_1, R_2 = H$	57 %	0.5 %
$R_1, R_2 = CH_3$	75 %	0.6 %
$R_1 = H, R_2 = Ph$	81 %	0.9 %

Figure 10. Reaction of lithium dimethyl cuprate with phenyl cyclopropyl ketones

Further, House^{53,54} performed a qualitative study of the decay of electrochemically generated phenyl cyclopropyl ketyl anions in DMF. By assuming unimolecular decay⁵⁴, the half lives of several cyclopropyl ketyl anions were estimated. The lifetimes of the radical anions were shown to be quite long and to decrease with substitution of radical stabilizing groups on the cyclopropane ring (Figure 11).

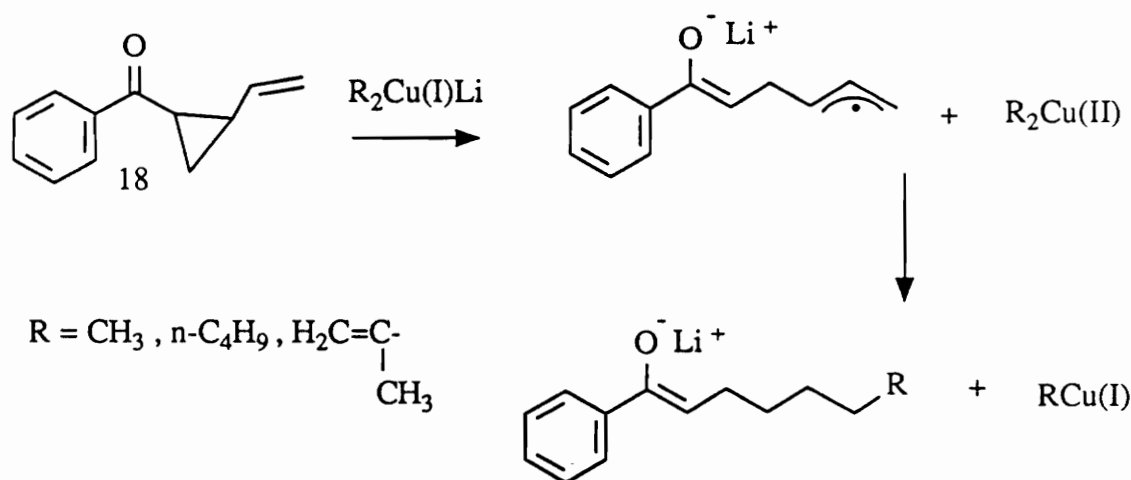


	$t_{1/2}$ (sec)
$R_1, R_2 = H$	~5
$R_1, R_2 = CH_3$	~4
$R_1 = H, R_2 = Ph$	$< 10^{-2}$

Figure 11. Estimated half lives of phenyl cyclopropyl ketyl anions

The addition of lithium dialkyl cuprates to 1-benzoyl-2-vinylcyclopropane (**18**) has been suggested to proceed through an electron transfer pathway (Eqn. 7).⁵⁵ Also, the addition of trialkyl boranes (R_3B) to this substrate leads to ring-opened product, but since the reaction is catalyzed by oxygen (O_2) it is believed that a free radical process and not an SET process is responsible for ring opening.⁵⁵

Eqn. 7



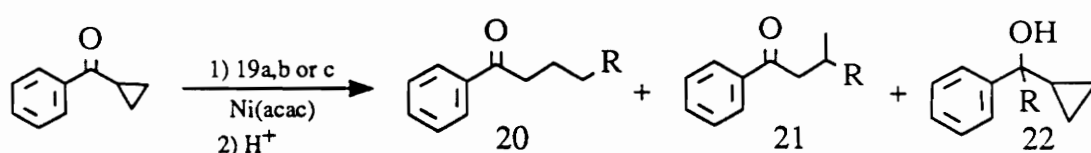
The current train of thought concerning the addition of dialkyl cuprates to carbonyl compounds is that addition can occur through at least three possible mechanisms depending on the reaction conditions and the substrate.⁵⁶ Based on the products derived from the addition of lithium dimethyl cuprate to various cyclopropyl ketones, including phenyl cyclopropyl ketone, the following three mechanisms are postulated to operate:

- 1) direct nucleophilic substitution (S_N2 like)
- 2) Michael-type substitution (S_N2' like)
- 3) electron transfer.

The dominant mechanism depends upon substrate (substitution on the cyclopropane, reduction potential of the compound, etc.) and the reaction conditions (solvent, temperature, etc.).

Addition of other common organometallics such as Grignard⁵⁷ and

organolithium⁵⁸ reagents to phenyl cyclopropyl ketone have been shown to yield only 1,2 addition products to the carbonyl with the cyclopropane ring remaining intact. The reactions of several other organometallic reagents with phenyl cyclopropyl ketones are believed to involve electron transfer because cyclopropyl ring opened products are found. The nickel catalyzed additions of trimethylaluminum (**19a**)^{59,60}, dialkylaluminum alkenyls (**19b**)⁶⁰, and alkenyl zirconiums (**19c**)⁶⁰ are members of this class (Figure 12).



19a. (CH ₃) ₃ Al	R = CH ₃	main	-	trace
19b. (i-Bu) ₂ AlR	R =	-	-	only product
19c. Cp ₂ Zr(Cl)R	R =	-	61 %	31 %

Figure 12. Nickel catalyzed additions of various organometallics to phenyl cyclopropyl ketones

The results of these experiments can be readily explained by invoking an electron transfer mechanism (Figure 13, I). One electron reduction of phenyl cyclopropyl ketone by low valent nickel leads to the intermediate ketyl anion (**23**). Trapping of the ketyl anion (path c) would eventually lead to ring closed species (i.e. **22**). If however, a nickel(I) species (path b) or a nickel(II) species (path a) oxidatively adds to the cyclopropane, ring opened products would be observed. Substitution on the terminus of the carbon chain to yield product such as (**20**) is explained directly by intermediates such as (**24**) and (**25**). However, to explain products like (**21**) a formal hydride shift from the β

carbon to the α carbon (Figure 13, II) has been postulated.

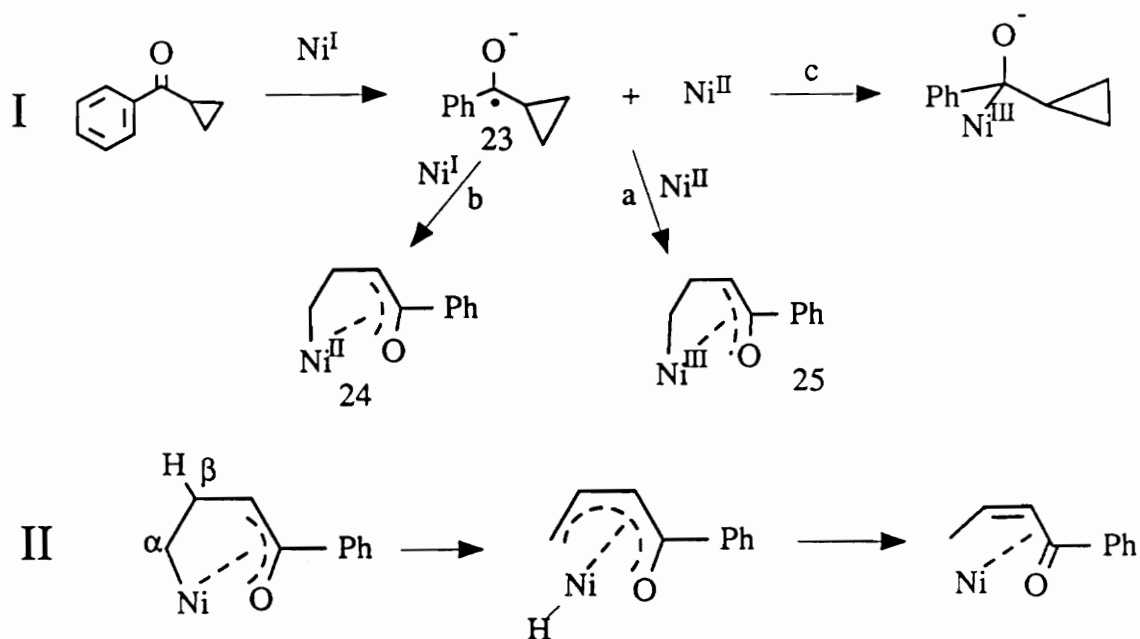
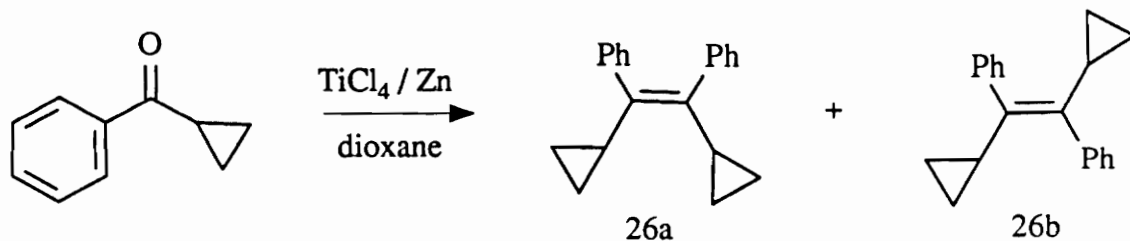


Figure 13. Proposed mechanism for nickel catalyzed addition of organometallics to phenyl cyclopropyl ketones

Nishida et al⁶¹ were surprised to find that they could synthesize heavily substituted cyclopropylethylenes through low valent titanium coupling of cyclopropyl ketones. Phenyl cyclopropyl ketone was coupled to a mixture of *cis*- and *trans*-1,2-dicyclopropylstilbenes (26) in about 25% overall yield with titanium tetrachloride and zinc (Eqn. 8).

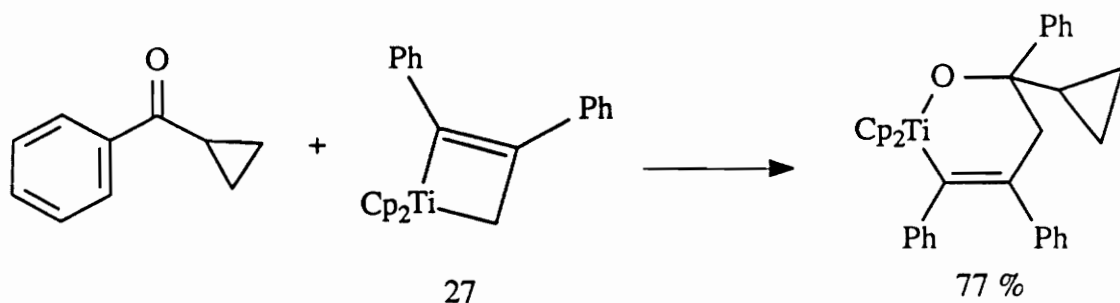
Eqn. 8



Also, it has been shown that bis(η^5 -cyclopentadienyl)titanacyclobutenes (27) can be

inserted into the carbonyl of phenyl cyclopropyl ketone without any cyclopropane ring opening (Eqn. 9).⁶² Despite the fact that no cyclopropyl ring open product is found, the authors are careful not to rule out an electron transfer mechanism.

Eqn. 9



It is generally accepted that dissolving metal reductions proceed through radical anions. Usually, dissolving metal reductions of cyclopropyl ketones lead to ring opening.⁶³ The cyclopropyl bond which is cleaved is governed by stereoelectronic considerations. The cyclopropane C-C bond which has the best overlap with the p-orbitals of the carbonyl group is broken (see page 73 for a discussion of the stereoelectronic requirements for ring opening). It has been proposed that for some cyclopropyl ketones, ring opened product may not arise from the ketyl anion but instead from the dianion.⁶⁴ Curiously, dissolving metal reduction of unsubstituted or alkyl substituted phenyl cyclopropyl ketones yields only benzyl cyclopropanes.^{65a,66} Reduction of trans-1-benzoyl-2-phenylcyclopropane or trans-1,2-dibenzoylcyclopropane, however, leads to both reduction of the carbonyl(s) and the cyclopropane ring (Figure 14).^{65a} Reduction of aryl cyclopropyl ketones with zinc chloride and/or zinc in refluxing ethanol leads to sluggish ring opening if the cyclopropane ring is substituted with an aromatic group. Starting material was recovered if the cyclopropane was substituted with only alkyl groups or hydrogen.^{65b}

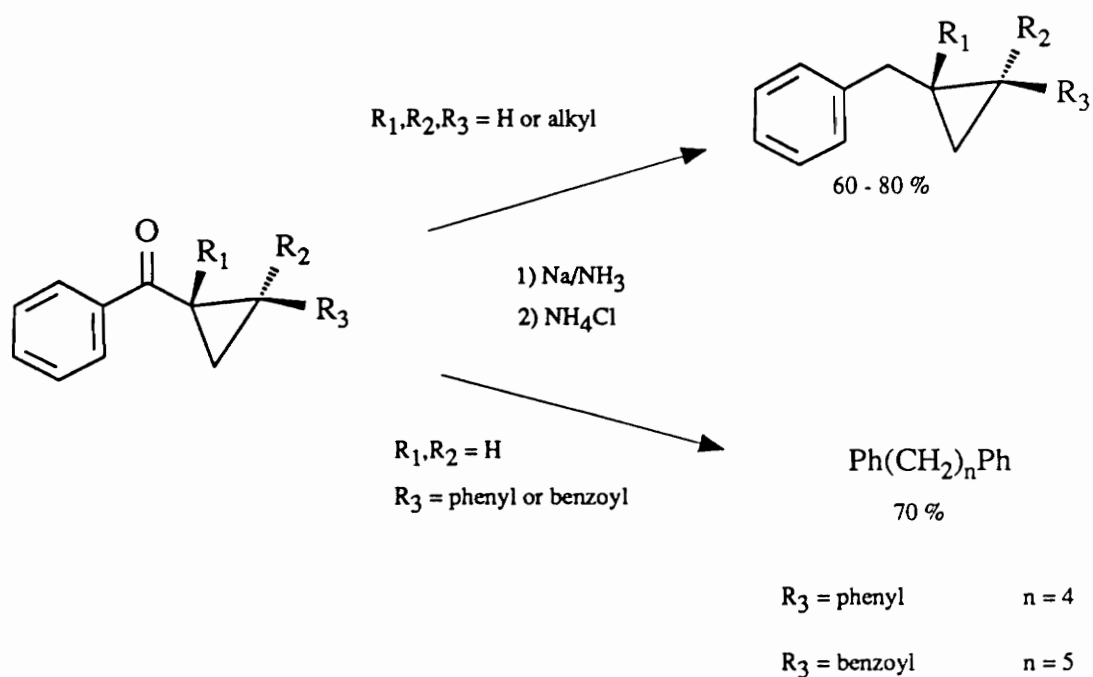


Figure 14. Dissolving metal reduction of phenyl cyclopropyl ketones

Cases where the radical anions of phenyl cyclopropyl ketones are unambiguously generated cast some doubt on the use of these substrates as probes for electron transfer processes. Electrolytic reduction⁶⁷ of phenyl cyclopropyl ketone in aqueous ethanol at a mercury cathode yields no ring-opened product.⁶⁸ Instead, monomeric alcohol and pinacol dimer are obtained (Figure 15). However, substitution of a phenyl group on the cyclopropane ring leads to ring opening under the same conditions.

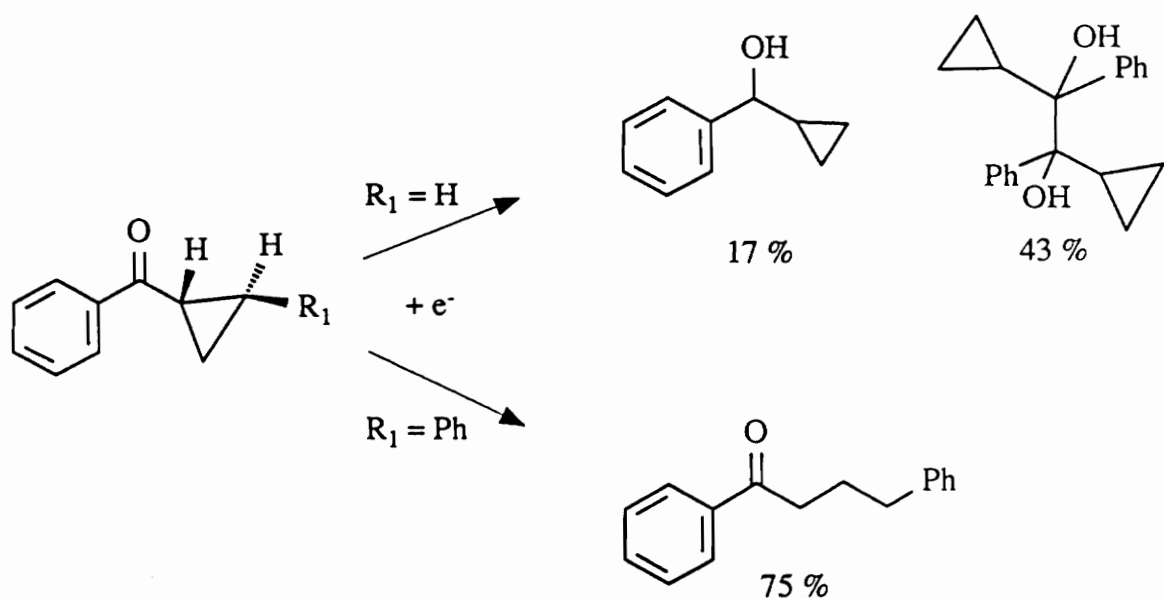
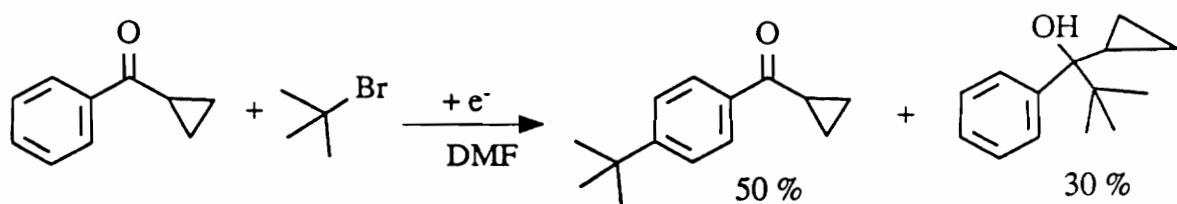


Figure 15. Electrochemical reduction of phenyl cyclopropyl ketones in aqueous ethanol

Also, electrochemical *t*-butylation of phenyl cyclopropyl ketone with *t*-butyl bromide yields only products with the cyclopropane ring intact (Eqn. 10).⁶⁹

Eqn. 10



House's⁵³ qualitative lifetime measurements of electrochemically generated phenyl cyclopropyl ketyl anions (Figure 11) show that they are apparently quite long lived. Also, the EPR spectrum of phenyl cyclopropyl ketyl anion (generated with K in DME) has been reported with no apparent difficulty.⁷⁰ This would not be expected if the ketyl anion were undergoing a rapid rearrangement. So, there is quite a bit of ambiguity as to whether aryl cyclopropyl ketyl anions rearrange or not.

SUMMARY

In order to be a good electron transfer probe, phenyl cyclopropyl ketyl anions need to rearrange rapidly and irreversibly. Literature precedence shows that these requirements are not necessarily met. Despite the lack of knowledge about phenyl cyclopropyl ketyl anion rearrangements, phenyl cyclopropyl ketones have been and are still being used as probes to detect electron transfer reaction mechanisms. It was our goal to find out if aryl cyclopropyl ketyl anions do rearrange and if they do rearrange, how fast this rearrangement occurs.

CHAPTER 2. ALKYL- AND UNSUBSTITUTED ARYL CYCLOPROPYL KETONES

INTRODUCTION

Using the earlier work of House⁵³ as a starting point, we set out to study what effect (if any) ion pairing had on the rate of ring opening of phenyl cyclopropyl ketyl anions. We were surprised to find that contrary to earlier reports which assumed unimolecular decay kinetics⁵³, phenyl cyclopropyl ketyl anion (**28a^{•-}**) underwent an apparent bimolecular decay. This initial finding led us to the realization that most of the current thinking regarding the rearrangements of these radical anions and their utilization as SET probes was in error.

To study the chemistry of phenyl cyclopropyl ketyl anions, we employed electrochemical techniques. Electrochemistry, and in particular voltammetry, is a powerful tool for unambiguously generating and subsequently probing the fate of radical ions. A thorough description of the voltammetric techniques employed in this study (cyclic voltammetry (CV), derivative cyclic voltammetry (DCV), and linear sweep voltammetry (LSV)) and their application to the elucidation of the mechanism of decay of electrode generated intermediates is contained in Appendix A.

In summary, voltammetric methods allow assignment of the rate law for decay of electrode generated species (Figure 16). Once the observed rate law and hence overall stoichiometry for decay is known, the rate constant for decay of the electrode generated intermediate can be extracted from experimental data by digital simulation, curve fitting, or empirical relationships already developed in the literature.

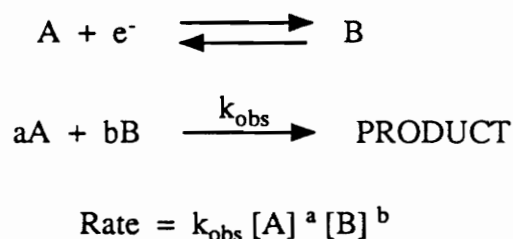
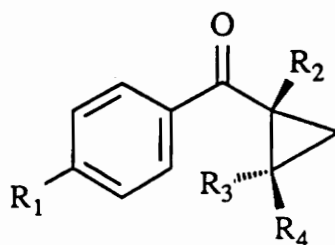


Figure 16. General scheme for decay of electrode generated intermediates

Phenyl cyclopropyl ketones with alkyl or hydrogen as the only substituents on the cyclopropane ring are the focus of this chapter (Figure 17). These substrates, and especially phenyl cyclopropyl ketone (**28a**) have seen extensive use as rearrangement probes for detection of electron transfer reaction mechanisms.



- 28a. $R_1, R_2, R_3, R_4 = H$
- 28b. $R_1, R_2, R_3 = H$ $R_4 = CH_3$
- 28c. $R_1, R_2 = H$ $R_3, R_4 = CH_3$
- 28d. $R_2, R_3, R_4 = H$ $R_1 = CH_3$
- 28e. $R_1, R_3, R_4 = H$ $R_2 = CH_3$

Figure 17. General structure of phenyl cyclopropyl ketones

KINETIC ANALYSIS OF KETYL ANION DECAY

The reduction potentials of variously substituted phenyl cyclopropyl ketones and the observed, integral order of the rate law for decay of their radical anions are shown in Table 2. All voltammetric measurements were performed at 23°C in anhydrous N,N-Dimethylformamide (DMF) with 0.5 M tetra-*n*-butylammonium tetrafluoroborate (*n*-Bu₄NBF₄) as the supporting electrolyte unless noted otherwise. The working electrode was a gold disk, and the reference electrode a silver wire in contact with 0.1 M silver nitrate in acetonitrile.

Utilizing derivative cyclic voltammetry (DCV) as delineated in Appendix A, we examined the mechanism of decay of the ketyl anions (**28a**^{•-}) through (**28d**^{•-}) and found them all to decay in a bimolecular fashion. At several concentrations of substrate, C_A, the sweep rate, *v*, was adjusted to keep the ratio of the anodic to cathodic DCV peaks (R_{DCV}) constant. A plot of log (*v*_c) vs. log (C_A) yields a straight line whose slope is related to the combined reaction order (R_{A/B}) in neutral ketone, A, and ketyl anion, B (Eqn. 11).⁷¹⁻⁷³

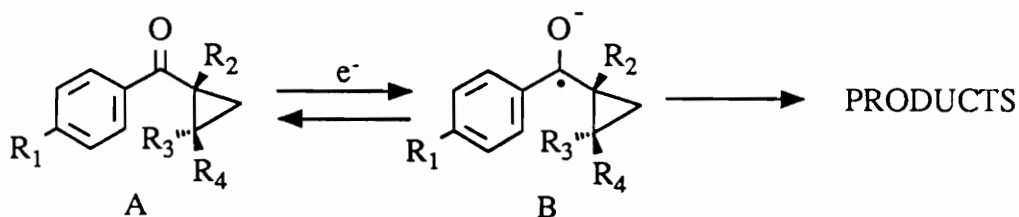
Eqn. 11

$$R_{A/B} = [\delta \log (v_c) / \delta \log (C_A)] + 1$$

Figures 18 through 21 show typical reaction order plots for the various substrates. The results of these experiments are summarized in Table 3.

Table 2.

Reduction potentials of phenyl cyclopropyl ketones and the observed integral orders for the rate laws of decay of their ketyl anions



cmpd	R ₁	R ₂	R ₃	R ₄	E ^o (V) ^{a,b}	Integral Reaction Order ^c
28a	H	H	H	H	-2.420	2
28b	H	H	H	CH ₃	-2.435	2
28c	H	H	CH ₃	CH ₃	-2.435	2
28d	CH ₃	H	H	H	-2.496	2
28e	H	CH ₃	H	H	-2.410	d

^a 0.5 M n-Bu₄NBF₄ / DMF, planar Au working electrode, Ag/AgNO₃ (0.1 M in CH₃CN) reference electrode

^b E^o = (E_{pa} + E_{pc}) / 2 when R_{DCV} = 1.00, see appendix A.

^c reaction order rounded off to integral value

^d decay too slow for DCV analysis, see discussion later in chapter

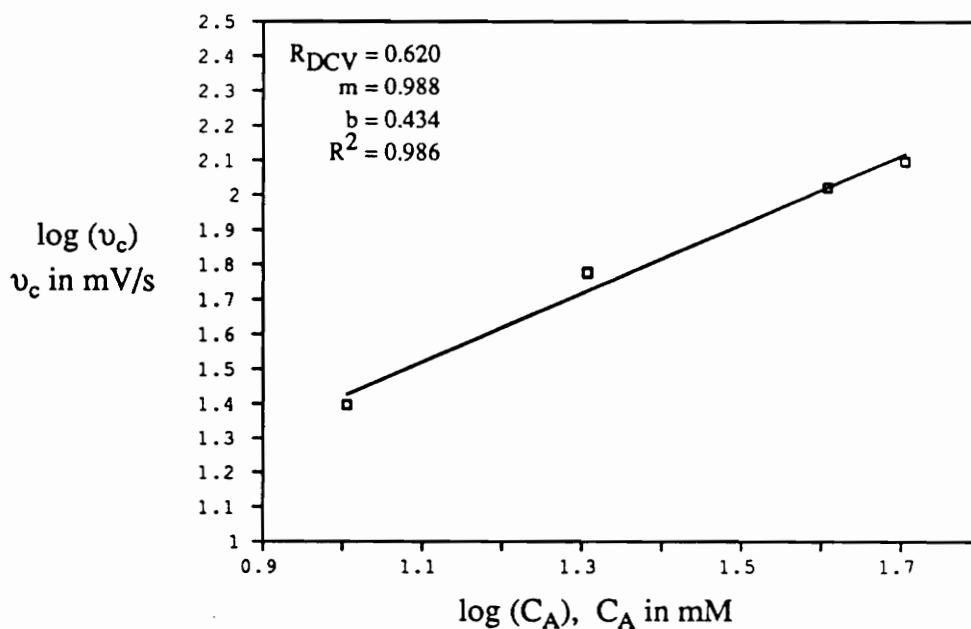


Figure 18.

DCV reaction order plot for decay of phenyl cyclopropyl ketyl anion (28a⁻)

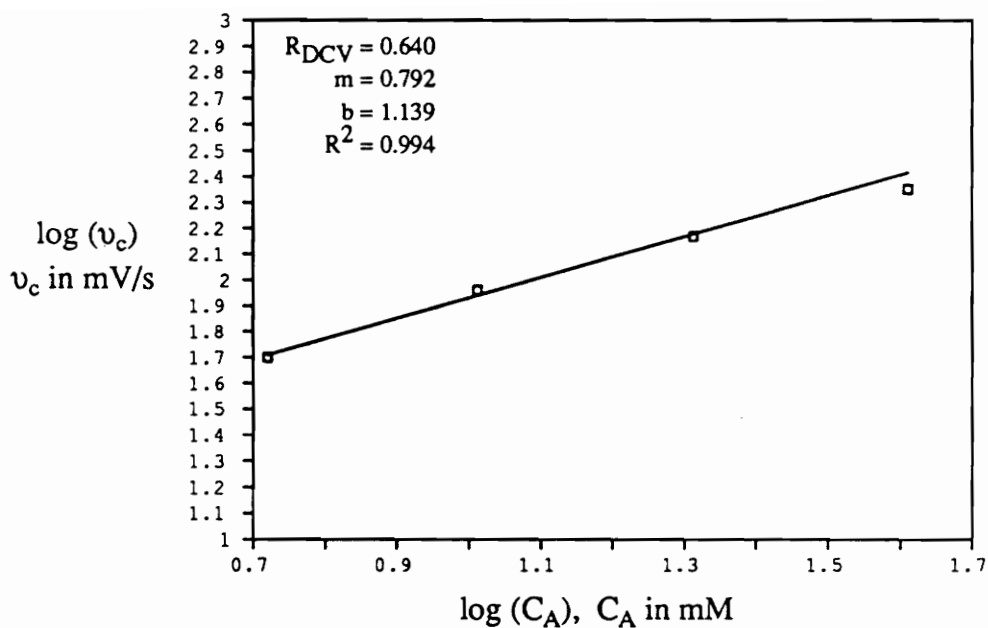


Figure 19. DCV reaction order plot for decay of trans-1-benzoyl-2-methylcyclopropyl ketyl anion (28b⁻)

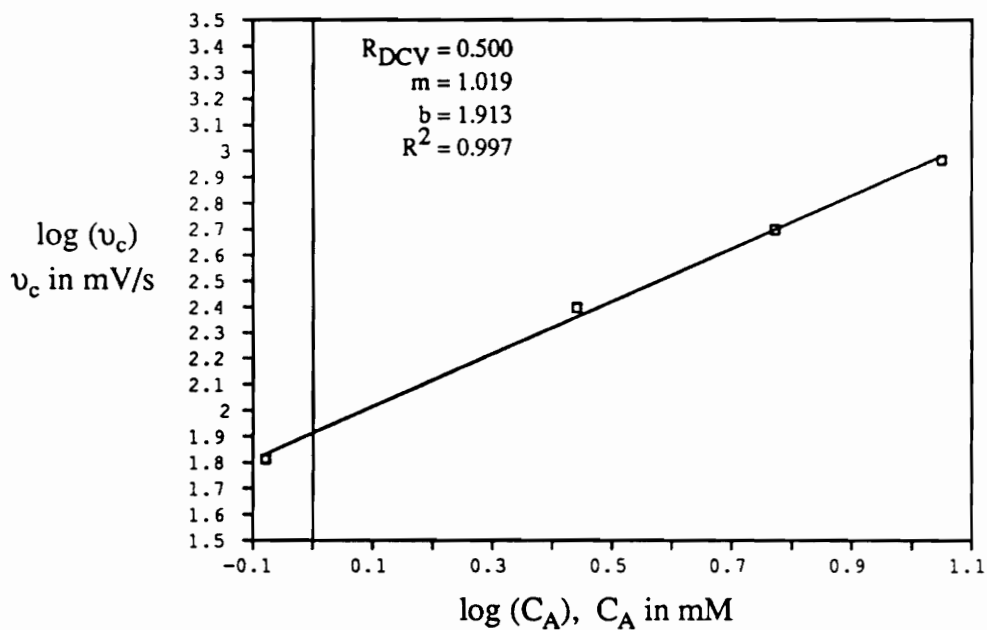


Figure 20. DCV reaction order plot for decay of 1-benzoyl-2,2-dimethylcyclopropyl ketyl anion (28c⁻)

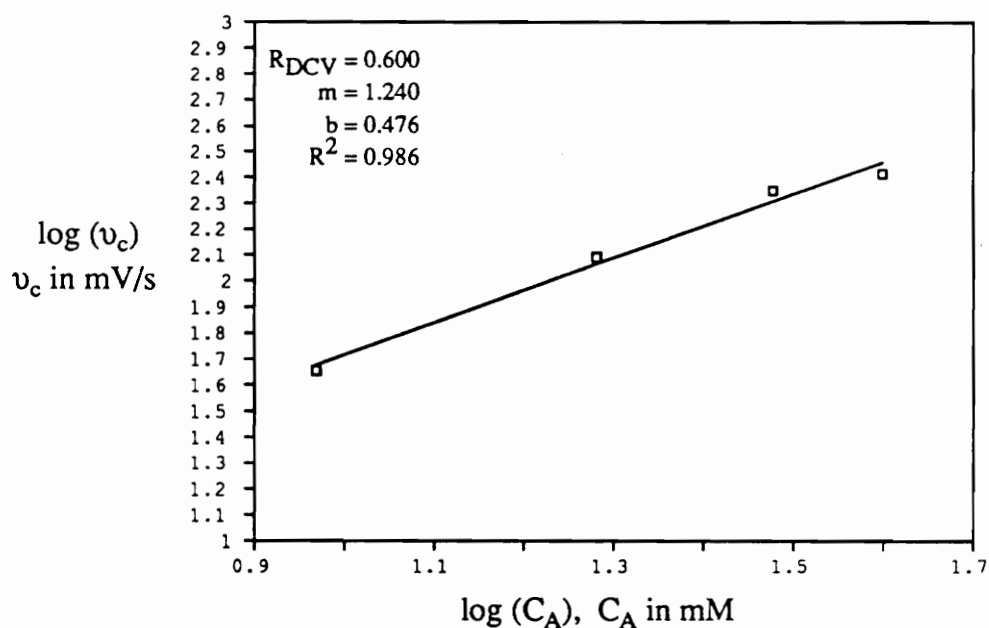
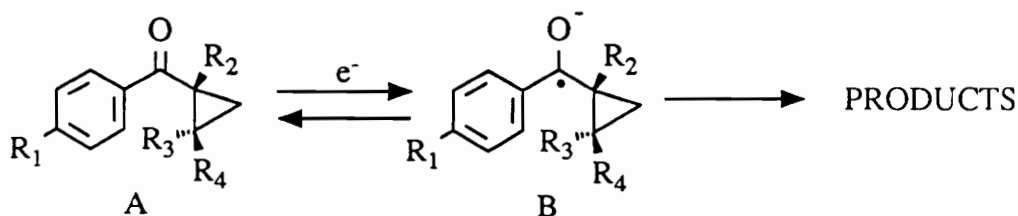


Figure 21. DCV reaction order plot for decay of p-tolyl cyclopropyl ketyl anion (28d^{•-})

Table 3. Experimentally observed reaction orders for decay of phenyl cyclopropyl ketyl anions



cmpd	R ₁	R ₂	R ₃	R ₄	R _{A/B} ^a
28a	H	H	H	H	2.0 ± 0.1
28b	H	H	H	CH ₃	1.8 ± 0.1
28c	H	H	CH ₃	CH ₃	2.0 ± 0.1
28d	CH ₃	H	H	H	2.2 ± 0.1
28e	H	CH ₃	H	H	b

^a 0.5 M n-Bu₄NBF₄ / DMF, planar Au working electrode, Ag/AgNO₃ (0.1 M in CH₃CN) reference electrode

^b decay too slow for DCV analysis, see discussion later in chapter

The DCV reaction order approach provides an overall order for the rate law but does not separate the individual reaction orders in neutral ketone, A, and ketyl anion, B. Deconvolution of the individual reaction orders in A and B was accomplished via linear sweep voltammetry (LSV). For voltammetric waves where no reverse current is observed, the shift in the forward peak potential, E_p , as a function of sweep rate, v , can be related to the reaction order, R_B , of the electrode generated intermediate, B (Eqn. 12).^{72,73}

Eqn. 12

$$\frac{\delta E_p}{\delta \log (v)} = \frac{-1}{(R_B + 1)} \times \frac{[\ln (10)] RT}{nF}$$

Similarly, the shift in peak potential, E_p , as a function of concentration of substrate, C_A , can be related to the reaction order, R_A , in the neutral substrate, A (Eqn. 13).⁷²⁻⁷³

Eqn. 13

$$\frac{\delta E_p}{\delta \log (C_A)} = \frac{R_A + R_B - 1}{(R_B + 1)} \times \frac{[\ln (10)] RT}{nF}$$

A sample of the LSV results for 1-benzoyl-2,2-dimethylcyclopropane (**28c**) is shown in Figures 22 and 23. A summary of the results plus the theoretical expectations for the two possible bimolecular rate laws as well as a unimolecular rate law for comparison are shown in Table 4. The results are consistent with a rate law which is second order in ketyl anion (B), $\text{Rate} = k_{\text{obs}}[\text{B}]^2$, not one which is first order in ketyl anion (B) and first order in neutral ketone (A), $\text{Rate} = k_{\text{obs}}[\text{A}][\text{B}]$. Decay kinetics for the other phenyl cyclopropyl ketyl anions (**28a^{•-}**), (**28b^{•-}**), (**28d^{•-}**), and (**28e^{•-}**) were too slow to analyze by LSV. We assumed and later demonstrated through product analyses that because of structural similarities, ketyl anions (**28a^{•-}**) and (**28b^{•-}**) decayed in an identical manner. Ketyl anions (**28d^{•-}**) and (**28e^{•-}**) decayed in a slightly different fashion as discussed later in this chapter.

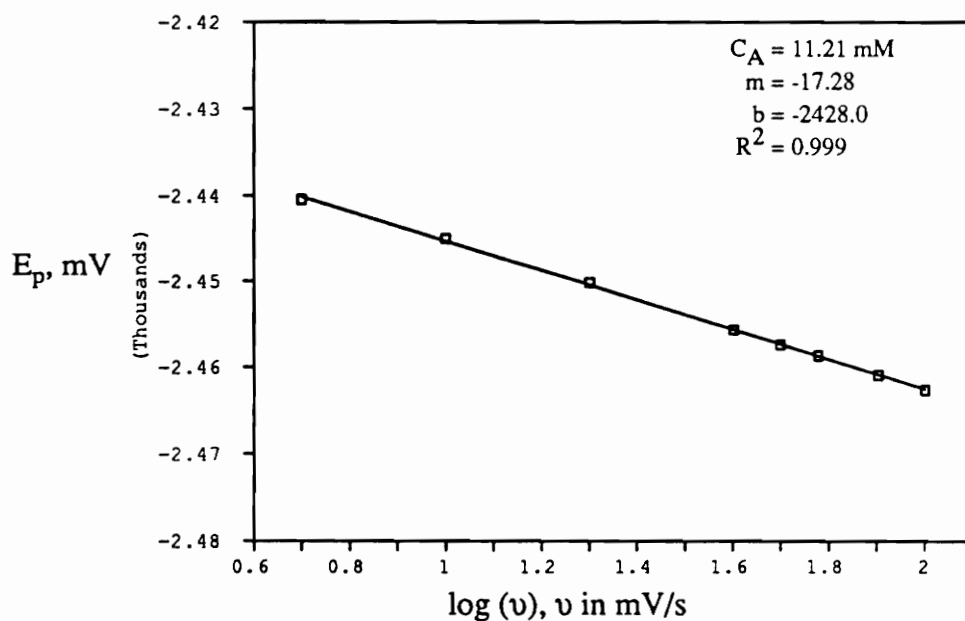


Figure 22. Linear sweep voltammetry reaction order plot for decay of 1-benzoyl-2,2-dimethylcyclopropyl ketyl anion ($28c^-$)

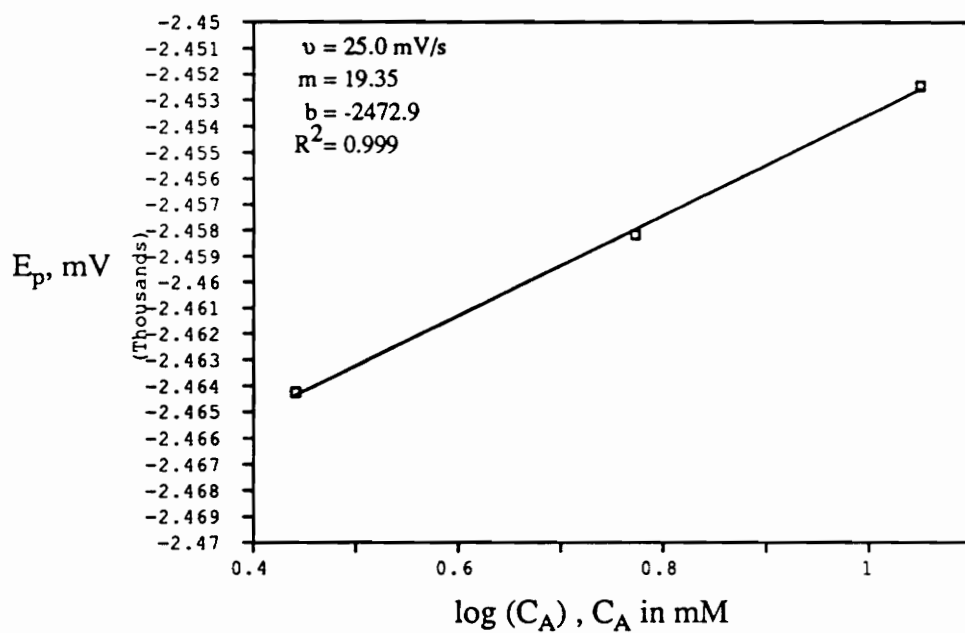
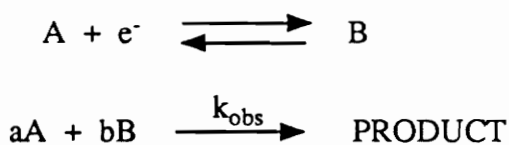


Figure 23. Linear sweep voltammetry reaction order plot for decay of 1-benzoyl-2,2-dimethylcyclopropyl ketyl anion ($28c^-$)

Table 4.

**Linear sweep voltammetry analysis of the decay of
1-benzoyl-2,2-dimethylcyclopropyl ketyl anion (28c⁻)**



Rate law	$\delta E_p / \delta \log (v)$ mV/decade	$\delta E_p / \delta \log (C_A)$ mV/decade
^b $k_{\text{obs}}[B]$	-29.5	0.0
^b $k_{\text{obs}}[B]^2$	-19.7	19.7
^b $k_{\text{obs}}[A][B]$	-29.5	29.5
^{a,c} $k_{\text{obs}}[B]^2$	-17.3 ± 0.2	19.4 ± 0.6

^a 0.5 M n-Bu₄NBF₄ / DMF, planar Au working electrode, Ag/AgNO₃ (0.1 M in CH₃CN) reference

^b theoretical response, see Ahlberg, E., Parker, V., *Acta. Chem. Scand.*, 1981, B35, 117.

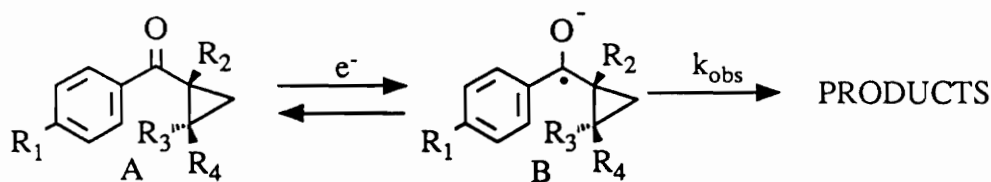
^c experimental response for 1-benzoyl-2,2-dimethylcyclopropane (28c)

With the rate law for decay of the ketyl anions in hand, it was possible to calculate the experimentally observed rate constants for their bimolecular disappearance. Parker has shown that at a given concentration of substrate (C_A), the sweep rate at which R_{DCV} is equal to 0.5 ($v_{0.5}$) can be related to the overall rate constant for decay of the radical ion.^{72,73} For dimerization of an electrode generated intermediate (EC_{DIM}) the expression is as shown in equation 14. The observed rate constants for decay of the ketyl anions calculated from this equation and verified by digital simulation^{74,75} are shown in Table 5.

Eqn. 14

$$k(\text{EC}_{\text{DIM}}) = 0.1173 (F/RT) v_{0.5} / C_A$$

Table 5. Observed rate constants for decay of phenyl cyclopropyl ketyl anions



cmpd	R ₁	R ₂	R ₃	R ₄	k _{obs} (M ⁻¹ s ⁻¹) ^{a,b}
28a	H	H	H	H	3.9 ± 0.4
28b	H	H	H	CH ₃	13.1 ± 1.5
28c	H	H	CH ₃	CH ₃	211 ± 30
28d	CH ₃	H	H	H	14.4 ± 3.4

^a 0.5 M n-Bu₄NBF₄ / DMF, planar Au working electrode, Ag/AgNO₃ (0.1 M in CH₃CN) reference

^b k_{obs} = k(EC_{DIM}) = 0.1173 (F/RT)(ν_{0.5}/C_A), see Parker, V. in "Topics in Organic Electrochemistry", Fry, A., Britton, W., eds., Plenum Press, New York, 1986, pp. 35-79.

To ensure that the best values for ν_{0.5} were used in calculating k_{obs}, plots of ln (R_{DCV}) vs. ln (1/ν) for several concentrations of substrate were employed. It has been shown that for decay of electrode generated intermediates equation 16 holds in the region R_{DCV} = 0.25 to 0.70.^{76a} The slope, m, and intercept, C, can be related to the mechanism of decay of the electrode generated intermediate. Fitting the voltammetric data for each concentration of substrate to the best line allows for the best values of ν_{0.5} to be extracted. Representative plots are shown in Figures 24 through 27.

Eqn. 16

$$\ln (R_{DCV}) = m [\ln (1 / \nu)] + C$$

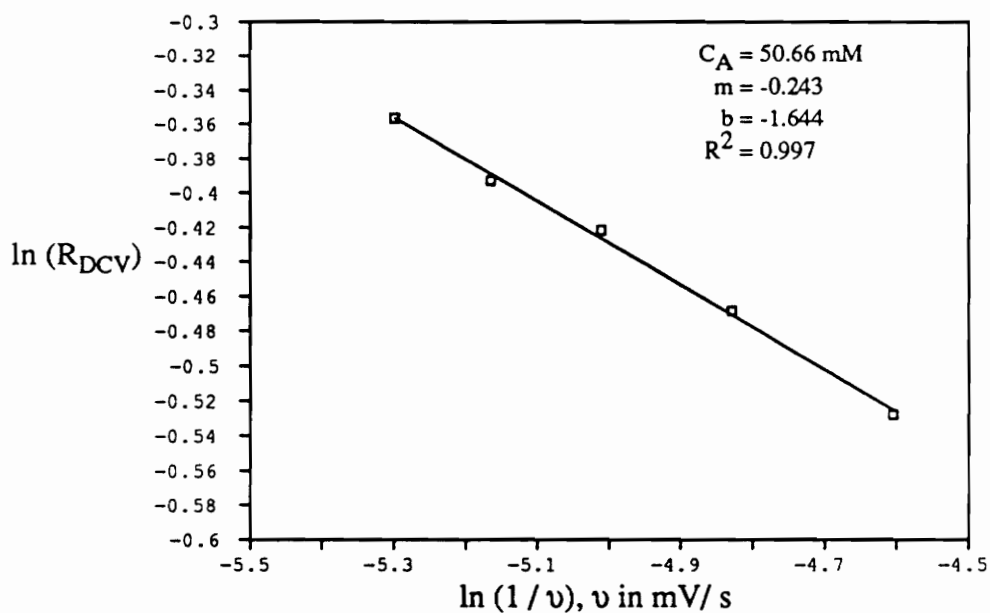


Figure 24. Plot for extraction of $v_{0.5}$ for phenyl cyclopropyl ketyl anion ($28a^-$)

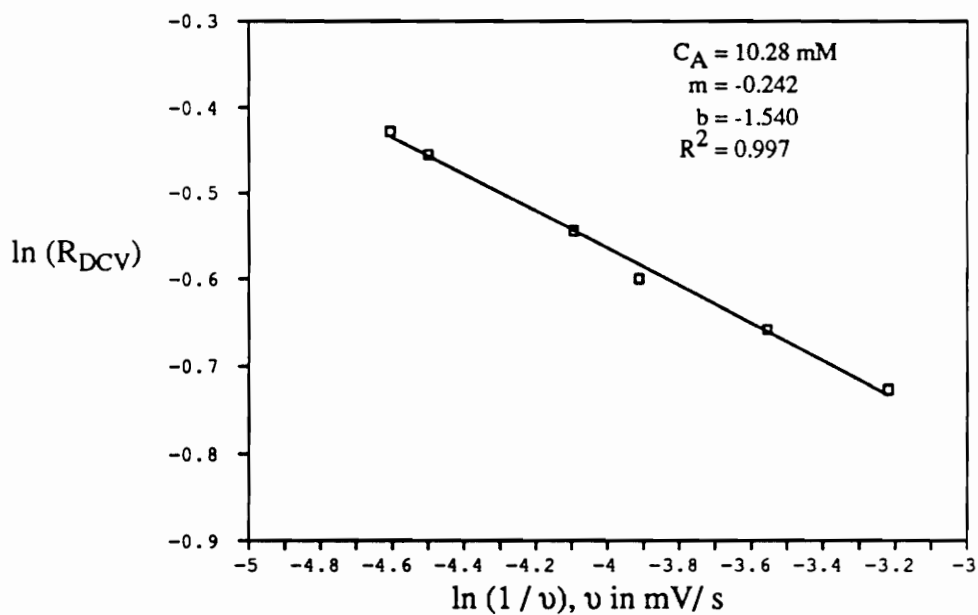


Figure 25. Plot for extraction of $v_{0.5}$ for trans-1-benzoyl-2-methylcyclopropyl ketyl anion ($28b^-$)

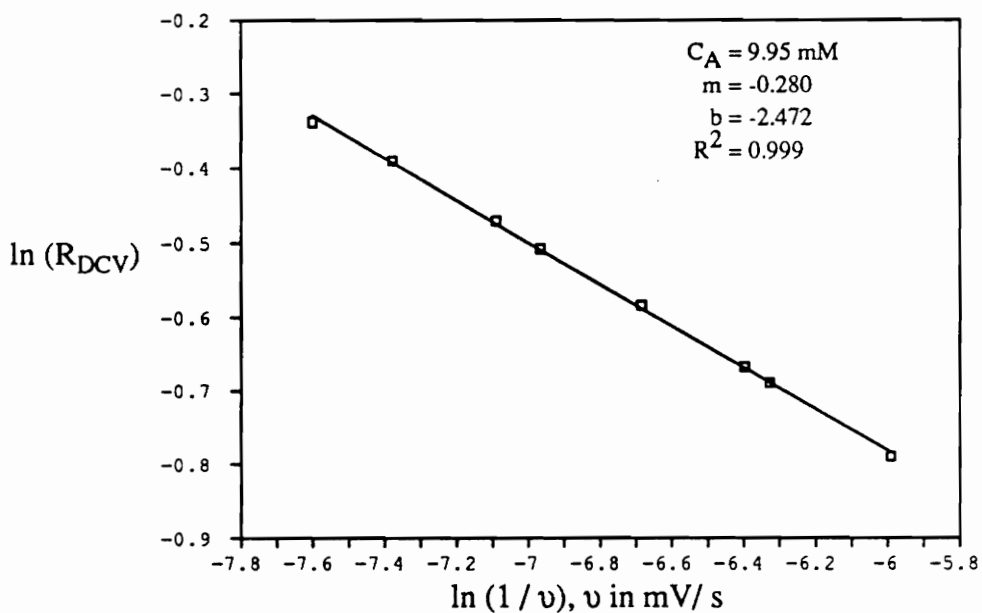


Figure 26. Plot for extraction of $v_{0.5}$ for 1-benzoyl-2,2-dimethylcyclopropyl ketyl anion ($28c^-$)

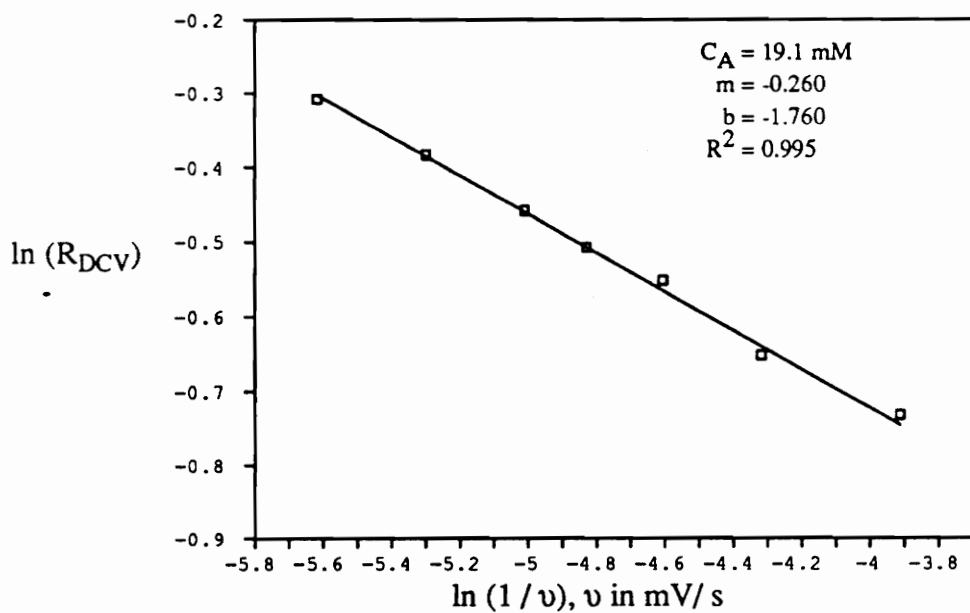
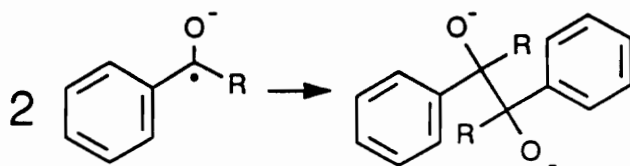


Figure 27. Plot for extraction of $v_{0.5}$ for p-tolyl cyclopropyl ketyl anion ($28d^-$)

On the surface, it appears that the phenyl cyclopropyl ketyl anions (**28a⁻**) through (**28d⁻**) are undergoing a simple ketyl dimerization reaction. Close examination of the rate constants for decay of the ketyl anions (Table 5) shows that increased alkyl substitution on the cyclopropane ring increases the observed bimolecular rate constant. This trend is exactly the opposite of what is expected for a typical ketyl dimerization reaction.^{76b} For the phenyl alkyl ketone series, increased steric bulk retards the rate of ketyl anion dimerization (Table 6). For example, acetophenone ketyl anion (R = CH₃) dimerizes quite rapidly; propiophenone ketyl anion (R = CH₂CH₃) dimerizes slower than acetophenone ketyl anion but much more rapidly than isobutyrophenone ketyl anion (R = CH(CH₃)₂). For all practical purposes under our reaction conditions, pivalophenone ketyl anion (R = C(CH₃)₃) is a stable radical anion.

Table 6. Relative stability of phenyl alkyl ketyl anions



R	C _A (mM)	v (mV/s)	R _{DCV} ^a
CH ₃	3	100	0.00
CH ₂ CH ₃	3	100	0.40
CH(CH ₃) ₂	3	100	0.96
C(CH ₃) ₃	3	100	1.00

^a 0.5 M n-Bu₄NBF₄ / DMF, planar Au working electrode, Ag/AgNO₃ (0.1 M in acetonitrile) reference electrode

The opposite trend in ketyl anion stability is observed for the phenyl cyclopropyl ketone series. Phenyl cyclopropyl ketyl anion (**28a⁻**) decays with a rate constant of about

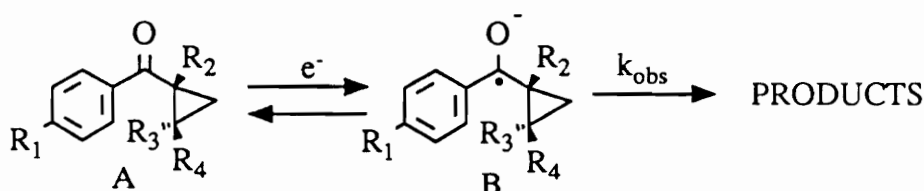
4 M⁻¹s⁻¹. Substitution of two methyl groups on the cyclopropane ring (**28c**⁻) increases the rate constant for decay by about fifty times to around 200 M⁻¹s⁻¹. The radical anion of the monomethyl derivative (**28b**⁻) decays at an intermediate rate of about 15 M⁻¹s⁻¹. Evidently something other than a simple dimer forming reaction is occurring for phenyl cyclopropyl ketyl anions.

Apparent activation energies, E_a , for the decay of these cyclopropyl ketyl anions were also obtained (Table 7). At several temperatures, T , the sweep rate, ν , was adjusted to keep R_{DCV} constant. An Arrhenius type plot of $\ln(\nu_c/T)$ vs. $1/T$ yields a straight line whose slope is related to the apparent activation energy for decay of the electrode generated intermediate (Eqn. 15).^{72,73,77}

Eqn. 15

$$\ln(\nu_c/T) = (-E_a/R)(1/T) + C$$

Table 7. Observed activation energies for the decay of phenyl cyclopropyl ketyl anions



cmpd	R ₁	R ₂	R ₃	R ₄	E_a (kcal/mol) ^{a,b}
28a	H	H	H	H	9.5 ± 0.2
28b	H	H	H	CH ₃	7.7 ± 0.1
28c	H	H	CH ₃	CH ₃	7.1 ± 0.2

^a 0.5 M *n*-Bu₄NBF₄ / DMF, planar Au working electrode, Ag/AgNO₃ (0.1 M in CH₃CN) reference electrode; temperature varied in range of -10°C to 60°C.

^b E_a calculated using $\ln(\nu_c/T) = (-E_a/R)(1/T) + C$, see Hammerlich, O., Parker, V., *Acta. Chem. Scand.*, 1983, B37, 379.

Figures 28 through 30 show representative plots for the calculation of apparent activation energies for the decay of ketyl anions (**28a⁻**), (**28b⁻**), and (**28c⁻**). As can be seen in Table 7, increased alkyl substitution on the cyclopropane ring decreases the observed activation energy for decay of the ketyl anions. Again, this trend is exactly the opposite of what would be expected for a "normal" ketyl dimerization. This trend is however what would be expected for unimolecular ring opening of the phenyl cyclopropyl ketyl anions.

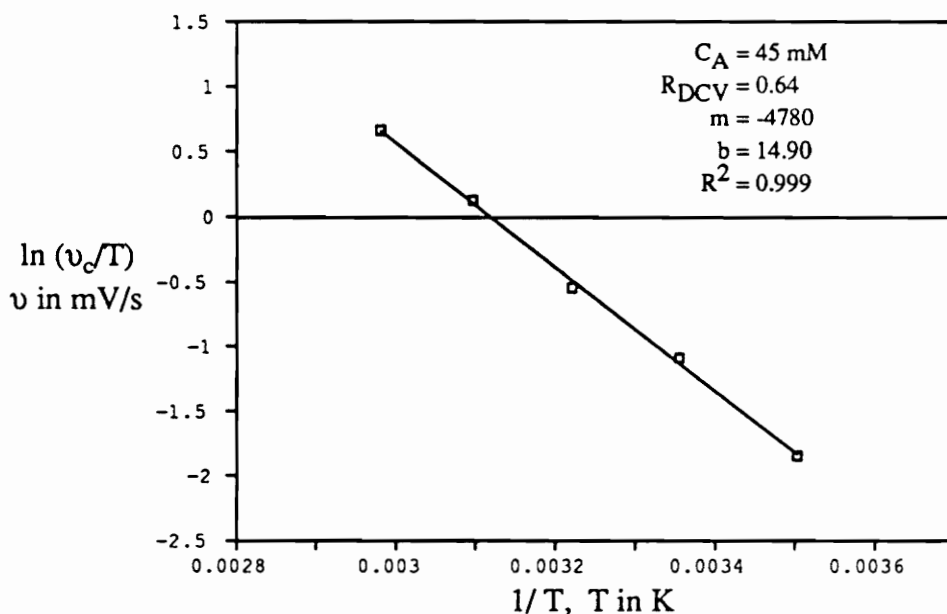


Figure 28. Plot for determination of activation energy for decay of phenyl cyclopropyl ketyl anion (**28a⁻**)

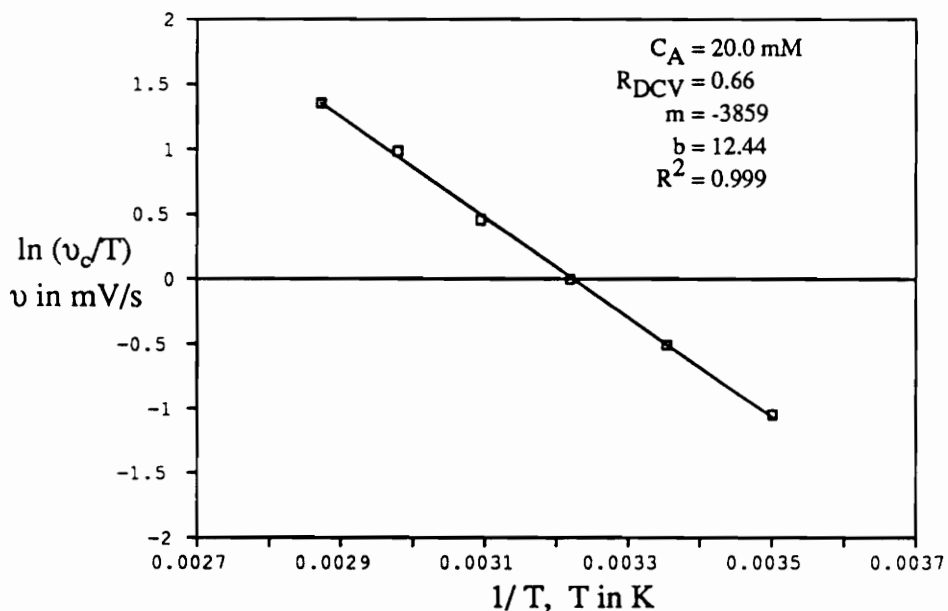


Figure 29. Plot for determination of activation energy for decay of trans-1-benzoyl-2-methylcyclopropyl ketyl anion (28b⁻)

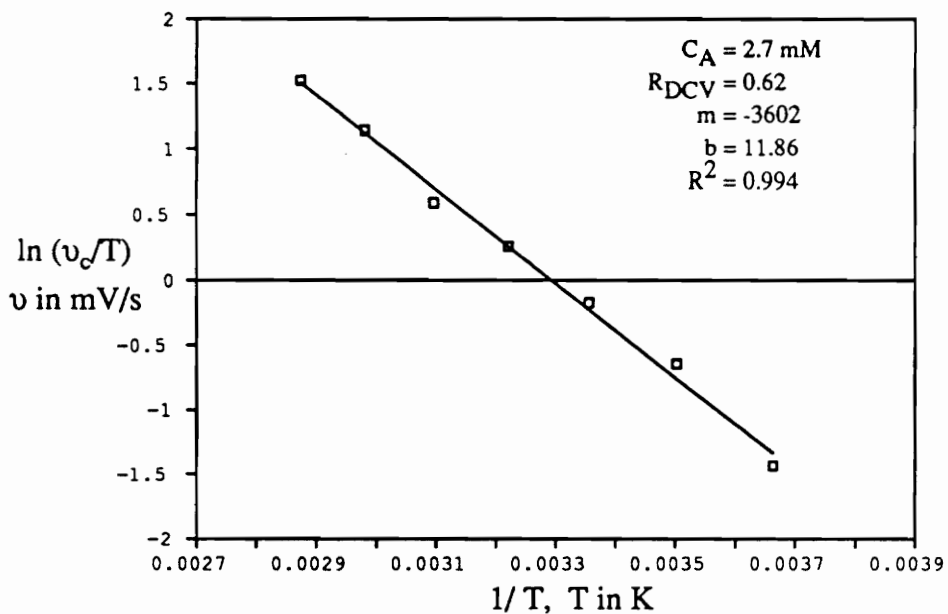
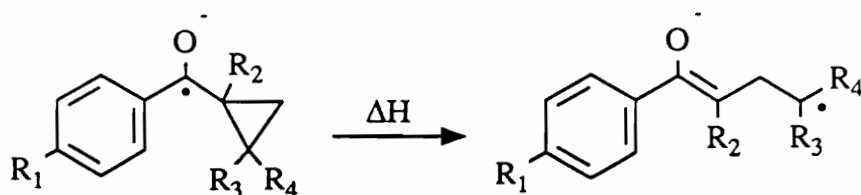


Figure 30. Plot for determination of activation energy for decay of 1-benzoyl-2,2-dimethylcyclopropyl ketyl anion (28c⁻)

The observed trend in activation energies manifests itself in the calculated enthalpies of ring opening of variously substituted phenyl cyclopropyl ketyl anions (Table 8). The heats of formation of the ketyl anions and corresponding distonic radical anions were calculated using AM1^{78a} implemented through MOPAC version 5.0 (QCPE #455). Full geometry optimizations were performed at the Unrestricted Hartree-Fock (UHF) level.^{78b}

Substitution on the cyclopropane ring takes the calculated enthalpy of ring opening from endothermic to exothermic. The enthalpy of ring opening of phenyl cyclopropyl ketyl anion (**28a⁻**) is endothermic by 7.9 kcal/mol. Substitution of two methyl groups on the cyclopropane ring (**28c⁻**) provides sufficient stabilization for the resulting distonic radical anion that the calculated enthalpy of ring opening becomes exothermic by 2.5 kcal/mol. As before, the monomethyl derivative (**28b⁻**) is intermediate between the unsubstituted and disubstituted cases with an endothermic enthalpy of ring opening of 2.5 kcal/mol.

Table 8. AM1 calculated enthalpies for ring opening of cyclopropyl ketyl anions



cmpd	R ₄	R ₃	R ₂	R ₁	ΔH (kcal/mol) ^a
28a ⁻	H	H	H	H	+ 7.9
28b ⁻	H	CH ₃	H	H	+ 2.5
28c ⁻	CH ₃	CH ₃	H	H	- 2.5
28d ⁻	H	H	H	CH ₃	+ 7.9
28e ⁻	H	H	CH ₃	H	+ 6.2

^a Heats of formation of the ketyl anions and their corresponding distonic radical anions calculated using AM1 implemented through MOPAC ver. 5.0 (QCPE #455). Full geometry optimization at UHF level.

The facts presented so far create quite a dichotomy. Steric and electronic effects point toward a unimolecular ring opening of the phenyl cyclopropyl ketyl anions. However, kinetic analysis of the decay of these species unambiguously points toward a bimolecular decomposition. Any successful mechanistic scheme describing the decay of phenyl cyclopropyl ketyl anions must reconcile these apparently conflicting facts.

All of the data presented is totally consistent with the mechanistic scheme presented in Figure 31. A *reversible* ring opening of the ketyl anion (29) yields distonic radical anion (30). The ring opened species (30) is then trapped by the ketyl anion (29) to yield dimer. Application of the steady state approximation to (30) yields the rate law delimited in equation 17.

Eqn. 17

$$\text{RATE} = \frac{k_1 k_2 [29]^2}{k_{-1} + k_2 [29]}$$

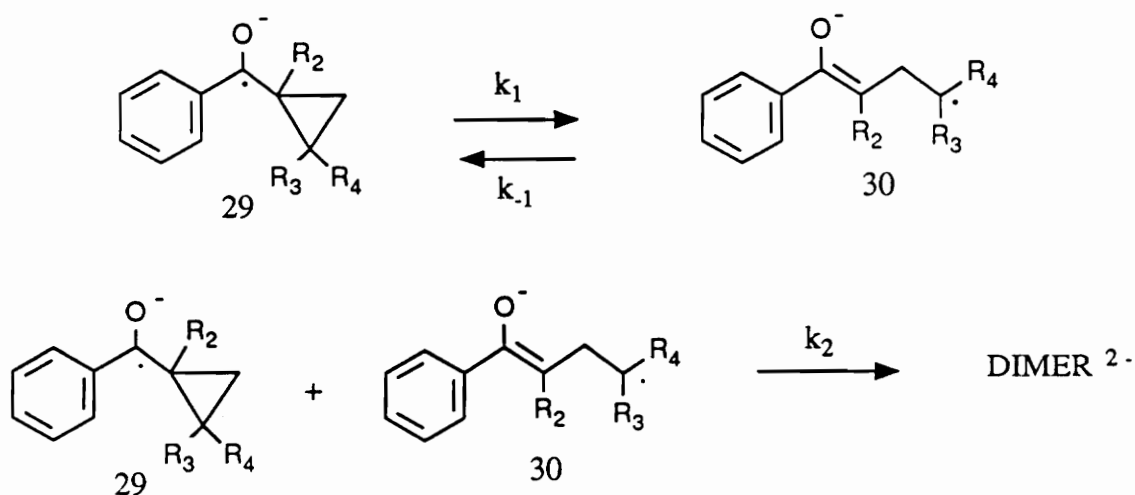


Figure 31. Proposed mechanism for the decay of phenyl cyclopropyl ketyl anions

Since the calculated rate law has a two term denominator, it can be viewed as being composed of three distinct cases depending upon the relative rates of the competing processes consuming the steady state intermediate. Once formed, the distonic radical anion (30) partitions itself between returning to the ring closed species (k_{-1}) and going on to product ($k_2[29]$). If formation of dimer is fast relative to ring closing ($k_2[29] \gg k_{-1}$), the denominator simplifies to $k_2[29]$ and the overall rate law becomes unimolecular, Rate = $k_1[29]$. If on the other hand ring closure is fast relative to dimer formation ($k_{-1} \gg k_2[29]$), the denominator reduces to k_{-1} and the overall rate law simplifies to Rate = $(k_1 k_2 / k_{-1})[29]^2$ or equivalently Rate = $k_{\text{obs}}[29]^2$; a simple second order rate law. The final case arises if ring closure and dimer formation occur at comparable rates ($k_{-1} \cong k_2[29]$). In this scenario, no simplifications can be made and the rate law remains as shown in equation 17.

In the concentration range available to us for study ($C_A = 0.1 - 50 \text{ mM}$), no deviation from second order kinetics was observed (Figures 18 through 21) suggesting that within this concentration regime, $k_{-1} \gg k_2[29]$. Thus, the rate law for decay of

cyclopropyl ketyl anions (**28a⁻**) through (**28c⁻**) can be described by $\text{Rate} = (k_1k_2/k_{-1})[\mathbf{29}]^2 = k_{\text{obs}}[\mathbf{29}]^2$. This rate law satisfies both the observed steric and electronic effects signalling cyclopropane ring opening and the bimolecular nature of decay of unsubstituted and alkyl substituted phenyl cyclopropyl ketyl anions.

ELECTROLYSIS PRODUCTS

Although not compulsory in a kinetic study, it is always desirable to know the product(s) of the chemical process under investigation. Bulk electrolyses of phenyl cyclopropyl ketones (28a), (28b), (28c), and (28e) yielded the products shown in Figure 32. Yields are summarized in Table 9. In all cases, dimers with the structure of (31) predominated. Electrolyses were performed in a standard H cell in anhydrous *N,N*-Dimethylformamide (DMF) containing 0.2 M tetra-*n*-butylammonium tetrafluoroborate (*n*-Bu₄NBF₄) as the supporting electrolyte. The working electrode was fashioned from gold foil and the auxiliary electrode from platinum mesh. The reference electrode was made from a silver wire in contact with 0.1 M silver nitrate in acetonitrile.

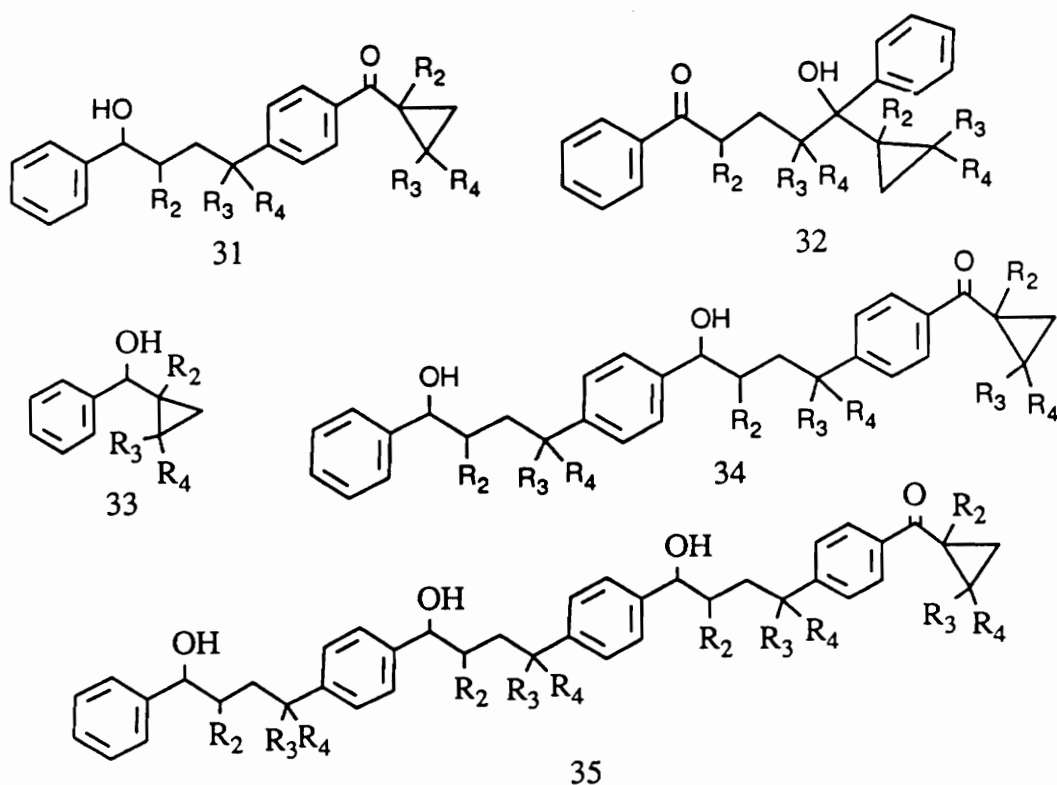
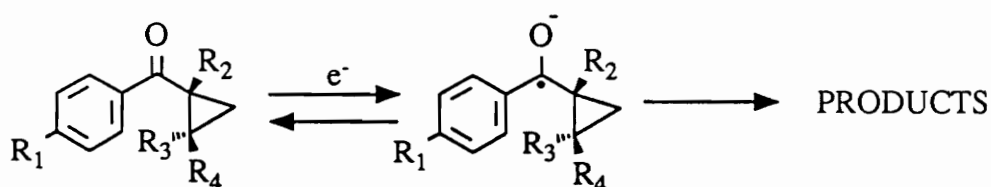


Figure 32. Electrolysis products for phenyl cyclopropyl ketones (28a), (28b), (28c), and (28e)

Table 9. Product yields for bulk electrolyses of phenyl cyclopropyl ketones (28a), (28b), (28c), and (28e)



cmpd	R ₁	R ₂	R ₃	R ₄	28	YIELDS (%) ^{a,b}				
						31	32	33	34	35
28a	H	H	H	H	14	41	7	c	11	c
28b	H	H	H	CH ₃	17	51	6	c	15	5
28c	H	H	CH ₃	CH ₃	17	40	c	c	17	7
28e	H	CH ₃	H	H	10	41	c	12	9	c

^a 0.2 M *n*-Bu₄NBF₄/DMF, Au working electrode, Pt auxiliary electrode, Ag/AgNO₃ (0.1 M in CH₃CN) reference electrode.

^b constant current electrolyses, 1 equivalent of electrons passed; constant potential electrolysis at potentials 300 mV beyond E^o yielded analogous results.

^c none detected

p-Tolyl cyclopropyl ketone (**28d**) gave slightly different electrolysis results. Since the para position of the ketyl anion is blocked by a methyl group, decay of this radical anion is expected to take an alternate route. Our initial hope was that substitution in the para position would shut down dimerization and allow us to study the reversible unimolecular ring opening directly. The voltammetric results presented earlier show this not to be the case (i.e. second order decay was observed, Figure 21). Controlled current electrolysis of (**28d**) (1 equivalent of electrons) yielded the products shown in Figure 33 as well as 22% recovered starting material and 4% of a trimer believed to be of structure (**39**). The formation of ring opened monomer (**38**) might be explained by the presence of a good hydrogen atom donor not present in the other cases (Eqn. 18).

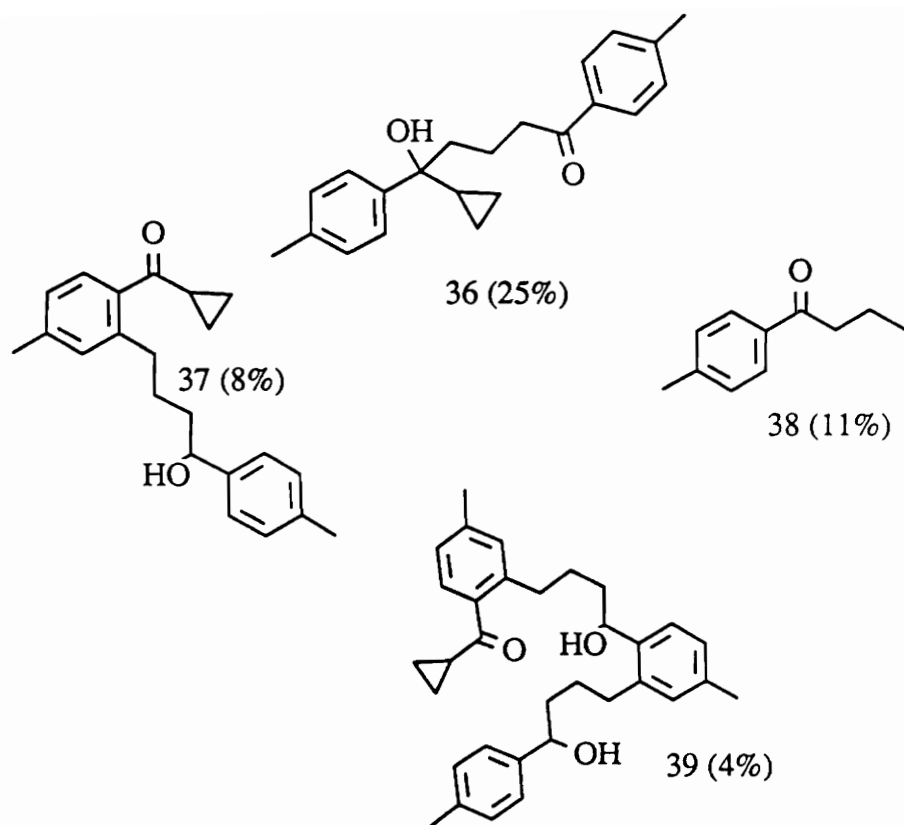
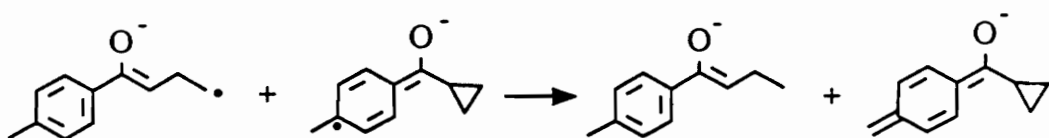


Figure 33. Products of the electrolysis of p-tolyl cyclopropyl ketone (28d)

Eqn. 18



Formation of the main dimer product (Figure 32, (31)) from decay of (28a^{•-}), (28b^{•-}), (28c^{•-}), and (28e^{•-}) provided an interesting digression from our kinetic pursuits. The product is envisioned to be formed through an initial coupling of the ketyl anion (29) and distonic radical anion (30) to yield the dianion (40) (Figure 34). Somehow in a process occurring after the rate limiting dimerization step or during workup, the dianion is converted into the final observed product.

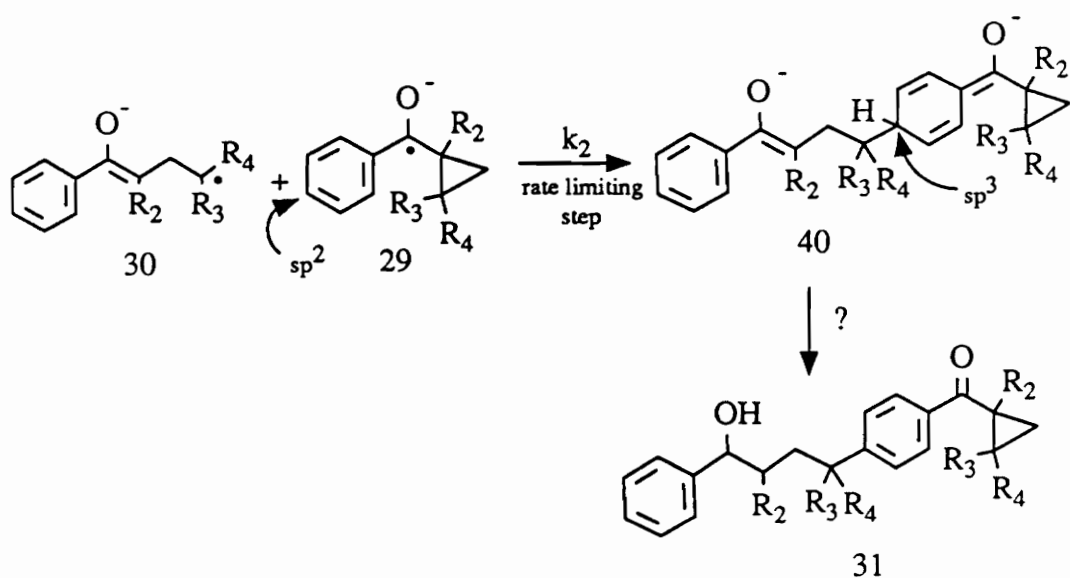


Figure 34. Coupling of ketyl anion and distonic radical anion to yield dianion

Cyclic voltammetry experiments on the phenyl cyclopropyl ketones reveal an anodic wave substantially more positive than the ketone/ketyl couple which we have assigned to oxidation of the dianion (*vide infra*). A CV trace of 1-benzoyl-2,2-dimethylcyclopropane showing these features is given in Figure 35. The "new" anodic wave shows no reverse current up to relatively fast scan rates (10 V/s).

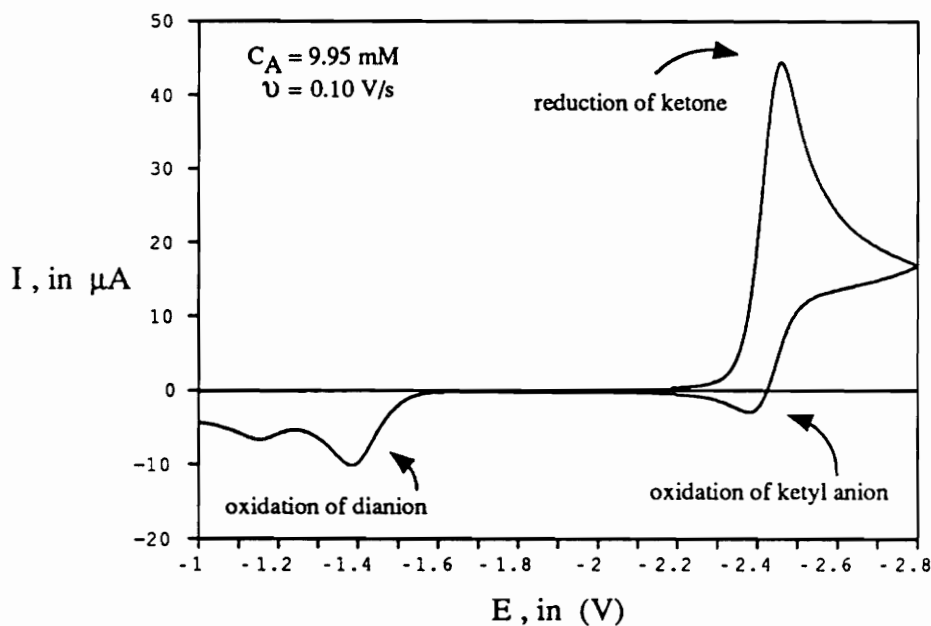
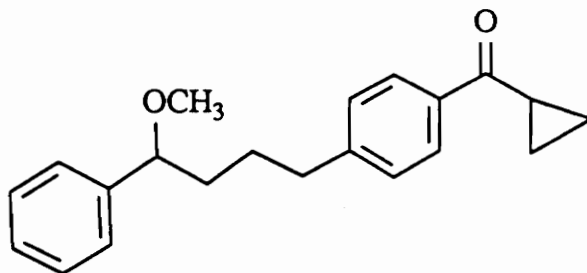


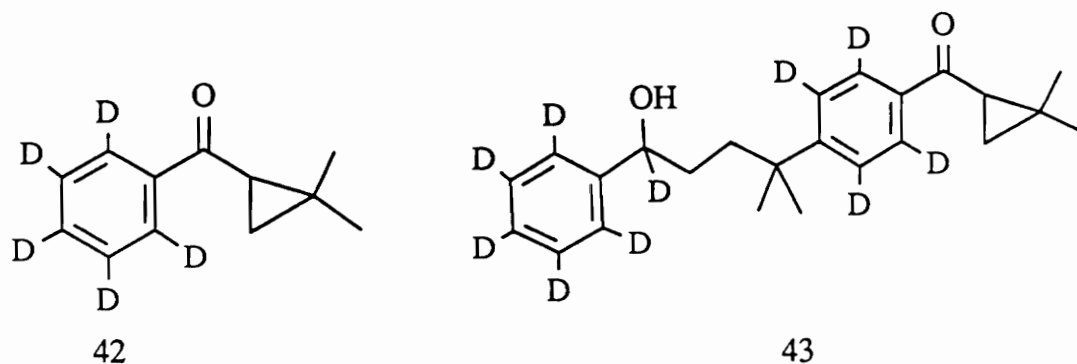
Figure 35. Cyclic voltammogram of 1-benzoyl-2,2-dimethylcyclopropane (28c)

Attempts to trap the dianion (40) following electrolysis of phenyl cyclopropyl ketones were ambiguous. For example, electrolysis of phenyl cyclopropyl ketone (28a) followed by quenching with D_2O / DCl led to no detectable deuterium incorporation in the final products (MS, 2H NMR). The same experiment followed by quenching with methyl iodide yielded oxygen methylated dimer (41). If the "new" anodic wave seen by CV is due to the dianion (40), these quenching experiments suggest that the dianion is converted into the final product (31) sluggishly but before quenching.



41

In an effort to gain a better understanding of how the dianion (**40**) is transformed into the final product (**31**), we electrolyzed the d-5 derivative of 1-benzoyl-2,2-dimethylcyclopropane (**42**).



We found complete deuterium incorporation at the benzylic alcohol carbon in the dimer product (**43**) providing strong evidence for a mechanism such as the one outlined in Figure 36. An initial protonation of the dianion to yield the keto/enol molecule (**44**) can be envisioned. A hydride transfer, reducing the ketone to an alcohol and oxidizing the cyclohexadiene to an aromatic nucleus, could then yield the final product.

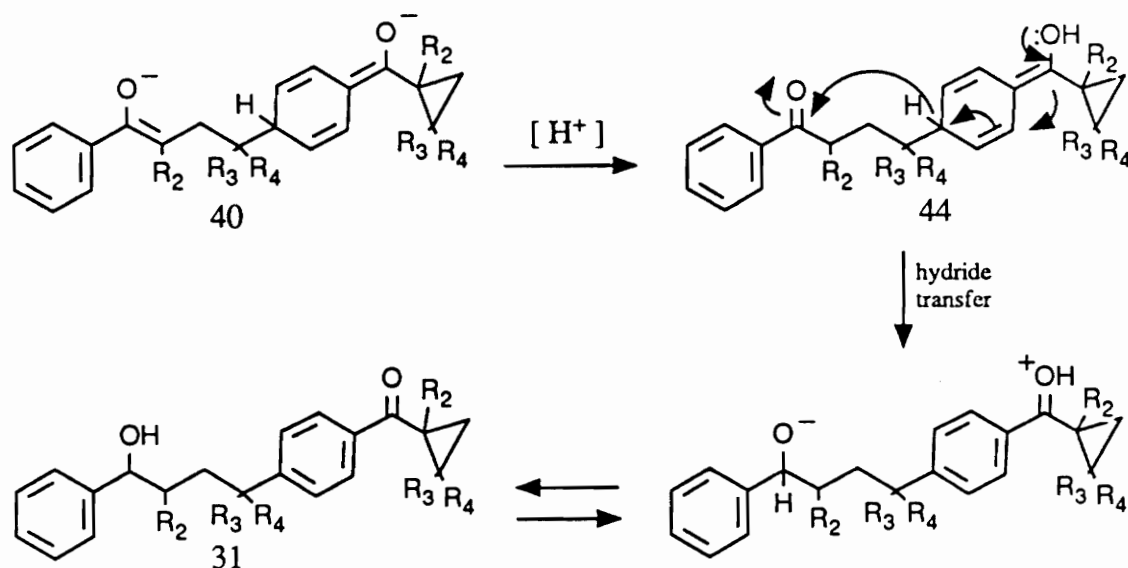


Figure 36. Proposed mechanism for formation of dimeric product

Our next step was to find the source of protons implicated in the mechanistic scheme (Figure 36). Possible sources of "H⁺" include solvent (DMF), electrolyte (*n*-Bu₄NBF₄), H⁺ generated at the anode by oxidation of solvent or electrolyte, starting ketone, product, or fortuitous moisture. The first two possible sources of "H⁺" would be fairly straightforward but expensive to test by employing deuterated solvent and electrolyte, but these sources seemed unlikely as proton donors because of the weak acidity of alkyl ammonium salts and N,N-dimethylformamide.^{79a,b,c} The third possible proton source, H⁺ generated in situ at the anode, is likely but would be extremely difficult to prove or disprove. The last three proton sources, starting material, product, and water appear to be likely candidates and can be qualitatively tested.

Electrolysis of 1-benzoyl-1-deuteriocyclopropane (**45**) followed by a methyl iodide quench led to loss of most of the deuterium label in both starting material and products (Figure 37).

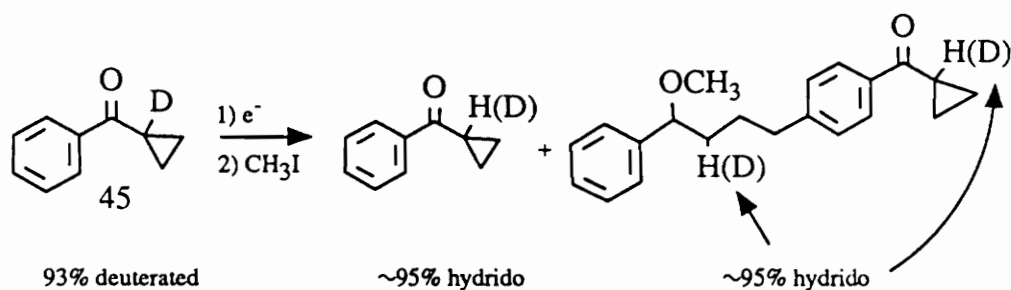


Figure 37. Results of electrolysis of 1-benzoyl-1-deuteriocyclopropane (45**)**

Also, electrolysis of phenyl cyclopropyl ketone (**28a**) in the presence of 3.0 mol equivalents of D₂O led to relatively high deuterium incorporation in both product and remaining starting material (Figure 38). These experiments implicate starting ketone, adventitious moisture, and possibly product as being potential sources of protons during electrolysis.

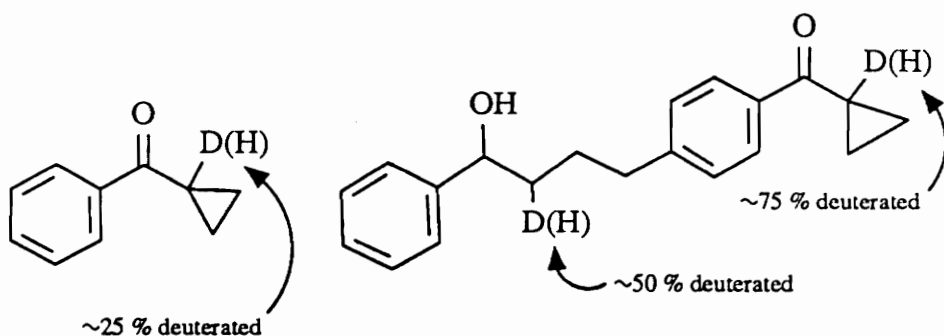


Figure 38. Results of electrolysis of phenyl cyclopropyl ketone (28a) in the presence of D_2O

The only remaining question concerning the formation of dimer (31) was whether the implicated hydride transfer occurs in an intramolecular fashion (as shown in Figure 36) or through an intermolecular pathway. At the outset, we favored an intramolecular process because compounds expected to be observed for an intermolecular process were not found in the electrolysis product mixture (Figure 39).

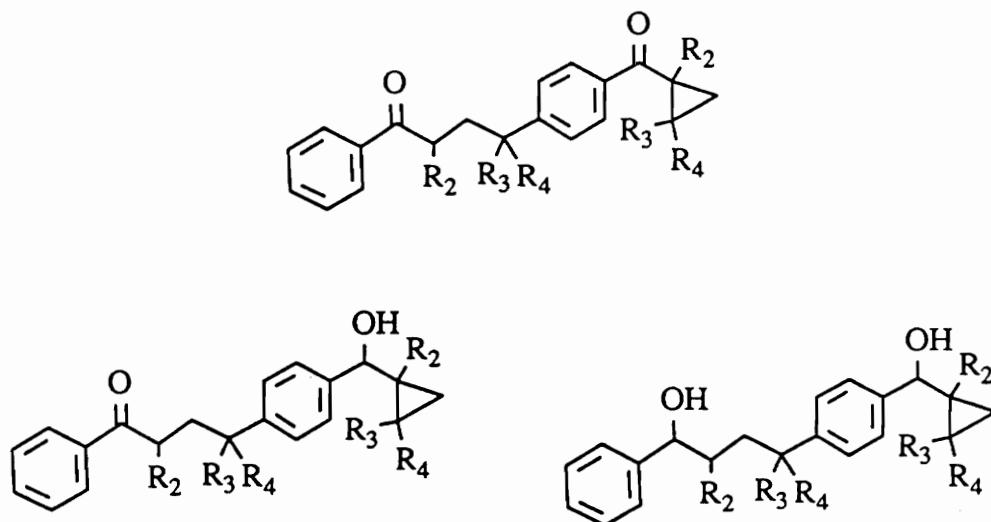


Figure 39. Compounds not observed in the electrolysis product mixture that would be expected if an intermolecular hydride transfer were operating

To address the question of intra- vs. intermolecular hydride transfer, we performed a coelectrolysis of an equimolar mixture of the d-5 labelled (42) and unlabelled (28c) 1-benzoyl-2,2-dimethylcyclopropanes and analyzed the products by mass spectrometry. If the hydride transfer occurs in an intramolecular fashion, four products with three distinct molecular weights should be observed (Figure 40). Further, assuming the dimerization step to be governed by simple statistics, one would expect to find d-0 compound (46), two d-5 compounds (47) and (48), and one d-10 compound (49) in the relative ratios shown in Table 10 (under column with $K_{eq} = 1$).

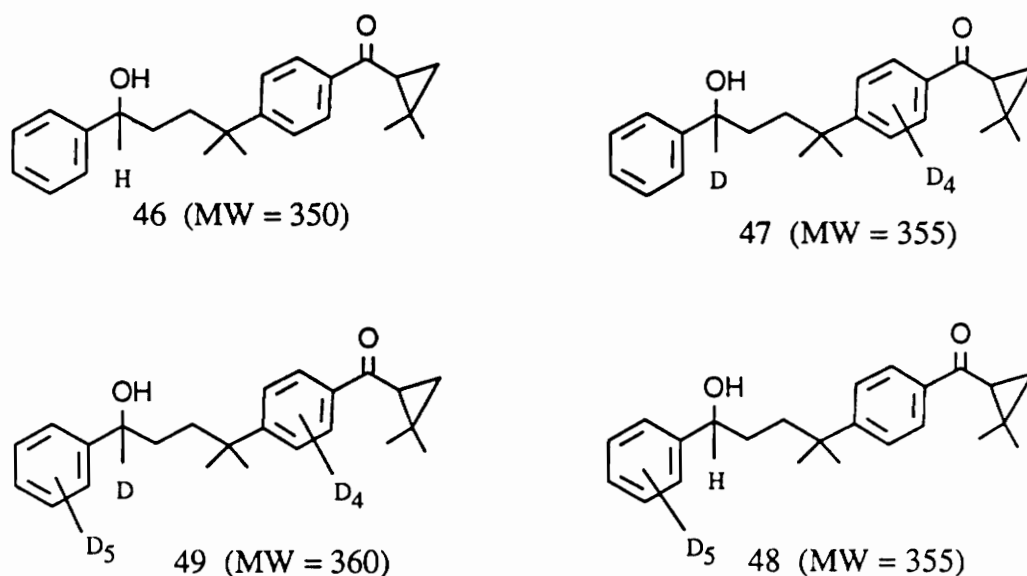


Figure 40. Dimer products expected for coelectrolysis of mixture of labelled (42) and unlabelled (28c) 1-benzoyl-2,2-dimethylcyclopropanes if hydride transfer is intramolecular

Table 10. Predicted and observed ratios of mass spectral peak intensities for coelectrolysis of labelled (42) and unlabelled (28c) 1-benzoyl-2,2-dimethylcyclopropanes

Mass	experimentally observed relative peak intensities	predicted ratio of peak intensities for intramolecular case		predicted ratio of peak intensities for intermolecular case ^c
		K _{eq} = 1.00	K _{eq} = 0.75	K _{eq} = 1.00
350	1.000	1.000 ^a	1.000	1.000
351	0.290	0.274 ^a	0.274	1.300
352	0.061	0.044 ^a	0.044	0.350
353	0.000	0.000	0.000	0.050
354	0.088	0.000	0.000	1.000
355	1.430	2.000	1.500	2.300
356	0.377	0.639 ^b	0.479	1.650
357	0.079	0.112 ^b	0.084	0.100
358	0.026	0.000	0.000	0.000
359	0.000	0.000	0.000	1.000
360	0.597	1.000 ^a	0.563	1.300
361	0.184	0.365 ^a	0.205	0.350
362	0.035	0.068 ^a	0.038	0.050

^a measured from mass spectrum of authentic sample

^b approximated based on average of d-0 compound (MW = 350) and d-10 compound (MW = 360)

^c approximated by letting (M⁺ + 1) = 30% of M⁺ and (M⁺ + 2) = 5% of M⁺

On the other hand, assuming the hydride transfer occurs through an intermolecular process, one would expect to find not only the products in Figure 40 but also the products shown in Figure 41. The d-1 compound (50), d-4 compound (51), d-6 compound (52), and d-9 compound (53) could only arise through an intermolecular process. For an intermolecular hydride transfer, assuming simple statistical dimerization, one would expect eight products with seven distinct molecular weights in the relative ratios shown in Table 10.

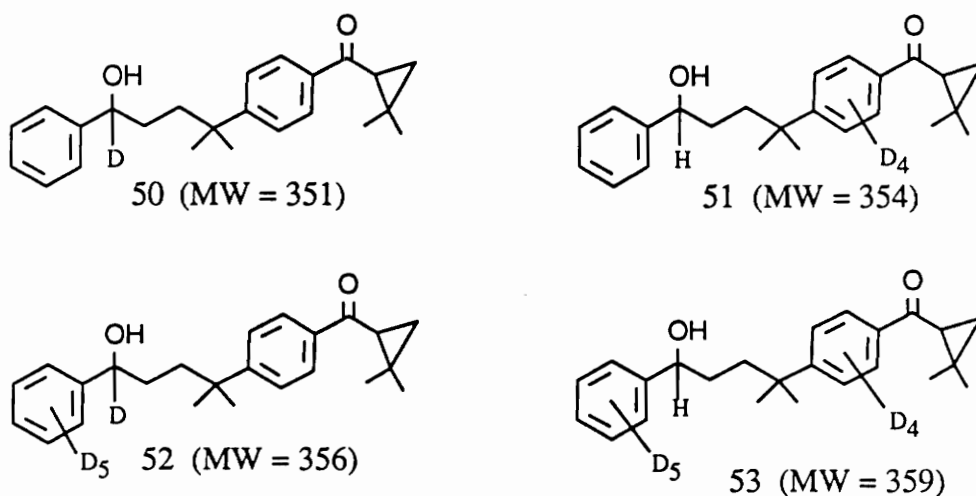
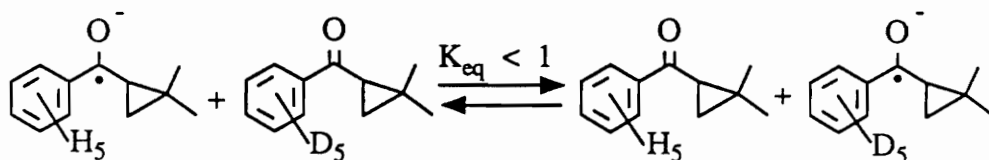


Figure 41. Dimer products expected for coelectrolysis of mixture of labelled (42) and unlabelled (28c) 1-benzoyl-2,2-dimethylcyclopropanes if hydride transfer is intermolecular

The results of the coelectrolysis were consistent with an intramolecular hydride transfer process (Table 10). The observed mass spectral peak intensities are best described by molecular ion peaks at 350, 355, and 360 mass units plus their natural isotope abundance peaks ($M^{\cdot+} + 1$, $M^{\cdot+} + 2$). Small peaks at 354 mass units (**51**?) and 358 mass units ($M^{\cdot+} + 2$ for (**52**)?) as well as small discrepancies in the intensities of the isotope peaks for the molecular ions at 350, 355, and 360 mass units might be accounted for by a small amount of competing intermolecular hydride transfer. The observed ratio of the molecular ion peaks at 350, 355, and 360 mass units is 1.00 : 1.43 : 0.60 not 1.00 : 2.00 : 1.00 as predicted by simple statistical analysis of the intramolecular case. This discrepancy might be rationalized with the following argument. An equimolar mixture of the labelled and unlabelled ketones does not ensure an equimolar mixture of their ketyl anions upon electrolysis (Eqn. 19).

Eqn. 19



This phenomena has been observed with several organic radical anions and their neutral isotopic isomers (Table 11).^{79d} An equilibrium constant less than one for equation 19 would skew the predicted statistical ratio of products in the direction of the observed ratio. An equilibrium constant, K_{eq} , of 0.75 would be expected to yield a ratio of products of 1.00 : 1.50 : 0.56 for the intramolecular case which is very close to the experimentally observed ratio of 1.00 : 1.43 : 0.60 (Table 10).

Table 11. Equilibrium between radical anions and neutral substrates of isotopic isomers

compound ^a	K_{eq} (25 °C) ^b
benzene	0.45
naphthalene	0.45
anthracene	0.50
pyrene	0.56
perylene	0.59

^a R = fully hydrido isomer, R* = fully deuterated isomer

^b see Stevenson, G., Sturgeon, B., *J. Org. Chem.*, 1990, 55, 4090.

Deviation from the ideal statistical ratio of mass spectral peak intensities for an intramolecular hydride transfer in the coelectrolysis of labelled and unlabelled materials could also arise from an isotope effect. A primary isotope effect for the hydride transfer (i.e. C-D harder to break than C-H) would skew the product ratio in the observed direction. If the proposed mechanism for ketyl anion decay (Figure 31) is correct, a primary isotope effect would not manifest itself because the hydride transfer occurs after the rate limiting dimerization step. Instead, the proposed mechanism would suggest the existence of a possible inverse, secondary isotope effect which would distort the observed product ratio in the opposite direction (i.e. favor deuterated products).^{79e} An inverse, α , secondary isotope effect can arise in the rate limiting dimerization of the distonic radical anion with the ketyl anion (Figure 34). The hybridization of the "para" carbon of the ketyl anion changes from sp^2 in the reactant to sp^3 in the dianion. A hydrogen (or deuterium) bonded to the carbon undergoing the hybridization change will experience increased resistance to C-H (C-D) bending in the transition state resulting from the change in hybridization. The hindrance of the bending mode will be greater for a C-H bond than for a C-D bond because the amplitude of the C-H vibration is greater than that for the C-D bond. Thus, substitution of deuterium on the para position of the aromatic ring of the ketyl anion would be expected to enhance the rate of dimerization, therefore, resulting in a small, inverse, α , secondary isotope effect (i.e. $k_H/k_D < 1$).

Voltammetric studies of the labelled derivative (42) analogous to those described earlier yielded $k_{Dobs} = 203 \pm 12 \text{ M}^{-1}\text{s}^{-1}$. Therefore, $k_{Hobs}/k_{Dobs} = 1.04 \pm 0.15$. If a small isotope effect exists, the precision of our measurements do not allow its detection. Figures 42 and 43 show representative reaction order plots for 1-(d5)benzoyl-2,2-dimethylcyclopropane (42).

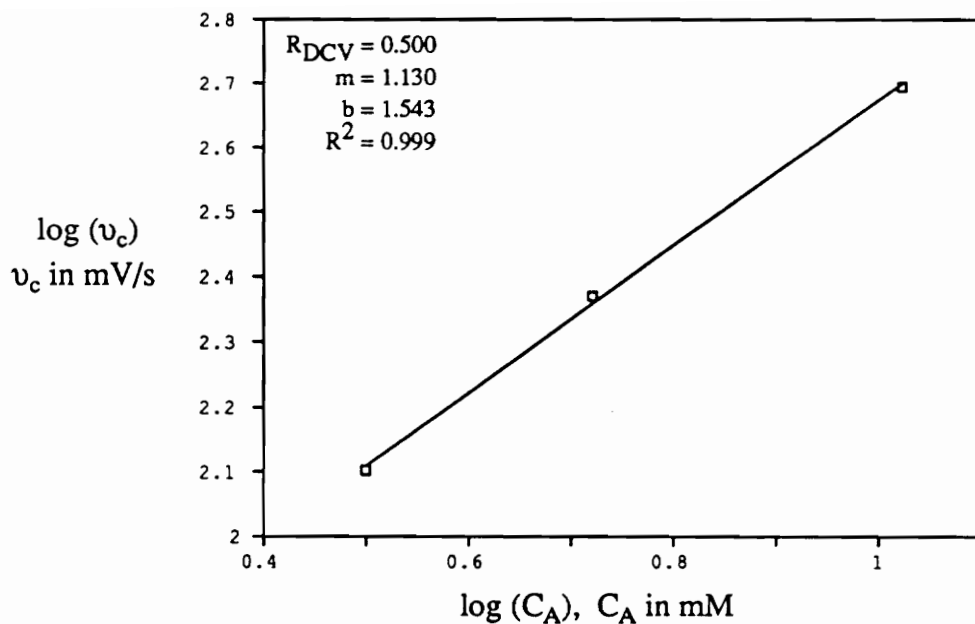


Figure 42. DCV reaction order plot for decay of 1-(d5)benzoyl-2,2-dimethylcyclopropyl ketyl anion (42^-)

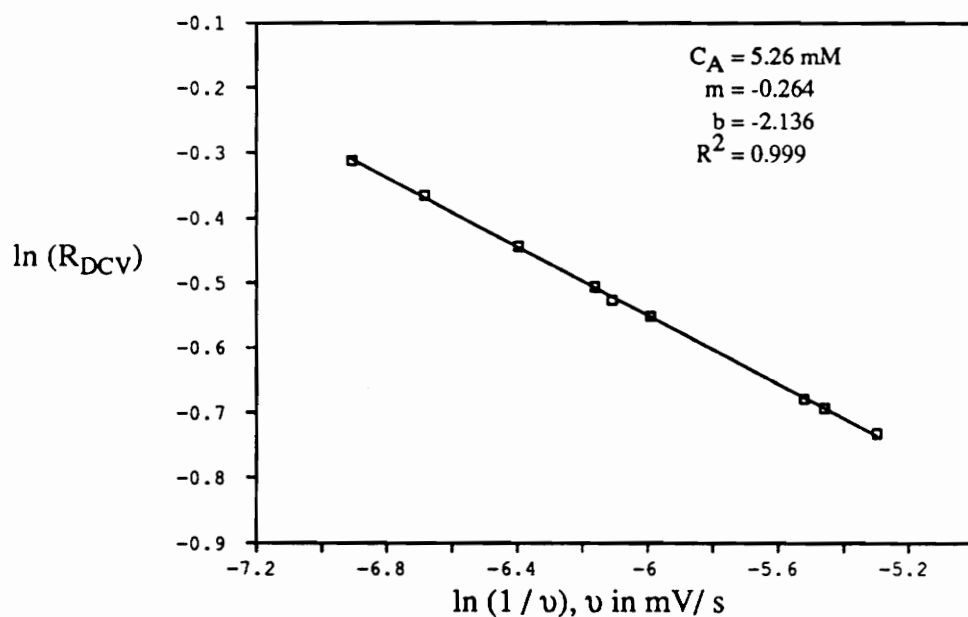


Figure 43. Plot for extraction of $v_{0.5}$ for 1-(d5)benzoyl-2,2-dimethylcyclopropyl ketyl anion (42^-)

In retrospect, the intramolecular hydride transfer can be explained by means of a very favorable transition state.^{80a} Figure 44 shows the MMX calculated least energy structure for hydride transfer.^{80b} The geometry of the minimized structure reveals that the intramolecular hydride transfer could proceed through a six-centered chair like transition state.

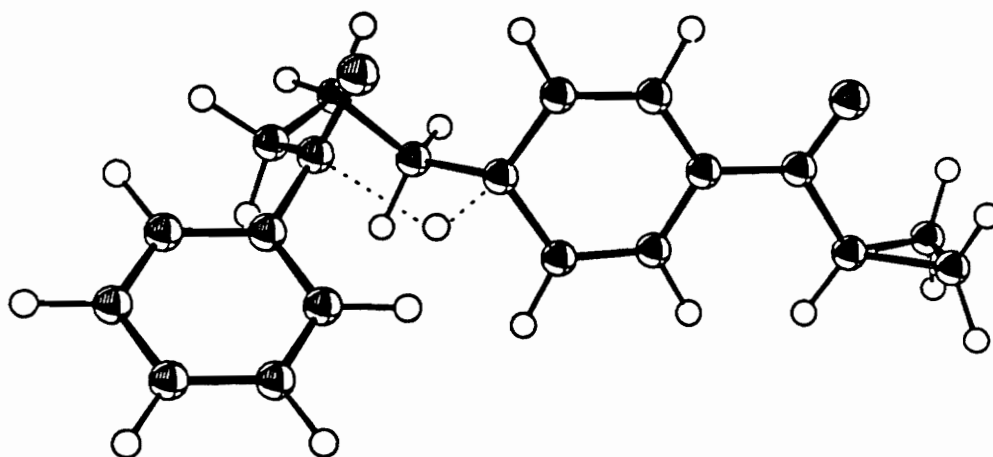


Figure 44. MMX calculated transition state for intramolecular hydride transfer

RATE CONSTANTS FOR KETYL ANION DECAY

The observed bimolecular rate constants for decay of the phenyl cyclopropyl ketyl anions show that they are quite long lived. These observed rate constants are each composed of three individual rate constants, $k_{\text{obs}} = k_1 k_2 / k_{-1}$ (See Figure 31). The magnitude of these individual rate constants, k_1 , k_{-1} , and k_2 , and not the magnitude of the observed rate constant will determine the utility of phenyl cyclopropyl ketyl anions as rearrangement probes for electron transfer. In order to begin picking apart the observed rate constants into their individual components, we set out to measure k_2 , the bimolecular rate constant for coupling of the distonic radical anion (30) with ketyl anion (29), independently. In order to make this measurement, it was assumed that the reactivity of the "radical portion" of distonic radical anion (30) could be approximated as an alkyl radical (i.e. the enolate and radical parts of (30) were assumed to be independent).

The Δ^5 -hexenyl radical (55) was generated in an excess of pivalophenone ketyl anion (54). The radical was formed from either the corresponding bromide or organomercurial by electron transfer from pivalophenone ketyl anion followed by concomitant disassociation of the newly created radical anion. Once formed, the Δ^5 -hexenyl radical partitions itself between two competing pathways. It can couple directly with pivalophenone ketyl anion (path a) or it can undergo an intramolecular cyclization followed by coupling with (54) (Figure 45, path b). The Δ^5 -hexenyl radical cyclizes to the cyclopentylcarbinyl radical with a known rate constant of $k_c = 1 \times 10^5 \text{ s}^{-1}$ at 25 °C.³³

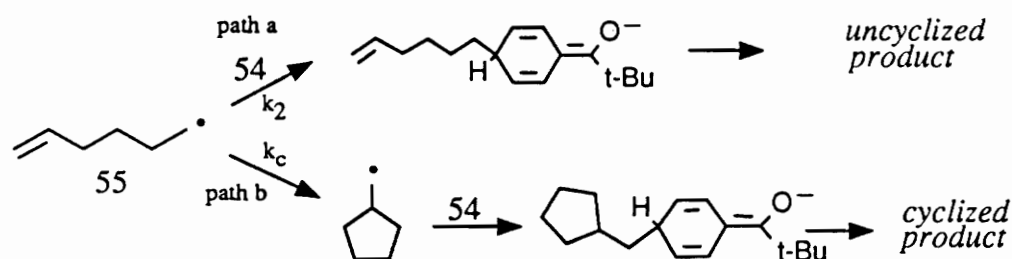
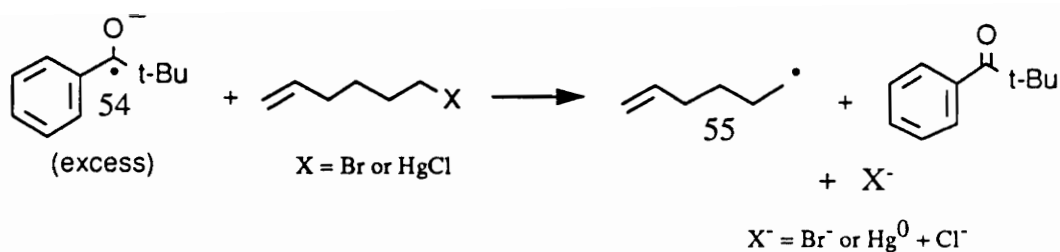


Figure 45. Estimation of the rate constant for coupling of a free radical with a ketyl anion

Assuming the concentration of ketyl anion (54) remains relatively constant during the course of the experiment, the bimolecular rate constant for coupling of a primary carbon centered radical with a ketyl anion, k_2 , can be easily calculated via equation 20.^{81a} Because the rate constant for cyclization of the Δ^5 -hexenyl radical, k_c , and the initial concentration of (54) are known, determination of the ratio of adducts containing the Δ^5 -hexenyl moiety (P_1^∞) to the adducts containing the cyclopentylcarbinyl moiety (P_2^∞) allows determination of k_2 .

Eqn. 20

$$k_2 = \frac{P_1^\infty}{P_2^\infty} \times \frac{k_c}{[54]}$$

The products resulting from coupling of the free radical with pivalophenone ketyl anion are shown in Figure 46. The bimolecular rate constant, k_2 , was determined to be

$8.4 \pm 2.0 \times 10^7 \text{ M}^{-1}\text{s}^{-1}$. Typical results are shown in Table 12. Product yields were obtained by gas chromatography utilizing diphenyl ether as an internal standard. Pivalophenone ketyl anion was generated by electrolysis and its concentration monitored with a second electrode by application of the Cottrell equation (Eqn. 21) to current vs. time data obtained by potential step methods. The diffusion coefficient, D_0 , was taken to be the same for pivalophenone and its ketyl anion.

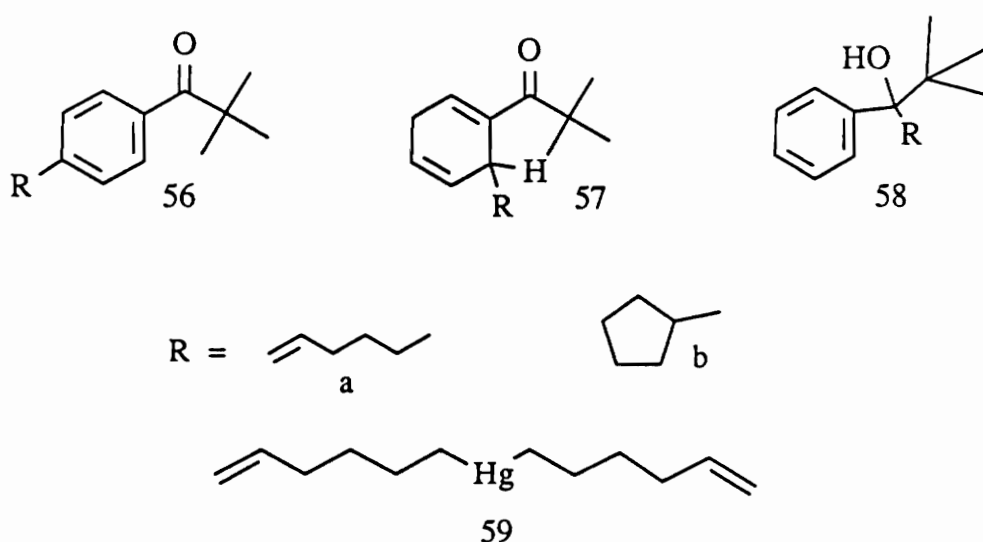


Figure 46. Products resulting from coupling of pivalophenone ketyl anion and Δ^5 -hexenyl radical

Eqn. 21

$$i(t) = \frac{n F A D_0^{1/2} C_o^*}{\pi^{1/2} t^{1/2}}$$

Our results are in good accord with a study performed on the coupling of lithium benzophenone ketyl anion with the Δ^5 -hexenyl radical in tetrahydrofuran ($k(25^\circ\text{C}) = 1.5 \times 10^8 \text{ M}^{-1}\text{s}^{-1}$).^{81b} Also, we can rule out addition of the free radical to neutral pivalophenone because addition of radicals to aromatic ketones has been shown to be slow.^{81c} The

addition of methyl radical to benzophenone occurs with a rate constant around $80 \text{ M}^{-1}\text{s}^{-1}$ at room temperature.^{81c,d} ($\text{Me}\cdot + \text{RH} \rightarrow \text{MeH} + \text{R}\cdot$; $k^A(25^\circ\text{C}) \cong 20 \text{ M}^{-1}\text{s}^{-1}$, $\text{RH} = \text{isoccatane}^{81d}$, $\text{Me}\cdot + \text{benzophenone} \xrightarrow{k^B} \text{adducts}$, $k^B/k^A(65^\circ\text{C}) = 4.2^{81c}$)

Table 12. Typical experimental results for coupling of Δ^5 -hexenyl radical with pivalophenone ketyl anion

Products	mMoles product (% yield)	
	Organomercurial radical source ^a	Bromide radical source ^b
56a	2.84×10^{-3} (30.2)	4.88×10^{-3} (37.9)
56b	4.21×10^{-4} (04.5)	2.76×10^{-4} (02.2)
57a	1.09×10^{-3} (11.6)	2.01×10^{-3} (15.6)
57b	1.94×10^{-4} (02.1)	1.60×10^{-4} (01.3)
58a	^c	^c
58b	1.69×10^{-4} (01.8)	9.59×10^{-4} (00.8)
59	1.01×10^{-3} (21.4)	
mass balance	73%	58%
P_1^∞ / P_2^∞	5.0	4.9
$k_2 \text{ ave}$	$6.7 \times 10^7 \text{ M}^{-1}\text{s}^{-1}$	$8.7 \times 10^7 \text{ M}^{-1}\text{s}^{-1}$

^a 9.4×10^{-3} mMol RHgCl added to 25 mL of 10.31 mM ketyl anion (54)

^b 1.29×10^{-2} mMol RBr added to 25 mL of 7.03 mM ketyl anion (54)

^c 58a and 57a not separable by G.C.

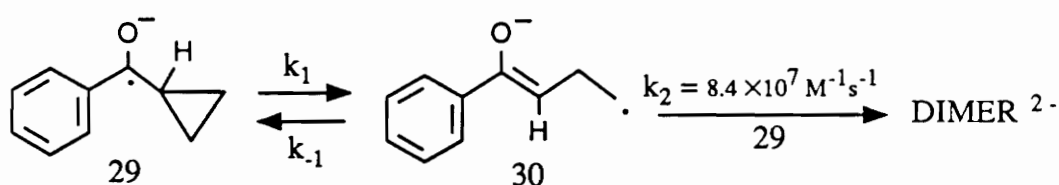
With k_2 and k_{obs} in hand, it is possible to estimate the equilibrium constant, K_1 , for the reversible ring opening of the ketyl anion to the distonic radical anion ($29 \rightleftharpoons 30$) (Eqn. 22).

Eqn. 22

$$\text{RATE} = \frac{k_1 k_2 [29]^2}{k_{-1} + k_2 [29]} \cong \frac{k_1 k_2 [29]^2}{k_{-1}} = K_1 k_2 [29]^2 = k_{\text{obs}} [29]^2$$

Also, a value for k_2 allows estimation of a minimum value for k_{-1} , the unimolecular rate constant for closing of the distonic radical anion to the ketyl anion ($30 \rightarrow 29$). This is possible because, for the calculated rate law to collapse to the observed rate law, dimerization must be the rate limiting step ($k_{-1} \geq 10k_2[29]$). Finally, with the equilibrium constant (K_1) and a minimum value for the reverse rate constant (k_{-1}), it is possible to estimate a maximum value for k_1 , the unimolecular rate constant for ring opening of the ketyl anion ($29 \rightarrow 30$). The results of this exercise are summarized in Table 13.

Table 13. Individual rate constants for the decay of phenyl cyclopropyl ketyl anion



cmpd	$k_{\text{obs}} (\text{M}^{-1}\text{s}^{-1})$	K_1^a	$k_{-1} (\text{s}^{-1})_{\text{min}}^b$	$k_1 (\text{s}^{-1})_{\text{max}}^c$
28a	3.9 ± 0.4	$4.6 \pm 1.2 \times 10^{-8}$	4.3×10^7	2.0

^a $K_1 = k_{\text{obs}}/k_2$

^b $k_{-1} \geq 10k_2[29]$, $[29]_{\text{max}} = 50 \text{ mM}$

^c $k_1 = K_1 k_{-1}$

The observed rate constants for decay of (28b^{•-}) and (28c^{•-}) could be broken apart in this same manner. However, our estimation for k_2 should only be applied to the primary distonic radical anion generated from phenyl cyclopropyl ketyl anion. Increased substitution on the cyclopropane ring β to the carbonyl would be expected to make the equilibrium constant (K_1) larger (i.e. stabilize the distonic radical anion), but make the rate constant for dimerization (k_2) smaller (i.e. steric bulk slows dimerization) relative to a substrate with no β substituents. Nevertheless, the large magnitude of k_2 and k_{-1} and the small magnitude of k_1 for decay of phenyl cyclopropyl ketyl anion allow similar conclusions to be extrapolated for the decay of the other systems (28b, 28c).

The data presented in Table 13 casts some serious doubt on the validity of using phenyl cyclopropyl ketones as electron transfer probes. The equilibrium constant for the reversible ring opening is on the order of 10^{-9} . This means that at equilibrium, for every one billion ketyl anions (29), only approximately one molecule exists in the ring open form (30). Also for that one distonic radical anion in a billion, any bimolecular reaction consuming it must proceed very rapidly to compete with the rapid unimolecular ring closing back to ketyl anion, or no ring opened products will be formed. Finally, the forward rate constant for ring opening of the ketyl anion is extremely small. This small forward rate constant causes equilibrium between the distonic radical anion (30) and ketyl anion (29) to be established very slowly; therefore, the estimation of one molecule in a billion existing in the ring open form at any given time is probably optimistic.

STEREOELECTRONIC EFFECTS IN RING CLEAVAGE

It is interesting to note that 1-benzoyl-1-methylcyclopropyl ketyl anion ($28e^-$) decays considerably slower than phenyl cyclopropyl ketyl anion ($28a^-$). The ketyl anion of 1-benzoyl-1-methylcyclopropane ($28e^-$) decays too slowly for its decomposition kinetics to be studied by derivative cyclic voltammetry. Based on the analogous electrolysis products isolated for the variously substituted phenyl cyclopropyl ketones (Figure 32, Table 9) and the structural similarity of ($28e^-$) to phenyl cyclopropyl ketone ($28a^-$) and its derivatives ($28b^-$, $28c^-$), we initially assumed that 1-benzoyl-1-methylcyclopropyl ketyl anion ($28e^-$) decayed via a rate law identical to that of the other substrates (Eqn. 22).

The sluggish decay of ($28e^-$) is not explained by thermodynamic considerations. The calculated enthalpy of ring opening of the ketyl anion of the α -methyl substituted derivative ($28e^-$) is about 2 kcal/mol more favorable than the corresponding ring opening for the unsubstituted case ($28a^-$) (Table 8). Also, there is no compelling reason to suspect that the activation barrier for the dimerization of the distonic radical anion with the ring closed ketyl anion would be significantly different for either substrate ($28a^-$) or ($28e^-$), since both involve coupling of a primary carbon centered radical with a ketyl anion. Thus, if the same rate law applies to the decay of both phenyl cyclopropyl ketyl anion ($28a^-$) and 1-benzoyl-1-methylcyclopropyl ketyl anion ($28e^-$), then the latter would be expected to decay at least as fast (if not faster) as ($28a^-$); however, this is not the case. Assuming bimolecular decay, digital simulation of experimental data for decay of 1-benzoyl-1-methylcyclopropyl ketyl anion places a maximum value of $0.04 \text{ M}^{-1}\text{s}^{-1}$ for the observed bimolecular rate constant^{82a}, a value which is two orders of magnitude smaller than the observed rate constant for decay of phenyl cyclopropyl ketyl anion (Table 5).

The discrepancy in reactivity yet similarity in products for the decay of 1-benzoyl-1-methylcyclopropyl ketyl anion ($28e^-$) and phenyl cyclopropyl ketyl anion ($28a^-$) might be explained by assuming that both decay by the same mechanism, but that the decay is described by different rate laws. The proposed mechanism for decay of phenyl cyclopropyl ketyl anions is reiterated in Figure 47. The calculated rate law for this mechanism, assuming distonic radical anion (30) to be a steady state intermediate, is given in equation 23.

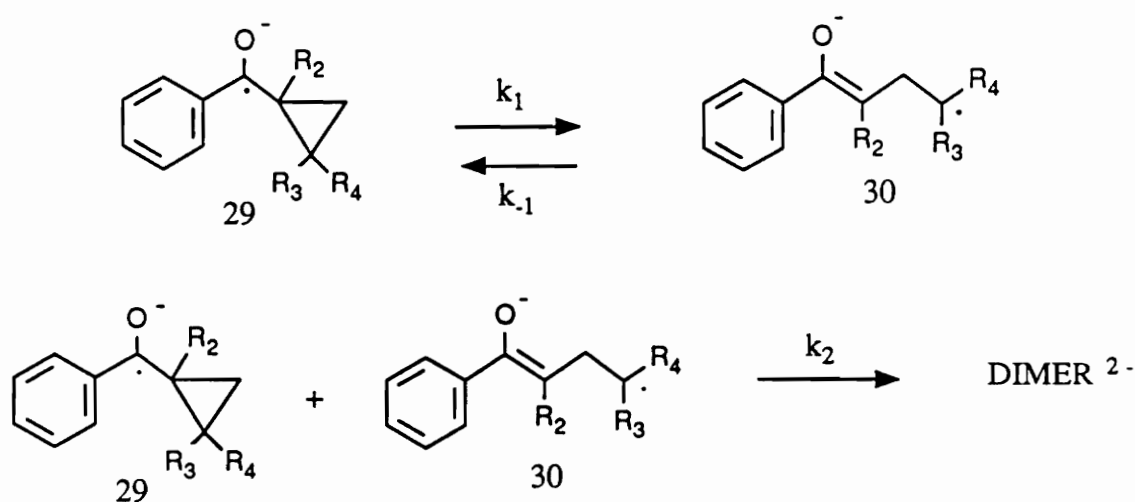


Figure 47. Proposed mechanism for decay of unsubstituted and alkyl substituted phenyl cyclopropyl ketyl anions

Eqn. 23

$$\text{RATE} = \frac{k_1 k_2 [29]^2}{k_{-1} + k_2 [29]}$$

For unsubstituted and alkyl-substituted phenyl cyclopropyl ketyl anions with only hydrogen on the cyclopropane α to the carbonyl group, dimerization is the rate limiting step (i.e. $k_{-1} \gg k_2[29]$). Therefore, the observed rate law for decay of these species collapses to $\text{Rate} = (k_1 k_2 / k_{-1}) [29]^2$ (vide supra). For 1-benzoyl-1-methylcyclopropyl ketyl

anion ($28e^-$), we believe that the rate limiting step is no longer dimerization, but instead ring opening of the ketyl anion (i.e. $k_2[29] \gg k_1$). Therefore, the observed rate law for decay of ($28e^-$) collapses to $\text{Rate} = k_1[29]$. Assuming this rate law is correct, digital simulation of experimental data places a maximum value for the observed rate constant at $k_{1(\text{max})} = 0.005 \text{ s}^{-1}$.^{82b} This rate constant is about four hundred times smaller than our estimate of the rate constant for unimolecular ring opening of phenyl cyclopropyl ketyl anion (Table 13).

Since the enthalpy of ring opening of 1-benzoyl-1-methylcyclopropyl ketyl anion ($28e^-$) is not significantly different from the enthalpy of ring opening of phenyl cyclopropyl ketyl anion ($28a^-$), the activation energies for the two processes must be quite different. This hypothesis is expressed pictorially in Figures 48 and 49. Figure 48 depicts the reaction coordinate where dimerization is the rate limiting step for decay of the ketyl anion. Once the distonic radical anion (**30**) is formed, it must partition itself between returning to ketyl anion and going on to product. If the activation energy for product formation ($E_a(2)$) is larger than the activation energy for returning to the ketyl anion ($E_a(-1)$), dimerization is the rate limiting step and second order decay of the ketyl anion will be observed. Note that in this preequilibrium scenario, the magnitude of the activation energy for opening of the ketyl anion ($E_a(1)$) is not important. Figure 48 could be used to describe the decay of ($28a^-$), ($28b^-$), and ($28c^-$).

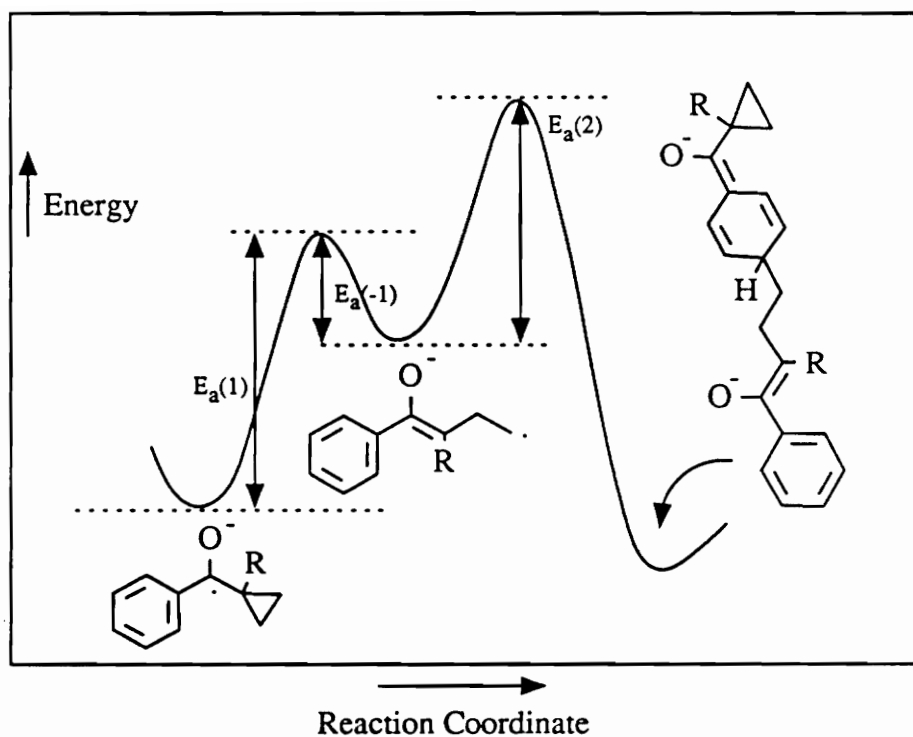


Figure 48. Plot of energy vs. reaction coordinate for the decay of phenyl cyclopropyl ketyl anions where dimerization is the rate limiting step

Figure 49 depicts the reaction coordinate where opening of the ketyl anion to the distonic radical anion is rate limiting. Again, once the distonic radical anion (30) is formed, it must partition itself between proceeding on to product and closing to the ketyl anion. In this instance however, the activation barrier for ring closure ($E_a(-1)$) is large relative to the activation barrier for dimerization ($E_a(2)$). Consequently, the magnitude of the activation energy for opening of the ketyl anion ($E_a(1)$) is large, and ring opening is the rate limiting step for decay of the ketyl anion. We believe that Figure 49 accurately describes the decay of ($28e^-$). The switch in the rate limiting step for the decay of 1-benzoyl-1-methylcyclopropyl ketyl anion ($28e^-$) can be explained as a stereoelectronic effect.

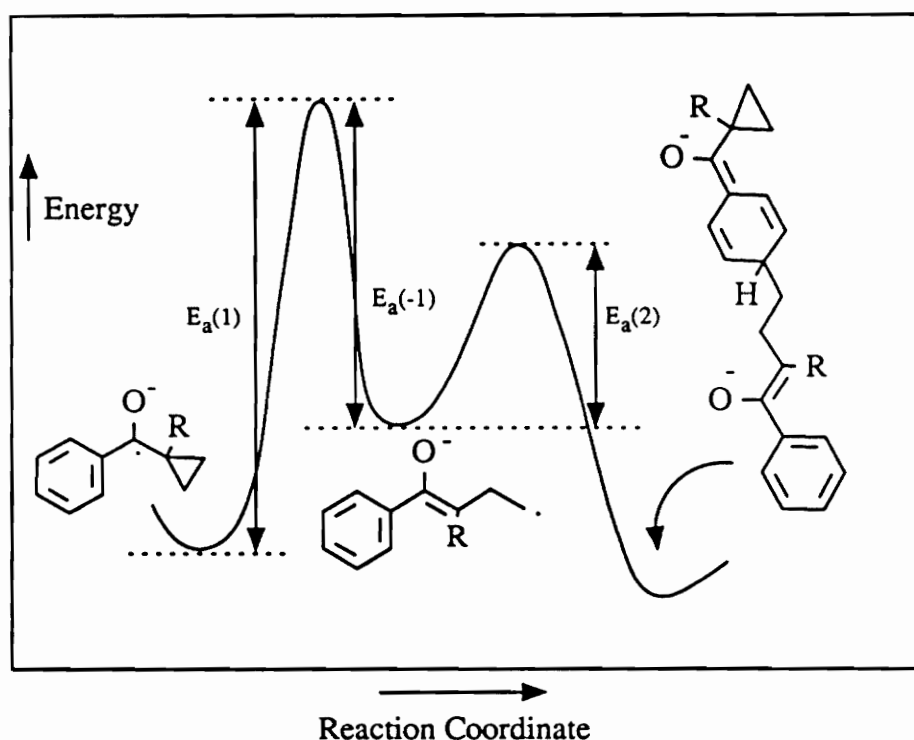


Figure 49. Plot of energy vs. reaction coordinate for the decay of phenyl cyclopropyl ketyl anions where cyclopropane ring opening is the rate limiting step

Cyclopropane can be envisioned as being built from three sp^2 hybridized methylene carbons with one sp^2 hybrid of each carbon pointing toward the center of the three membered ring and three unhybridized p orbitals laying in the plane of the cyclopropane ring⁸³ (Figure 50).

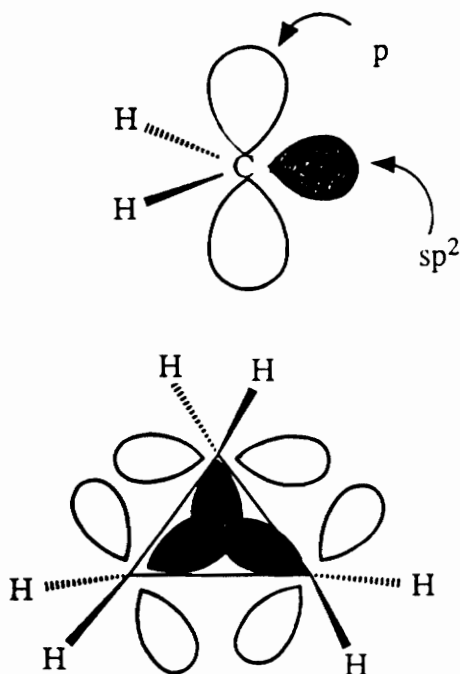


Figure 50. Walsh (Sugden) model for cyclopropane

Therefore, cyclopropane has a π system but it is unlike conventional π systems because it lies in the plane of the ring not orthogonal to it. Cyclopropane can adopt two extreme conformations with respect to an adjacent π system^{83d} (Figure 51). In the bisected conformation, the p orbitals of cyclopropane are aligned with the adjacent π system allowing for good electronic communication between the two moieties. In the perpendicular conformation, the p orbitals of cyclopropane are orthogonal to the p orbitals of the adjacent π system, effectively electronically insulating the two moieties from each other. In general, the bisected conformation is preferred because of favorable interactions

between the cyclopropyl HOMO and benzoyl LUMO, but steric considerations sometimes necessitate that the cyclopropane adopt a perpendicular conformation (or some conformation intermediate between bisected and perpendicular).^{83d,84}

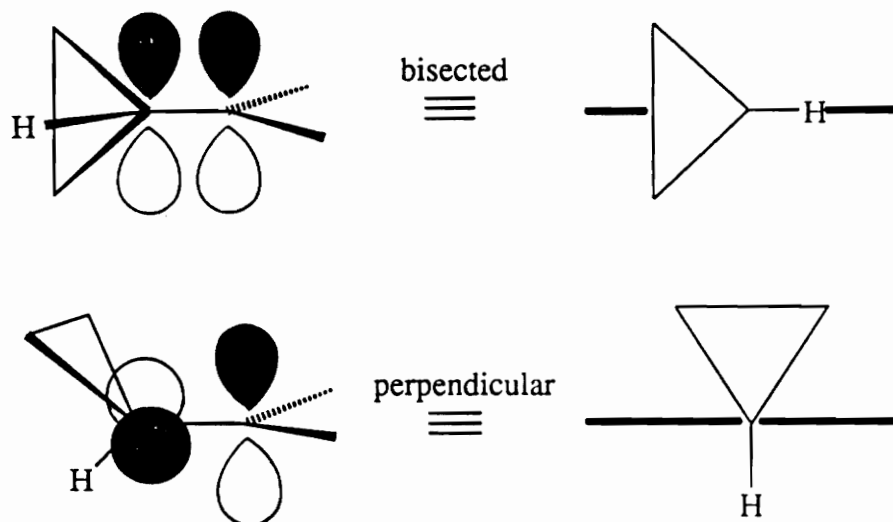


Figure 51. Conformations of cyclopropane relative to an adjacent π system

We propose that the difference in reactivity between 1-benzoyl-1-methylcyclopropyl ketyl anion (**28e⁻**) and phenyl cyclopropyl ketyl anion (**28a⁻**) can be explained by a difference in the conformation of the cyclopropane ring with respect to the benzoyl group.⁶³ For ketyl anions in the bisected conformation, the π component of the vicinal cyclopropyl bonds (C_1-C_2 and C_1-C_3) is aligned with the π -system of the benzoyl group. This alignment of the π -systems allows a transition state for cyclopropane ring opening which is stabilized by the adjacent benzoyl group. In the perpendicular conformation, the π component of the vicinal cyclopropyl bonds is orthogonal to the π -system of the adjacent benzoyl group; therefore, the transition state for cyclopropyl ring opening is not stabilized by the benzoyl group and the rate of ring opening is retarded (Figure 52).

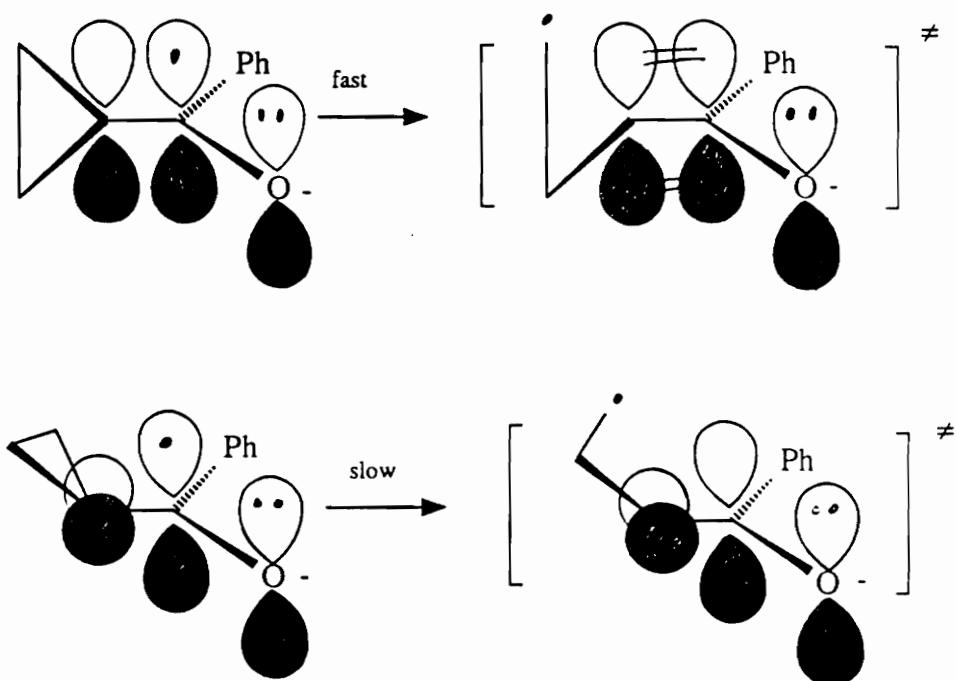


Figure 52. Effect of conformation on the rate of ring opening of cyclopropyl ketyl anions

The AM1⁷⁸ minimized geometries for the radical anions of phenyl cyclopropyl ketone (**28a^{•-}**) and 1-benzoyl-1-methylcyclopropane (**28e^{•-}**) are shown in Figures 53 and 54. Phenyl cyclopropyl ketyl anion exists in a *s-cis* bisected conformation⁸⁵ which allows for good electronic communication between the benzoyl group and the cyclopropane and therefore facile ring opening (i.e. low activation energy).

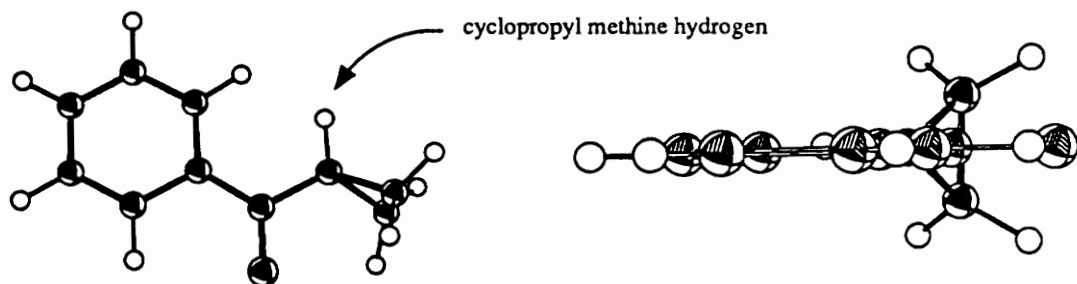


Figure 53. AM1 calculated least energy geometry for phenyl cyclopropyl ketyl anion (**28a^{•-}**)

The ketyl anion of 1-benzoyl-1-methylcyclopropane prefers a perpendicular conformation. In this conformation, the benzoyl group and cyclopropane ring are electronically insulated from each other. Ring opening of this isomer is stereoelectronically turned off (i.e. high activation energy).

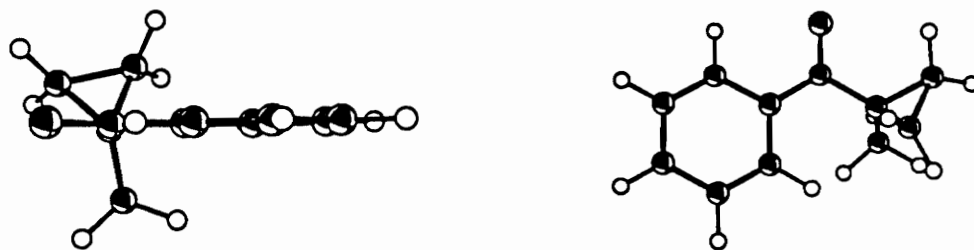


Figure 54. AM1 calculated least energy geometry for 1-benzoyl-1-methylcyclopropyl ketyl anion ($28e^-$)

In summary, the rate law and rate constant for decay of 1-benzoyl-1-methylcyclopropyl ketyl anion ($28e^-$) have not been experimentally determined. Based upon observation that the rate of decay of ($28e^-$) does not fit the trend established by the rates of decay of ($28a^-$), ($28b^-$), and ($28c^-$), but that the products of decay of all of these ketyl anions are analogous, we propose a change in the rate limiting step for decay of ($28e^-$) from dimerization to cyclopropane ring opening. A stereoelectronic effect has been used to rationalize the stark difference in reactivity of this ketyl anion. We propose that the rate law for decay of ($28e^-$) in anhydrous DMF is unimolecular with a maximum rate constant of $k_{1(max)} = 0.005 \text{ s}^{-1}$. Work in our laboratory is currently being pursued to confirm or disprove these conjectures. Kinetic techniques such as chronoamperometry and coulometry (by itself and coupled with UV or EPR) have the necessary "time window" to examine the decay of species with long half-lives such as ($28e^-$).

SUMMARY

In this chapter it has been shown that phenyl cyclopropyl ketyl anions with no substituents or alkyl substituents on the cyclopropane ring undergo a slow reversible bimolecular decay. The ketyl anions ring open slowly and reversibly with the equilibrium constant highly favoring the ring closed form. Based upon the results presented in this chapter, it can be shown that these substrates will fail to detect electron transfer reaction mechanisms.

Suppose that phenyl cyclopropyl ketone (**28a**) is treated with a reagent, Y^- , which definitely reacts with ketones by electron transfer (Figure 55). Following the electron transfer, the first distinct entity along the reaction pathway is a caged pair consisting of the ketyl anion (**29a**) and neutral radical, Y^\cdot . If coupling of the ketyl anion and radical occurs within the cage, the only product observed will be ring closed species (**60**, path a). The lifetime of a cage is on the order of picoseconds⁸⁷ while the lifetime of the radical anion towards ring opening is on the order of seconds. Thus, the ketyl anion will not have time to ring open if coupling occurs within the cage.

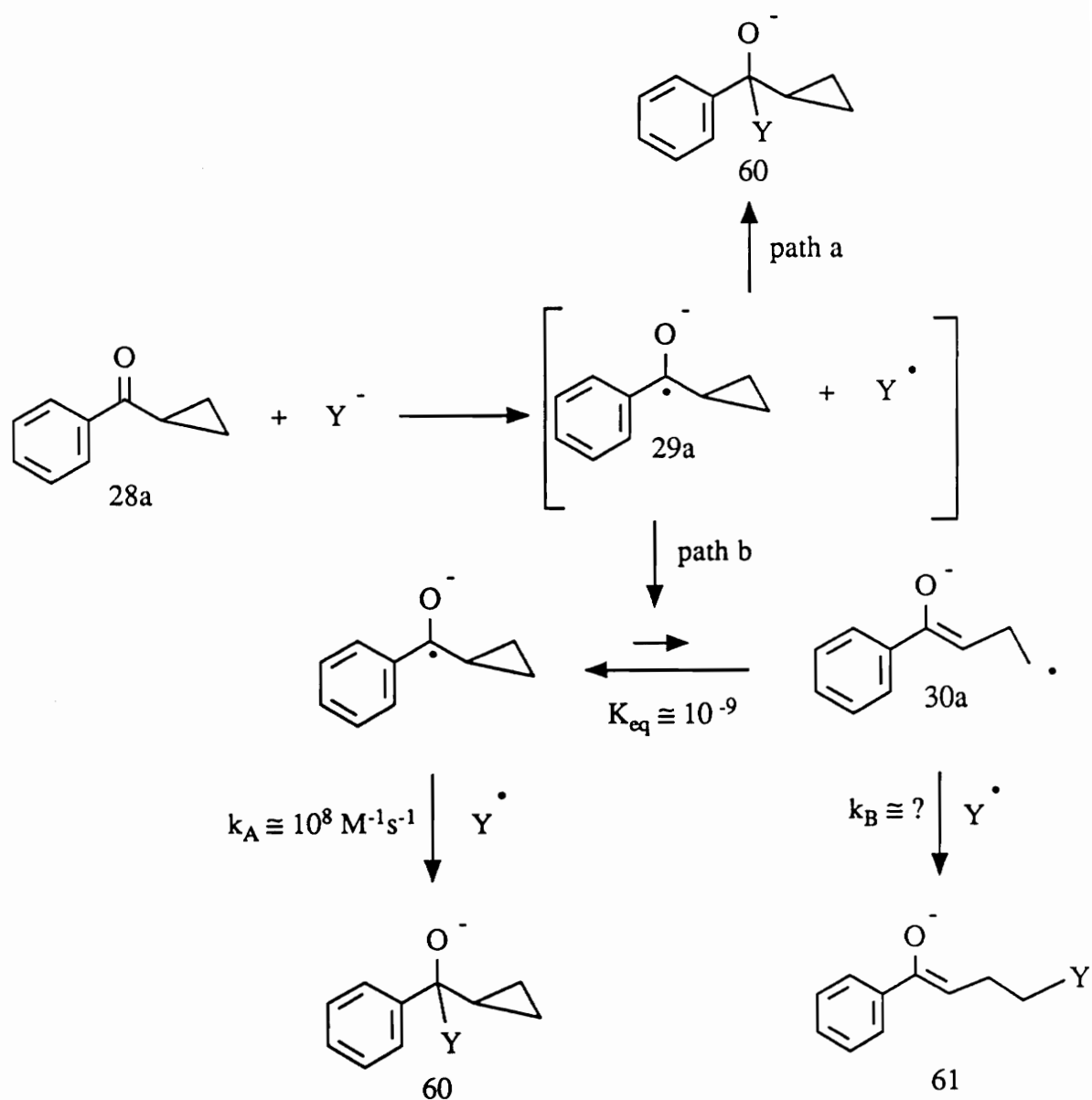


Figure 55. Electron transfer reaction mechanism involving phenyl cyclopropyl ketone

Perhaps the geometry of the reagents in the cage is not correct for adduct formation, so they diffuse apart into bulk solution (path b). Now the ketyl anion (29a) can equilibrate with its ring opened form. At equilibrium the concentration of the ring closed species (29a) is approximately one billion times greater than the concentration of the ring

opened species (30a). In order to observe any ring opened adduct (61) in the final reaction mixture, the rates of formation of the ring closed and ring opened adducts must be at least comparable in magnitude. To keep the rate of formation of the ring opened adduct similar to the rate of formation of the ring closed adduct, the bimolecular rate constant for coupling of the distonic radical anion (30a) with $Y\cdot$ must make up for the huge concentration difference between ring closed and ring opened radical anions (i.e. $k_A[29a] \cong k_B[30a]$). The rate constant for formation of the ring closed adduct is fairly large, $k_A \cong 10^8 \text{ M}^{-1}\text{s}^{-1}$ (if $Y\cdot$ is a primary carbon centered radical); the rate constant for formation of ring opened adduct must be about nine orders of magnitude larger, $k_B \cong 10^{8+9} = 10^{17} \text{ M}^{-1}\text{s}^{-1}$, in order to observe any ring open adduct at all. This rate constant, $k_B = 10^{17} \text{ M}^{-1}\text{s}^{-1}$, is clearly ridiculous. It is about seven orders of magnitude above the diffusion controlled limit. Therefore, even though the reaction definitely proceeds through an electron transfer mechanism, no ring opened product would be observed. Needless to say, phenyl cyclopropyl ketone and its alkyl substituted analogs are not reliable rearrangement probes for electron transfer processes.

CHAPTER 3. DEVELOPMENT AND STUDY OF POTENTIAL ELECTRON TRANSFER PROBES

INTRODUCTION

Although unsubstituted and alkyl substituted phenyl cyclopropyl ketones are unreliable probes for electron transfer, we envisioned several potentially reliable electron transfer probes involving ring opening of "appropriately substituted" cyclopropyl containing ketyl anions. Two basic design strategies were pursued. The first was to move the cyclopropane elsewhere in the molecule in hopes of locating a carbon center with higher spin density than the ketyl carbon to attach the cyclopropane to. The second was to preserve the phenyl cyclopropyl ketone structure but to substitute the cyclopropane with groups capable of stabilizing the distonic radical anion through resonance interactions.

In this chapter, the design and study of three substrates is discussed. Unlike the previous chapter, each substrate will be treated individually because of the unique and diverse chemistry that each exhibits.

p-CYCLOPROPYL ACETOPHENONE

p-Cyclopropyl acetophenone (**62**) was chosen for study because its corresponding ketyl anion might possess considerable spin density α to the cyclopropyl group. Aromatic ketyl anions are expected to exhibit extensive delocalization of the unpaired electron (Figure 56).

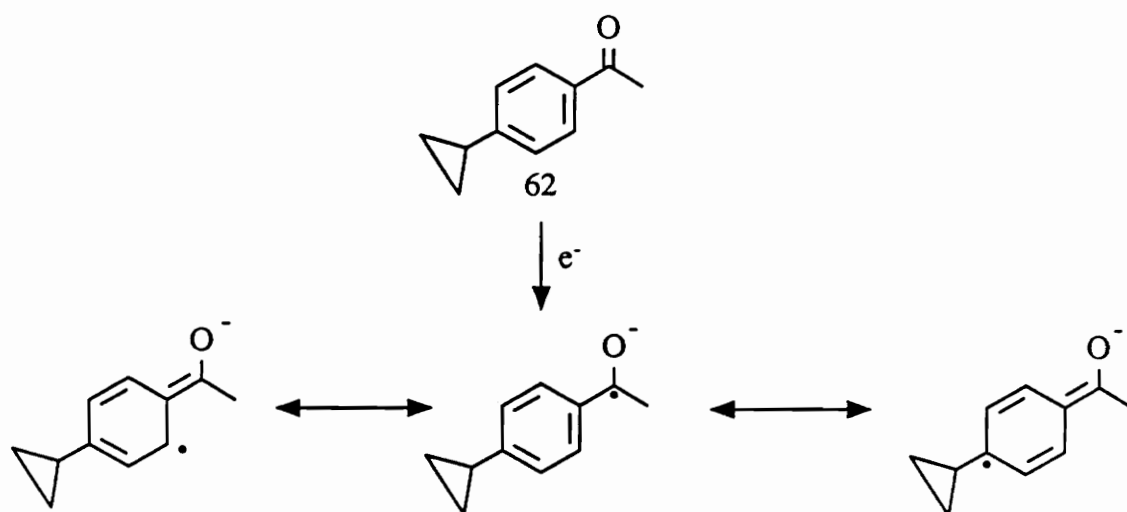
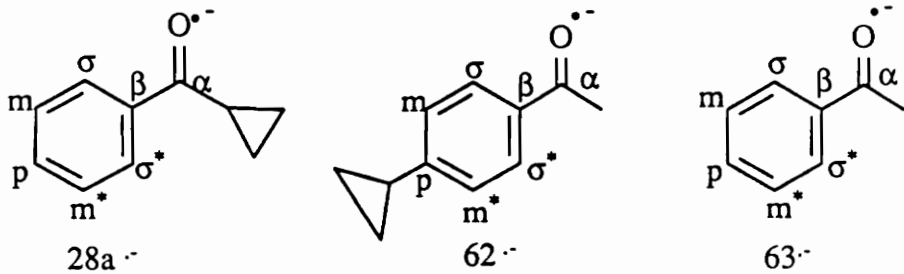


Figure 56. Resonance structures of p-cyclopropyl acetophenone ketyl anion (**62^{•-}**)

The head to tail dimers, trimers, and tetramers obtained from electrolysis of phenyl cyclopropyl ketones (**28a**), (**28b**), (**28c**), and (**28e**) illustrate that considerable spin density exists at the para position of these aromatic ketyl anions (Figure 32). If the para carbon of (**62^{•-}**) possesses high spin density, opening of a cyclopropane at this position might be expected to be rapid. Calculation⁷⁸ of atomic orbital spin populations (ρ^{π_i}) in the p_z orbitals (π system) of phenyl cyclopropyl ketyl anion (**28a^{•-}**) and p-cyclopropyl acetophenone ketyl anion (**62^{•-}**) are reported in Table 14. In both cases, the extra electron

is highly delocalized with considerable spin density at the para position. These calculations parallel the experimentally observed distribution of spin density for acetophenone ketyl anion (**63**^{•-}, Table 14).⁸⁸ The AM1⁷⁸ calculated enthalpy of ring opening of (**62**^{•-}) is endothermic by 1.6 kcal/mol, 6.3 kcal/mol more favorable than ring opening of phenyl cyclopropyl ketyl anion (**28a**^{•-}) (see Table 8).

Table 14. AM1^a calculated atomic orbital spin populations (ρ^{π_i}) in the p_z orbitals of phenyl alkyl and phenyl cyclopropyl ketyl anions



	$ a^{\text{H}_i} $ (Gauss)	p_z orbital spin populations (ρ^{π_i})		
	^b 63 ^{•-}	^c 63 ^{•-}	^a 28a ^{•-}	^a 62 ^{•-}
O	---	---	0.242	0.211
C α	6.735	0.248	0.114	0.072
C β	---	---	0.058	0.129
C σ	3.712	0.157	0.311	0.251
C σ^*	4.251	0.179	0.345	0.303
C m	0.875	0.037	-0.254	-0.202
C m^*	1.070	-0.045	-0.291	-0.256
C p	6.597	0.278	0.465	0.455

^a AM1 implemented through MOPAC ver. 5.0 (QCPE #455). Full geometry optimizations were performed at the UHF level.

^b measured from EPR spectrum of acetophenone ketyl anion in DMF/*n*-Bu₄NClO₄; see Steinberger, N., Fraenkel, G., *J. Chem. Phys.*, 1964, 40(3), 723.

^c calculated from experimentally observed hyperfine splittings using the McConnell equation, see reference in footnote b and also Bolton, J., in "Radical Ions", Kaiser, E., Kevan, L., eds., Interscience, 1968, pp. 1-33; $a^{\text{H}_i} = 23.7(\rho^{\pi_i})$ except for methyl proton splitting where $a^{\text{H}_i} = 27.2(\rho^{\pi_i})$.

We were disappointed to find that in anhydrous DMF containing 0.5 M $n\text{-Bu}_4\text{NBF}_4$ ($62^{\cdot-}$) underwent an apparent slow, bimolecular decay.⁸⁹ Due to the sluggish decay of the ketyl anion, it is not rigorously correct to apply the DCV reaction order approach to *p*-cyclopropyl acetophenone in the concentration range available to us for study ($C_A \leq 50$ mM). A reaction order plot with $R_{\text{DCV}} = 0.82$ (usable range $R_{\text{DCV}} = 0.25 - 0.70$)^{76a} is however shown in Figure 57. Assuming that a bimolecular decay of the radical anion is occurring (EC_{DIM}), we can estimate the rate constant for its decay to be $k_{\text{obs}} = 2.8 \pm 1.3 \text{ M}^{-1}\text{s}^{-1}$.^{72,73} The reduction potential of this substrate as measured by cyclic voltammetry is -2.482 V (vs. Ag/Ag^+) in anhydrous DMF at a gold electrode.⁸⁹

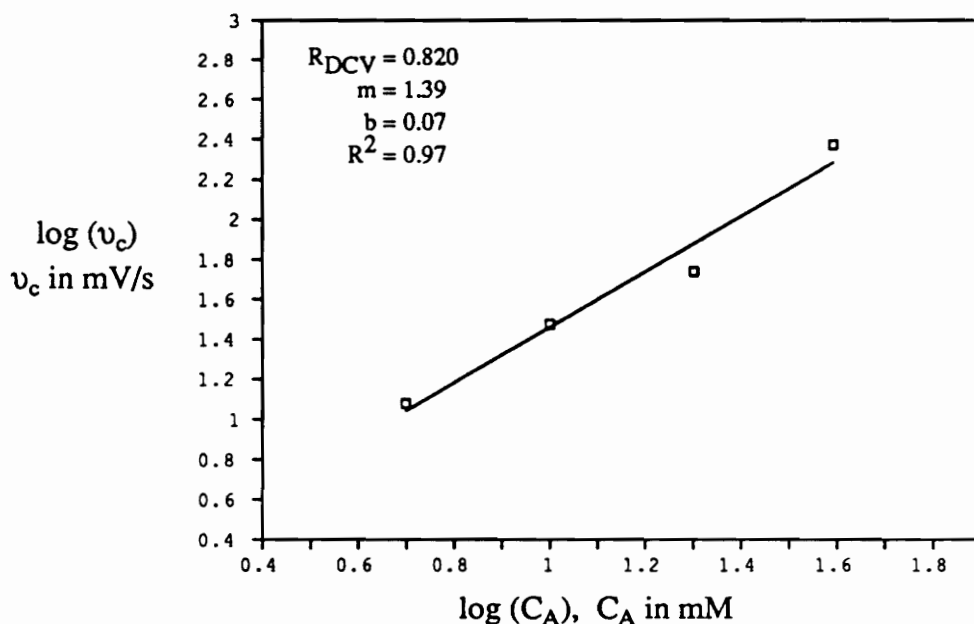
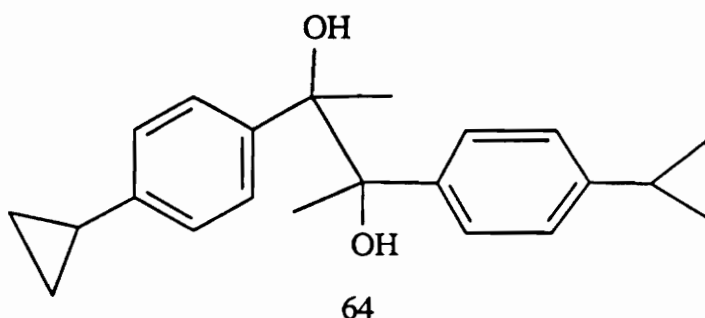


Figure 57. DCV reaction order plot for *p*-cyclopropyl acetophenone (62)

Constant current electrolysis (1 equivalent of electrons) of *p*-cyclopropyl acetophenone in anhydrous DMF at a gold electrode yielded starting material (22%) and a dimer product (40%). The product (**64**) was a simple pinacol dimer with the cyclopropane rings intact.



The above experiments show that despite calculational results which hint at the contrary, *p*-cyclopropyl acetophenone ketyl anion is not a good rearrangement probe for electron transfer. If cyclopropane ring opening does occur, it must be at least an order of magnitude slower than the rate of pinacolization for this substrate. Increasing steric bulk α to the carbonyl would slow the rate of pinacolization and possibly allow study of any chemistry that the cyclopropyl moiety might be undergoing. This was not pursued. Any ring opening of a ketyl anion of this basic structure is too slow to be of use as an electron transfer rearrangement probe.

Our results for the decay of *p*-cyclopropyl acetophenone ketyl anion suggest that 4-cyclopropylnitrobenzene would also be a poor probe for detection of electron transfer reaction mechanisms. 4-Cyclopropylnitrobenzene (**65**) has been used to help rule out an electron transfer mechanism in favor of a nucleophilic addition for the fluoride catalyzed coupling of silyl enol ethers and aromatic nitro compounds (Figure 58).⁹⁰ Since no products with the cyclopropane ring opened were isolated, an electron transfer reaction mechanism was discounted.

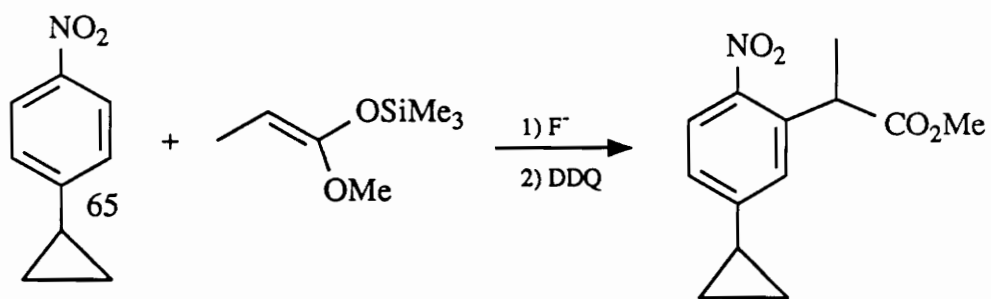


Figure 58. Fluoride catalyzed addition of silyl enol ethers to 4-cyclopropylnitrobenzene (65)

trans-1-BENZOYL-2-PHENYLCYCLOPROPANE

With the previous results in mind, we decided to return to the basic phenyl cyclopropyl ketone substrate, but to substitute the cyclopropane moiety with good resonance stabilizing groups. As demonstrated earlier by both electrolysis⁶⁸ and chemical reduction,⁶⁵ substitution of a phenyl group on the cyclopropane ring (**66**) is expected to facilitate ring opening of the ketyl anion because the resulting distonic radical anion (**68**) is stabilized (Figure 59). The AM1⁷⁸ calculated enthalpy of ring opening of trans-1-benzoyl-2-phenylcyclopropyl ketyl anion (**67**) is exothermic by 5.9 kcal/mol.

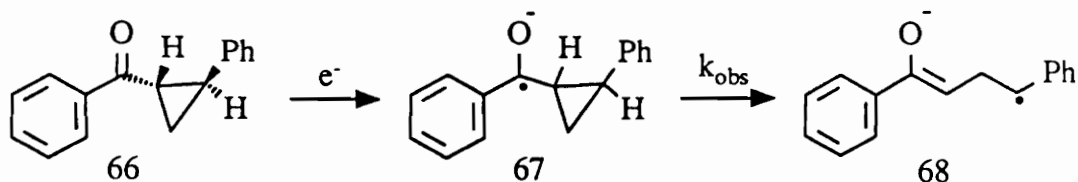


Figure 59. Ring opening of 1-benzoyl-2-phenylcyclopropyl ketyl anion (**67**)

The decay of (**67**) proved to be too fast for DCV reaction order analysis with our current equipment. LSV analysis of the decay of (**67**) at a gold electrode in anhydrous DMF containing 0.5 M $n\text{-Bu}_4\text{NBF}_4$ yielded $\delta E_p/\delta \log(v) = 33.4 \pm 1.3$ and $\delta E_p/\delta \log(C_A) = -2.7 \pm 1.7$, indicating that the radical anion decays by a unimolecular process that is first order in ketyl anion and zero order in ketone, $\text{Rate} = k_{obs}[\mathbf{67}]$ (see Table 4 for theoretical responses). Figures 60 and 61 show typical linear sweep voltammetry reaction order plots for this substrate.

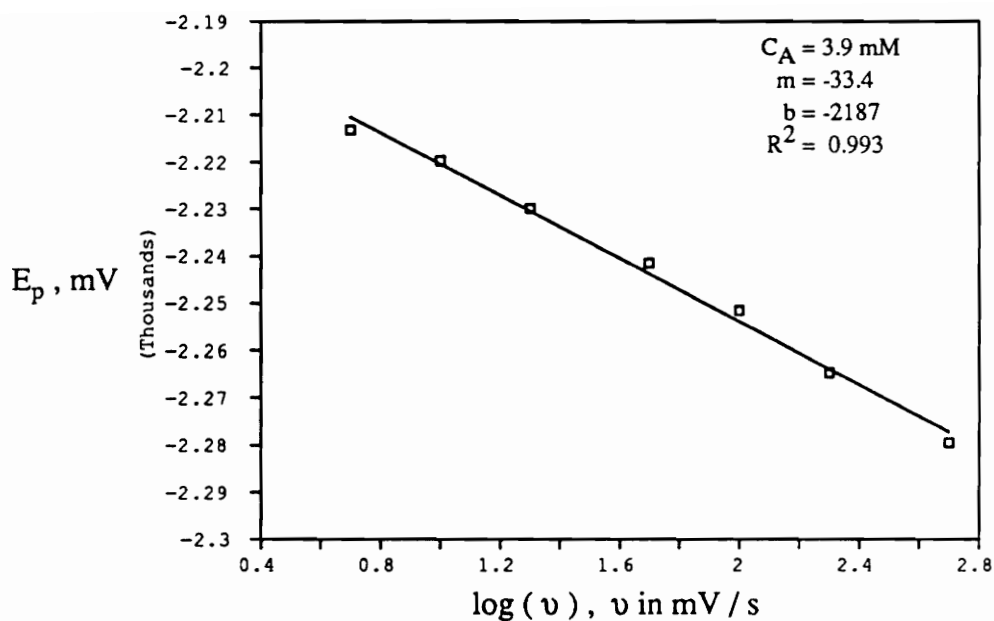


Figure 60. Linear sweep voltammetry reaction order plot for decay of 1-benzoyl-2-phenylcyclopropyl ketyl anion (67)

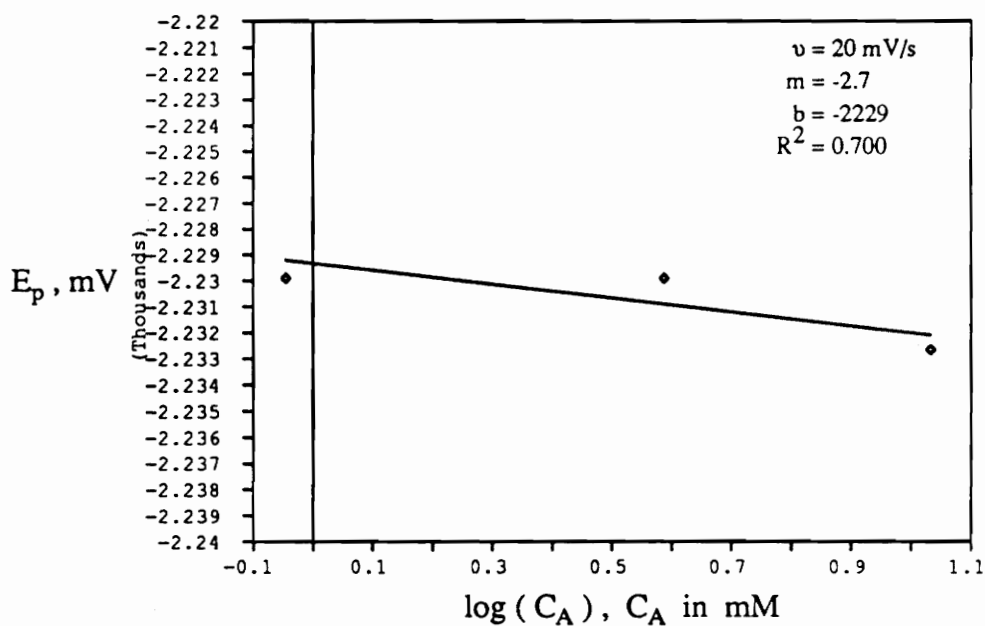


Figure 61. Linear sweep voltammetry reaction order plot for decay of 1-benzoyl-2-phenylcyclopropyl ketyl anion (67)

No reverse wave corresponding to the oxidation of (67) was observed by cyclic voltammetry, even at high sweep rates ($v \leq 50$ V/s) and low temperatures ($T \geq -20^\circ\text{C}$). The cyclic voltammetry peak potential at $v = 50$ mV/s was approximately -2.24 V (Ag/Ag⁺).⁸⁹ Since no reverse current is observed, we cannot unambiguously assign the rate constant for the decay of 1-benzoyl-2-phenylcyclopropyl ketyl anion (67), but we can bracket it using digital simulation. The lower limit for the unimolecular rate constant for ring opening can be estimated by simulating the proposed mechanism of decay (EC) of the ketyl anion and decreasing the homogeneous rate constant until a reverse wave (ketyl oxidation) is observed. The largest rate constant which gives some reverse current is taken to be the lower limit of the rate constant for decay of the ketyl anion. We estimate the lower limit of the unimolecular rate constant for decay of (67) to be 10^3 s⁻¹.^{91a}

An upper limit for the unimolecular rate constant can also be estimated. A plot of the simulated cathodic peak potential less the true reduction potential ($E_{pc} - E^0$) vs. log of the homogeneous rate constant is shown in Figure 62 for the proposed mechanism of decay of the ketyl anion (EC mechanism). If the true reduction potential (E^0) of the ketone were known, the rate constant for decay of the ketyl anion could be read directly from the graph by measuring only the cathodic peak potential (E_{pc}) from a LSV experiment. The catch is that the true reduction potential of the ketone is not known because the ketyl anion decays so quickly that a reliable value cannot be measured. However, it is reasonable to assume that the reduction potential of phenyl cyclopropyl ketone, 28a (-2.42 V (Ag/Ag⁺), see Table 2), is a lower limit for the reduction potential of trans-1-benzoyl-2-phenylcyclopropane, 66 (i.e. 28a is just as hard (if not harder) to reduce as 66).⁹² Using the experimentally observed cathodic peak potential, $E_{pc} = -2.24$ V ($v = 50$ mV/s), and the estimated lower limit for the true reduction potential ($E^0 = -2.42$ V), the upper limit for the rate constant of decay of 1-benzoyl-2-phenylcyclopropyl ketyl anion (67) can be estimated at 10^7 s⁻¹. Thus, the rate constant for decay of (67) lies in the range

of 10^3 - 10^7 s⁻¹.

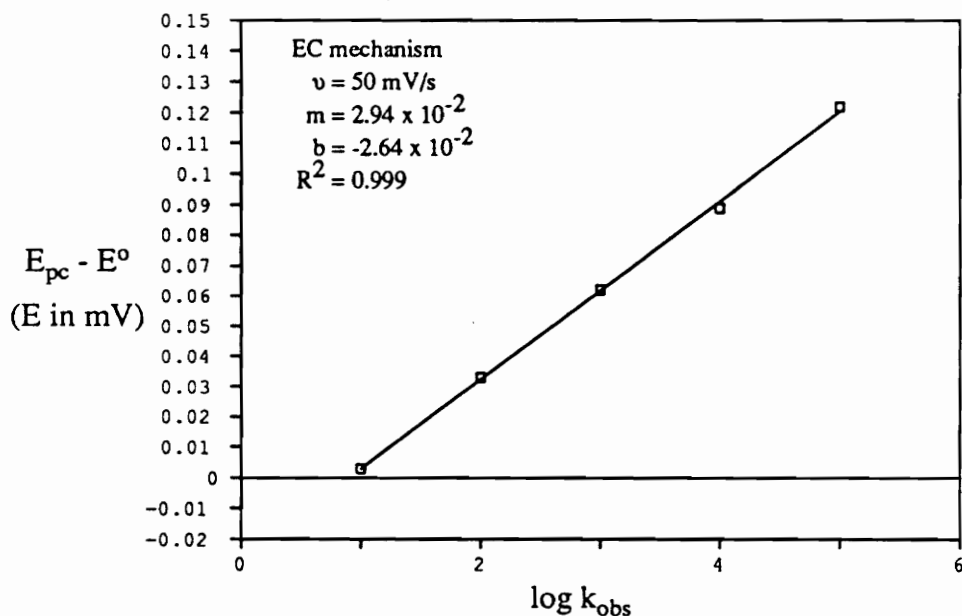


Figure 62. Working curve for estimation of the upper limit of the unimolecular rate constant for ketyl anion decay

Controlled potential electrolysis of (66) (1.6 equivalents of electrons) at a gold electrode in anhydrous DMF yielded 21% recovered starting material and 73% γ -phenylbutyrophenone (71). We envision (71) to be formed through a mechanism such as the one depicted in Figure 63. Ring opening of the ketyl anion (67) yields distonic radical anion (68). The distonic radical anion is then rapidly reduced to the dianion (69) because the reduction potential of the newly created benzyl radical (-1.77 V vs. Ag/Ag⁺(0.1M))⁹³ is considerably more positive than the reduction potential of the starting ketone. Since ring opening (67 \rightarrow 68) is the rate determining step, it is not possible to distinguish whether a heterogeneous (ECE, 68 + e⁻ \rightarrow 69) or a homogeneous (ECE_h, 67 + 68 \rightarrow 66 + 69) electron transfer yields the dianion.⁹⁴ Nonetheless, the dianion is not long lived. The benzyl anion is a potent base and is rapidly protonated. The enolate (70) is

stable until work up.

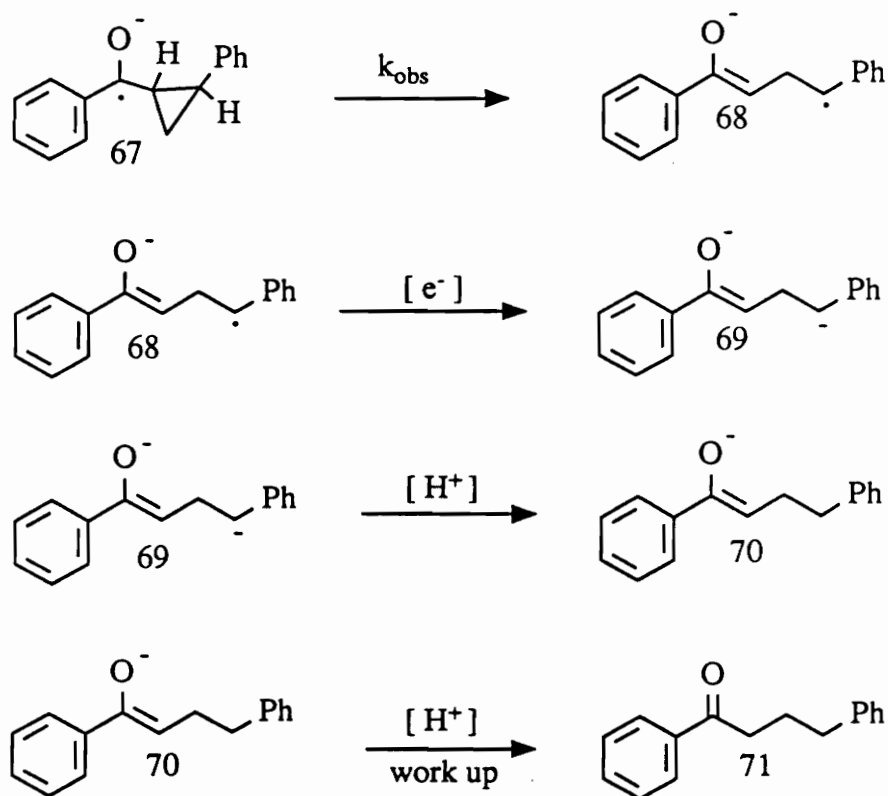


Figure 63. Proposed mechanism for the decay of 1-benzoyl-2-phenylcyclopropyl ketyl anion (67)

Controlled current electrolysis of (66) (0.68 equivalents of electrons) at a gold electrode in anhydrous DMF followed by a methyl iodide quench gave the products shown in Figure 64 plus 54% recovered starting material. Products (72) and (73) arise from methylation of the ring opened enolate (70) but product (74) must arise from the enolate of starting material.

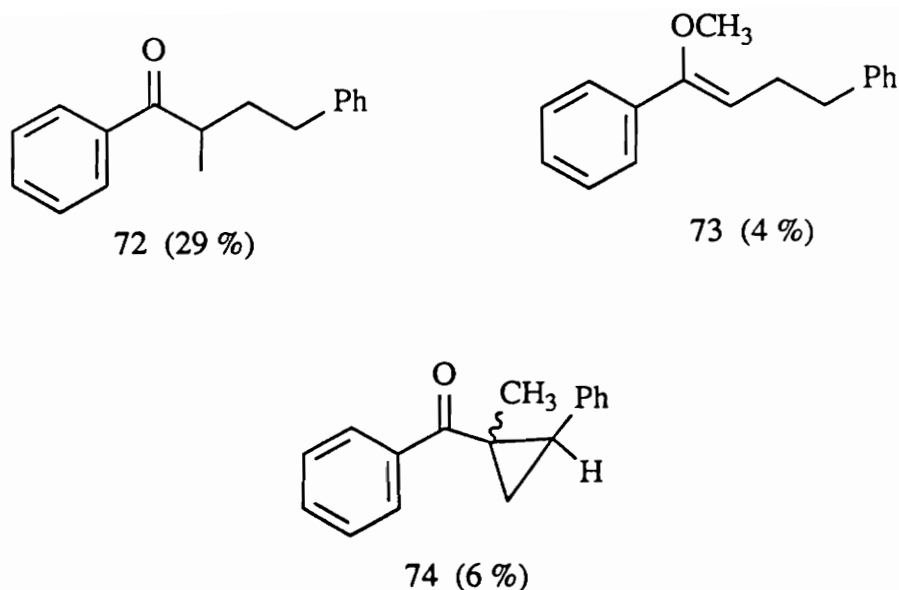


Figure 64. Results of methyl iodide quench after electrolysis of trans-1-benzoyl-2-phenylcyclopropane (66)

Controlled current electrolysis of 1-benzoyl-1-deuterio-2-phenylcyclopropane (**75**) (1.5 equivalents of electrons) at a gold electrode in anhydrous DMF yielded the results shown in Figure 65. Recovered starting material (25%) maintained only 10% of its deuterium label. The ring opened product (71%) contained 11% deuterium label. The deuterium in the ring opened product was shown to be distributed between the positions α and γ to the carbonyl in a ratio of 2.5 : 1 by deuterium NMR. The results of electrolysis of (**66**) followed by a MeI quench and the electrolysis of (**75**) show that the enolate (**70**) is stable under our reaction conditions but the benzylic anion (**69**) is not, and that starting ketone is a source of protons (albeit a small source) for quenching of the benzylic anion. Other researchers have shown that tetraalkyl ammonium salts (i.e. the supporting electrolyte) readily protonate potent bases such as a benzylic anion.^{79a-c}

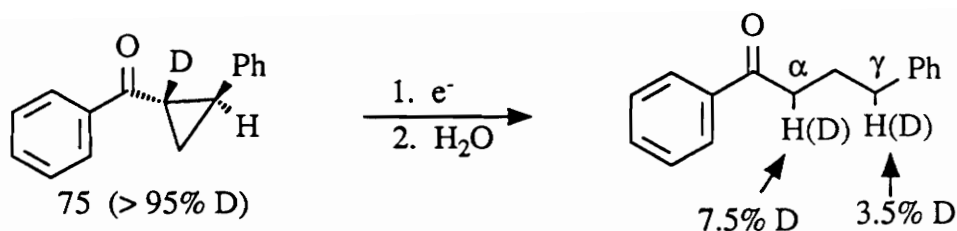


Figure 65. Results of electrolysis of 1-benzoyl-1-deuterio-2-phenylcyclopropane (75)

CV experiments on trans-1-benzoyl-2-phenylcyclopropane (66) reveal an anodic wave far positive of the reduction wave for the starting ketone (Figure 66). We have ascribed this anodic wave to oxidation of the ring opened enolate (vide infra). The oxidation of enolates has been studied in attempts to correlate their oxidation potentials to quantities such as homolytic bond dissociation energies^{95a} and pKa's of their conjugate acids^{95b}, as well as to the feasibility of enolates to act as single electron donors instead of nucleophiles.^{30c,95c} Although similar reduction potentials are not sufficient criteria to assign the nature of our anodic wave, it is satisfying to note that the oxidation potential of the sodium enolate of phenyl acetone ($\text{Ph}(\text{CH}_3\text{CO})\text{CH}^-\text{Na}^+$) at a mercury coated platinum electrode is -0.54 V (vs. Ag/Ag^+).^{30c}

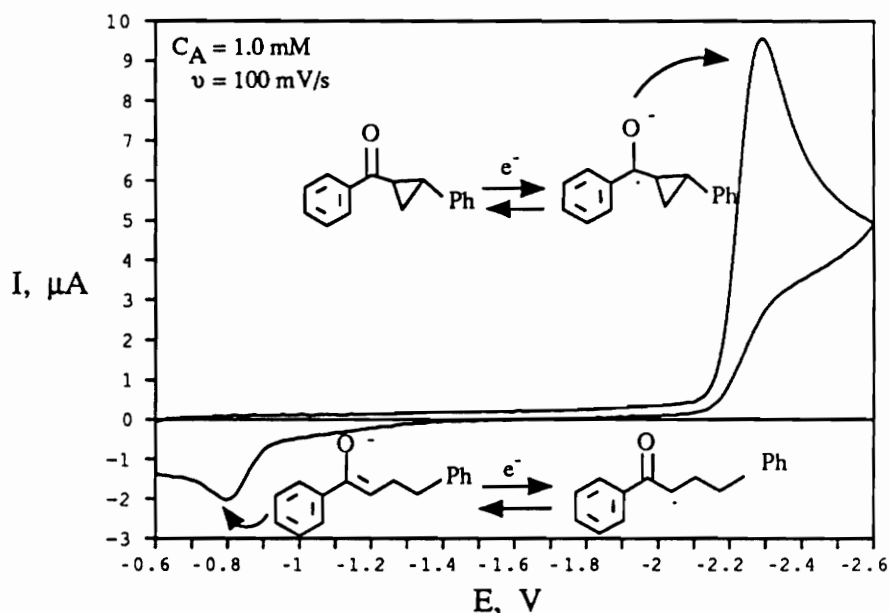


Figure 66. Cyclic voltammogram of trans-1-benzoyl-2-phenylcyclopropane (**66**)

We have experimentally shown that the "new" anodic wave is due to the ring opened enolate (**70**). An electrolysis of (**66**) was monitored with cyclic voltammetry. As the peak corresponding to reduction of the ketone diminished, the peak ascribed to oxidation of the enolate grew (Figure 67). Quenching with methyl iodide destroyed the anodic peak ascribed to the enolate and yielded methylated products arising from (**70**) which were analogous to those reported earlier in this section for electrolysis of (**66**) followed by a methyl iodide quench. The electrolytic reduction of "appropriately substituted" phenyl cyclopropyl ketones appears to provide a convenient and novel method to generate enolates in the presence of a host of different counterions. This methodology could prove to be useful for generation of enolates for synthetic purposes and/or for generating enolates to study the effect of ion pairing on their reactivity.

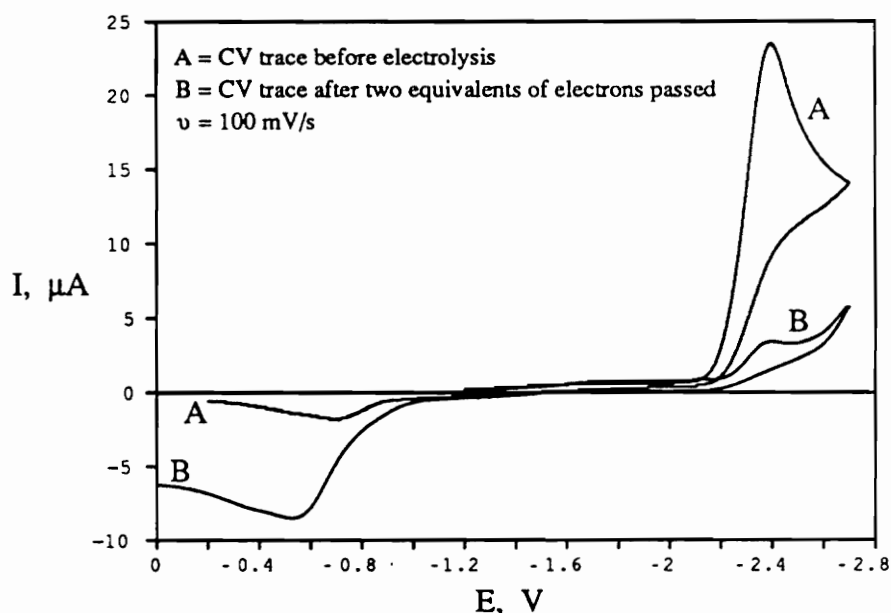


Figure 67. Cyclic voltammograms before and after electrolysis of trans-1-benzoyl-2-phenylcyclopropane (66)

trans-1-Benzoyl-2-phenylcyclopropane (66) is a potentially useful rearrangement probe for electron transfer. Its ketyl anion undergoes a rapid and seemingly irreversible unimolecular decay. The rate constant for ring opening of the ketyl anion (67) was too fast to measure with our equipment, but lies in the range of 10^3 - 10^7 s^{-1} . It is possible to directly measure rate constants for rapid decay of electrode generated intermediates such as (67) by performing extremely fast voltammetric experiments with ultramicroelectrodes and specialized instruments to initiate and monitor the experiment.⁹⁶ This may be pursued at a later date, but for now, caution should be employed if applying trans-1-benzoyl-2-phenylcyclopropane as a probe for electron transfer because the rate constant for ring opening of its ketyl anion is not known.

1-BENZOYL-2-VINYLCYCLOPROPANE

The last substrate studied was 1-benzoyl-2-vinylcyclopropane (76). We hoped to induce an overall vinylcyclopropane \rightarrow cyclopentene rearrangement⁹⁷ initiated by electron transfer (Figure 68). A vinylcyclopropane \rightarrow cyclopentene radical cation rearrangement has recently been reported for the chemical oxidation of variously substituted *p*-anisyl-2-vinylcyclopropanes.⁹⁸ Also, radical cation vinylcyclobutane \rightarrow cyclohexene rearrangements have been observed.⁹⁹ A good review covering radical cation pericyclic reactions has been compiled by Bauld.¹⁰⁰

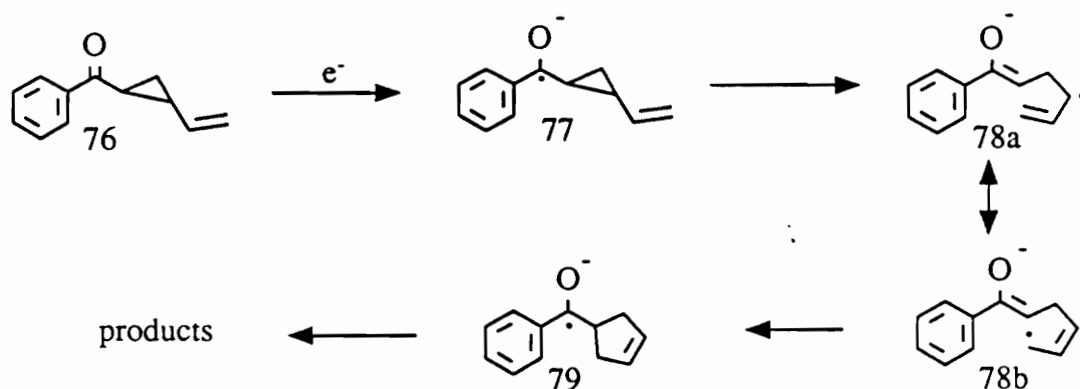


Figure 68. Electron transfer induced vinylcyclopropane \rightarrow cyclopentene rearrangement

Structural rearrangements of the Δ^5 -hexenyl type have been reported for appropriately substituted ketyl anions.^{28,29} Also, several studies have centered upon the regiochemistry of rearrangement of alkyl cyclopropyl ketyl anions.⁶³ The vinylcyclopropane \rightarrow cyclopentene rearrangement of ketones is of considerable synthetic utility and has been induced by thermolysis, transition metal catalysis, photolysis, and nucleophilic opening / alkylative reclosure.^{63c,97} We observed that

1-benzoyl-2-vinylcyclopropane (**76**) might be a good candidate for a *new* electron transfer induced vinylcyclopropane → cyclopentene rearrangement of its ketyl anion. If the rearrangement (**77** → **79**) were to proceed rapidly, (**76**) would have potential to be an excellent diagnostic probe for electron transfer.

The AM1⁷⁸ calculated thermodynamic driving force for this rearrangement is enormous. The enthalpy of ring opening of the ketyl anion (**77**) to the distonic radical anion (**78**) is exothermic by 6.3 kcal/mol. The enthalpy of closing of the distonic radical anion (**78**) to the phenyl cyclopentyl ketyl anion (**79**) is exothermic by 23.2 kcal/mol. Therefore, the overall calculated enthalpy for rearrangement of the cyclopropyl ketyl anion (**77**) to the cyclopentyl ketyl anion (**79**) is exothermic by 29.5 kcal/mol. When the cyclopropyl ketyl anion (**77**) is formed it would be expected to rapidly ring expand to the cyclopentyl ketyl anion (**79**), therefore signalling that electron transfer had occurred.

As with the phenyl substituted derivative, the decay of (**77**) proved to be too fast for DCV reaction order analysis with our equipment. Linear sweep voltammetry reaction order analysis yielded $\delta E_p/\delta \log(\nu) = 38.9 \pm 3.1$ and $\delta E_p/\delta \log(C_A) = 0.7 \pm 1.7$ indicating that the ketyl anion decays by a unimolecular process which is first order in ketyl anion and zero order in ketone, Rate = $k_{\text{obs}}[\text{77}]$ (see Table 4 for theoretical LSV responses). Figures 69 and 70 show typical linear sweep voltammetry reaction order plots for this substrate. No reverse wave was observed by cyclic voltammetry for this species even at high scan rates ($\nu \leq 50$ V/s). The cyclic voltammetry peak potential at $\nu = 50$ mV/s was approximately -2.28 V (Ag/Ag⁺).⁸⁹ Since no reverse current is observed, we cannot assign the rate constant for decay of 1-benzoyl-2-vinylcyclopropyl ketyl anion, but we can bracket it using digital simulation.⁹¹ The same simulation methodology that was used to describe the decay of 1-benzoyl-2-phenylcyclopropyl ketyl anion was used to model the decay of (**77**) (vide supra, see Figure 62 and related discussion). The rate constant for decay of 1-benzoyl-2-vinylcyclopropyl ketyl anion lies between 10^3 and 10^5 s⁻¹.

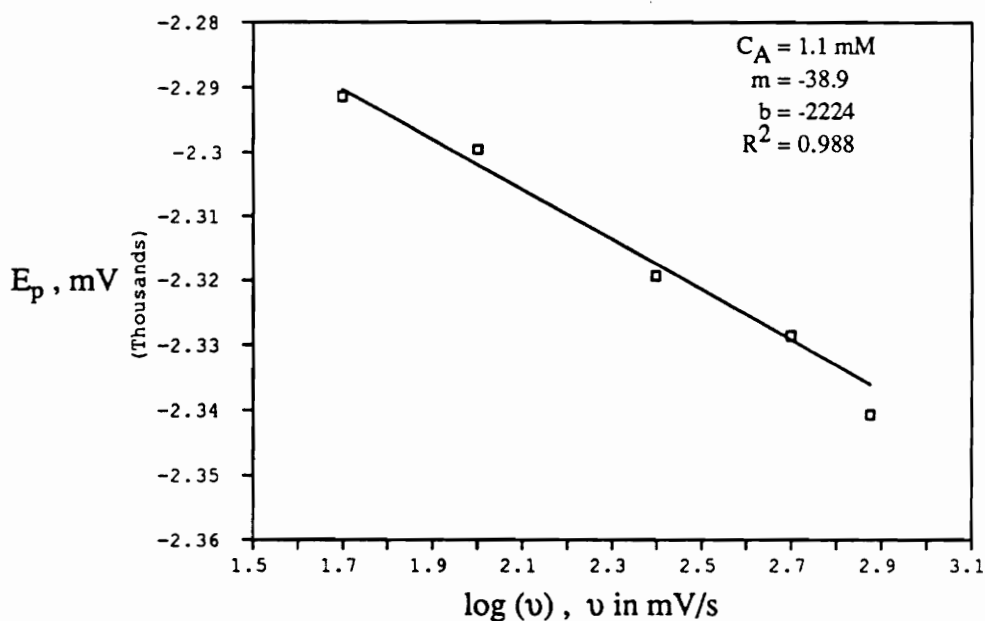


Figure 69. Linear sweep voltammetry reaction order plot for 1-benzoyl-2-vinylcyclopropane (76)

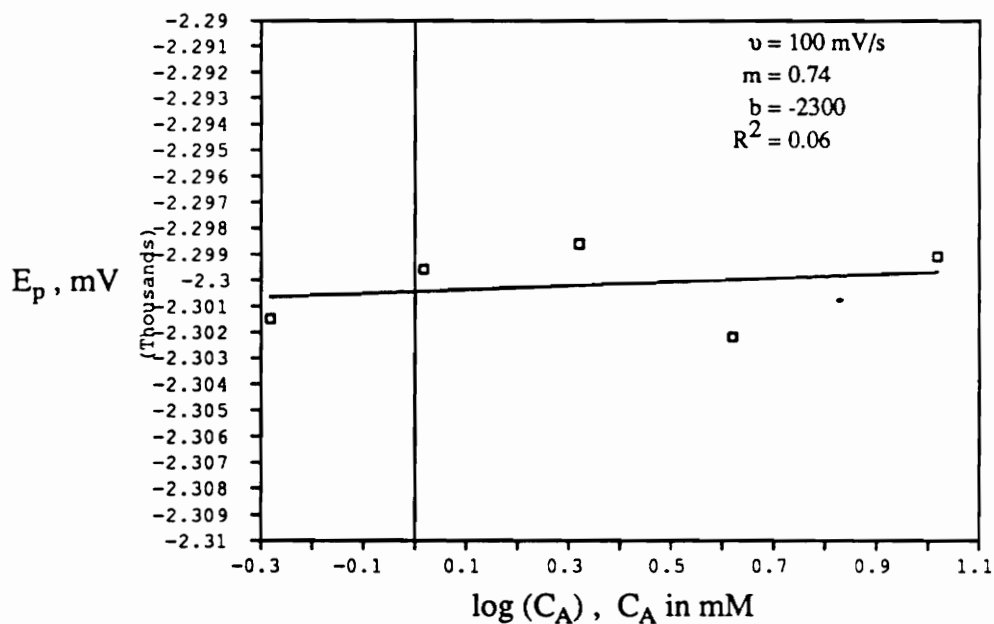


Figure 70. Linear sweep voltammetry reaction order plot for 1-benzoyl-2-vinylcyclopropane (76)

Constant current electrolysis of (**76**) (1 equivalent of electrons) yielded not the cyclopentene containing products we expected, but instead ring opened monomer (**80**) in 28% yield and head to head dimer (**81**) in 23% yield as well as 26% recovered starting material (Figure 71).

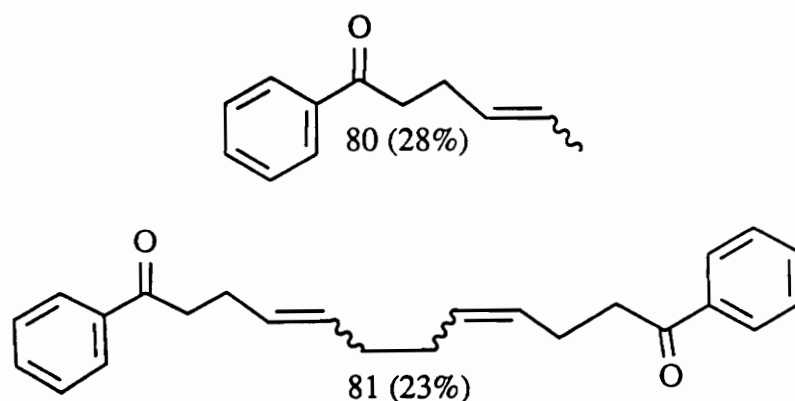


Figure 71. Electrolysis products of 1-benzoyl-2-vinylcyclopropane (**76**)

The formation of ring opened monomer (**80**) can be rationalized by a mechanism similar to that for decay of the phenyl substituted derivative (Figure 72, path A). As for the formation of head to head dimer, dimerization must compete successfully with further reduction of (**78**). Dimerization could occur by coupling of two distonic radical anions ($78 + 78 \rightarrow \text{dimer}^{2-}$, $k \approx 10^9 \text{ M}^{-1}\text{s}^{-1}$)¹⁰¹ and/or by coupling of a distonic radical anion with a ring closed ketyl anion ($78 + 77 \rightarrow \text{dimer}^{2-}$, $k \approx 10^8 \text{ M}^{-1}\text{s}^{-1}$, vide supra) (Figure 72, path B). Evidently, the rate of closure of the distonic radical anion to the cyclopentyl ketyl anion is slow compared with the rapid consumption of (**78**) via further reduction or dimerization.

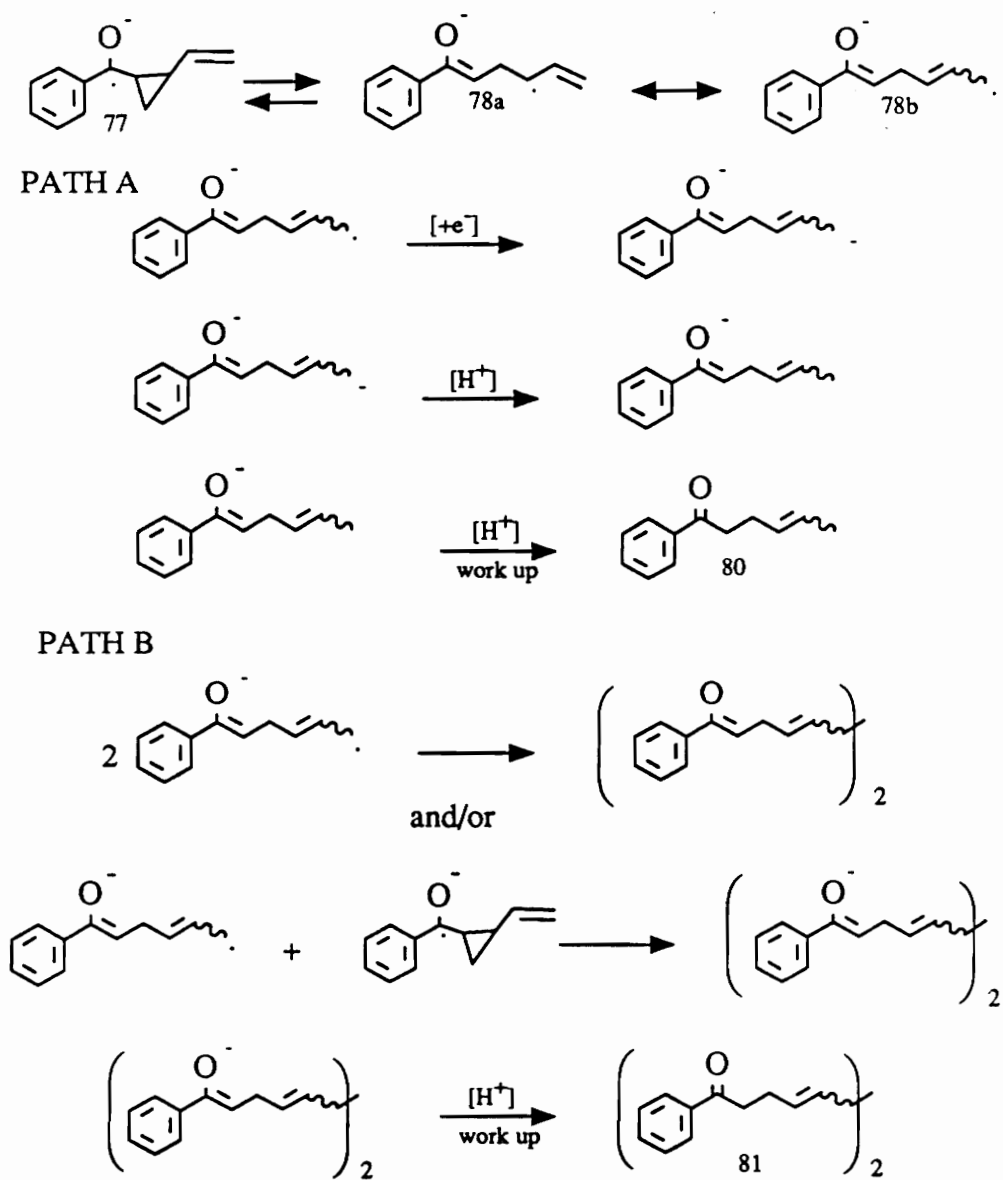


Figure 72. Proposed mechanism for decay of 1-benzoyl-2-vinylcyclopropyl ketyl anion (77)

As with the other phenyl cyclopropyl ketone substrates, an anodic peak substantially more positive than the reduction peak of the ketone is observed by voltammetry. As before, this peak is ascribed to oxidation of an enolate moiety (both monomer and dimer enolates) (Figure 73).

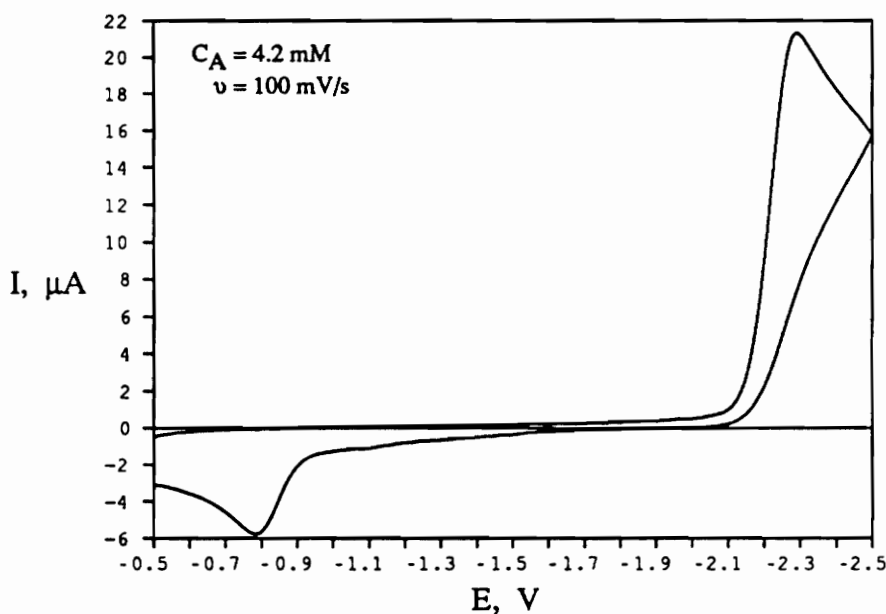


Figure 73. Cyclic voltammogram of 1-benzoyl-2-vinylcyclopropane (76)

Even though the rearrangement of this ketyl anion did not proceed as far as we had hoped, it is still a potentially useful rearrangement probe for electron transfer because the cyclopropane rapidly ring opens. In order to have any hope of electrochemically generating cyclopentene containing products, extremely dilute reaction conditions would have to be employed to circumvent dimerization for this substrate; perhaps products which have cyclized to the cyclopentene could be obtained if alternate methods are employed to generate the ketyl anion (i.e. $h\nu$, chemical reductants). As with the phenyl substituted derivative (67), ring opening of 1-benzoyl-2-vinylcyclopropyl ketyl anion (77) occurs too fast for us to measure with our equipment, but lies in the range of 10^3 to 10^5 s^{-1} .

It should be possible to directly measure the rate of decay of (77) voltammetrically by using ultramicroelectrodes.⁹⁶ Presently, caution should be exercised if 1-benzoyl-2-vinylcyclopropane (76) is employed as an electron transfer probe because the rate constant for ring opening of its ketyl anion is not known.

SUMMARY

By appropriately substituting the cyclopropane ring with groups capable of stabilizing the distonic radical anion, phenyl cyclopropyl ketyl anions can be persuaded to ring open rapidly. The rate constants for ring opening of the ketyl anions of 1-benzoyl-2-vinylcyclopropane and 1-benzoyl-2-phenylcyclopropane are greater than 10^3 s^{-1} and less than 10^5 s^{-1} and 10^7 s^{-1} respectively. Although potentially excellent probes for electron transfer, extreme caution should be exercised if employing these species because their absolute rate constants for ring opening are not yet known. *p*-Cyclopropyl acetophenone was shown to be a poor diagnostic electron transfer probe because electrochemical generation of its ketyl anion yielded only slow bimolecular decay to products with the cyclopropane ring intact.

It is fair to ask what the rate constant for rearrangement of a cyclopropyl ketyl anion to a distonic radical anion must be in order to make a substrate a good electron transfer probe. However, this question is not easy to answer. The best response is that the unimolecular rate of rearrangement of the probe must be competitive with the bimolecular rate of adduct formation.

This is best illustrated with an example (Figure 74). Assume that a reagent, Y^\cdot , which unambiguously reacts with ketones by electron transfer, is combined with a cyclopropyl ketone (**82**) whose ketyl anion (**83**) undergoes a rapid, irreversible ring opening with a rate constant k_{OP} . To make life easy, assume that adduct formation cannot occur within the cage that the intermediates are formed in. If it does, there is very little chance for any rearrangement probe to be effective because of the short (picosecond) lifetime of a cage.⁸⁷

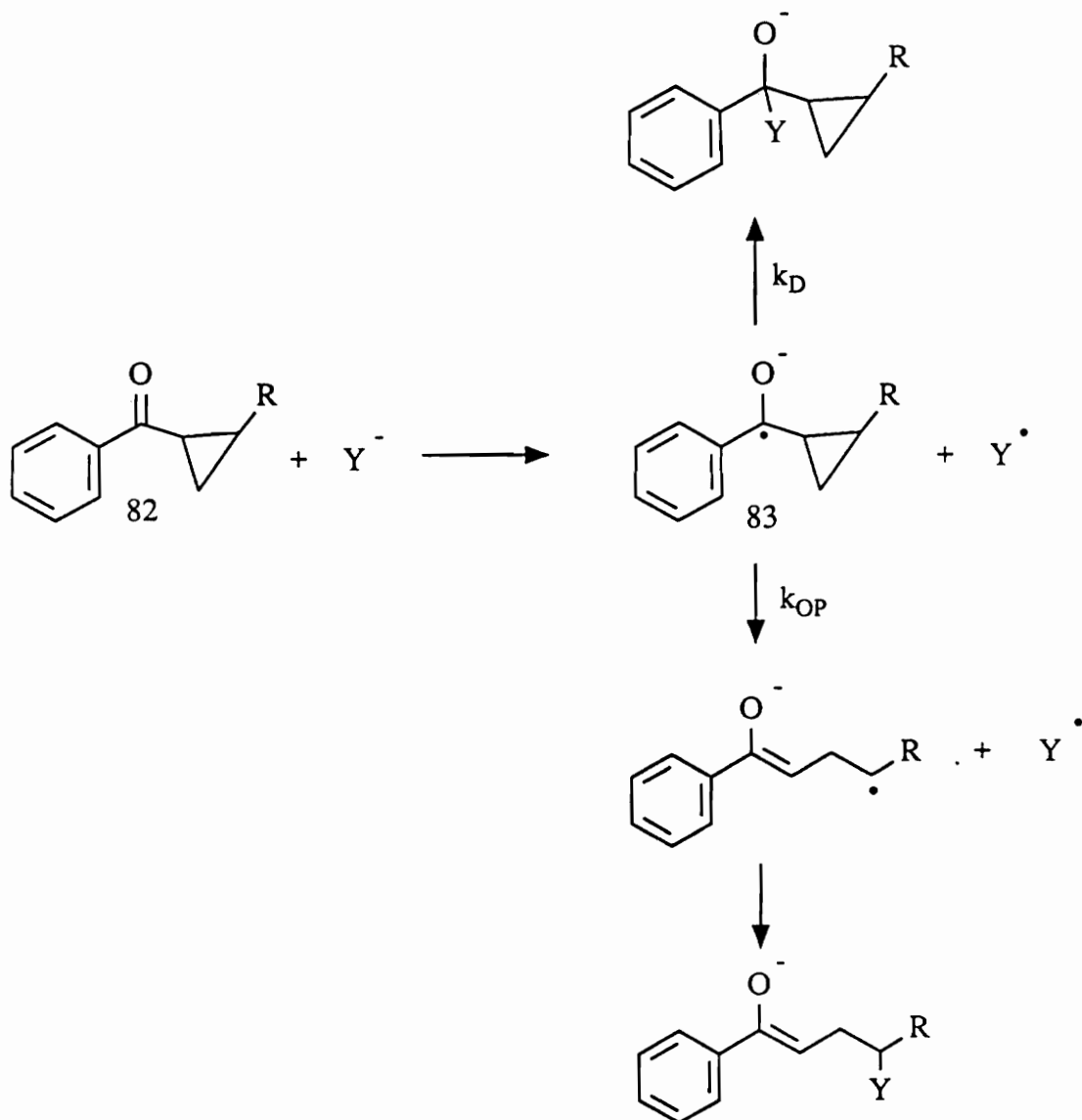


Figure 74. Requirements for an effective electron transfer rearrangement probe

To observe an equal mixture of ring opened and ring closed adducts, the ketyl anion (**83**) must partition itself equally between the two processes competing for it (i.e. $k_D[\mathbf{83}][\mathbf{Y}\cdot] = k_{OP}[\mathbf{83}]$ or more simply $k_D[\mathbf{Y}\cdot] = k_{OP}$). Estimating k_D as $10^8 \text{ M}^{-1}\text{s}^{-1}$ (vide supra) and giving $[\mathbf{Y}\cdot]$ the arbitrary but reasonable value of 0.1 M requires that $k_{OP} = 10^7$

s^{-1} in order to observe equal amounts of ring opened and ring closed adducts. If k_{OP} is two orders of magnitude slower, absolutely no ring opened product would be observed. So, without prior knowledge or at least good estimations of the rate constants and concentrations involved in a chemical transformation, the use of rearrangement probes to detect or reject a specific mechanistic process is a dangerous proposition.

CHAPTER 4. CONCLUSION

The studies presented in the previous pages detail the rich chemistry of aryl cyclopropyl ketyl anions. Alkyl- and unsubstituted phenyl cyclopropyl ketones, including phenyl cyclopropyl ketone, 1-benzoyl-1-methylcyclopropane, trans-1-benzoyl-2-methylcyclopropane, 1-benzoyl-2,2-dimethylcyclopropane, and *p*-tolyl cyclopropyl ketone, have been shown to be extremely unreliable rearrangement probes for electron transfer reaction mechanisms. The ketyl anions of these substrates undergo a *slow* and *reversible* cyclopropyl carbinyl type rearrangement followed by dimerization of the ring opened and ring closed radical anions. In all cases, except for the decay of 1-benzoyl-1-methylcyclopropyl ketyl anion, dimerization is the rate limiting step, therefore, yielding an overall bimolecular rate law. The slow decay of 1-benzoyl-1-methylcyclopropyl ketyl anion is postulated to be first order due to stereoelectronic inhibition of cyclopropane ring opening.

The equilibrium for the reversible ring opening of alkyl- and unsubstituted phenyl cyclopropyl ketyl anions lies highly in favor of the ring closed form. For example, the equilibrium constant for the reversible ring opening of phenyl cyclopropyl ketyl anion was shown to be extremely small, $K_1 \approx 4.6 \times 10^{-8}$. It was determined that the maximum rate constant for ring opening and minimum rate constant for ring closing of this ketyl anion were approximately 2.0 s^{-1} and $4.3 \times 10^7 \text{ s}^{-1}$ respectively. Semiempirical molecular orbital calculations (AM1) also indicate that the ring opening of phenyl cyclopropyl ketyl anion is not favored ($\Delta H = 7.9 \text{ kcal/mol}$). Similar results were obtained for the other aryl cyclopropyl ketyl anions in this class.

The utility of phenyl cyclopropane derivatives (with no substituents or alkyl substituents on the cyclopropane ring) as diagnostic probes for electron transfer has also

been cast in doubt. *p*-Cyclopropyl acetophenone ketyl anion was shown to undergo slow bimolecular decay to its corresponding pinacol dimer. No evidence was found to indicate that the decay of this ketyl anion involved opening of the cyclopropane ring.

Aryl cyclopropyl ketyl anions with good radical stabilizing groups on the cyclopropane ring have been shown to undergo rapid unimolecular decay. The rate constants for opening of trans-1-benzoyl-2-phenylcyclopropyl ketyl anion and 1-benzoyl-2-vinylcyclopropyl ketyl anion to their corresponding distonic radical anions are greater than 10^3 s^{-1} but probably less than 10^7 s^{-1} and 10^5 s^{-1} respectively. Thermodynamic calculations indicate that the enthalpy for cyclopropane ring opening of both the phenyl and vinyl substituted ketyl anions is exothermic ($\Delta H \approx -6 \text{ kcal/mol}$), confirming that rupture of the cyclopropane ring should be favorable. Aryl cyclopropyl ketones, with substituents on the cyclopropane ring capable of stabilizing the radical portion of the corresponding ring opened distonic radical anion, may prove to be useful diagnostic probes for electron transfer. Although relatively fast, the absolute rate constants for rearrangement of trans-1-benzoyl-2-phenylcyclopropyl ketyl anion and 1-benzoyl-2-vinylcyclopropyl ketyl anion are not known; therefore, extreme caution should be exercised in applying these substrates as electron transfer rearrangement probes.

In summary, chemists generally believe that a cyclopropane ring is an extremely fragile moiety that will rapidly rupture whenever desired. In the past, the design and implementation of cyclopropane containing substrates as diagnostic electron transfer rearrangement probes has been based on this precept. In this work, we have shown that the strain energy relieved by rupture of a cyclopropane is not always great enough to drive the ring cleavage process. For alkyl- and unsubstituted phenyl cyclopropyl ketyl anions and *p*-cyclopropyl phenone ketyl anions, it is apparent that the loss in resonance energy associated with the conversion of the ketyl anion to the distonic radical anion is not offset by the energy released by cleavage of the cyclopropane ring (Figure 75). If the distonic

radical anion is resonance stabilized (i.e. radical portion allylic, benzylic, etc.), the relief of strain energy accompanying cleavage of the cyclopropane ring is sufficient to drive the cyclopropyl carbinyl type rearrangement of aryl cyclopropyl ketyl anions. These principles are not restricted to the rearrangement of cyclopropane containing aryl ketyl anions, and should be kept in mind whenever utilizing the rearrangement of a cyclopropane containing substrate.

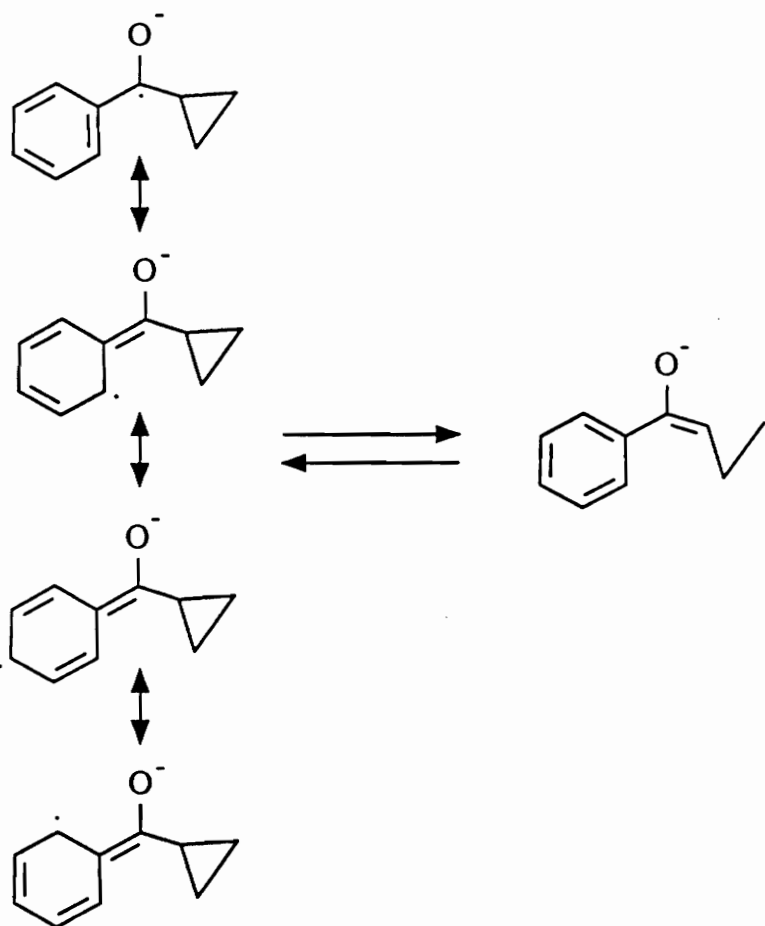


Figure 75. Cleavage of a delocalized aryl cyclopropyl ketyl anion to its corresponding distonic radical anion

CHAPTER 5. EXPERIMENTAL

INSTRUMENTATION

Melting points were determined on a Thomas Hoover capillary melting point apparatus and are uncorrected. Nuclear magnetic resonance spectra (^1H , ^2H , ^{13}C) were obtained on either a 200 MHz or 270 MHz Bruker FT NMR spectrometer. All chemical shift values are reported in δ units relative to Me_4Si (δ 0.00 ppm) in deuteriochloroform (^2H spectra run in CHCl_3). Infrared spectra were recorded on a Perkin-Elmer model 1600 FT-IR spectrometer and IR bands are reported in cm^{-1} . Ultraviolet spectra were obtained on a Beckman Du-50 spectrophotometer and are reported with λ in units of nm and ϵ in units of $\text{M}^{-1}\text{cm}^{-1}$. Both low and high resolution mass spectral data were obtained from a VG Analytical model 7070 E-HF double focusing, magnetic sector, high resolution mass spectrometer. Electron impact ionization (70eV) was employed unless otherwise stated. Low resolution GC/MS was performed on a Hewlett Packard model 5890 gas chromatograph with an HP methylsilicone capillary column (12 m \times 0.2 mm) interfaced with an HP 5097B EI mass spectrometer and an HP series computer. Gas chromatographic analyses were performed on a Hewlett Parkard HP 5890 instrument equipped with both FID and TCD detectors, and an HP 3393A reporting integrator. Analyses were accomplished on either an Alltech RSL-200 (nonpolar) capillary column (30m \times 0.25mm) or a Supelco SE-54 (low polarity) capillary column (15m \times 0.25mm). Analytical and preparative HPLC separations were accomplished on a Rainin HPXL instrument using a Microsorb C-18 reverse phase column (anal. 5 μm , 4.6 mm ID \times 25 cm; prep. 5 μm , 21.4 mm ID \times 25 cm) with acetonitrile / water solvent mixtures. Flash

chromatography¹⁰² was performed on silica gel (EM Science, 230-400 mesh) using hexane/ethyl acetate solvent mixtures (weight ratio of silica to substrate \approx 200:1). Thin layer chromatography (TLC) was performed on precoated silica gel 60 F-254 plates purchased from EM Science. Electrochemical measurements were performed on an EG&G Princeton Applied Research (EG&G/PAR) Model 273 potentiostat/galvanostat interfaced to an IBM XT personal computer equipped with a 16 MHz accelerator board. Experiments were initiated and analyzed by subroutines written in FORTH and implemented through ASYST (see appendix B). An oscilloscope (Telequipment Model S51B) was employed to monitor either current or potential as an aid in setting positive feedback IR compensation.

MATERIALS AND PURIFICATIONS

All materials were purchased from the suppliers indicated in brackets after the reagent and were used as received unless indicated otherwise.

Purification of Ethers

Diethyl ether (Fisher or Baker) and tetrahydrofuran (Fisher or Baker) were dried prior to use. The ether was refluxed (under Ar) over sodium (≈ 2 g/L) for two hours and then benzophenone (≈ 2 g/L) was added. Reflux was continued until the solution turned royal blue due to the presence of sodium benzophenone ketyl anion. The ether was then distilled under an inert atmosphere and immediately used.

Activation of Neutral Alumina

Neutral alumina (activated, neutral, Brockmann I, 150 mesh, Aldrich) was placed under vacuum (0.5 mm Hg) and heated with a flame until bumping subsided (15 - 60 min). The flask was cooled under vacuum, filled with argon, and stoppered tightly. Alumina activated in this fashion was used within two weeks.

Purification of N,N-Dimethylformamide¹⁰³

Aldrich HPLC grade (99.9 + %) N,N-dimethylformamide (DMF) was stirred over anhydrous copper(II)sulfate (Aldrich) (10 g/L) and activated neutral alumina (30 g/L) under argon for three days and then distilled (bp. 35 °C, 7 mm Hg). The middle cut ($\approx 3/4$ of total volume) was saved and stored over anhydrous CuSO_4 under argon. DMF purified in this manner was not stored over two weeks prior to being used. Before use, the DMF was passed through a column of activated neutral alumina (2.5 cm \times 20 cm) under positive argon pressure into a receptacle blanketed with argon.

Purification of Argon

Commercially available argon (Airco UN-1006) was passed through an oxygen removal tower (5.4 cm \times 84.5 cm, Kontes) packed with 1 kg of BASF oxygen binding catalyst R3-11.¹⁰⁴ The catalyst bed was operated at 125°C by heating the tower with a heat cord. The argon was then passed through a moisture trap (4.4 cm \times 45.7 cm, American Scientific) packed with 4 Angstrom indicating molecular sieves. The argon was conducted through 1/8" copper tubing from the tank to the purifying towers and on to the electrochemical cell.

SYNTHESIS OF STARTING MATERIALS

Phenyl cyclopropyl ketones were generally prepared by the action of two equivalents of phenyl lithium on one equivalent of the corresponding cyclopropyl carboxylic acid. This methodology has been used to produce a variety of phenyl cyclopropyl ketones including (28c) and (28e) but no procedure was given.¹⁰⁵ The general procedure developed in our laboratory to perform this transformation is outlined below for the synthesis of (28b).

trans-1-Benzoyl-2-methylcyclopropane (28b). A flame dried flask equipped with a mechanical stirrer and under an argon atmosphere was charged with 2.5g (25 mmol) of 2-methylcyclopropane carboxylic acid (Aldrich) and 50 mL of dry tetrahydrofuran. The flask was cooled in an ice/salt bath and then 30 mL (54 mmol) of 1.8 M PhLi in 70/30 cyclohexane/diethyl ether (Aldrich) was slowly added dropwise. After addition, the reaction mixture was slowly warmed to room temperature and stirred for one hour and then quenched with 15 mL of 20% aqueous HCl, and acidified with conc. HCl. The reaction mixture was extracted three times with 30 mL portions of diethyl ether. The organic layers were combined and washed twice with water, once with saturated aqueous sodium bicarbonate solution and dried over magnesium sulfate. Flash chromatography (5% ethyl acetate/95% hexane) followed by short path distillation (bp. 48 °C, 0.25mm Hg, lit.^{106a} 128 °C, 18 mm Hg) yielded 2.5 g (63%) trans-1-benzoyl-2-methylcyclopropane (28b): ¹H NMR (CDCl₃) δ 0.85 (m, 1H), 1.25 (d, 3H, J = 8.1 Hz), 1.52 (m, 2H), 2.41 (m, 1H), 7.45 (m, 3H), 8.0 (m, 2H).

Other synthetic routes to this compound have been reported.¹⁰⁶

1-Benzoyl-1-methylcyclopropane (28e)¹⁰⁵ was prepared by the action of two equivalents of phenyl lithium on one equivalent of 1-methylcyclopropane carboxylic acid (Aldrich) as described in the previous procedure. Yield 69% (bp. 38 °C, 0.25 mm Hg, lit.^{107a} 58-60 °C, 0.3 mm Hg): ¹H NMR (CDCl₃) δ 0.80 (m, 2H), 1.3 (m, 2H), 1.47 (s, 3H), 7.45 (m, 3H), 7.82 (m, 2H).

Other synthetic routes to (28e) have been reported.¹⁰⁷

1-Benzoyl-2-vinylcyclopropane (76) (mixture of cis and trans) (bp. 44-46 °C, 0.1 mm Hg) was prepared in 32% yield from reaction of one equivalent of 2-vinylcyclopropane carboxylic acid¹⁰⁸ with two equivalents of phenyl lithium as described earlier. It has been reported that (76) was prepared by reaction of acetophenone with 1,4-dibromo-2-butene but no procedure or spectroscopic data was given⁵⁵: ¹H NMR (CDCl₃) δ 1.1 - 1.4 (m, 1H), 1.7 (m, 1H), 2.25 (m, 1H), 2.7 (m, .58H), 2.95 (m, .42H), 4.9 - 5.3 (m, 2H), 5.95 - 6.3 (m, 1H), 7.5 (m, 3H), 8.0 (m, 2H); ¹³C NMR (CDCl₃) δ 14.29 and 18.06 (cyclopropyl methylene), 25.88, 26.67, 28.18, and 29.39 (cyclopropyl methines), 115.01, and 116.18 (vinylic methylene), 128.06, 128.54, 132.68, 132.79, 134.97, and 138.5 (methines), 198.67 (carbonyl carbon); IR 3083, 3006, 2957, 2932, 2871, 1668, 1637, 1598, 1580, 1450, 1386, 1224, 1018, 907, 705; MS (GC/MS) m/e (relative intensity) 172 (M⁺ 1.2), 171 (2.2), 157 (3.0), 128 (4.0), 115 (6.7), 105 (100), 77 (40.2).

2-Vinylcyclopropane carboxylic acid¹⁰⁸ was prepared by hydrolysis of 10 g (71 mmol) of its ethyl ester by refluxing for 2 hours in 40 mL of 50% aqueous methanol containing 7.8 g (140 mmol) of potassium hydroxide. The solution was concentrated to remove the alcohol solvent and acidified with 2 M aqueous HCl. The free acid was extracted with

four 50 mL portions of ether. The ether layers were combined, dried over magnesium sulfate and concentrated. Short path distillation (bp. 51-54 °C, 0.05 mm Hg, lit.^{108a} 52-54 °C, 0.05 mm Hg) yielded 7.0 g (88%) of a colorless oil: ¹H NMR (CDCl₃) δ 1.05 (m, .52H), 1.3 - 1.5 (m, 1.58H), 1.65 (m, .48H), 1.9 - 2.2 (m, 1.48H), 5.0 - 5.5 (m, 2H), 5.8 (m, 1H), 10.4 (s, 1H); IR 3086, 1698, 1639, 1436, 1304, 1289, 1235, 985, 907, 861.

Ethyl 2-vinylcyclopropane carboxylate¹⁰⁸ was prepared by the reaction of butadiene (Aldrich) with ethyl diazoacetate (Aldrich) in a sealed steel cylinder by the method of Vogel^{108a}. Short path distillation (bp. 64 °C, 12 mm Hg, lit. 61-62 °C, 12 mm Hg) yielded the colorless ester in 75% yield: ¹H NMR (CDCl₃) δ 0.95 (m, .45H), 1.2 - 1.3 (m, 4.5H), 1.65 (m, .55H), 1.85-2.1 (m, 1.5H), 4.15 (q, 2H, J = 6.9 Hz), 4.9 - 5.9 (m, 3H); IR 3085, 2983, 1727, 1638, 1400, 1383, 1183, 1096, 1036, 995, 907.

1-Benzoyl-2,2-dimethylcyclopropane (28c) was prepared equally well by either the method of Watson¹⁰⁹ or by reaction of one equivalent of 2,2-dimethylcyclopropane carboxylic acid¹¹⁰ with two equivalents of phenyl lithium as described in the earlier procedures¹⁰⁵: Colorless oil (bp. 55°C, 0.1 mm Hg); ¹H NMR (CDCl₃) δ 0.9 (m, 1H), 1.1 (s, 3H), 1.35 (s, 3H), 1.55 (m, 1H), 2.45 (m, 1H), 7.50 (m, 3H), 7.95 (m, 2H).

Other syntheses of (28c) have also been reported.¹¹¹

1-(d-5)Benzoyl-2,2-dimethylcyclopropane (42). A mechanically stirred, flame dried flask under argon was charged with 1.94g (17 mmol) of 2,2-dimethylcyclopropane carboxylic acid¹¹⁰ in 20 mL of dry diethyl ether. The flask was cooled to -78 °C (dry

ice/acetone) and the lithium salt of the acid was generated by slow addition of 7.1 mL (17.85 mmol) of 2.5 M *n*-butyllithium in hexane (Aldrich) with stirring.

A second flame dried flask under argon (magnetically stirred) was charged with 2.50 g (15.4 mmol) of bromobenzene-*d*₅ (Aldrich) in 20 mL of dry diethyl ether. The flask was cooled to -78 °C (dry ice/acetone) and 6.5 mL (16.2 mmol) of 2.5 M *n*-butyllithium in hexane (Aldrich) was slowly added with stirring. The reaction mixture was stirred and allowed to warm to 0 °C over the course of two hours.

The phenyl lithium-*d*₅ (at 0°C) was then slowly transferred via a cannula into the lithium salt of 2,2-dimethylcyclopropane carboxylic acid (at -78°C). The reaction mixture was allowed to warm to room temperature over the course of 1.5 hours and then stirred for one hour more at room temperature. The flask was cooled to 0°C and the reaction mixture quenched with 20 mL of saturated aqueous ammonium chloride solution and acidified with concentrated HCl. The organic layer was separated, washed twice with water, dried over magnesium sulfate and concentrated. Flash chromatography (5% ethyl acetate, 95% hexane) followed by short path distillation yielded 42% of a colorless oil (bp. 52-56 °C, 0.1 mm): ¹H NMR (CDCl₃) δ 0.9 (m, 1H), 1.1 (s, 3H), 1.35 (s, 3H), 1.55 (m, 1H), 2.45 (m, 1H); ²H NMR (CHCl₃) δ 7.50 (s, 3D), 8.0 (s, 2D); IR 2949, 2871, 2280, 1669, 1564, 1458, 1436, 1401, 1181, 1117, 991; MS *m/e* (relative intensity) 181 (0.9), 180 (6.5), 179 (M⁺ 37), 178 (2.6), 177 (2.0), 164 (19), 155 (21), 110 (100).

***p*-Tolyl cyclopropyl ketone (28d)** (mp. 49°C) was prepared in 35% yield by Friedel-Crafts coupling of toluene and cyclopropane carboxylic acid chloride (Aldrich) in accordance with the procedure of Rovnyak et al.¹¹²: ¹H NMR (CDCl₃) δ 1.0 (m, 2H), 1.2 (m, 2H), 2.4 (s, 3H), 2.65 (m, 1H), 7.25 (d, 2H, *J* = 8.5 Hz), 7.95 (d, 2H, *J* = 8.5 Hz); IR 3096, 3008, 2958, 2920, 1658, 1604, 1568, 1407, 1381, 1230, 982, 826, 742.

p-Cyclopropyl acetophenone (62) was prepared in 60% yield by Friedel-Crafts coupling of phenyl cyclopropane (Aldrich) and acetyl chloride (Aldrich) by the method of Hart and Levitt.¹¹³ $^1\text{H NMR}$ (CDCl_3) δ 0.7 (m, 2H), 1.05 (m, 2H), 1.90 (m, 1H), 2.55 (s, 3H), 7.05 (d, 2H), 7.80 (d, 2H); IR 3083, 3005, 2929, 1681, 1606, 1562, 1414, 1359, 1270, 1186, 1045, 1016, 958, 900, 822.

trans-1-Benzoyl-2-phenylcyclopropane (66) was prepared in 35% yield by the method of Corey¹¹⁴ from chalcone and trimethyl sulfoxonium iodide: $^1\text{H NMR}$ (CDCl_3) δ 1.55 (m, 1H), 1.95 (m, 1H), 2.7 (m, 1H), 2.95 (m, 1H), 7.1 - 7.6 (m, 8H), 8.05 (m, 2H); MS (GC/MS) m/e (relative intensity) 224 (0.28), 223 (3.05), 222 (M^+ , 17.06), 221 (14.98), 207 (4.98), 131 (3.6), 117 (17.6), 116 (12), 115 (21.1), 106 (7.6), 105 (100), 91 (7.65), 77 (46).

1-Benzoyl-1-deuteriocyclopropane (45)¹¹⁵. A flame dried flask under argon was charged with 30 mL of D_2O and 1.7 g (74 mmol) of sodium. Phenyl cyclopropyl ketone (Aldrich) (2.75g, 19 mmol) in 30 mL of 1,4-dioxane (Fisher) was then added to the flask. The reaction mixture was refluxed for three days, poured into 100 mL of water and extracted three times with 30 mL portions of diethyl ether. The organic layers were combined, washed with water, dried over magnesium sulfate and concentrated. The yellow residue was purified by Kugelrohr distillation (0.1 mm Hg, air bath temperature 60-80 °C) to yield 1.8 g of product which contained 93% deuterium label as determined by comparison of the mass spectra of the deutero and hydrido isomers: $^1\text{H NMR}$ (CDCl_3) δ 1.05 (m, 2H), 1.30 (m, 2H), 7.55 (m, 3H), 8.05 (m, 2H); $^2\text{H NMR}$ (CHCl_3) δ 2.65 (s); IR 3061, 3009, 1668, 1596, 1579, 1448, 1334, 1207, 996, 720; MS m/e (relative intensity) 148 (2.6), 147 (M^+ , 24.4), 146 (9.0), 145 (0.6), 106 (7.8), 105 (100), 77 (55); MS m/e (relative intensity) for

the hydrido derivative (i.e. phenyl cyclopropyl ketone (**28a**)) 147 (2.9), 146 (M^+ , 22.7), 145 (7.8), 117 (2.5), 106 (7.6), 105 (100), 77 (55).

1-Benzoyl-1-deuterio-2-phenylcyclopropane (75) was prepared from trans-1-benzoyl-2-phenylcyclopropane¹¹⁴ by treatment with NaOD/D₂O as described in the previous procedure. The crude viscous oil was crystallized from petroleum ether to yield 50% of a white solid (mp. 44-45 °C) containing better than 95% deuterium label as determined by comparison of the MS spectra of the deutero and hydrido isomers: ¹H NMR (CDCl₃) δ 1.55 (m, 1H), 1.95 (m, 1H), 2.7 (m, 1H), 7.1 - 7.6 (m, 8H), 8.05 (m, 2H); ²H NMR (CHCl₃) δ 2.94 (s); MS (GC/MS) m/e (relative intensity) 224 (2.9), 223 (M^+ , 17.8), 222 (14.7), 221 (1.2), 118 (16.9), 117 (11.8), 116 (17.8), 105 (100), 77 (44); MS (GC/MS) m/e (relative intensity) for hydrido derivative (i.e. trans-1-benzoyl-2-phenylcyclopropane (**56**)) 224 (0.28), 223 (3.05), 222 (M^+ , 17.06), 221 (14.98), 207 (4.98), 131 (3.6), 117 (17.6), 116 (12), 115 (21.1), 106 (7.6), 105 (100), 91 (7.65), 77 (46).

Tetra-n-butylammonium tetrafluoroborate (n-Bu₄NBF₄)¹¹⁶ was prepared by treatment of tetra-n-butylammonium iodide (Aldrich) with aqueous HBF₄ (Fisher) using the method of House¹¹⁶. The crude salt was thoroughly dried under vacuum (0.1 mm Hg), and then recrystallized four times from ethyl acetate/pentane. After recrystallization, the salt was placed under vacuum (0.1 mm Hg) until dry. The salt was stored under argon until needed.

VOLTAMMETRY

Solution Preparation

Unless otherwise stated all voltammetric measurements were performed on solutions which contained 0.5 M $n\text{-Bu}_4\text{NBF}_4$ in N,N-dimethylformamide (DMF). The solutions were prepared by carefully weighing $n\text{-Bu}_4\text{NBF}_4$ into an appropriately sized volumetric flask and then placing the volumetric flask in a desiccator under vacuum (0.02 - 0.05 mm Hg) for approximately 24 hours to remove any last traces of moisture from the electrolyte. The desiccator was then filled with argon and the volumetric flask removed and sealed with a septum. The appropriate quantity of electro-active substrate was then added to the volumetric flask. DMF (purified as described earlier) was percolated under argon through a column of neutral activated alumina (2.5 cm \times 20 cm) into the awaiting volumetric flask (blanketed with argon). The flask was then sealed with a septum and parafilm and stored in an argon filled desiccator prior to use (no solution was stored over 48 hours before use). The voltammetric solutions were added to the argon filled, oven dried, electrochemical cell through a short plug of activated neutral alumina (1cm \times 5cm) under positive argon pressure.

Voltammetric Cell

The voltammetric cell (part no. K0060) and cap (part no. K0066) were purchased from EG&G/PAR. The cell was stored in a drying oven at 150 °C and cooled in a desiccator containing indicating DRIERITE prior to use. The cell was kept under a stream

of argon while approximately 0.5 g of activated neutral alumina, a small stir bar, and the electrodes were assembled in the cell. The solution was then added to the cell as described before. The solution was purged with argon and stirred with neutral activated alumina for 20-30 minutes before the experiments were begun. See Figure 76 for a pictorial representation of the voltammetric set-up.

Working Electrode

The working electrode, purchased from Bioanalytical Systems (BAS), (part no. MF-2014) was a planar gold button with a diameter of 1.6 mm and encased in a Kel-F plastic sheath. The electrode was prepared for use by polishing with alumina slurry as outlined in the BAS electrode polishing kit (part no. MF-2056).

Auxiliary Electrode

The auxiliary electrode was fabricated by melting a 0.8 mm \times 8 cm piece of platinum wire (Fisher) to a length of 1.0 mm diameter silver wire (Aldrich). The platinum portion of the wire was then sealed in a 4 mm OD pyrex tube leaving the Pt outside and the Ag inside the tube. The platinum was then coiled into a tight spiral with a diameter of about 5 mm. The electrode was then attached to a bridge tube (Figure 76) with Teflon heat shrink tubing (BAS part no. MF-2027) for easy introduction into the voltammetric cell. Planar platinum working electrodes were also made in this fashion. A shorter piece of Pt wire of desired diameter was melted to a silver wire and then sealed in a 4 mm OD pyrex tube. The excess Pt and glass was ground off with coarse sandpaper and the

electrode polished to a mirror finish with a BAS electrode polishing kit (part no. MF-2056).

Reference Electrode

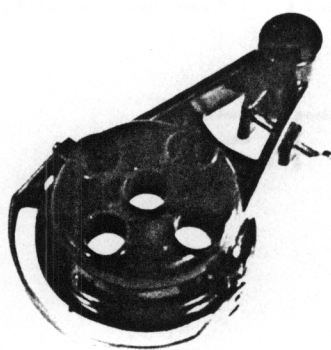
The reference electrode was made by sealing a 5 mm length of 4 mm diameter porous Vycor rod (BAS part no. MF-1080) to a 4 mm OD Pyrex tube with Teflon heat shrink tubing (BAS part no. MF-2027). The other end of the Pyrex tube was attached to a bridge tube with Teflon heat shrink tubing. The electrode case was filled with 0.1 M AgNO_3 in acetonitrile (EG&G/PAR part no. G0028) and a silver wire (1.0 mm diameter, Aldrich), inserted through a septum, was placed in contact with the filler solution. This produces a reference electrode which is 337 mV positive of SCE. The filler solution and Vycor tip were replaced after one day of use.

Positive Feedback IR Compensation¹¹⁷

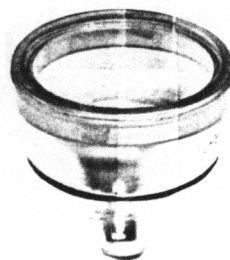
After the allotted degassing period, the solution was blanketed with argon and the stirring stopped. Positive feedback IR compensation was set by monitoring the current response (oscilloscope) to a square potential step waveform applied to the electrometer (EG&G/PAR model 273) by the potentiostat. IR compensation was increased until the potentiostat began to oscillate and was then backed off to 85% of that value. Typical IR compensation values for our voltammetric setup were in the neighborhood of 150 ohms.

Voltammetric Runs

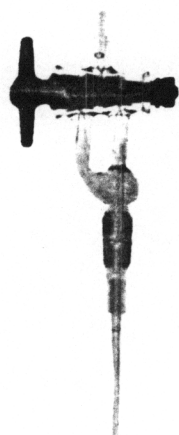
All experiments were performed at ambient temperature (23°C) unless otherwise stated. Variable temperature studies were performed using a jacketed electrochemical cell (EG&G/PAR part no. K0064) and a variable temperature circulating bath (50% ethylene glycol, 50% water) purchased from Fisher Scientific (Isotemp Refrigerated Circulator Model 9500). The solutions were blanketed (positive pressure) with argon throughout the experimental sequence. Each result represents a minimum of three experiments. The simple numerical average of the raw data was used in further data handling (i.e. DCV reaction order plots, E_a plots, etc.). Errors in values are reported as population standard deviations and errors are propagated through calculations by taking the square root of the sum of the squares of either the absolute or relative errors as appropriate.¹¹⁸



A



B



C



D

- A. Voltammetry cell top
- B. Voltammetry cell bottom
- C. Purge valve
- D. Bridge tube

Figure 76. Voltammetry cell and cap, two way purge valve, and bridge tube

ELECTROLYSES

Solution Preparation

All electrolysis experiments were performed on solutions which contained 0.2 M $n\text{-Bu}_4\text{NBF}_4$ in DMF. The blank solutions were prepared as delineated in the voltammetry section. Fifty milliliters of the electrolyte solution was partitioned equally between the two compartments of a flame dried, fully assembled H cell under argon (See Figure 77). The electro-active substrate was added to the cathodic compartment. Both anodic and cathodic compartments were then degassed for at least 30 minutes with argon before electrolysis.

Electrolysis Cell

The electrolysis cell was a conventional H cell with the two compartments separated by a medium glass frit (22 mm in diameter). Each compartment was fabricated from a pyrex tube 3 cm in diameter and 13 cm long sealed on one end. The frit was positioned so that 25 mL of electrolyte solution in each side of the cell easily covered the entire frit. Electrodes, purge tubes and purge vents were introduced through 14/20 ground glass joints on the sides of the cell or through the top of the compartments through a no. 6 rubber stopper (Figure 77).

Working Electrode

The working electrode was built from a 0.127 mm × 25 mm × 25 mm piece of gold foil (Aldrich). A 0.5 mm diameter by 4.0 cm piece of Pt wire (Fisher) was melted to a 1.0 mm diameter piece of silver wire (Aldrich). The Pt wire was sealed in a 4 mm OD pyrex tube leaving the Pt outside and the Ag inside the tube. The gold foil was then spot welded to the platinum wire. The gold foil was bent to conform to the electrolysis cell.

Auxiliary Electrode

The auxiliary electrode was fabricated in a fashion similar to that for the working electrode. The only difference was that a piece of platinum gauze (45 mesh) 30 mm × 50 mm (Fisher) was spot welded to the platinum wire instead of gold foil. The platinum gauze was shaped to conform to the electrolysis cell.

Reference Electrode

The reference electrode for bulk electrolyses was identical to the reference electrode used in the voltammetric experiments.

Experimental Runs

All electrolysis experiments were performed at ambient temperature (23°C). Constant current electrolyses were performed at currents from 35 to 50 mA. Constant potential electrolyses were performed at potentials approximately 300 mV beyond the cyclic voltammetry peak potential. Positive feedback IR compensation for controlled potential electrolyses was set as described earlier for voltammetry (typical values around 5 ohms). The cathodic compartment was stirred and both anodic and cathodic compartments purged with argon throughout the experiment. After the allotted time, the electrolysis was stopped and the cathodic compartment quenched with an appropriate reagent (5% aqueous HCl, 5% aqueous(D₂O) DCl, MeI, etc.). The contents of the cathodic compartment were then poured into 30-40 mL of water and extracted 4 times with 20 mL portions of diethyl ether. The organic layers were combined and washed three times with water and then dried over magnesium sulfate and concentrated. The products were then separated by flash column chromatography.¹⁰²

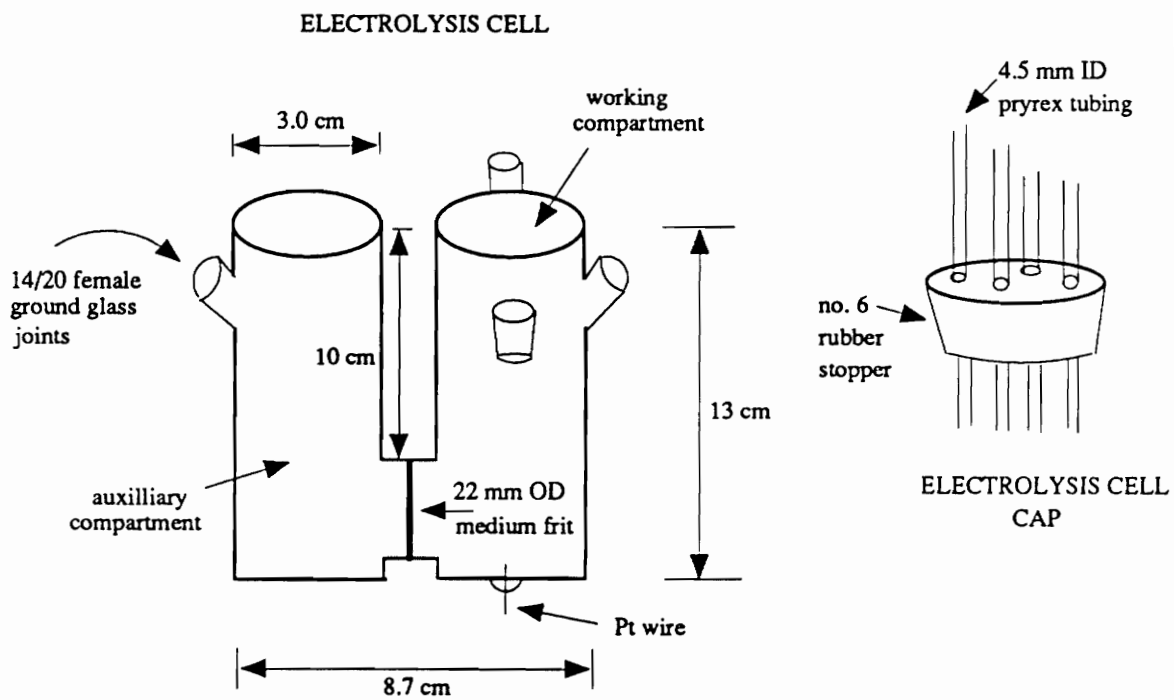


Figure 77. Electrolysis cell (H-cell) and cap

SPECIFIC ELECTROLYSES

Phenyl Cyclopropyl Ketone (28a)

Electrolysis of (28a) with H_3O^+ quench

Phenyl cyclopropyl ketone [148 mg (1.01 mmol)] was electrolyzed at 35 mA for 45 minutes passing 0.98 mmol (0.97 equivalents) of electrons. The reaction was quenched with 5% aqueous HCl, worked up, and flash chromatographed with a solvent gradient starting with 25/75 and ending with 50/50 ethyl acetate/hexane to yield:

recovered starting material - 21 mg (14%)

dimer (**31a**) - 61 mg (41%)

$^1\text{H NMR}$ (CDCl_3) δ 0.95 (m, 2H), 1.15 (m, 2H), 1.5 - 1.8 (m, 4H), 2.0 (s, 1H), 2.6 (m, 3H), 4.6 (m, 1H), 7.25 (m, 7H), 7.85 (m, 2H); $^{13}\text{C NMR}$ (CDCl_3) δ 11.29 (cyclopropyl methylenes), 16.91 (cyclopropyl methine), 27.15, 35.67, and 38.47 (aliphatic methylenes), 74.34 (alcoholic methine), 125.77, 127.56, 128.18, and 128.47 (aromatic methines), 135.83, 144.67, 147.64 (aromatic quarts), 200.15 (carbonyl carbon); IR 3448, 3028, 2938, 2860, 1664, 1606, 1568, 1385, 1230, 994, 701; MS m/e (relative intensity) 294 (M^+ 11), 276 (48), 253 (10) 172 (80), 160 (100), 104 (95), 79 (45); **HIGH RES. MS** for $\text{C}_{20}\text{H}_{22}\text{O}_2$, calc. 294.1619802, found 294.158203, error: 12.8 ppm.

dimer (**32a**) - 11 mg (7%)

^1H NMR (CDCl_3) δ 0.2 - 0.5 (m, 4H), 1.3 (m, 1H), 1.6 - 2.1 (m, 5H), 2.95 (t, 2H, $J = 6.1$ Hz), 7.2 - 7.6 (m, 8H), 7.95 (m, 2H); ^{13}C NMR (CDCl_3) δ 0.78, 1.57, and 18.68 (methylenes), 22.19 (methine), 38.68, and 41.88 (methylenes), 75.01 (alcoholic quart), 125.71, 126.74, 128.65, and 132.99 (aromatic methines), 137.28, and 146.51 (aromatic quarts), 200.34 (carbonyl carbon); IR 3476, 3008, 2931, 1678, 1597, 1580, 1446, 754, 599; MS m/e (relative intensity) 276 ($\text{M}^+ - \text{H}_2\text{O}$, 14), 253 (8), 171 (14), 147 (68), 129 (35), 105 (100), 91 (22), 77 (57).

trimer (**34a**) - 16.5 mg (11%)

^1H NMR (CDCl_3) δ 0.95 (m, 2H), 1.15 (m, 2H), 1.5 - 1.9 (m, 10H), 2.65 (m, 5H), 4.6 (m, 2H), 7.1 - 7.4 (m, 11H), 7.95 (m, 2H); IR 3417, 3026, 2936, 2859, 1657, 1606, 1568, 1385, 1230, 993, 758, 700; MS m/e (relative intensity) 424 ($\text{M}^+ - \text{H}_2\text{O}$, 7), 406 ($\text{M}^+ - 2\text{H}_2\text{O}$, 27), 289 (40), 247 (25), 160 (48), 129 (95), 117 (98), 91 (100), 69 (75).

*note - repeating the above experiment with a 5% DCl in D_2O quench gave identical results with no detectable deuterium incorporation in products or remaining starting material by mass spec or deuterium NMR.

Electrolysis of (28a) with CH₃I quench

Phenyl cyclopropyl ketone [199 mg (1.36 mmol)] was electrolyzed at 35 mA for 62.5 minutes passing 1.36 mmol (1 equivalent) of electrons. The reaction was quenched with 400 μ L (6.3 mmol, 4.5 equivalents) of methyl iodide, worked up and flash chromatographed with a solvent gradient starting with 15/85 and finishing with 50/50 ethyl acetate/hexane to yield:

recovered starting material - 27 mg (14%)

O-methylated dimer (**41**) - 53 mg (25%)

¹H NMR (CDCl₃) δ 1.0 (m, 2H), 1.25 (m, 2H), 1.6 - 1.9 (m, 4H), 2.65 (m, 3H), 3.2 (s, 3H), 4.1 (t, 1H, J = 7.5 Hz), 7.3 (m, 7H), 7.95 (d, 2H, 8 Hz); ¹³C NMR (CDCl₃) δ 11.21 (cyclopropyl methylene), 16.90 (cyclopropyl methine), 27.21, 35.76, and 37.64 (aliphatic methylenes), 56.56 (O-methyl), 83.84 (methine), 126.59, 126.95, 127.50, 128.11, 128.34, and 128.47 (aromatic methines), 135.82, 142.15, 147.70 (aromatic quarts), 200.15 (carbonyl carbon); IR 3084, 3060, 3006, 2934, 2860, 2821, 1667, 1607, 1569, 1493, 1452, 1416, 1384, 1229, 1103, 993, 702; MS m/e (relative intensity) 308 (M⁺, 2.5), 276 (65), 172 (80), 147 (50), 104 (100), 91 (75), 77 (90).

dimer (**31a**) - 52 mg (26%)

dimer (**32a**) - 11 mg (5%)

trimer (**34a**) - 15 mg (7%)

Electrolysis of (28a) in presence of D₂O

Phenyl cyclopropyl ketone [225 mg (1.5 mmol)] was electrolyzed at 35 mA for 69 minutes passing 1.5 mmol (1 equivalent) of electrons in an electrolyte solution containing 3 mole equivalents of D₂O. The cathodic compartment was quenched with 5% aqueous HCl, worked up, and flash chromatographed with a solvent gradient starting with 10/90 and finishing with 50/50 ethyl acetate/hexane yielding:

recovered starting material - 29 mg (13%)

¹H NMR (CDCl₃) δ 1.05 (m, 2H), 1.25 (m, 2H), 2.65 (m, .75H), 7.5 (m, 3H), 8.0 (m, 2H);

²H NMR δ 2.65 (s).

Deuterium incorporation in recovered starting material at the cyclopropyl methine position estimated to be 25% based on ¹H NMR integration of signal at 2.65 ppm relative to the rest of the spectrum and the presence of a strong signal in ²H NMR at 2.65 ppm.

dimer (31a) - 106 mg (48%)

¹H NMR (CDCl₃) δ 0.95 (m, 2H), 1.15 (m, 2H), 1.5 - 1.8 (m, 3.5 H), 2.3 (s, 1H), 2.6 (m, 2.25H), 4.6 (m, 1H), 7.25 (m, 7H), 7.85 (d, 2H, J = 9 Hz); ²H NMR (CHCl₃) δ 1.7 (s), 2.6 (s); MS 297 (13.5), 296 (19.5), 295 (17.5), 294 (9.2), 280 (17.7), 279 (47.4), 278 (92.5), 277 (100), 276 (45.4).

The total deuterium incorporated in this sample was estimated by comparison of the mass spectrum of this sample with the mass spectrum of an authentic sample of the fully hydrido isomer. The amount of deuterium incorporated at specific sites in the molecule was estimated by the low integration in ¹H NMR of signals centered at 2.6 and 1.7 ppm and the presence of strong signals in ²H NMR at the same chemical shift in the relative ratio of 1.5 to 1. We estimate that 50% of one hydrogen β to the benzylic alcohol and

75% of the cyclopropyl methine hydrogen have been replaced by deuterium.

dimer (**32a**) - 22 mg (10%)

^1H NMR (CDCl_3) same as reported earlier; ^2H NMR (CHCl_3) δ 1.3 (small peak); no MS obtained because M^+ not observed for this species. Deuterium incorporation estimated to be no more than 10% at the cyclopropyl methine position for this sample. This estimation was arrived at by considering that the sensitivity of NMR experiments to detect deuterium incorporation lies in the 5-10% range. We observe a weak signal in ^2H NMR due to substitution of deuterium on the cyclopropyl methine but ^1H NMR integration does not reveal any deviation from the results obtained for the fully hydrido isomer.

trimer (**34a**) - 53 mg (24%)

^1H NMR (CDCl_3) same as reported earlier; ^2H NMR (CHCl_3) δ 1.7 (s), 2.6 (s); no MS obtained because M^+ not observed for this species. Deuterium incorporation in this trimer is postulated to be similar in magnitude and distribution to the deuterium incorporation in dimer (**31a**), although we have no firm experimental data upon which to base this claim. The ^2H NMR shows strong signals at 1.7 and 2.6 ppm in the relative ratio of 1 to 1; however, the ^1H NMR integration shows no deviation from the integration of the ^1H NMR spectrum of the fully hydrido isomer (traditionally it is difficult to get good integration for ^1H NMR spectra of compounds with high molecular weight).

1-Benzoyl-1-deuteriocyclopropane (45)

Electrolysis of 212 mg (1.44 mmol) of 1-benzoyl-1-deuteriocyclopropane at 35 mA for 66 minutes passed 1.44 mmol (1 equivalent) of electrons. Quenching with 400 μ L (4 mol equivalents) of methyl iodide, work up, and flash chromatography with a solvent gradient starting at 10/90 and finishing with 50/50 ethyl acetate/hexane yielded:

recovered starting material - 34 mg (16%)

$^1\text{H NMR}$ (CDCl_3) δ 1.05 (m, 2H), 1.25 (m, 2H), 2.65 (m, .95H), 7.5 (m, 3H), 8.0 (m, 2H);

$^2\text{H NMR}$ (CHCl_3) δ 2.65 (s).

We estimate that the recovered starting material maintained only 5% of its deuterium label at the cyclopropyl methine position based on the integration of the $^1\text{H NMR}$ spectrum and the presence of only a weak signal in $^2\text{H NMR}$ at 2.65 ppm.

O-methylated dimer (41) - 47 mg (21%)

$^1\text{H NMR}$ (CDCl_3) same as reported earlier; $^2\text{H NMR}$ (CHCl_3) δ 1.7 (s), 2.65 (s), extremely weak signals.

We estimate that this compound has no more than 5% deuterium label distributed between the positions β to the benzylic ether and α to the carbonyl at the cyclopropyl methine. We base this on the observation that integration of the $^1\text{H NMR}$ spectrum of this sample does not deviate from the integration of the $^1\text{H NMR}$ spectrum of the fully hydrido isomer and that the $^2\text{H NMR}$ spectrum shows only two extremely weak signals at 1.7 and 2.65 ppm in the relative ratio of 1 to 2.

dimer (**31a**) (loss of >95% of label) - 54 mg (25%)

$^1\text{H NMR}$ (CDCl_3) same as reported earlier; $^2\text{H NMR}$ (CHCl_3) δ 1.7 (s), 2.60 (s), extremely weak signals.

We estimate that this compound has no more than 5% deuterium label distributed between the positions β to the benzylic alcohol and α to the carbonyl at the cyclopropyl methine.

We base this on the observation that integration of the $^1\text{H NMR}$ spectrum of this sample does not deviate from the integration of the $^1\text{H NMR}$ spectrum of the fully hydrido isomer and that the $^2\text{H NMR}$ spectrum shows only two extremely weak signals at 1.7 and 2.65 ppm in the relative ratio of 1 to 2.

dimer (**32a**) - 12 mg (5%)

No deuterium label found by $^2\text{H NMR}$. $^1\text{H NMR}$ same as for fully hydrido isomer.

trimer (**34a**) - 17 mg (8%)

No deuterium label found by $^2\text{H NMR}$. $^1\text{H NMR}$ same as for fully hydrido isomer.

trans-1-Benzoyl-2-methylcyclopropane (28b)

Electrolysis of 166 mg (1.03 mmol) of *trans*-1-benzoyl-2-methylcyclopropane at 35 mA for 47 minutes passed 1.02 mmol (0.99 equivalents) of electrons. Quenching with 5% aqueous HCl, work up, and flash chromatography with a solvent gradient beginning with 20/80 and ending with 50/50 ethyl acetate/hexane yielded:

recovered starting material - 29 mg (17%)

dimer (**31b**) - 85 mg (51%)

¹H NMR (CDCl₃) δ 0.85 (m, 1H), 1.25 (m, 6H), 1.4 - 1.8 (m, 6H), 2.1 (s, 1H), 2.35 (m, 1H), 2.8 (m, 1H), 4.6 (m, 1H), 7.3 (m, 7H), 7.9 (m, 2H); **¹³C NMR** δ 18.44 (methyl), 20.08 (methylene), 21.18 (methine), 22.35 (methyl), 26.47 (methine), 34.16, 37.20 (methylene), 40.15(methine), 74.70 (methine), 126.02, 127.28, 127.67, 128.46, and 128.61 (aromatic methines), 136.35, 144.85, and 152.70 (aromatic quarts), 199.87 (carbonyl carbon); **IR** 3448, 3028, 2967, 2928, 2868, 1660, 1605, 1569, 1493, 1331, 1228, 1182, 850, 700; **MS** m/e (relative intensity) 322 (M⁺, 4), 304 (26), 267 (9), 161 (100), 145 (85), 117 (45), 107 (50), 79 (55); **HIGH RES. MS** for C₂₂H₂₆O₂, calc. 322.1932803, found 322.1920, error: 4.0 ppm..

dimer (**32b**) - 10 mg (6%)

¹H NMR (CDCl₃) δ 0.1 (m, 2H), 0.3 (m, 1H), 0.45 (m, 1H), 0.8 -1.1 (m, 6H), 1.4 (m, 2H), 2.0 - 2.2 (m, 2H), 2.9 (m, 2H), 7.2 - 7.5 (m, 8H), 7.9 (m, 2H); **IR** 3512, 3059, 2962, 1680, 1598, 1580, 1447, 1267, 1077, 1031, 796, 700; **MS** m/e (relative intensity) 322 (0.5), 304 (1.8), 161 (100), 143 (25), 105 (81), 77 (32).

trimer (**34b**) - 34 mg (15%)

$^1\text{H NMR}$ (CDCl_3) δ 0.85 (m, 1H), 1.1 - 1.3 (m, 9H), 1.4 - 1.9 (m, 12H), 2.35 (m, 1H), 2.8 (m, 2H), 4.6 (m, 2H), 7.1 - 7.4 (m, 11H), 7.9 (m, 2H); **IR** 3420, 3027, 2958, 2930, 2868, 1658, 1605, 1569, 1509, 1493, 1228, 1030, 911, 758, 700; **MS** m/e (relative intensity) 466 ($\text{M}^+ - \text{H}_2\text{O}$, 12), 448 ($\text{M}^+ - 2\text{H}_2\text{O}$, 25), 362 (18), 331 (48), 188 (100), 145 (90), 105 (50), 91 (65), 83 (70), 77 (25).

tetramer (**35b**) - 9 mg (5%)

$^1\text{H NMR}$ (CDCl_3) δ 0.85 (m, 1H), 1.25 (m, 12H), 1.4 - 1.8 (m, 17H), 2.35 (m, 1H), 2.6 - 2.9 (m, 3H), 4.6 (m, 3H), 7.1 - 7.4 (m, 15H), 7.9 (m, 2H); **IR** 3416, 3026, 2960, 2927, 2868, 1659, 1605, 1569, 1509, 1493, 1454, 1261, 1227, 910, 836, 800, 759, 734, 701; **MS** m/e (relative intensity) 628 ($\text{M}^+ - \text{H}_2\text{O}$, 0.2), 610 ($\text{M}^+ - 2\text{H}_2\text{O}$, 1.3), 592 ($\text{M}^+ - 3\text{H}_2\text{O}$, 1), 448 (9), 362 (10), 331 (50), 188 (100).

1-Benzoyl-2,2-dimethylcyclopropane (28c)

Electrolysis of 158 mg (0.91 mmol) of 1-benzoyl-2,2-dimethylcyclopropane at 35 mA for 42 minutes passed 0.91 mmol (1 equivalent) of electrons. Quenching with 5% aqueous HCl, work up, and flash chromatography with a solvent gradient beginning with 10/90 and finishing with 50/50 ethyl acetate/hexane yielded:

recovered starting material - 27 mg (17%)

dimer (31c) - 63 mg (40%)

$^1\text{H NMR}$ (CDCl_3) δ 0.9 (m, 1H), 1.1 (s, 3H), 1.30 (two close singlets, 6H), 1.35 (s, 3H), 1.4 - 1.6 (m, 5H), 2.0 (s, 1H), 2.45 (m, 1H), 4.55 (m, 1H), 7.2 - 7.4 (m, 7H), 7.9 (m, 2H); $^{13}\text{C NMR}$ (CDCl_3) δ 18.55 (methyl), 21.92 (methylene), 26.53 (quart.), 27.07, 28.73, and 28.20 (methyl), 32.85 (methine), 34.19 (methylene), 37.87 (quart.), 40.04 (methylene), 74.99 (methine), 125.92, 127.57, 127.94, and 128.49 (aromatic methines), 136.70, and 154.11 (aromatic quarts.), 198.30 (carbonyl carbon); IR 3450, 3030, 2959, 2868, 1659, 1609, 1560, 1455, 1391, 1272, 1222, 1188, 1103, 1047, 997, 906, 857, 801, 759, 695; MS m/e (relative intensity) 350 (M^+ , 35), 332 (12), 281 (30), 263 (12), 215 (100); **HIGH RES. MS** for $\text{C}_{24}\text{H}_{30}\text{O}_2$, calc. 350.2245805, found 350.225220, error: 1.8 ppm.

trimer (**34c**) - 28 mg (17%)

$^1\text{H NMR}$ (CDCl_3) δ 0.9 (m, 1H), 1.1 (s, 3H), 1.3 - 1.4 (5 singlets, 15H), 1.5 - 1.65 (m, 9H), 1.9 (m, 2H), 2.45 (m, 1H), 4.55 (m, 2H), 7.2 - 7.4 (m, 11H), 7.9 (m, 2H); $^{13}\text{C NMR}$ (CDCl_3) δ 18.68, 22.03, 26.72, 27.19, 29.14, 32.89, 34.38, 37.43, 38.06, 40.28, 74.93, 75.16, 125.80, 126.05, 127.61, 128.07, 128.54, 154.33, 198.24; **IR** 3440, 3060, 3028, 2962, 2870, 1663, 1605, 1566, 1409, 1387, 1225, 999, 911, 757, 734, 701.

tetramer (**35c**) - 13 mg (7%)

$^1\text{H NMR}$ (CDCl_3) δ 0.9 (m, 1H), 1.1 (s, 3H), 1.2 - 1.4 (7 singlets, 21H), 1.4 - 1.6 (m, 13H), 1.8 (m, 3H), 2.45 (m, 1H), 4.55 (m, 3H), 7.1 - 7.4 (m, 15H), 7.9 (m, 2H); **IR** 3418, 3088, 3058, 3027, 2961, 2869, 1661, 1605, 1566, 1409, 1387, 1225, 910, 733.

1-(d5)Benzoyl-2,2-dimethylcyclopropane (42)

Electrolysis of 150 mg (0.84 mmol) of 1-(d5)benzoyl-2,2-dimethylcyclopropane at 35 mA for 25 minutes passed 0.54 mmol (0.64 equivalents) of electrons. Quenching with 5% aqueous HCl, work up, and flash chromatography with a solvent gradient beginning with 15/85 and ending with 50/50 ethyl acetate/hexane yielded:

recovered starting material - 35 mg (23%)

dimer (43) - 36 mg (24%)

$^1\text{H NMR}$ (CDCl_3) δ 0.9 (m, 1H), 1.1 (s, 3H), 1.30 (two close singlets, 6H), 1.35 (s, 3H), 1.4 - 1.6 (m, 5H), 1.9 (m, 1H), 2.45 (m, 1H); $^2\text{H NMR}$ (CHCl_3) δ 4.45 (s, 1D), 7.2 - 7.4 (s, 7D), 7.9 (s, 2D); IR 3447, 2951, 2869, 2276, 2113, 1663, 1577, 1540, 1458, 1418, 1387, 1182, 1116, 1089, 991; MS m/e (relative intensity) 360 (M^+ , 55), 342 (22), 291 (45), 219 (100).

trimer (34c-d15) - 20 mg (13%)

$^1\text{H NMR}$ (CDCl_3) δ 0.9 (m, 1H), 1.1 (s, 3H), 1.3 - 1.4 (5 singlets, 15H), 1.5 - 1.65 (m, 9H), 1.9 (m, 2H), 2.45 (m, 1H); $^2\text{H NMR}$ (CHCl_3) δ 4.55 (s, 2D), 7.1 - 8.0 (broad s, 13D); IR 3425, 2960, 2869, 2275, 2113, 1577, 1386, 1182, 1089, 991, 755.

tetramer (35c-d20) - 9 mg (6%)

$^1\text{H NMR}$ (CDCl_3) δ 0.9 (m, 1H), 1.1 (s, 3H), 1.2 - 1.4 (7 singlets, 21H), 1.4 - 1.6 (m, 13H), 1.8 (m, 3H), 2.45 (m, 1H); $^2\text{H NMR}$ (CHCl_3) δ 4.55 (s, 3D), 7.0 - 8.0 (broad s, 17D); IR 3422, 2960, 2869, 2273, 2113, 1662, 1577, 1457, 1386, 1366, 1183, 1089, 991, 756.

Coelectrolysis of 1-benzoyl-2,2-dimethylcyclopropane (28c) and 1-(d5)benzoyl-2,2-dimethylcyclopropane (42)

Electrolysis of 70.2 mg (0.39 mmol) and 68.5 mg (0.39 mmol) of each of the labelled and unlabelled substrates respectively (total 0.78 mmol) for 36 minutes at 35 mA passed 0.78 mmol (1 equivalent) of electrons. Quenching with 5% aqueous HCl, work up, and flash chromatography with a solvent gradient beginning at 15/85 and finishing with 50/50 ethyl acetate/hexane yielded:

recovered starting material (mixture of H/D) - 19 mg (~14%)

dimer (31c) (mixture of H/D) - 38 mg (~27%)

MS m/e (relative intensity) 350 (1.000), 351 (0.290), 352 (0.061), 353 (0), 354 (0.088), 355 (1.430), 356 (0.377), 357 (0.079), 358 (0.026), 359 (0), 360 (0.597), 361 (0.184), 362 (0.035); MS m/e (relative intensity) of fully hydrido dimer 350 (1.000), 351 (0.274), 352 (0.044); MS m/e (relative intensity) of fully deuterio dimer 360 (1.000), 361 (0.365), 362 (0.068).

trimer (34c) (mixture of H/D) - 27 mg (~19%)

tetramer (34 Ψ c) (mixture of H/D) - 11mg (~8%)

p-Tolyl cyclopropyl ketone (28d)

Electrolysis of 153 mg (0.95 mmol) of *p*-tolyl cyclopropyl ketone at 35 mA for 44 minutes passed 0.96 mmol (1.01 equivalents) of electrons. Quenching with 5% aqueous HCl, work up, and flash chromatography with a solvent gradient beginning at 8/92 and finishing with 50/50 ethyl acetate/hexane yielded:

recovered starting material - 27 mg (22%)

p-tolyl propyl ketone (38) - 17 mg (11%)

$^1\text{H NMR}$ (CDCl_3) δ 1.0 (t, 3H, $J = 8.3$ Hz), 1.8 (m, 2H), 2.4 (s, 3H), 2.95 (t, 2H, $J = 8.2$ Hz), 7.25 (d, 2H, $J = 12.0$ Hz), 7.85 (d, 2H, $J = 12.0$ Hz); $^{13}\text{C NMR}$ (CDCl_3) δ 13.87 (methyl), 17.92 (methylene), 21.53 (methyl), 40.43 (methylene), 128.18, and 129.19 (aromatic methines), 134.81, 143.50 (aromatic quarts.), 201.32 (carbonyl carbon); **IR** 3031, 2962, 2930, 2874, 1683, 1607, 1573, 1457, 1409, 1366, 1274, 1223, 1208, 1181, 1000, 897, 809, 748; **MS** m/e (relative intensity) 162 (12), 147 (15), 119 (100), 91 (47), 65 (22).

dimer (36) - 38 mg (25%)

$^1\text{H NMR}$ (CDCl_3) δ 0.35 (m, 2H), 0.45 (m, 2H), 1.3 (m, 1H), 1.6 - 2.1 (m, 5H), 2.3 (s, 3H), 2.4 (s, 3H), 2.95 (t, 2H), 7.1 - 7.4 (m, 6H), 7.8 (m, 2H); $^{13}\text{C NMR}$ (CDCl_3) δ 0.66 and 1.36 (cyclopropyl methylenes), 18.63 (methylene), 20.94, and 21.59 (methyls), 21.99 (methine), 38.47 and 41.83 (methylenes), 74.80 (methine), 125.52, 128.17, 128.72, and 129.18 (aromatic methines), 134.60, 136.06, 143.33, and 143.63 (aromatic quarts.), 199.98 (carbonyl carbon); **IR** 3476, 3005, 2922, 2870, 1677, 1607, 1572, 1512, 1453, 1407, 1181, 1020, 807; **MS** m/e (relative intensity) 322 (0.8), 304 (10), 281 (4), 185 (35), 158 (55), 143

(86), 119 (100), 105 (40), 91 (80).

dimer (37) - 12 mg (8%)

$^1\text{H NMR}$ (CDCl_3) δ 0.9 - 1.1 (m, 2H), 1.2 - 1.4 (m, 2H), 1.6 - 1.8 (m, 5H), 2.2 - 2.4 (m, appears to be two closely spaced singlets masking a multiplet, 7H), 2.75 - 2.85 (m, 2H), 4.7 (m, 1H), 7.1 - 7.3 (m, 6H), 7.65 (d, 1H); **IR** 3473, 3007, 2925, 2858, 1671, 1609, 1513, 1457, 1377, 1219, 1063, 1034, 990, 817; **MS** m/e (relative intensity) 322 (0.8), 304 (9), 174 (65), 161 (100), 119 (82), 105 (30), 91 (45), 77 (21).

trimer (39) - 7 mg (4%)

$^1\text{H NMR}$ (CDCl_3) δ 0.8 - 1.3 (m, 4H), 1.4 - 1.8 (m, 10H), 2.3 - 2.5 (m, 10H), 2.6 - 2.9 (m, 4H), 4.65 (m, 2H), 7.0 - 7.4 (m, 9H), 7.9 (d, 1H); **IR** 3456, 2929, 2857, 1676, 1608, 1512, 1452, 1408, 1379, 1263, 1219, 1181, 816, 732.

1-Benzoyl-1-methylcyclopropane (28e)

Electrolysis of 157 mg (0.98 mmol) of 1-benzoyl-1-methylcyclopropane for 45 minutes at 35 mA passed 0.98 mmol (1 equivalent) of electrons. Quenching with 5% aqueous HCl, work up, and flash chromatography with a solvent gradient starting with 20/80 and ending with 50/50 ethyl acetate/hexane yielded:

recovered starting material - 15 mg (10%)

dimer (**31e**) - 65 mg (41%)

$^1\text{H NMR}$ (CDCl_3) δ 0.65 (m, 2H), 0.85 (d, 3H), 1.1 (m, 2H), 1.35 (m, 4H, looks like singlet of 3H masking multiplet of 1H), 1.7 (m, 2H), 1.9 (s, 1H), 2.55 (m, 2H), 4.5 (m, 1H), 7.0- 7.3 (m, 7H), 7.65 (d, 2H); $^{13}\text{C NMR}$ (CDCl_3) δ 14.49 (methyl), 14.80 (cyclopropyl methylene), 22.09 (methyl), 25.35 (quart.), 33.40, and 34.41 (methylenes), 39.65, and 77.93 (methine), 126.32, 127.33, 128.18, and 128.58 (aromatic methines), 134.97, 143.43, and 146.85 (aromatic quarts.), 203.58 (carbonyl carbon); **IR** 3463, 3084, 3060, 3023, 2964, 2931, 2875, 1670, 1606, 1568, 1452, 1333, 1216, 1176, 1026, 988, 702; **MS** m/e (relative intensity) 322 (4.5), 304 (2.5), 267 (6), 174 (100), 118 (45), 107 (50); **HIGH RES. MS** for $\text{C}_{22}\text{H}_{26}\text{O}_2$, calc. 322.1932803, found 322.1962, error: 9.0 ppm.

1-methylcyclopropyl phenyl carbinol (**33e**) - 19 mg (12%)

$^1\text{H NMR}$ (CDCl_3) δ 0.3 (m, 2H), 0.6 (m, 2H), 0.9 (s, 3H), 1.8 (s, 1H), 4.1 (s, 1H), 7.1 - 7.4 (m, 5H); $^{13}\text{C NMR}$ (CDCl_3) δ 11.20 (methylene), 18.33 (methyl), 21.84 (quart.), 79.74 (methine), 126.22, 127.16, 127.97, 128.26, 128.57; **IR** 3442, 3064, 2961, 1450, 1026, 725, 700; **MS** m/e (relative intensity) 162 (1.5), 161 (2.8), 160 (2.0), 134 (100), 91 (25).

trimer (**34e**) - 14 mg (9%)

$^1\text{H NMR}$ (CDCl_3) δ 0.65 (m, 2H), 0.85 (m, 6H), 1.2 (m, 2H), 1.35 (m, 5H), 1.6 - 1.9 (m, 6H), 2.55 (m, 4H), 4.5 (m, 2H), 7.0 - 7.3 (m, 11H), 7.7 (m, 2H); $^{13}\text{C NMR}$ (CDCl_3) δ 14.41, 14.60, 14.89, 22.11, 25.39, 29.69, 30.10, 33.09, 33.46, 34.43, 34.78, 35.04, 35.22, 38.79, 39.69, 40.93, 77.98, 126.07, 126.37, 127.28, 128.19, 128.59, 129.27, 140.85, 141.16, 143.64; **IR** 3444, 3060, 3026, 2963, 2931, 2874, 1665, 1606, 1452, 1333, 1216, 1177, 1027, 988, 758, 702; **MS** m/e (relative intensity) 466 ($\text{M}^+ - \text{H}_2\text{O}$, 3), 448 ($\text{M}^+ - 2\text{H}_2\text{O}$, 6), 360 (7), 174 (100), 145 (40), 131 (35), 105 (42), 91 (65).

p-Cyclopropyl acetophenone (62)

Electrolysis of 160 mg (1.0 mmol) of *p*-cyclopropyl acetophenone for 46 minutes at 35 mA passed 1.0 mmol (1 equivalent) of electrons. Quenching with 5% aqueous HCl, work up, and flash chromatography with a solvent gradient starting with 10/90 and finishing with 20/80 ethyl acetate/hexane yielded:

starting material - 35 mg (22%)

dimer (64) - 65 mg (40%)

¹H NMR (CDCl₃) δ 0.65 (m, 4H), 0.95 (m, 4H), 1.45 (s, 6H), 1.90 (m, 2H), 2.6 (s, 2H), 6.95 (d, 4H, J = 11.5 Hz), 7.1 (d, 4H, J = 11.5 Hz); ¹³C NMR (CDCl₃) δ 9.17 (methylene), 14.96 (methine), 25.03 (methyl), 78.75 (quart.), 124.36, and 127.27 (aromatic methines), 140.62, and 142.62 (aromatic quarts.); IR 3456, 3081, 3001, 2935, 2872, 1613, 1514, 1459, 1371, 1193, 1144, 1069, 922, 903, 830, 733; MS m/e (relative intensity) 322 (0.2), 304 (0.3), 286 (0.5), 261 (24), 161 (100).

trans-2-Phenyl-1-benzoylcyclopropane (66)

Electrolysis of (66) with H_3O^+ quench

Electrolysis of 120 mg (0.54 mmol) of trans-1-benzoyl-2-phenylcyclopropane at -2.35 V for one hour passed 82 coulombs of current (1.6 equivalents of electrons). Quenching with 5% aqueous HCl, and work up yielded a viscous yellow oil which was two components (GC, HPLC) but was not separable by flash column chromatography or TLC. One component was shown to be starting material by comparison of the 1H NMR spectrum of the mixture to the 1H NMR spectrum of the starting ketone and also by GC coinjection. Exhaustive constant current electrolysis of trans-2-phenyl-1-benzoylcyclopropane provided a pure sample of the other component, 4-phenylbutyrophenone. GC response factors on authentic samples were determined relative to diphenyl ether and the reaction mixture analyzed by GC:

starting material - 25 mg (21%)

4-phenylbutyrophenone (71) - 89 mg (73%)

1H NMR ($CDCl_3$) δ 2.1 (m, 2H), 2.7 (t, 2H, $J = 7.6$ Hz), 2.95 (t, 2H, $J = 7.6$ Hz), 7.1 - 7.6 (m, 8H), 7.95 (m, 2H).

Electrolysis of (66) with a MeI quench

Electrolysis of 211 mg (0.95 mmol) of trans-1-benzoyl-2-phenylcyclopropane for 30 minutes at 35 mA passed 0.65 mmol (0.68 equivalents) of electrons. Quenching with 300 μ L (4 mole equivalents) of methyl iodide, work up, and flash chromatography with 7/93 ethyl acetate/hexane yielded:

recovered starting material - 113 mg (54%)

2-methyl-4-phenylbutyrophenone (**72**) - 66mg (29%)

$^1\text{H NMR}$ (CDCl_3) δ 1.15 (d, 3H, $J = 8.3$ Hz), 1.65 (m, 1H), 2.05 (m, 1H), 2.55 (t, 2H, $J = 7.8$ Hz), 3.4 (m, 1H), 7.0 - 7.5 (m, 8H), 7.8 (m, 2H); **IR** 3061, 3026, 2968, 2938, 2860, 1682, 1596, 1579, 1496, 1448, 1226, 974, 700.

methyl enol ether of 4-phenylbutyrophenone (**73**) - 8.5 mg (4%)

$^1\text{H NMR}$ (CDCl_3) δ 2.5 - 2.8 (m, 4H), 3.4 (s, 3H), 5.4 (t, 1H, $J = 7.8$ Hz), 7.0 - 7.5 (m, 5H); **IR** 3083, 3060, 3025, 2929, 2854, 1601, 1493, 1452, 1629, 1074.

1-benzoyl-1-methyl-2-phenylcyclopropane (**74**) - 14 mg (6%)

$^1\text{H NMR}$ (CDCl_3) δ 1.3 (s, 3H), 1.6 (m, 1H), 2.0 (m, 1H), 2.45 (m, 1H), 7.1 - 7.6 (m, 8H), 7.8 (m, 2H); **IR** 3060, 3027, 2970, 2940, 1670, 1497, 1448, 1224, 974, 700.

Electrolysis of (66) monitored by cyclic voltammetry

Electrolysis of 141 mg (0.63 mmol) of trans-1-benzoyl-2-phenylcyclopropane at 35 mA for 68 minutes passed 1.48 mmol (2.3 equivalents) of electrons. The electrolysis was monitored with a planar platinum electrode (0.5 mm in diameter) before, during and after the electrolysis experiment. Voltammetry in the electrolysis cell was performed by shutting down the electrolysis and switching the working electrode lead from the gold flag to the platinum voltammetry electrode and the auxiliary lead from the platinum mesh to the large gold flag electrode. Purging and stirring were stopped and voltammetric experiments run. The electrode leads were then switched back to electrolysis positions, purging and stirring resumed, and the electrolysis continued. This procedure was repeated every 10 minutes during the electrolysis. The cathodic compartment was quenched with 4 mole equivalents of methyl iodide, worked up and analyzed by GC. Response factors for authentic samples (obtained from the previously described experiment) were determined relative to diphenyl ether.

recovered starting material - 11 mg (8%)

methyl enol ether of 4-phenylbutyrophenone (73) - 6 mg (4%)

2-methyl-4-phenylbutyrophenone (72) - 93 mg (62%)

4-phenylbutyrophenone (71) - 2 mg (1%)

1-benzoyl-1-methyl-2-phenylcyclopropane (74) - 6 mg (4%)

1-Benzoyl-1-deuterio-2-phenylcyclopropane (75)

Electrolysis of 136 mg (0.61 mmol) of 1-benzoyl-1-deuterio-2-phenylcyclopropane at 30 mA for 50 minutes passed 0.93 mmol (1.5 equivalents) of electrons. Quenching with 5% aqueous HCl and work up yielded a viscous yellow oil. Yields were determined by GC. The GC response factors relative to diphenyl ether were assumed to be the same as those determined for the corresponding fully hydrido isomers.

recovered starting material (scrambled label) - 33 mg (24%)

MS (GC/MS) m/e (relative intensity) 224 (0.81), 223 (5.52), 222 (24.32), 221 (18.91), 219 (0.24), 105 (100)

Approximately 90% of the deuterium label was lost in the recovered starting material.

This was estimated by comparing the mass spectrum of this sample to the mass spectrum of the authentic hydrido and deutero isomers.

4-phenylbutyrophenone (71) - 97 mg (71%)

MS (GC/MS) m/e (relative intensity) 226 (0.50), 225 (4.08), 224 (15.14), 120 (100), 105 (50.27), 91 (13.3), 77 (37.02); ^2H NMR (CHCl_3) δ 2.7 (s), 2.9 (s), relative ratio 1 : 2.5.

The total deuterium incorporated into this product was estimated by comparison of the mass spectrum of this sample to the mass spectrum of the fully hydrido isomer. The distribution of deuterium in the molecule was estimated based upon the relative intensity of signals in the ^2H NMR spectrum of this sample. We estimate a total deuterium incorporation of 11% distributed between the positions α and γ to the carbonyl in a ratio of 2.5 to 1.

1-Benzoyl-2-vinylcyclopropane (76)

Electrolysis of 148 mg (0.86 mmol) of 1-benzoyl-2-vinylcyclopropane at 35 mA for 40 minutes passed 0.87 mmol (1.01 equivalents) of electrons. Quenching with 5% aqueous HCl, work up, and flash column chromatography with a solvent gradient starting at 2.5/97.5 and finishing at 5/95 ethyl acetate/hexane yielded:

recovered starting material - 39 mg (26%)

5-benzoyl-2-pentene (**80**) (mixture of cis & trans) - 42 mg (28%)

$^1\text{H NMR}$ (CDCl_3) δ 1.65 (m, 3H, looks like two doublets close together), 2.45 (m, 2H), 3.05 (t, 2H, $J = 7.6$ Hz), 5.5 (m, 2H), 7.5 (m, 3H), 7.9 (m, 2H); $^{13}\text{C NMR}$ (CDCl_3) δ 12.66, and 17.80 (cis and trans methyls), 21.69, 27.13, 38.37, and 38.48 (cis and trans methylenes), 125.08 (methine), 125.88 (quart.), 128.00, 128.50, 128.85, and 132.86 (methines), 199.74 (carbonyl carbon); **IR** 3061, 3016, 2919, 2857, 1688, 1598, 1580, 1449, 1409, 1358, 1203, 969, 744, 690; **MS** m/e (relative intensity) 175 (1.2), 174 (10.1), 159 (4.8), 145 (5.7), 120 (16.3), 105 (100), 77 (46.6); **HIGH RES. MS** for $\text{C}_{12}\text{H}_{14}\text{O}$, calc. 174.1044652, found 174.102890, error: 9.0 ppm.

1,10-dibenzoyl-3,7-decadiene (**81**) - 34 mg (23%)

$^1\text{H NMR}$ (CDCl_3) δ 2.1 (m, 4H), 2.45 (m, 4H), 3.0 (t, 4H, $J = 8.1$ Hz), 5.5 (m, 4H), 7.5 (m, 6H), 7.95 (m, 4H); $^{13}\text{C NMR}$ (CDCl_3) δ 27.22, 32.47, 38.56 (methylenes), 128.06, 128.55, 128.97, and 132.92 (methines), 137.10 (quart.), 199.73 (carbonyl carbon); **IR** 3061, 2922, 2850, 1686, 1597, 1580, 1448, 1410, 1363, 1203, 970, 743, 690; **MS** m/e (relative intensity) 348 (0.2), 347 (1.8), 346 (6.2), 328 (8.2), 278 (7.6), 227 (11.3), 226 (20), 208 (4.6), 199 (7.0), 173 (18.8), 120 (9.2), 105 (100), 77 (40); **HIGH RES. MS** for $\text{C}_{24}\text{H}_{26}\text{O}_2$, calc. 346.1932803, found 346.191605, error: 4.8 ppm.

COMPETITION KINETICS

The set up for these experiments was very similar to the set up for the previously described electrolysis experiments (Figure 77). A mercury (triply distilled, Bethlehem) pool was used as a working electrode instead of a gold flag. Electrical contact to the mercury pool (30 mm in diameter) was achieved by sealing a 0.5 mm diameter Pt wire through the bottom of the cathodic compartment of the H cell to attach the working electrode lead to. A platinum voltammetry electrode (0.5 mm diameter) was inserted into the cathodic compartment. The auxiliary (Pt gauze) and reference (Ag/Ag⁺) electrodes were the same as described earlier for electrolysis experiments. In voltammetry mode, the 0.5 mm Pt electrode was used as the working electrode and the Hg pool as the auxiliary electrode. Positive feedback IR compensation was set as described earlier.

The anodic compartment was charged with 25 mL of 0.2 M *n*-Bu₄NBF₄ in DMF and the cathodic compartment charged with an identical solution also containing a known concentration of pivalophenone (Aldrich). The cell was stirred and purged with argon for 30 minutes and then blanketed with argon. The potential of the voltammetry electrode was stepped to -2.9 V (pivalophenone E^o = -2.48 V (Ag/Ag⁺)) and the current decay was monitored as a function of time in order to measure the constant term ($nFAD_o^{1/2}/\pi^{1/2}$) in the Cottrell equation. Since the initial concentration of pivalophenone is known, a plot of $i(t)$ vs. $1/t^{1/2}$ yields a line from which the constant term of the Cottrell equation can be computed. (Cottrell equation: $i(t) = [nFAD_o^{1/2}/\pi^{1/2}][C_o^*/t^{1/2}]$, note that the diffusion coefficient, D_o , is taken to be the same for both pivalophenone and its ketyl anion.) The stirring and purging was restarted and the electrode leads switched to electrolysis mode. Constant current electrolysis (50 mA) was performed to generate pivalophenone ketyl anion. The cell was then switched back to voltammetry mode. The potential of the Pt

voltammetry electrode was stepped to -1.9 V and current decay monitored as a function of time to give an upper limit for the ketyl anion concentration (i.e. since all terms in the Cottrell equation are known except for the concentration of the ketyl anion, a plot of $i(t)$ vs. $1/t^{1/2}$ yields a line from which the concentration of the ketyl anion can be determined). A small amount (\leq one twentieth of the amount (moles) of ketyl anion present) of 1-bromo-5-hexene (Aldrich) or 5-hexenylmercuric chloride¹¹⁹ dissolved in 1 mL of DMF was then added dropwise to the cathodic compartment with vigorous stirring and purging. After addition was complete, the potential of the voltammetry electrode was stepped to -1.9 V and current decay monitored as a function of time to give a lower limit for the ketyl anion concentration.

The cathodic compartment was quenched with 5% aqueous HCl and poured into water. A known amount of diphenyl ether was added, and the solution extracted four times with 20 mL portions of diethyl ether. The organic layers were combined, washed three times with water and dried over magnesium sulfate. The product distribution was assessed by GC. Response factors for independently synthesized authentic samples (vide infra) were determined relative to diphenyl ether. Results are tabulated in Tables 15 and 16.

Table 15. Results of competition experiments using 1-bromo-5-hexene as the radical source

	Run 1	Run 2	Run 3
$^a P_1^\infty / P_2^\infty$	9.4	4.9	12.7
mass balance	61%	58%	57%
$[54]_{\max}$	1.14×10^{-2}	6.61×10^{-3}	1.15×10^{-2}
$[54]_{\min}$	8.29×10^{-3}	4.90×10^{-3}	8.78×10^{-3}
$^b k_{2 \max} (M^{-1}s^{-1})$	1.1×10^8	1.0×10^8	1.4×10^8
$^b k_{2 \min} (M^{-1}s^{-1})$	8.2×10^7	7.4×10^7	1.1×10^8
$^c k_{2 \text{ ave}} (M^{-1}s^{-1})$	9.6×10^7	8.7×10^7	1.2×10^8

^a P_1^∞ is total mmoles of coupling adducts containing the Δ^5 -hexenyl moiety and P_2^∞ is total mmoles of coupling adducts containing the cyclopentyl carbinyl moiety.

^b $k_2 = (P_1^\infty/P_2^\infty)(k_c/[54])$, $k_c = 1 \times 10^5 \text{ s}^{-1}$

^c $k_{2 \text{ ave}} = (k_{2 \max} + k_{2 \min})/2$

Table 16. Results of competition experiments using 5-hexenylmercuric chloride as the radical source

	Run 1	Run 2	Run 3
$^a P_1^\infty / P_2^\infty$	4.6	5.0	4.0
mass balance	80%	73%	68%
$[54]_{\max}$	8.64×10^{-3}	9.39×10^{-3}	8.31×10^{-3}
$[54]_{\min}$	4.73×10^{-3}	6.40×10^{-3}	5.82×10^{-3}
$^b k_{2 \max} (M^{-1}s^{-1})$	9.7×10^7	7.8×10^7	6.9×10^7
$^b k_{2 \min} (M^{-1}s^{-1})$	5.3×10^7	5.3×10^7	4.8×10^7
$^c k_{2 \text{ ave}} (M^{-1}s^{-1})$	7.5×10^7	6.6×10^7	5.9×10^7

^a P_1^∞ is total mmoles of coupling adducts containing the Δ^5 -hexenyl moiety and P_2^∞ is the total mmoles of coupling adducts containing the cyclopentyl carbinyl moiety

^b $k_2 = (P_1^\infty/P_2^\infty)(k_c/[54])$, $k_c = 1 \times 10^5 \text{ s}^{-1}$

^c $k_{2 \text{ ave}} = (k_{2 \max} + k_{2 \min})/2$

INDEPENDENT SYNTHESIS OF PIVALOPHENONE KETYL ANION/FREE RADICAL COUPLING PRODUCTS

Constant current electrolyses of pivalophenone were performed in an H cell with a gold electrode as described earlier. During the course of the electrolysis either 1-bromo-5-hexene (Aldrich) or (bromomethyl)cyclopentane¹²⁰ in 2 mL of DMF was slowly added dropwise. Addition of the bromide was controlled so that the ketyl anion color (reddish/black) was never fully dissipated. After the electrolysis/addition was complete, the cathodic compartment was quenched with 5% aqueous HCl and poured into water. The aqueous layer was extracted four times with 25 mL portions of diethyl ether. The organic layers were combined, washed 3 times with water, dried over magnesium sulfate and concentrated. The crude reaction mixtures were separated by preparative HPLC.

Coupling of Pivalophenone Ketyl Anion and Δ^5 -hexenyl Radical

Pivalophenone [252 mg (1.56 mmol)] was electrolyzed for 72 minutes at 35 mA passing 1.56 mmol (1 equivalent) of electrons. After 10 minutes of electrolysis, addition of 140 mg (0.86 mmol) of 1-bromo-5-hexene in 2 mL of DMF was begun. Slow addition was continued over the remainder of the electrolysis. The cathodic compartment was quenched, worked up, and chromatographed (80% acetonitrile, 20% water) to yield:

58a - 17 mg (8%)

$^1\text{H NMR}$ (CDCl_3) δ 0.8 (s, 9H), 1.0 - 1.4 (m, 4H), 1.5 - 2.2 (m, 5H), 4.85 (m, 2H), 5.7 (m, 1H), 7.1 - 7.4 (m, 5H); $^{13}\text{C NMR}$ (CDCl_3) δ 23.48 (methylene), 25.82 (methyl), 29.58, 33.64, and 34.57 (methylene), 38.48, and 80.99 (quart.), 114.27 (methylene), 126.15, 127.09, 127.55, 138.89 (methines), 143.34 (quart.); IR 3608, 3061, 3023, 2959, 2872, 1640, 1603, 1493, 1481, 1496, 1446, 1393, 1366, 1262, 1108, 1071, 909, 805, 757, 709; MS (GC/MS) m/e (relative intensity) 231 (M^+-15 , 0.8), 189 (34.14), 171 (3.16), 133 (6.06), 105 (100), 91 (9.43), 77 (16.65).

57a - 15 mg (7%)

$^1\text{H NMR}$ (CDCl_3) δ 1.1 - 1.4 (m, 15H), 1.95 (m, 2H), 2.75 (m, 2H), 3.25 (m, 1H), 4.85 (m, 2H), 5.7 (m, 3H), 6.4 (m, 1H); $^{13}\text{C NMR}$ (CDCl_3) δ 25.20, and 26.92 (methylenes), 28.60 (methyl), 29.10, 33.72, and 34.97 (methylenes), 35.20 (methine), 43.95 (quart.), 114.19 (methylene), 122.24, 129.75, 130.37, and 139.04 (methines), 140.14 (quart.), 209.83 (carbonyl carbon); **IR** 3076, 3028, 2930, 2859, 1661, 1640, 1630, 1477, 1461, 1418, 1394, 1366, 1262, 1155, 910; **UV** (methanol) 244 (2516); **MS** (GC/MS) m/e (relative intensity) 247 (0.71), 246 (M^+ , 5.15), 245 (7.96), 189 (29.56), 163 (15.77), 145 (9.20), 129 (20.79), 105 (49.32), 91 (100), 77 (31.63), 57 (82); **HIGH RES. MS** for $\text{C}_{17}\text{H}_{26}\text{O}$, calc. 246.1983657, found 246.196077, error: 9.3 ppm.

*note - see Appendix C for explanation of how UV spectrometry aided in identifying this product.

56a - 48 mg (23%)

$^1\text{H NMR}$ (CDCl_3) δ 1.3 - 1.5 (m, 11H, singlet for t-butyl masking multiplet), 1.6 (m, 2H), 2.05 (m, 2H), 2.6 (t, 2H, $J = 6.9$ Hz), 4.95 (m, 2H), 5.8 (m, 1H), 7.15 (d, 2H, $J = 8.3$ Hz), 7.65 (d, 2H, $J = 8.3$ Hz); $^{13}\text{C NMR}$ (CDCl_3) δ 28.09 (methyl), 28.40, 30.44, 33.49, 35.59, and 114.43 (methylenes), 122.48, 127.95, and 128.26 (methines), 138.57, 145.99 (quarts); **IR** 3076, 3026, 2969, 2931, 2858, 1672, 1640, 1607, 1477, 1461, 1412, 1394, 1366, 1277, 1196, 1172, 962, 910, 762, 708; **MS** m/e (relative intensity) 245 (0.7), 244 (M^+ , 3.5), 187 (100), 91 (65), 77 (21), 57 (60); **HIGH RES. MS** for $\text{C}_{17}\text{H}_{24}\text{O}$, calc. 244.1827156, found 244.181885, error: 3.4 ppm.

Coupling of Pivalophenone Ketyl Anion and Cyclopentyl Carbinyl Radical

Pivalophenone [244 mg (1.50 mmol)] was electrolyzed for 69 minutes at 35 mA passing 1.50 mmol (1 equivalent) of electrons. After 10 minutes of electrolysis, addition of 135 mg (0.83 mmol) of (bromomethyl)cyclopentane in 2 mL of DMF was begun. Slow addition was continued over the remainder of the electrolysis. The cathodic compartment was quenched, worked up, and chromatographed (80% acetonitrile, 20% water) to yield:

58b - 20 mg (10%)

¹H NMR (CDCl₃) δ 0.8 (s, 9H), 1.0 - 1.8 (m, 11H), 2.3 (m, 1H), 7.1 - 7.5 (m, 5H); **¹³C NMR** (CDCl₃) δ 25.90 (methyl), 34.26, and 34.84 (methylenes), 36.53 (methine), 38.63 (quart.), 40.59 (methylene), 81.53 (quart.), 126.07, 126.93, and 127.64 (methines), 144.05 (quart.); **IR** 3630, 3086, 3058, 3022, 2955, 2870, 1600, 1446, 1393, 1365, 1071, 757, 709; **MS** (GC/MS) m/e (relative intensity) 231 (M⁺-15, 0.5), 189 (100), 121 (20), 105 (32), 91 (15), 77 (30), 57 (45).

57b - 22 mg (10%)

$^1\text{H NMR}$ (CDCl_3) δ 0.7 - 1.8 (m, 20H), 2.8 (m, 2H), 3.3 (m, 1H), 5.65 (m, 1H), 5.9 (m, 1H), 6.4 (m, 1H); $^{13}\text{C NMR}$ (CDCl_3) δ 25.18 (methylene), 28.63 (methyl), 32.23, 33.79, (methylene), 34.75, 37.39 (methine), 42.62 (methylene), 43.87 (quart.), 121.85, 129.88, and 130.13 (methine), 141.00 (quart.), 209.76 (carbonyl carbon); **IR** 3030, 2956, 2860, 1661, 1630, 1476, 1460, 1418, 1394, 1365, 1261, 1155, 1024, 801, 708; **UV** (methanol) 242 (1820); **MS** (GC/MS) *m/e* (relative intensity) 247 (0.45), 246 (2.77), 189 (4.45), 164 (12.42), 107 (100), 93 (4.59), 77 (10.22), 57 (21.88); **HIGH RES. MS** for $\text{C}_{17}\text{H}_{26}\text{O}$, calc. 246.1983657, found 246.199417, error: 4.3 ppm.

*note - see Appendix C for explanation of how UV spectrometry aided in identifying this product.

56b - 58 mg (29%)

$^1\text{H NMR}$ (CDCl_3) δ 1.35 (s, 9H), 1.4 - 1.8 (m, 8H), 2.05 (m, 1H), 2.6 (d, 2H, $J = 9.1$ Hz), 7.15 (d, 2H, $J = 10.2$ Hz), 7.65 (d, 2H, $J = 10.2$ Hz); $^{13}\text{C NMR}$ (CDCl_3) δ 24.91 (methylene), 28.18 (methyl), 32.50 (methylene), 41.65 (methine), 41.95 (methylene), 44.06 (quart.), 128.24, and 128.40 (methines), 135.70, and 145.82 (quarts.); **IR** 2962, 2869, 1675, 1607, 1476, 1458, 1411, 1261, 1098, 1019, 801; **MS** (GC/MS) *m/e* (relative intensity) 245 (0.12), 244 (M^+ , 0.64), 201 (0.84), 187 (100), 119 (6.08), 91 (14.19), 77 (2.22), 57 (5.76); **HIGH RES. MS** for $\text{C}_{17}\text{H}_{24}\text{O}$, calc. 244.1827156, found 244.180450, error: 9.3 ppm.

Synthesis of di(5-hexenyl)mercury (59)

Pivalophenone [255 mg (1.57 mmol)] was electrolyzed for 60 minutes at 35 mA passing 1.3 mmol (0.83 equivalents) of electrons. After electrolysis, 171.5 mg (0.54 mmol) of 5-hexenylmercuric chloride was added (neat) to the cathodic compartment. The reaction was stirred for 5 minutes under argon, quenched with 5% aqueous HCl, worked up, and flash chromatographed with 5/95 ethyl acetate/hexane to yield:

di(5-hexenyl)mercury (59) - 84 mg (42%)

$^1\text{H NMR}$ (CDCl_3) δ 1.05 (t, 4H, $J = 8.1$ Hz), 1.45 (m, 4H), 1.85 (m, 4H), 2.05 (m, 4H), 4.95 (m, 4H), 5.80 (m, 2H); $^{13}\text{C NMR}$ (CDCl_3) δ 28.30, 33.70, 34.68, 44.07, and 114.06 (methylenes), 139.33 (methine); IR 3075, 2921, 2845, 1640, 1458, 994, 908; MS (chemical ionization) m/e (relative intensity) 369 (7.5), 368 (6.7), 367 (27.0), 366 (15.1), 365 (19.8), 364 (13.5), 363 (7.1), 117 (100).

LITERATURE CITED

1. Andrieux, C., Bouchiat, J., Saveant, J., J. Electroanal. Chem., **1978**, *88*, 43.
2. House, H., "*Modern Synthetic Reactions*", W.A. Benjamin Inc., Philippines, 1972.
3. Schlesener, C., Amatore, C., Kochi, J., J. Am. Chem. Soc., **1984**, *106*, 7472.
4. Bordwell, F., Cheng, J., J. Am. Chem. Soc., **1989**, *111*, 1792
5. a) Ortiz de Montellano, P., ed., "*Cytochrome P-450: Structure, Mechanism, and Biochemistry*", Plenum Press, New York, 1986.
b) Groves, J., J. Chem. Ed., **1985**, *62(11)*, 928.
6. Norris, J., Schiffer, M., Chem. and Eng. News, **1990**, *68(31)*, 22.
7. Kochi, J., Pure and Applied Chem., **1980**, *52*, 571.
8. a) Garst, J., in "*Free Radicals, Vol I*", Kochi, J., ed., Wiley, New York, 1973, p. 503.
b) Ebersson, L., "*Electron Transfer Reactions in Organic Chemistry*", Springer Verlag, New York, 1987.
9. Sankaraman, S., Haney, W., Kochi, J., J. Am. Chem. Soc., **1987**, *109*, 5235.
10. Masnovi, J., Sankaraman, S., Kochi, J., J. Am. Chem. Soc., **1989**, *111*, 2263.
11. Lund, T., Lund, H., Acta. Chem. Scand., **1986**, *B40*, 470.
12. a) Rossi, de Rossi, in "*Aromatic Substitution by the S_{RN}1 Mechanism*", American Chemical Society, Washington, 1983.
b) Rossi, Acc. Chem. Res., **1982**, *15*, 164.
c) Carey, F., Sundberg, R., "*Advanced Organic Chemistry, 2nd ed., Part A*", Plenum Press, New York, 1984, p. 683.
13. Ashby, E., Wiesemann, T., J. Am. Chem. Soc., **1978**, *100(1)*, 189.
14. Ashby, E., Pure and Applied Chem., **1980**, *52*, 545.
15. Blomberg, C., Salinger, R., Mosher, H., J. Org. Chem., **1969**, *34(8)*, 2385.
16. a) Holm, T., Crossland, I., Acta. Chem. Scand., **1971**, *25*, 59.
b) Bordwell, F., Harrelson, J., Satish, A., J. Org. Chem., **1989**, *54*, 3101.
c) Bordwell, F., Bausch, M., J. Am. Chem. Soc., **1986**, *108*, 1985.
d) Bordwell, F., Clemens, A., J. Org. Chem., **1981**, *46*, 1037.
17. Ashby, E., Goel, A., DePriest, R., J. Am. Chem. Soc., **1980**, *102*, 7779.
18. Ward, H., Lawler, R., Cooper, R., J. Am. Chem. Soc., **1969**, *91*, 746.

19. Lepley, R., Landau, R., J. Am. Chem. Soc., 1969, 91, 748.
20. Russell, G., Larson, D., J. Am. Chem. Soc., 1969, 91, 3967.
21. Russell, G., Janzen, E., Strom, E., J. Am. Chem. Soc., 1964, 86(9), 1807.
22. Ashby, E., Wiesmann, T., J. Am. Chem. Soc., 1978, 100(10), 3101.
23. House, H., Weeks, P., J. Am. Chem. Soc., 1975, 97(10), 2770.
24. House, H., Weeks, P., J. Am. Chem. Soc., 1975, 97(10), 2778.
25. Chung, S., Dunn, K., Larson, B., J. Org. Chem., 1984, 49, 935.
26. Renaud, P., Fox, M.A., J. Org. Chem., 1988, 53, 3745.
27. Ashby, E., Pham, T., Park, B., Tetrahedron Lett., 1985, 26, 4691.
28. a) Kariv-Miller, E., Machachi, T., J. Org. Chem., 1986, 51, 1041.
b) Swartz, J., Mahachi, T., Kariv-Miller, E., J. Am. Chem. Soc., 1988, 110, 3622.
29. a) Penn, J., Cox, E., J. Org. Chem., 1986, 51, 4447.
b) Belotti, S., Cossy, J., Pete, J., Portella, C., J. Org. Chem., 1986, 51, 4196.
30. a) House, H., Snoble, K., J. Org. Chem., 1976, 41(9), 3076.
b) House, H., McDaniel, W., Sieloff, R., Vandever, D., J. Org. Chem., 1978, 43(22), 4316.
c) House, H., Acc. Chem. Res., 1976, 9, 59.
d) MacInnes, I., Nonhebel, D., Orszulik, S., Suckling, C., J. Chem. Soc., Chem. Commun., 1982, 121.
e) Nonhebel, D., Orszulik, S., Suckling, C., J. Chem. Soc., Chem. Commun., 1982, 1146.
31. Wilt, J., in *"Free Radicals, Vol. I"*, Kochi, J., ed., Wiley, 1973, pp. 334-501.
32. Beckwith, A., Ingold, K., in *"Rearrangements in Ground and Excited States, Vol I."*, DeMayo, P., ed., Academic Press, 1980, pp. 161-310.
33. Griller, D., Ingold, K., Acc. Chem. Res., 1980, 13, 317.
34. Hirota, N., J. Chem. Phys., 1962, 37, 1884.
35. Hirota, N., J. Am. Chem. Soc., 1967, 89, 32.
36. Masnovi, J., Samsel, E., Bullock, R., J. Chem. Soc., Chem. Commun., 1989, 1044.
37. Bowry, V., Luszyk, J., Ingold, K., J. Chem. Soc., Chem. Commun., 1990, 923.
38. Bowry, V., personal communication, submitted J. Org. Chem.
39. Neckers, D., Schaap, A., Hardy, J., J. Am. Chem. Soc., 1966, 88(6), 1265.
40. Neckers, D., Tetrahedron Lett., 1965, 23, 1889.

41. Godet, J., Pereyre, M., Pommier, J., Chevolleau, D., J. Organomet. Chem., 1973, 55, C15.
42. Yang, D., Tanner, D., J. Org. Chem., 1986, 51, 2267.
43. Pereyre, M., Godet, J., Tetrahedron Lett., 1970, 42, 3653.
44. Godet, J., Pereyre, M., J. Organomet. Chem., 1972, 40, C23.
45. Godet, J., Pereyre, M., Bull. Chim. Soc. Fr., 1976, 7/8, 1105.
46. Degueil-Castaing, M., Rahm, A., J. Org. Chem., 1986, 51, 1672.
47. Tanner, D., Diaz, G., Potter, A., J. Org. Chem., 1985, 50, 2149.
48. a) Pierre, J., Arnaud, P., Bull. Soc. Chim. Fr., 1967, 6, 2107.
b) Caubere, P., Moreau, J., Bull. Soc. Chim. Fr., 1971, 9, 3276.
c) McCormick, J., Fitterman, A., Barton, D., J. Org. Chem., 1981, 46(23), 4708.
49. Neidig, P., Sun, S., J. Org. Chem., 1969, 34(6), 1854.
50. Hwu, J., J. Chem. Soc., Chem. Commun., 1985, 8, 452.
51. Krapcho, A., Seidman, D., Tetrahedron Lett., 1981, 179.
52. Chung, S., J. Org. Chem., 1981, 46, 5457.
53. House, H., Prabhu, A., Wilkins, J., Lee, L., J. Org. Chem., 1976, 41(19), 3067.
54. Bowers, K., Giese, R., Grimshaw, J., House, H., Kolodny, N., Kronberger, K., Roe, D., J. Am. Chem. Soc., 1970, 92(9), 2783.
55. Miyaura, N., Itoh, M., Sasaki, N., Suzuki, A., Synthesis, 1975, 5, 317.
56. Bertz, S., Dabbagh, G., J. Org. Chem., 1984, 49(10), 1739.
57. a) Breuer, E., Segall, E., Stein, Y., Sarel, S., J. Org. Chem., 1972, 37(14), 2242.
b) Traas P., Boeleus, H., Takken, H., Recl. Trav. Chim Pays-Bas, 1976, 95(3), 57.
c) Schliemann, W., Buege, A., Reppel, L., Pharmazie, 1980, 35(3), 140.
58. a) Hall, S., Sha, C., Jordan, F., J. Org. Chem., 1976, 41(9), 1494.
b) Blumbergs, P., LaMontagne, M., Stevens, J., J. Org. Chem., 1972, 37(8), 1248.
59. Bagnell, L., Meisters, A., Mole, T., Aust. J. Chem., 1975, 28, 821.
60. Loots, M., Dayrit, F., Schwartz, J., Bull. Soc. Chim. Belg., 1980, 89, 897.
61. Nishida, S., Kataoka, F., J. Org. Chem., 1978, 43(8), 1612.
62. Meinhart, J., Grubbs, R., Bull. Chem. Soc. Jpn., 1988, 61(1), 171.

63. a) Dauben, W., Deviny, E., *J. Org. Chem.*, **1966**, *31*, 3979.
 b) Staley, S., in *"Selective Organic Transformations"*, Thyagarajan, B., ed., Wiley Interscience, New York, 1972, vol 2, pp. 309-348.
 c) Wong, H., Hon, Y., Tse, C., Yip, Y., Tanko, J., Hudlicky, T., *Chem. Rev.*, **1989**, *89*, 165.
64. Bellamy, A., Campbell, E., Hall, R., *J. Chem. Soc., Perkin Trans II*, **1974**, 1347.
65. a) Shiota, H., Ohkata, K., Hanafusa, T., *Chem. Lett.*, **1974**, *10*, 1153.
 b) Murphy, W., Wattanasin, S., *Tetrahedron Lett.*, **1981**, *22*, 659.
66. Hall S., Sha, C., *Chem Ind (London)*, **1976**, *5*, 216.
67. For a review of cyclopropane electrochemistry, see: Becker, J., in *"The Chemistry of the Cyclopropyl Group"*, Rappoport, Z., ed., Wiley, New York, 1987, pp 915-958.
68. Mandell, L., Johnston, J., Day, R., *J. Org. Chem.*, **1978**, *43*(8), 1616.
69. Kristensen, L., Lund, H., *Acta. Chem. Scand.*, **1979**, *B33*, 735.
70. Kostyanovskii, R., Solodovnikov, S., Yuzhakova, O., *Izv. Akad. Nauk. SSSR, Ser. Khim.*, **1966**, *4*, 735.
71. Parker, V., In *"Topics in Organic Electrochemistry"*, Fry A., Britton, W., eds., Plenum Press, New York, **1986**, pp. 35-79.
72. Parker, V., In *"Advances in Physical Organic Chemistry"*, Vol. 19, Gold, V., Bethell, D., eds., Academic Press, New York, **1983**, pp. 131-223.
73. Parker, V., *Electroanal. Chem.*, **1986**, *14*, 1.
74. Britz, D. *"Digital Simulation in Electrochemistry"*, Springer-Verlag, New York, **1981**.
75. Maloy, J., In *"Laboratory Techniques in Electroanalytical Chemistry"*, Kissinger, P., Heineman, W., eds., Marcel Dekker, New York, **1984**, pp. 417-461.
76. a) Ahlberg, E., Parker, V., *Acta. Chem. Scand.*, **1981**, *B35*, 117.
 b) Egashira, N., Minami, T., Kondo, T., Hori, F., *Electrochimica Acta*, **1986**, *31*, 463.
77. a) Parker, V., *Acta. Chem. Scand.*, **1981**, *B35*, 233.
 b) Hammerlich, O., Parker, V., *Acta. Chem. Scand.*, **1983**, *B37*, 379.
78. a) semiempirical molecular orbital theory, AM1 approximation. see, Dewar, M., Zoebisch, E., Healy, E., Stewart, J., *J. Am. Chem. Soc.*, **1985**, *107*, 3902.
 b) AM1 implemented through MOPAC ver. 5.0 (QCPE #455). Full geometry optimizations were performed at the UHF level. see, Clark, T., *"A Handbook of Computational Chemistry, A practical guide to chemical structure and energy calculations"*, John Wiley and Sons, New York, 1985.

79. a)Vieira, K., Mubarak, M., Peters, D., *J. Am. Chem. Soc.*, **1984**, *106*, 5372.
 b)Alvarado de la Torre, R., Sease, J., *J. Am. Chem. Soc.*, **1979**, *101*(7), 1687.
 c)Grimshaw, J., Trocha-Grimshaw, J., *J. Chem. Soc., Perkin Trans. II*, **1975**, 218
 d)Stevenson, G., Sturgeon, B., *J. Org. Chem.*, **1990**, *55*, 4090.
 e)Carey, F., Sundberg, R., in "*Advanced Organic Chemistry 2nd ed., Part A: Structure and Mechanisms*", Plenum Press, New York, 1984, pp. 190-194.
80. a)Dorigo, A., McCarrick, M., Loncharich, R., Houk, K., *J. Am. Chem. Soc.*, **1990**, *112*, 7508.
 b)MMX, Serena Software, Bloomington, IN 47402-3076. This program derived from MM2 (QCPE #395) with MMP1 π -subroutines included and is run on either an IBM PS/2 Model 50 or VAX 8800.
81. a)Espenson, J., "*Chemical Kinetics and Reaction Mechanisms*", McGraw Hill, New York, **1981**, pp. 57-59.
 b)Garst, J., Smith, C., *J. Am. Chem. Soc.*, **1976**, *98*(6), 1520.
 c)Smid, J., Szwarc, M., *J. Am. Chem. Soc.*, **1956**, *78*, 3322.
 d)Schuler, R., Kuntz, R., *J. Phys. Chem.*, **1963**, *67*, 1004.
82. a)C.V. simulation, Turbo Pascal Ver. 5, David K. Gosser Jr., The City College of the City University of New York, Dept. of Chemistry.
 EC_{DIM} mechanism simulated, $E_{red} = -2.410$ V, $E_i = -2.0$ V, $E_{sw} = -2.7$ V, $E_f = -2.0$ V, $v = 100$ mV/s, $T = 298.15$ K, $D = 1 \times 10^{-5}$ cm²/s, $k_{het} = 100$ cm/s, $\alpha = 0.5$, $C_A = 0.05$ M, k_{obs} = homogeneous, bimolecular rate constant for decay of the ketyl anion, $k_{obs(max)}$ = value of k_{obs} above which R_{DCV} dipped below 1.00 for the above conditions.
 b)C.V. simulation, Turbo Pascal Ver. 5, David K. Gosser Jr., The City College of the City University of New York, Dept. of Chemistry.
 EC mechanism simulated, $E_{red} = -2.410$ V, $E_i = -2.0$ V, $E_{sw} = -2.7$ V, $E_f = -2.0$ V, $v = 100$ mV/s, $T = 298.15$ K, $D = 1 \times 10^{-5}$ cm²/s, $k_{het} = 100$ cm/s, $\alpha = 0.5$, k_1 = homogeneous, unimolecular rate constant for decay of the ketyl anion, $k_{1(max)}$ = value of k_1 above which R_{DCV} dipped below 1.00 for the above conditions.
83. a)Walsh, A., *Nature(London)*, **1947**, *159*, 167, 712.
 b)Walsh, A., *Trans. Faraday Soc.*, **1949**, *45*, 179.
 c)Sugden, T., *Nature(London)*, **1947**, *160*, 367.
 d)Drumright, R., Mas, R., Merola, J., Tanko, J., *J. Org. Chem.*, **1990**, *55*, 4098.
84. a)Hoffmann, R., *Tetrahedron Lett.*, **1970**, 2907.
 b)Hoffmann, R., Davidson, R., *J. Am. Chem. Soc.*, **1971**, *93*, 5699.
 c)Clark, T., Spitznagel, G., Klose, R., Schleyer, P., *J. Am. Chem. Soc.*, **1984**, *106*, 4412.
 d)Tanko, J., Mas, R., Suleman, K., *J. Am. Chem. Soc.*, **1990**, *112*, 5557.
85. For conformational studies on phenyl cyclopropyl ketone see:
 a)Aroney, M., Calderbank, K., Stootman, H., *J. Chem. Soc., Perkin Trans. (II)*, **1973**, 1365.
 b)Andrieu, C., Lemarie, B., Paquer, P., *Org. Magn. Reson.*, **1974**, *6*, 479.
86. Bard, A., Faulkner, L., "*Electrochemical Methods, Fundamentals and Applications*", John Wiley and Sons, New York, 1980, pp. 429-487.

87. a)Raner, K., Lusztyk, J., Ingold, K., J. Am. Chem. Soc., **1988**, *110*, 3519.
 b)Eisenthal, K., Acc. Chem. Res., **1975**, *8*, 118.
 c)Koenig, T., Fischer, H., in "*Free Radicals, Vol I*", Kochi, J., ed., Wiley, New York, 1973, pp. 157-189.
88. Steinberger, N., Fraenkel, G., J. Chem. Phys., **1964**, *40(3)*, 723.
89. 0.5 M tetra-n-butylammonium tetrafluoroborate, DMF, 0.1 M AgNO₃/Ag in CH₃CN (+.337 vs. SCE), Au working electrode.
90. RajanBabu, T., Reddy, G., Fukunaga, T., J. Am. Chem. Soc., **1985**, *107*, 5473.
91. a)C.V. simulation, Turbo Pascal Ver. 5, David K. Gosser Jr., The City College of the City University of New York, Dept. of Chemistry.
 EC mechanism simulated, $E_{red} = -2.42$ V, $E_i = -2.0$ V, $E_{sw} = -2.8$ V, $E_f = -2.0$ V, $v = 50$ V/s, $T = 298.15$ K, $D = 1 \times 10^{-5}$ cm²/s, $k_{het} = 100$ cm/s, $\alpha = 0.5$, $k_{obs} =$ varied to find maximum homogeneous rate constant where reverse current is observed under the above conditions.
 b)C.V. simulation, Turbo Pascal Ver. 5, David K. Gosser Jr., The City College of the City University of New York, Dept. of Chemistry.
 EC mechanism simulated, $E_{red} = -2.42$ V, $E_i = -2.0$ V, $E_f = -2.8$ V, $v = 50$ mV/s, $T = 298.15$ K, $D = 1 \times 10^{-5}$ cm²/s, $k_{het} = 100$ cm/s, $\alpha = 0.5$, $k_{obs} =$ homogeneous rate constants large enough so that no reverse current would be observed for a full cycle.
92. House, H., Huber, L., Umen, M., J. Am. Chem. Soc., **1972**, *94*, 8471.
93. Wayner, D., McPhee, D., Griller, D., J. Am. Chem. Soc., **1988**, *110*, 132.
94. a)Amatore, C., Saveant, J., J. Electroanal. Chem., **1977**, *85*, 27.
 b)Amatore, C., Saveant, J., J. Electroanal. Chem., **1978**, *86*, 227.
95. a)Bordwell, F., Harrelson, J., Satish, A., J. Org. Chem., **1989**, *54*, 3101.
 b)Kern, J., Federlin, P., Tetrahedron, **1978**, *34*, 661.
 c)Ebersson, L., Acta. Chem. Scand., **1984**, *B38*, 439.
96. Andrieux, C., Hapiot, P., Saveant, J., Chem. Rev., **1990**, *90*, 723.
97. Hudlicky, T., Kutchan, T., Naqvi, S., in "*Organic Reactions, Vol. 33*", Kende, A., ed., John Wiley and Sons, New York, 1985, pp. 247-335.
98. a)Dinnocenzo, J., Schmittel, M., J. Am. Chem. Soc., **1987**, *109*, 1561.
 b)Dinnocenzo, J., Conlon, D., J. Am. Chem. Soc., **1988**, *110*, 2324.
99. Reynolds, D., Harirchian, B., Chiou, H., Marsh, K., Bauld, N., J. Phys. Org. Chem., **1989**, *2(1)*, 57.
100. Bauld, N., Bellville, D., Harirchian, B., Lorenz, K., Pabon, R., Reynolds, D., Wirth, D., Chiou, H., Marsh, K., Acc. Chem. Res., **1987**, *20*, 371.

101. a) Ingold, K., in *"Free Radicals, Vol. I"*, Kochi, J., ed., John Wiley and Sons, New York, 1973, pp. 37-112.
 b) *"Landolt-Bornstein, Numerical Data and Functional Relationships in Science and Technology, Radical Reaction Rates in Liquids"*, Vol. 13, subvolumes a-e, Springer Verlag, Berlin, 1984.
102. Still, W., Kahn, M., Mitra, A., *J. Org. Chem.*, **1978**, *43*(14), 2923.
103. a) Lines, R., Jensen, B., Parker, V., *Acta. Chem. Scand.*, **1978**, *B32*, 510.
 b) Mann, C., in *"Electroanalytical Chemistry, Vol. 3"*, Bard, A., ed., Marcel Dekker, New York, 1969, pp. 57-134.
104. BASF, "BTS Catalyst Booklet" BASF Corporation, E 221 State Highway 4, P.O. Box 289, Paramus, New Jersey, 07652, (201)-316-3000.
105. Miller, R., McKean, D., *J. Org. Chem.*, **1981**, *46*, 2412.
106. a) Agami, C., *Bull. Soc. Chim. Fr.*, **1967**, *4*, 1391.
 b) Cannon, G., Santali, A., Shenan, P., *J. Am. Chem. Soc.*, **1959**, *81*, 1665.
 c) Masuyama, Y., Ueno, Y., Okawara, M. *Chem. Lett.*, **1977**, 1439.
107. a) Bumgardner, C., McDaniel, K., *J. Am. Chem. Soc.*, **1969**, *91*, 6821.
 b) Handel, H., Pasquini, M., Pierre, J. *Bull. Soc. Chim. Fr.*, **1980**, (7-8, Pt. 2), 351.
 c) Ando, R., Sugawara, T., Shimizu, M., Kuwajima, I., *Bull. Chem. Soc. Jpn.*, **1984**, *57*, 2897.
 d) Takei, S., Dawano, Y., *Tetrahedron Lett.*, **1975**, *49*, 4389.
 e) Posner, G., Mallamo, J., Black, A., *Tetrahedron*, **1981**, *37*(23), 3921.
108. a) Vogel, E., Erb, R., Lenz, G., Bothner-By, A., *Ann*, **1964**, 682, 1.
 b) Arai, M., Crawford, R., *Can. J. Chem.*, **1972**, *50*(13), 2158.
109. Watson, J., Irvine, J., Roberts, R., *J. Am. Chem. Soc.*, **1973**, *95*(10), 3348.
110. Nelson, E., Maienthal, M., Lane, L., Benderly, A., *J. Am. Chem. Soc.*, **1957**, *79*, 3467.
111. Johnston, L., Scaiano, J., Sheppard, J., *Chem. Phys. Lett.*, **1986**, *124*(6), 493.
112. Rovnyak, G., Diassi, P., Levine, S., Sheehan, J., *J. Med. Chem.*, **1973**, *16*(5), 487.
113. Hart, H., Levit, G., *J. Org. Chem.*, **1959**, *24*, 1261.
114. Corey, E., Chaykovsky, M., *J. Am. Chem. Soc.*, **1965**, *87*(6), 1353.
115. Boggs, G., Gerig, J., *J. Org. Chem.*, **1969**, *34*(5), 1484.
116. House, H., Feng, E., Peet, N., *J. Org. Chem.*, **1971**, *36*(16), 2371.

117. a)EG&G/PAR "*Potential Error Correction (iR Compensation)*", Technical Note 101, EG&G Princeton Applied Research, Electrochemical Instruments Division, P.O. Box 2565, Princeton, NJ, 08543, 609-452-2111.
 b)Whitson, P., VandenBorn, H., Evans, D., Anal. Chem., **1973**, *45*(8), 1298.
 c)Ahlberg, E., Parker, V., J. Electroanal. Chem., **1980**, *107*, 197.
 d)Ahlberg, E., Parker, V., J. Electroanal. Chem., **1981**, *121*, 57.
118. a)Harris, D., "*Quantitative Chemical Analysis*", W.H. Freeman and Company, San Francisco, 1982, pp. 27-79.
 b)Christian, G.D., "*Analytical Chemistry 3rd ed.*", John Wiley and Sons, New York, 1980, Chapter 4, pp. 59-87.
119. Costa, L., Young, G., Whitesides, G., J. Organomet. Chem. , **1977**, *134*, 151.
120. a)Samsel, E., Kochi, J., J. Am. Chem. Soc., **1986**, *108*(16), 4790.
 b)Wiley, G., Hershkowitz, R., Rein, B., Chung, B., J. Am. Chem. Soc., **1964**, *86*, 964.
121. a)Adams, R.N. "*Electrochemistry at Solid Electrodes*", Marcel Dekker, New York, 1969.
 b)Bard, A., Faulkner, L., "*Electrochemical Methods, Fundamentals and Applications*", John Wiley and Sons, New York, 1980.
122. "*Organic Electrochemistry, an introduction and a guide*", Baizer, M., Lund, H., eds., Marcel Dekker, New York, 1983.
123. Evans, D., Acc. Chem. Res., **1977**, *10*(9), 313.
124. a)Mabbott, G., J. Chem. Ed., **1983**, *60*(9), 697.
 b)Kissinger, P., Heineman, W., J. Chem. Ed., **1983**, *60*(9), 702.
125. Electrochemical reversibility requires that electron transfer from the electrode to the electro-active species and vice versa is fast enough to maintain concentrations of oxidized and reduced forms required by the Nernst equation at the electrode surface. This phenomena relates to heterogeneous charge transfer kinetics and should not be confused with homogeneous reaction kinetics which deal with chemical reactions coupled to the electron transfer process. Therefore, be careful not to confuse electrochemical reversibility with chemical reversibility. They are distinctly different concepts.
126. a)Perone, S., Mueller, T., Anal. Chem., **1965**, *37*(1), 2.
 b)Evins, C., Perone, S., Anal. Chem., **1967**, *39*, 309.
 c)Ahlberg, E., Parker, V., J. Electroanal. Chem., **1981**, *121*, 73.
127. a)Parker, V., Acta. Chem. Scand., **1980**, *B34*, 359.
 b)Parker, V., Acta. Chem. Scand., **1981**, *B35*, 259.
 c)Parker, V., Acta. Chem. Scand., **1981**, *B35*, 373.
 d)Parker, V., Acta. Chem. Scand., **1984**, *B38*, 243.
128. a)Nicholson, R., Shain, I., Anal. Chem., **1964**, *36*(4), 706.
 b)Olmstead, M., Hamilton, R., Nicholson, R., Anal. Chem., **1969**, *41*(2), 261.

129. "Asyst 2.0. A Scientific System," Macmillan Software Co., New York, 1987. Module 1 (Tutorial/Glossaries), Module 2 (Analysis), and Module 3 (GPIB/IEEE-488).
130. "Cyclic Voltammetry, v. 4.0," James M. Tanko, Virginia Polytechnic Institute and State University (unpublished source code).
131. Blackman, R.B., Tukey, J.W., "*The Measurement of Power Spectra from the Point of View of Communications Engineering*", Dover Publications, New York, 1958.
132. Ackroyd, M.H., Digital Filters, in "*Computers in Medicine Series*", Hill, D.W., ed., Butterworth and Co. Ltd., London, 1973.
133. a) Silverstein, R., Bassler, G., Morrill, T., "*Spectrometric Identification of Organic Compounds, 4th ed.*", John Wiley and Sons, New York, 1981.
b) Cooper, J., "*Spectroscopic Techniques for Organic Chemists*", John Wiley and Sons, New York, 1980.

APPENDIX A. USE OF VOLTAMMETRY FOR MECHANISTIC STUDIES

INTRODUCTION

Voltammetry is a powerful tool for investigating chemical reaction mechanisms. Reactive intermediates can be generated and studied all in one voltammetric experiment. In this appendix, cyclic voltammetry (CV), derivative cyclic voltammetry (DCV), and linear sweep voltammetry (LSV) are discussed in the context of their application to mechanism elucidation. This appendix is neither a rigorous nor complete account, but instead is intended as a practical guide to the application of voltammetric techniques to mechanistic and kinetic problems. Thorough treatises of electrochemical methods and their applications are readily available.¹²¹⁻¹²³

CYCLIC AND DERIVATIVE CYCLIC VOLTAMMETRY

In order to understand the utility of cyclic voltammetry and related voltammetric methods, a brief introduction to the CV experiment is in order. Good articles on both basic theory and applications of CV have appeared.¹²⁴ To perform a voltammetric experiment, the potential of a working electrode (Hg, Pt, Au, C, etc.) is varied relative to a reference electrode (SCE, Ag/Ag⁺, etc.) and the resulting current is monitored. In cyclic voltammetry, the potential of the working electrode is varied linearly from an initial value, E_i , to a switching potential, E_λ , and then on to a final potential, E_f (See Figure 78). The rate at which the potential is varied, ν (known as sweep rate), can be controlled and is simply the absolute value of the slope of the triangular potential waveform applied to the working electrode. The current response (cyclic voltammogram) to this potential waveform is shown in Figure 79.

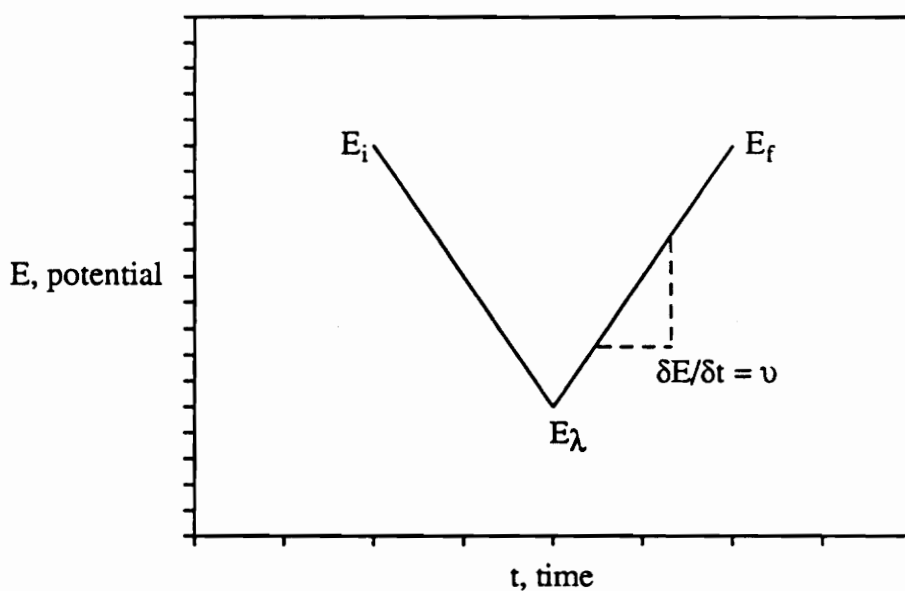


Figure 78. Potential waveform for cyclic voltammetry

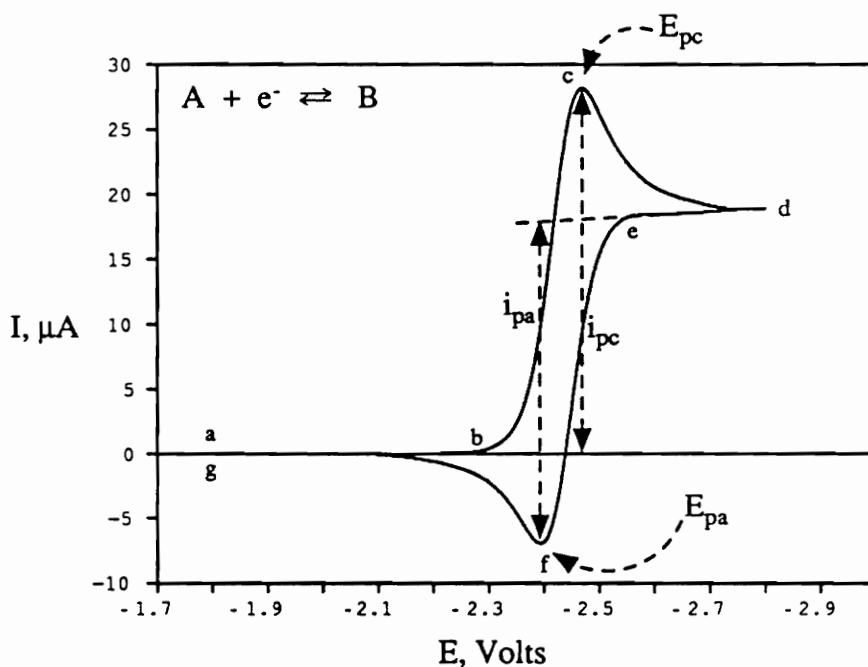


Figure 79. Cyclic voltammogram

Consider a substrate, A, with a reduction potential of E° which can be reduced to B ($A + e^- \rightleftharpoons B$). The cyclic voltammetry experiment is started at a potential (point a, E_i) positive of the reduction potential of the substrate and then scanned to more negative (less positive) values. At point b cathodic current begins to flow indicating that the electrode is a sufficiently strong reductant to reduce A to B. The current then rapidly increases, peaks, and then decays ($b \rightarrow c \rightarrow d$) as the concentration of A in the vicinity of the electrode is diminished. At point d (the switching potential, E_λ) the polarity of the electrode is reversed and the electrode is scanned to more positive potentials. Even though the polarity of the electrode has been reversed, its potential is still sufficiently negative to reduce A, so cathodic current continues to flow. Eventually (between points e & f), the potential of the working electrode becomes sufficiently positive (less negative) to oxidize B, whose concentration has been increasing in the vicinity of the electrode, back to A.

The anodic current then rapidly increases, peaks, and then decays ($e \rightarrow f \rightarrow g$) as the concentration of B is depleted in the vicinity of the electrode. At point g (the final potential, E_f) the experiment is complete. Qualitative profiles depicting how the concentration of A and B vary during the CV experiment with respect to both electrode potential and distance from the electrode are shown in Figure 80.

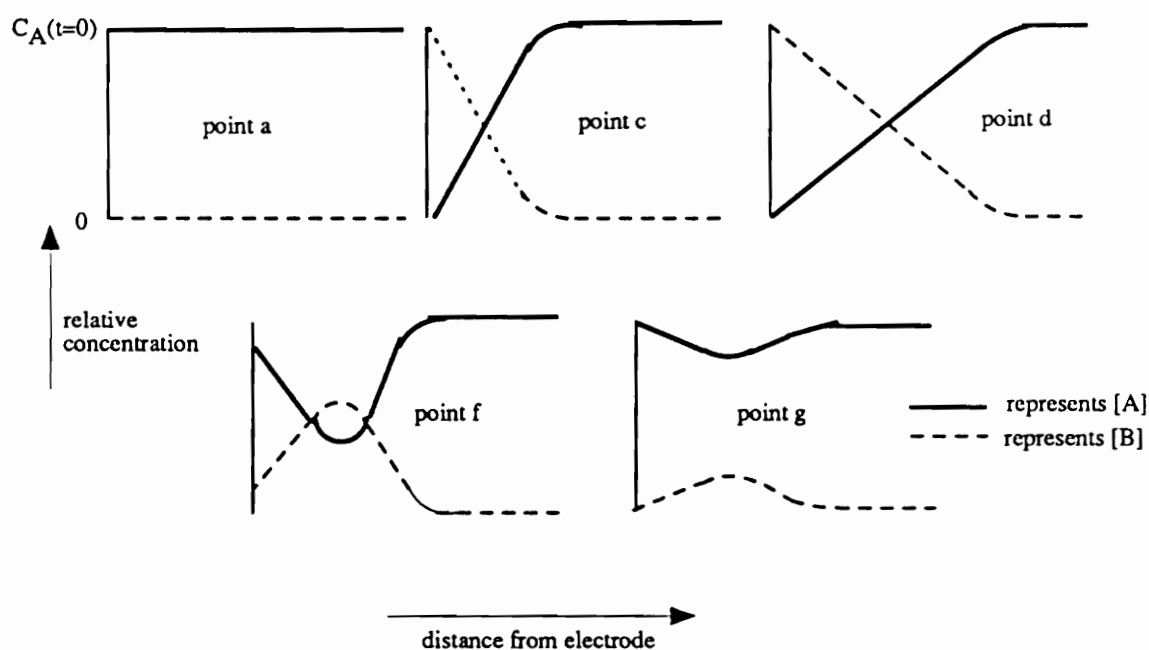


Figure 80. Concentration profiles for both oxidized and reduced species during a CV experiment

To summarize, in the first half of a CV experiment, B is electrochemically generated from A as indicated by the cathodic current. In the second half of the experiment, B is oxidized back to A as indicated by the anodic current. Therefore, CV is capable of rapidly generating an intermediate on the forward scan and then probing its fate on the reverse scan.

In a slightly more rigorous vein, the CV experiment can be explained by considering the relationship between the electrode potential and the concentration of

species at the electrode surface as governed by the Nernst equation (Eqn. 24). The potential applied to the working electrode (E) controls the ratio of [B]/[A] at the electrode surface. An initial value of E which is positive of E° maintains a ratio of [B]/[A] which is very small (i.e. A predominates). As the potential is scanned to more negative (less positive) values, A must be converted to B to satisfy the Nernst equation, so current flows. When E becomes more negative than E° , the ratio [B]/[A] must be large (i.e. B predominates). On the reverse scan, the potential applied to the working electrode forces the ratio of [B]/[A] to respond in an analogous but opposite manner.

Eqn. 24

$$E = E^\circ - \frac{RT}{nF} \left(\ln \frac{[B]_s}{[A]_s} \right)$$

E = applied potential	E° = formal reduction potential
R = gas constant (8.31441 VxC/Kxmol)	T = temperature (K)
F = Faraday's constant (9.648456 x 10 ⁴ C/mol)	n = # of electrons transferred
[A] _s = concentration of oxidized species at the electrode surface	[B] _s = concentration of reduced species at the electrode surface

Important information gleaned from a cyclic voltammogram include the cathodic peak potential (E_{pc}) and anodic peak potential (E_{pa}) as well as the magnitudes of the cathodic peak current (i_{pc}) and anodic peak current (i_{pa}). The formal reduction potential (E°) for an electrochemically reversible couple is centered between E_{pc} and E_{pa} as shown in equation 25 (please see footnote no. 125 for an explanation of electrochemical reversibility). Also, from a qualitative standpoint, the cathodic peak height (i_{pc}) is indicative of the amount of B initially generated, and the anodic peak height (i_{pa}) is indicative of the amount of B remaining when it is oxidized back to A. Therefore, the ratio of i_{pa}/i_{pc} is a qualitative measure of the stability of B.

Eqn. 25

$$E^\circ = \frac{E_{pa} + E_{pc}}{2}$$

The most elementary method for measuring the peak currents involves extrapolation of an estimated baseline current and then measuring the distance from the extrapolated baseline to the peak apex (Figure 79). It is essential to establish a good baseline to get accurate peak current measurements, but this is not always straightforward. Electrode couples complicated with homogeneous chemical reactions often do not give rise to clean CV traces (Figure 81). To circumvent the ambiguity in measuring CV peak heights, it is advantageous to take the derivative of the CV current with respect to time yielding a derivative cyclic voltammogram¹²⁶ (Figure 82). The two derivative peaks, $I'_{pc} = (dI/dt)_{\max}$ and $I'_{pa} = (dI/dt)_{\min}$, correspond to the inflection points on the cathodic and anodic waves of the corresponding cyclic voltammogram. The absolute heights of the two derivative cyclic voltammetry peaks are easily measured, but unfortunately have no meaning in themselves. However, the ratio of the two peaks, $R_{DCV} = I'_{pa}/I'_{pc}$, is an indirect measure of the stability of the electrode generated intermediate.

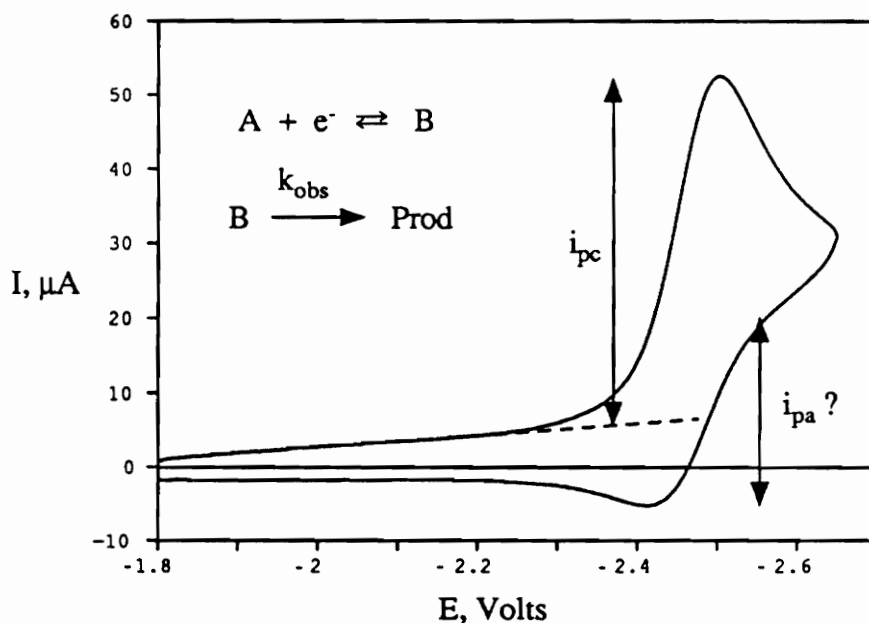


Figure 81. Cyclic voltammogram of system where the electrode generated species is involved in a homogeneous chemical reaction

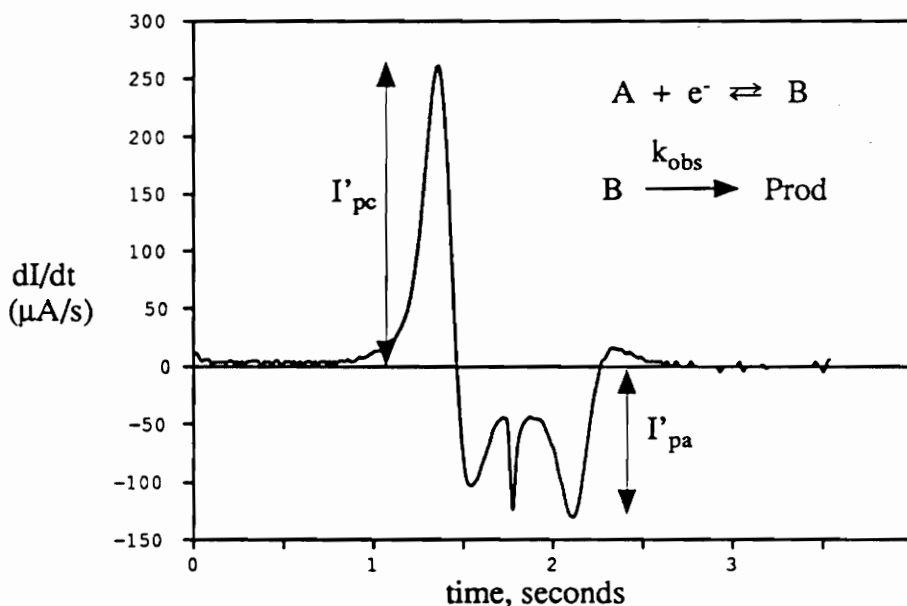


Figure 82. Derivative cyclic voltammogram of system where the electrode generated species is involved in a homogeneous chemical reaction

As an example, suppose that the CV trace in Figure 81 and the corresponding DCV trace in Figure 82 arise from a fast, reversible, heterogeneous charge transfer ($A + e^- \rightleftharpoons B$) coupled with a homogeneous chemical step consuming B ($B \rightarrow \text{products}$). The amount of B consumed by the reaction during the course of the CV experiment will depend upon the rate of the chemical reaction consuming it and the CV scan rate. If $R_{DCV} = 1$, no chemical reaction occurred in the time frame of the experiment. If on the other extreme $R_{DCV} = 0$, all B was consumed by the chemical step in the time frame of the experiment.

Intermediate values of R_{DCV} ($0.8 \leq R_{DCV} \leq 0.3$), obtained when the scan rate is in the same "time window" as the reaction rate, are extremely useful for determination of the rate law for decay of electrode generated intermediates. The duration of the experiment is controlled by the scan rate chosen. By varying the scan rate and observing how R_{DCV} changes, a map of relative concentration change with respect to time is obtained. This is

the basis of mechanistic and kinetic explorations using derivative cyclic voltammetry.

The "reaction order approach" reviewed extensively by Parker^{71,72} provides a means of assessing the rate law for decay of an electrode generated intermediate. During DCV analysis, the concentration of substrate, C_A , is varied and the sweep rate, ν , is adjusted to keep R_{DCV} at a constant value. Equation 26 shows that a plot of the log of the sweep rate necessary to maintain R_{DCV} at a constant value ($\log \nu_c$) vs. the log of the bulk concentration of substrate ($\log C_A$) yields a straight line whose slope is related to the combined reaction order ($R_{A/B}$) in substrate (A) and electrode generated intermediate, B ($R_{A/B} = R_A + R_B$ where $\text{Rate} = k_{\text{obs}}[A]^{R_A}[B]^{R_B}$).

Eqn. 26

$$R_{A/B} = [\delta \log (\nu_c) / \delta \log (C_A)] + 1$$

$R_{A/B}$ = combined reaction order in A and B
 ν_c = sweep rate necessary to maintain R_{DCV} at a constant value
 C_A = bulk concentration of substrate

Suppose that after performing several experiments it is found that $R_{A/B} = 2$. Two simple rate laws must be considered. The first rate law, $-\delta[B]/\delta t = k_{\text{obs}}[B]^2$, is second order in electrode generated intermediate ($R_B = 2$). The second possible rate law, $-\delta[B]/\delta t = k_{\text{obs}}[A][B]$, is first order in both substrate and electrode generated intermediate giving a combined reaction order of two ($R_A = R_B = 1$). Derivative cyclic voltammetry can not be used to distinguish between these two rate laws.

LINEAR SWEEP VOLTAMMETRY

A linear sweep voltammetry (LSV) experiment is essentially half of a cyclic voltammetry experiment (Figure 83). For kinetic experiments, the observable in LSV is the peak potential, E_p . As discussed earlier, the potential of the working electrode at any given time governs the relative ratio of oxidized and reduced species at the electrode surface as dictated by the Nernst equation.

$$E = E^\circ - \frac{RT}{nF} \left(\ln \frac{[B]_s}{[A]_s} \right)$$

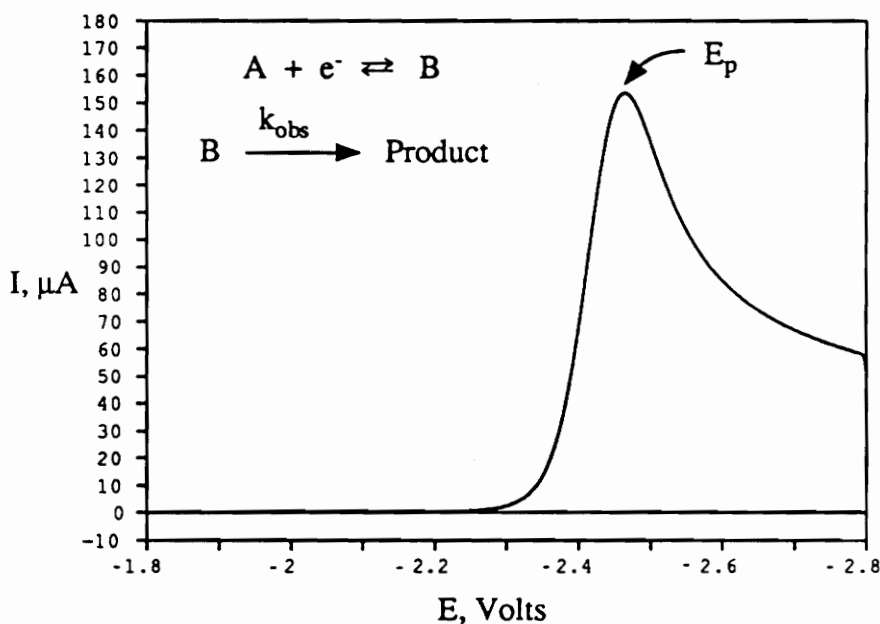


Figure 83. Linear sweep voltammogram

As before, consider a fast, reversible, heterogeneous charge transfer ($A + e^- \rightleftharpoons B$) coupled with a homogeneous chemical step consuming B ($B \rightarrow \text{products}$). Even when an electrode generated intermediate decays through a homogeneous chemical reaction, the Nernst equation must be obeyed. Since B is being consumed, the "missing" B must be replaced to satisfy the requirements of the Nernst equation. The only way to replace the "missing" B is to electrochemically make more; therefore, more current flows. The net result is that more current flows at less negative (more positive) potentials giving rise to a positive shift in the observed peak potential.

The peak potential shift caused by a chemical reaction's consumption of an electrode generated intermediate can be related to the reaction order in that intermediate (Eqn. 27).^{71,72,127} A plot of the observed peak potential (E_p) as a function of the log of scan rate ($\log v$) gives a line whose slope is directly related to the reaction order in B, R_B .

Eqn. 27

$$\frac{\delta E_p}{\delta \log v} = \frac{1}{R_B + 1} (\ln 10) \frac{RT}{nF} = \frac{1}{R_B + 1} \quad (59.2)$$

E_p = observed peak potential

v = scan rate

R_B = reaction order in electrode generated intermediate

Similarly, at a constant scan rate (v_c), the change in the observed peak potential (E_p) as a function of substrate concentration (C_A) can be related to both the reaction order in substrate (A) and electrode generated intermediate, B (Eqn. 28). A plot of the observed peak potential (E_p) as a function of the log of the substrate concentration ($\log C_A$) gives a line whose slope is directly related to the reaction orders in A, R_A , and in B, R_B . LSV reaction order analysis allows the reaction orders in substrate and electrode generated intermediate to be deconvoluted.

Eqn. 28

$$\frac{\delta E_p}{\delta \log C_A} = \frac{R_A + R_B - 1}{R_B + 1} (\ln 10) \frac{RT}{nF} = \frac{R_A + R_B - 1}{R_B + 1} \quad (59.2)$$

E_p = observed peak potential
 C_A = bulk concentration of substrate
 R_B = reaction order in electrode generated intermediate
 R_A = reaction order in substrate

RATE CONSTANTS

Once the rate law for decay of an electrode generated intermediate has been determined, it is possible to assign the rate constant for the observed decay. Empirical relationships and working curves for rate constant calculation from DCV⁷¹ and CV¹²⁸ data for various mechanisms are available. Also, rate constants can be obtained by digital simulation of the postulated mechanism.^{74,75} The rate constant is adjusted until the results of the digital simulation match the experimental results. In practice, it is best to estimate the rate constant by use of the empirical relationships and working curves and then fine tune the value with digital simulation.

SUMMARY

Voltammetric techniques provide a convenient way to synthesize and study reactive intermediates. In this appendix, cyclic voltammetry, derivative cyclic voltammetry, and linear sweep voltammetry are discussed. CV, DCV and LSV are complimentary electrochemical techniques. These voltammetric techniques yield a wealth of information about the mechanism and rate of decay of electrode generated intermediates, but each has its limitations. CV and DCV are best suited for studying slow to moderately fast homogeneous chemical reactions and give information about the overall order of the reaction and its observed rate constant. LSV can only be used for studying moderately to extremely fast homogeneous chemical reactions and gives specific information about the reaction's rate law but no information about its homogeneous rate constant unless the true reduction potential of the electrode couple is known. The technique of choice will depend on the relative rate and the information desired about the chemical reaction under investigation.

Appendix B. Collection and Handling of Electrochemical Data

Electrochemical experiments were performed using an EG&G Princeton Applied Research Model 273 potentiostat/galvanostat, interfaced (GPIB/IEEE-488) to an IBM PC-XT computer. The triangular waveform for cyclic voltammetry was generated using the Model 273's digital program generator. Data acquisition was accomplished using the Model 273 internal (100 μ s) A/D converter. Using the ASYST operating language,¹²⁹ on-site software was produced¹³⁰ for controlling the potentiostat functions, data transfer to the PC, and subsequent data analysis and storage. This menu-driven software allows the user to run an experiment, store/recall data from a disk file, and perform a variety of data analysis operations including plot (I vs. t, I vs. E, dI/dt vs. t, or I vs. E plot superimposed with data from a disk file), data smoothing/filtration, subtraction of data in a disk file from data in memory, and transfer of the data to a Lotus 123 worksheet.

Derivative cyclic voltammograms were generated from the raw current vs. time data from the potentiostat by interpolating a second-order polynomial through consecutive datapoints, and taking the first derivative of the polynomial. This derivative trace was then digitally filtered, using the "smooth" function in ASYST.¹³⁰ Via a fast Fourier transformation, the frequency spectrum of the derivative data array is generated. Convolution of the data is achieved by multiplication of the data spectrum by the inverse Fourier transform of the "Blackman window" for convolution weights.^{131,132} The cut-off frequency for the low pass filter (f_o), measured in cycles per point, was set according to the total number of datapoints:

$$f_o = \frac{100}{\text{total number of datapoints}}$$

(within the range $0.03 \leq f_o \leq 0.5$)

The total number of datapoints (which varied with the scan rate and the magnitude of the potential scan) was always set to maximize resolution, and was in the range $400 \leq \#$ of datapoints ≤ 6144 .

I (R.E. Drumright) would like to acknowledge and thank Dr. James M. Tanko for composing both this appendix and the software described within it.

APPENDIX C. STRUCTURAL DETERMINATION BY UV SPECTROSCOPY

Addition of Δ^5 -hexenyl and cyclopentyl carbinyl radicals to pivalophenone ketyl anion led to several products (Figure 46). Through ^1H NMR, ^{13}C NMR, IR and mass spectrometry, we were able to conclusively identify all of the products except for one which contained a cyclohexadiene ring at the expense of an aromatic nucleus. Based upon the aforementioned spectroscopic data, we were unable to distinguish between the three structural isomers shown in Figure 84 for the identity of the cyclohexadiene containing compound.

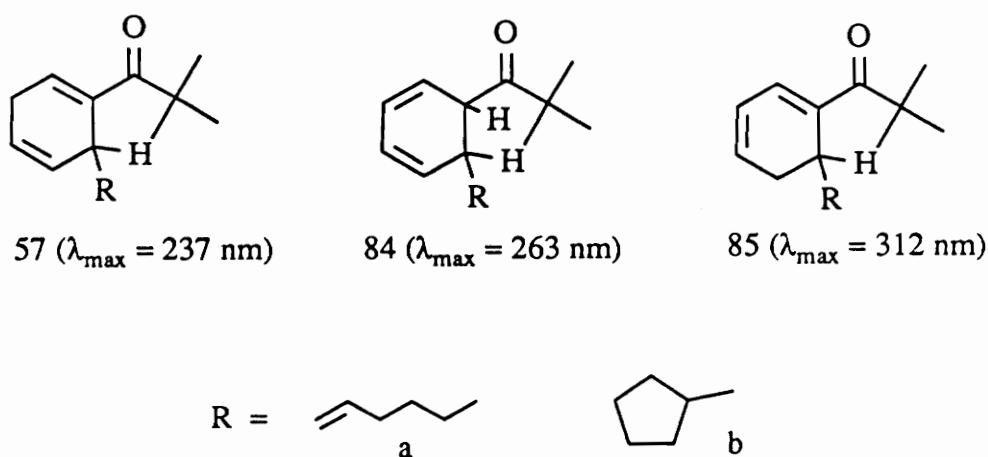


Figure 84. Possible isomeric structures for the cyclohexadiene containing product resulting from coupling of a free radical with pivalophenone ketyl anion

Ultraviolet (UV) spectroscopy allowed us to distinguish between the three possible choices. Rules for predicting the position of absorption (λ_{max}) of organic compounds are readily available.¹³³ The calculated values for λ_{max} are 237 nm, 263 nm, and 312 nm for (57), (84), and (85) respectively. The experimentally observed values for λ_{max} are 244 nm

and 242 nm for the Δ^5 -hexenyl and cyclopentyl carbinyl substituted compounds respectively. Therefore, the cyclohexadiene containing products have the structure of (57) and not the structure of isomers (84) or (85).

It is interesting to note that coupling of aryl cyclopropyl ketyl anions with their distonic radical anions does not yield any detectable cyclohexadiene containing products (see Chapter 2). Evidently, the "built in" hydride acceptor present in the ketyl anion/distonic radical anion adducts and not present in the ketyl anion/free radical adducts allows for an extremely facile rearomatization process to occur via our proposed intramolecular hydride transfer mechanism (see Figures 32, 33, and 36).

VITA

Ray Eugene Drumright was born on September 23, 1965 in Emporia, Kansas, USA to Patricia Ann and Arthur Lee Drumright. He began grade school in Emporia, continued in Richmond, Virginia, USA, and finished the bulk of it in Collingwood, Ontario, Canada. He began high school in Collingwood, continued in Frederick, Oklahoma, USA, and finished at Plano, Texas, USA.

In the fall of 1983 he enrolled at Oklahoma State University, Stillwater, Oklahoma, USA with aspirations of becoming a veterinarian but was soon whisked away from this field by a growing curiosity about the physical sciences. He landed in chemistry and worked in an organic chemistry laboratory under the supervision of Dr. Richard A. Bunce. He received a Bachelor of Science in Chemistry from Oklahoma State in the spring of 1987.

In the summer of 1987, he entered the doctoral program at Virginia Polytechnic Institute and State University where he worked in the area of physical organic chemistry under the guidance of Dr. James M. Tanko. He received a Doctor of Philosophy in Chemistry in January, 1991 from VPI&SU.

He married Susan DeAnn Nichols on August 19, 1989 in Stillwater, Oklahoma, USA and currently has no children. He will commence his career with Dow Chemical in Midland, Michigan, USA.

A handwritten signature in black ink that reads "Ray Drumright". The signature is written in a cursive, flowing style with a large initial "R" and "D".